PHYSIOLOGICAL INSIGHTS INTO A NOVEL ANAEROBIC HG(II) REDUCTION PATHWAY IN ANOXYGENIC PHOTOTROPHS

NOÉMIE LAVOIE

Thesis submitted to the University of Ottawa
in partial fulfillment of the requirements for the
Doctorate in Philosophy degree in Biology

Department of Biology
Faculty of Sciences
University of Ottawa

Abstract

Mercury (Hg) is a pollutant of global concern and a potent neurotoxin that bioaccumulates and biomagnifies in terrestrial and aquatic food webs as methylmercury (MeHg). Though now heavily regulated, over a century of legacy anthropogenic emissions and releases of Hg into the environment still affect us today. Anaerobic microorganisms are principally responsible for producing MeHg from new and legacy pollution, a process which depends on the bioavailability of inorganic Hg. Hg redox reactions, such as Hg^{II} reduction to gaseous elemental Hg^{0}, play a key role in determining the availability of Hg in the environment. In anoxic environments, certain anaerobic and phototrophic microbes can catalyze the reduction of Hg^{II} and may compete for other vital resources and nutrients with Hg methylators. Currently, the physiological mechanisms driving this anaerobic redox reaction are poorly understood. The main objective of my thesis is to uncover physiological and environmental controls of anaerobic and phototrophic Hg^{II} reduction pathways. I used a combination of microbial physiology, molecular biology, and trace Hg analytical techniques to study Hg^{II} reduction by anoxygenic phototrophs and fermenters from the Heliobacteria family. In Chapter 2, I discovered a novel Hg^{II}-reducing Heliobacteria from rice paddies. The magnitude of Hg^{II} reduced was enhanced by assimilating reduced sulphur sources, leading us to propose that anabolic pathways that consume reducing power can influence Hg^{II} reduction. In Chapter 3, I investigated the influence of nitrogen availability and metabolism on the magnitude of Hg^{II} reduction. Here, contrary to sulphur assimilation, nitrogen did not influence the magnitude of Hg^{II} reduced. In Chapter 4, I demonstrated how the ability to reduce Hg^{II} is tied to phototrophic and fermentative reducing power-generating machinery. In Chapter 5, I showed that Hg^{II} reduction depends on interactions between Hg and cellular thiols. Lastly, in Chapter 6, I explored the possibility of Hg^{II} reduction in phylogenetically distant anoxygenic phototrophs from the Chloroflexota phylum. At its core, my thesis underscores the relationships between Hg^{II} reduction and cellular pathways that produce or consume reducing power. Though still unresolved, my thesis significantly contributes to uncovering the cellular mechanism catalyzing anaerobic Hg^{II} reduction.

Résumé

Le mercure (Hg) est un polluant préoccupant à l'échelle mondiale et une neurotoxine puissante qui se bioaccumule et se bioamplifie dans les réseaux trophiques terrestres et aquatiques sous forme de méthylmercure (MeHg). Bien qu'elles soient maintenant fortement réglementées, plus d'un siècle d'émissions anthropiques et de rejets de mercure dans l'environnement nous affectent encore aujourd'hui. Les micro-organismes anaérobies sont principalement responsables de la production de MeHg tant à partir d'anciennes que de nouvelles émissions, un processus qui dépend de la biodisponibilité du mercure inorganique. Les réactions d'oxydoréduction du mercure, telles que la réduction de Hg^{II} en Hg^{0} élémentaire gazeux, jouent un rôle clé dans la détermination de la disponibilité du mercure dans l'environnement. Dans les environnements anoxiques, certains microbes anaérobies et phototrophes peuvent catalyser la réduction du Hg^{II} et peuvent entrer en compétition pour d'autres ressources vitales et nutriments avec les méthylateurs de mercure. Actuellement, les mécanismes physiologiques qui alimentent cette réaction redox anaérobie sont mal compris. L'objectif principal de ma thèse est de découvrir des contrôles physiologiques et environnementaux sur les voies anaérobies et phototrophiques de réduction de Hg^{II}. J'ai utilisé une combinaison de techniques en physiologie microbienne, biologie moléculaire et analyse du mercure afin d'étudier la réduction du Hg^{II} par des phototrophes anoxygènes et fermenteurs de la famille des héliobactéries. Dans le chapitre 2, j'ai découvert q'une nouvelle héliobactérie, provenant de rizières, est capable de réduire le Hg^{II}. Ici, l'ampleur du Hg^{II} réduit a été augmentée par l'assimilation de sources de soufre réduites, nous menant à proposer que les voies anaboliques qui consomment du pouvoir réducteur peuvent influencer la réduction du Hg^{II}. Dans le chapitre 3, j'ai étudié l'influence de la disponibilité de l'azote et de son métabolisme sur l'ampleur de la réduction du Hg^{II}. Ici, contrairement à l'assimilation du soufre, l'azote n'a pas influencé l'ampleur de la réduction du Hg^{II}. Dans le chapitre 4, j'ai démontré comment la capacité de réduire le Hg^{II} est liée à la production de pouvoir réducteur par les voix cellulaires phototrophiques et fermentatives. Dans le chapitre 5, j'ai montré que la réduction de Hg^{II} dépend aussi des intéractions entre le Hg et les thiols cellulaires. Enfin, dans le chapitre 6, j'ai exploré la possibilité de réduction du Hg^{II} chez des phototrophes anoxygènes de l'embranchement de Chloroflexota. À la base, ma thèse souligne les relations entre la réduction du Hg^{II} et les voies cellulaires qui produisent ou

consomment du pouvoir réducteur. Bien que toujours inconnu, ma thèse contribue de manière significative à l'élucidation du mécanisme cellulaire catalysant la réduction anaérobie du Hg^{II}.

Acknowledgements

Many great works of writing start with a cliché statement. This is MY greatest work, and I argue that it does in fact take a village to raise a PhD.

To my supervisor, Alexandre Poulain, I owe so much of the scientist I have become to you. Your mentorship, a balance of trust, high expectations, and respect, has given me the confidence to follow my scientific intuition and to push through and solve often-frustrating technical challenges. Thank you for the wonderful journey.

To my committee members, Marina Cvetkovska, Clément Bataille, Amy Rand, and Thomas Hanson, I am grateful for your support and feedback throughout the years, and your final evaluation of my thesis. I remember mentioning my distress over having amassed so many null results during a TAC meeting, and Clément sympathized with me, saying he was in a very similar situation during his PhD. This gave me peace of mind and the courage to embrace my null- but very robust results and to be proud of my contributions to this burgeoning scientific field.

I also extend my gratitude to my many lab mates over the years who offered feedback on my research and made the lab a welcoming and caring place; Mija, Martin, Ben, Dan, Galen, Jess, Michelle, Rui, Jake, and David. Benjamin Stenzler, you get a special shoutout. Thank you for all the support and scientific advice that usually took the form of a complex and nebulous metaphor. My years of friendship with you have given me one very special superpower, and that is to read between the lines of what you are saying to find a deeper meaning. A special thank you to Michelle Hotchkiss as well. You initiated me to many wonderful things I had been missing out on: dessert Mondays, D&D, bookclubs, boardgame nights, new friends, and the complex digestive system of bumblebees and the five microbes that call it home.

Speaking of old lab mates, thank you, Daniel Grégoire, for the mentorship, training, and teamwork in the early days when I joined the lab. I learned so much from you, including that plumber's tape, zip ties, and superstitious rituals are essential tools in any self-respecting microbiologist's toolbox. As much as you joke it's your fault, and you're very sorry I got tricked into studying anaerobic mercury reduction, I wouldn't choose a different outcome for myself. Some of my best memories in the lab include the time I got to spend working with you, MacGyvering bioreactors, figuring out how to grow frustrating microbes, developing hypotheses,

and testing them. I don't mean it lightly when I say I think I owe the other half of the scientist I have become to you.

I have to thank Emmanuel Yumvihoze, Dave Eickmeyer, and Linda Kimpe for their support and for letting me borrow tools when I had to MacGyver a solution, usually involving high-pressure gas, tubing, and zip ties. I especially have to thank you, Emmanuel, for helping me with all things mercury, whether it be analyzing samples, developing new methods, or figuring out why the Tekran isn't working again.

To my friends and family, including my new in-laws, thank you for being part of my life. Thank you for the hangouts, the holiday dinners, the weekend BBQs, the boardgame and D&D nights. I owe much of my emotional wellbeing to you and our time together. Merci à ma mère, Sophie Savoie, pour ton amour inconditionnel. C'est toi qui a planté cette première graine de curiosité scientifique en moi et c'est toi qui l'a arrosé et l'a encouragé à grandir pendant tant d'années.

Last, and most importantly, I have to thank my wife, Perrin Bryson. I couldn't have finished my PhD without your immense love and support. From driving me to the lab to check on my bacteria Saturdays and Sundays, to picking me up from work because the transit system in Ottawa is a joke, to motivating me to write my thesis with little treats, to holding me as I cry my anguish and anxiety into your shoulder. You believed I could do it, so I did too. I love you more than words can express.

Table of Contents

List of Figures

List of Tables

Chapter 1

Introduction

1.1 HG AS A CONTAMINANT OF CONCERN

1.1.1 Transport

Mercury (Hg) is a globally distributed priority contaminant mainly emitted in its elemental and gaseous form, Hg^0 [1]. Atmospheric Hg^0 emissions occur naturally, such as from volcanoes and forest fires, but are predominantly from anthropogenic sources like coal burning and small-scale artisanal gold mining [1,2]. Hg^0 can be transported in the atmosphere over long distances for up to 1.7 years [3] before being oxidized to divalent Hg^{II} and deposited on land or into aquatic ecosystems. An estimated 1070 Gg of Hg has been released into these ecosystems from anthropogenic activities in the last 500 years [4]. Once deposited, Hg^{II} can undergo further abiotic and biotic transformations, altering its toxicity and environmental fate. Hg^{II} can be re-emitted to the atmosphere as Hg^0, sequestered in soils and sediments, or converted to its organic form, monomethylmercury (MeHg), through the activity of certain microorganisms [5].

1.1.2 Toxicity

Although all forms of Hg are toxic, MeHg is of most concern to human and ecosystem health. Hg^{II}'s toxicity is attributable to its tendency to bind to thiols such as those from the amino acid cysteine. This in turn can cause widespread disruptions to protein structures and cellular functions [6]. Conversely, MeHg is considered a neurotoxin to humans as it can cross the blood-brain barrier and interfere with neurological functions and brain development [7]. Exposure to MeHg has also been associated with fatal heart attacks [8]. Furthermore, a recent estimate of MeHg-related health impacts valued its annual global economic cost at $117 billion USD [9].

MeHg can easily cross cell membranes, and due to relatively slower rates of MeHg elimination compared with other toxins, it can bioaccumulate to higher concentrations than ambient levels in exposed organisms [10]. In aquatic environments, MeHg in phytoplankton and zooplankton is biomagnified through trophic levels [11,12]. Consequently, concerns about Hg stem primarily from the risk of regularly consuming predatory fish like sharks, swordfish, and some larger tuna species [10,13]. However, growing health concerns surrounding rice contaminated with MeHg have also emerged over the last decade in countries with high burdens of Hg pollution and where rice is a dietary staple [14,15].

1.1.3 Global policies to regulate Hg pollution

The importance of Hg as a chemical of concern to human health is underscored by the ratification of the UNEP Minamata Convention on Mercury in 2017, which mandates the now 140 signatory governments to regulate Hg emissions and their environmental impacts [16]. The latest UNEP Global Hg Assessment highlights knowledge gaps that need addressing to facilitate the implementation of this international treaty. The assessment emphasizes the need for a greater scientific understanding of the links between Hg deposition, methylation, and uptake by organisms and how these processes will be altered in response to global environmental change [17]. By addressing these knowledge gaps, scientists aim to provide the basis for new technologies and policies to protect human health and the environment from the adverse effects of Hg pollution.

1.2 HG CYCLING AND MICROBE-MEDIATED TRANSFORMATIONS

As part of my PhD research, I investigate the mechanism of a novel microbial Hg transformation pathway that can control the mobility and toxicity of Hg in the environment. The following sections aim to provide context on microbial Hg methylation, Hg redox cycling, microbe-mediated Hg^{II} reduction, and what is currently known of their varied mechanisms.

1.2.1 Microbial methylation:

MeHg is formed from inorganic Hg by certain anaerobic microorganisms in low-oxygen habitats such as marine and freshwater sediments and flooded soils [18–21]. The predominant Hg methylating microbes include certain sulphate reducing bacteria (SRB) [22], iron reducing bacteria (IRB) [19], and methanogenic archaea [23], though metagenomic sequencing continuously reveals new putative methylators [2,21,24–27]. Hg methylation is genetically encoded by a two-gene cluster *hgcA* and *hgcB* [28], where HgcA, a corrinoid protein, likely partakes in transferring a methyl group from a carbon substrate to Hg^{II}, and HgcB, a dicluster ferredoxin, is involved in delivering Hg^{II} to HgcA and releasing MeHg [28–31]. At the time of writing, it is still unclear if the transformation serves a detoxification purpose for these microbes. However, growing evidence supports that Hg methylation may be an accidental process co-occurring during the operation of cellular carbon metabolism [28,32–34]. Laboratory experiments demonstrated that two different Hg methylating bacteria could use Hg^0 and Hg^{II} to produce MeHg, although cells produced less MeHg from Hg^0 [35]. The prevalence of this ability among different Hg methylators is poorly understood, though it suggests that the availability of Hg^{II} and Hg^0 species likely influences the amount of MeHg produced in the environment.

1.2.2 Hg redox cycling

Hg redox transformations control the speciation of Hg and thus can affect its availability to methylators [1,36,37]. Reduction of Hg^{II} to volatile Hg^0 may favour its partitioning to the atmosphere [38] , thereby limiting methylation [37], whereas the oxidation of Hg^0 to Hg^{II} may enhance methylation [35,39]. Whether in the aqueous phase or complexed with minerals and organic matter, recently deposited Hg^{II} in oxic surface environments can undergo photochemical redox reactions [40–42]. Hg^{II} photoreduction is a primary process driving Hg transformation in both surface aquatic

and terrestrial environments[40,43,44]. However, in dark conditions such as bottom waters and anoxic sediments, Hg^{II} reduction can also occur due to abiotic reactions with iron hydroxides [45], magnetite [46,47], and reactive sites on dissolved organic matter [48,49]. In addition, diverse microorganisms are involved in Hg transformations controlling the relative abundance of Hg species in the environment [32]. While MeHg is produced by some anaerobic bacteria and archaea, microorganisms can also influence the fate of Hg via MeHg degradation [50] or redox reactions [36]. **Figure 1.1** serves to broadly illustrate Hg transport and transformation pathways in the environment.

1.2.3 Microbial Hg^{II} reduction

1.2.3.1 Mer operon

As Hg^{II} has a high electrophilic affinity for thiol-bearing molecules (SH-), this renders essential amino acids like cysteine most vulnerable to attack, and this can result in oxidative damage, protein misfolding, loss of metabolic functions, and decreased fitness for vulnerable organisms [6]. Certain microorganisms can reduce Hg^{II} to Hg^0 which lessens its toxicity, as the latter is relatively inert and can passively diffuse out of cells [51]. Certain archaea and bacteria have evolved a suite of proteins encoded by the *mer* operon to interact with and minimize Hg^{II} toxicity to the cell environment, conferring resistance to high μM-levels of Hg^{II} [52]. The *mer* operon contains a series of Hg-specific proteins involved in transcription regulation, Hg transportation, and Hg catalysis. The expression of *mer* components is regulated by MerR, which acts as a transcriptional activator of other *mer* operon genes in the presence of toxic Hg^{II} concentrations [52]. Hg^{II} readily enters cells, however *mer*-mediated resistance strategies also employ dedicated Hg^{II} transporters to import Hg^{II} directly to other cytosolic *mer* proteins [53]. In Gram-negative bacteria, MerP acts as a 'scavenger' for Hg^{II} that enters the periplasm and then transfers it to the inner membrane-bound MerT transporter. MerT is responsible for delivering Hg^{II} to MerA situated in the cytoplasm [54,55].

MerA, a flavin-containing disulphide oxidoreductase enzyme, reduces Hg^{II} to volatile Hg^0 using the reduced redox cofactor NAD(P)H as a source of reducing power [56].

Phylogenetic reconstructions suggest that *mer*-mediated Hg resistance originated in a thermophilic bacterial lineage at a time after the widespread oxygenation of the Earth [51,53]. This oxygenation event led to a major change in the redox state of photic environments. Consequently, the composition of environmental Hg species would have shifted from predominantly volatile Hg^0 and precipitated cinnabar (HgS), as found in anoxic geothermal settings [57], to more toxic and bioavailable oxidized Hg^{II} species [51]. Supporting this aerobic origin, the *mer* operon is predominantly found among modern-day obligate and facultative aerobes [51,53]. However, as there are always exceptions to the rule, *merA* genes have, in rarer instances, been found in facultative and strict anaerobes, including *Clostridium* spp., *Escherichia* spp., *Shewanella* spp., and certain members of the Desulfobacterota phylum [58–62]. Furthermore, there are a handful of reported cases of anaerobes capable of Hg^{II} reduction in the absence of *merA* [47,63–70]. Anaerobes thrive in anoxic conditions also inhabited by Hg methylators and thus may be key drivers of Hg^{II} reduction [63–65] and stand to exert influence on the formation of MeHg. However, these alternate pathways of Hg^{II} reduction are poorly characterized. Uncovering their mechanisms could also provide insights into the evolution of metal resistance strategies that predate the rise of oxygen.

1.2.3.2 Dissimilatory metal-reducing bacteria (anaerobic respiration)

One anaerobic Hg^{II} reduction pathway occurs in certain dissimilatory metal-reducing bacteria (DMRB). They are so named for their ability to use a variety of metals as terminal electron acceptors (e.g. Fe, U, Mn) when coupled to anaerobic respiration. The genus *Geobacter* contains members extensively studied for their environmental importance as Hg methylators [71], but some representatives can also mediate Hg^{II} reduction [69], Hg^0 oxidation, and MeHg degradation under

anoxic conditions; in the case of *Geobacter bemidjiensis*, all of these reactions can occur within the same strain [72]. The biochemical mechanism of anaerobic Hg^{II} reduction has been most thoroughly studied in *Geobacter sulfurreducens* PCA. This strain can reduce Hg^{II} in the absence of any electron acceptor suggesting that Hg^{II} is yet another metal it can use as a terminal electron acceptor for anaerobic respiration [70]. As a potential mechanism, it was proposed that outer membrane cytochromes could offload electrons onto extracellular Hg^{II}. This mechanism is substantiated by the role certain cytochromes already play in transferring electrons from the respiratory electron transport chain to extracellular metal acceptors [73,74]. A mutant strain of PCA deficient for 5 outer membrane c-type cytochromes had a 50% decrease in Hg^{II} reduction compared to the wild-type strain [70]. Another PCA mutant deficient in *hgcAB*, the Hg methylation genes, exhibited an increased ability to reduce Hg^{II} and, in turn, had a higher abundance of cytochromes [67]. Overall, these findings show that in *Geobacter,* cytochromes are, at least in part, involved in Hg^{II} reduction. It is interesting to note that here Hg^{II} reduction occurs in association and seemingly as a "by-product" of the activity of the electron transport chain (ETC). Perhaps certain anaerobic microorganisms may not have had to develop separate and dedicated Hg detoxification strategies because components of their ETC could already fulfill that function.

Shewanella oneidensis MR-1, another facultative anaerobe DMRB, can also reduce Hg^{II} via a non-*mer* mediated pathway [69]. Its mode of Hg^{II} reduction is currently undetermined but appears to be associated with components of the anaerobic ETC as providing different electron donors and acceptors influences the rate and extent of Hg^{II} reduction [69]. A recent study also showed that *S. oneidensis* MR-1 reduced more Hg^{II} in the presence of natural organic matter (NOM); authors suggested that NOM can mediate the transfer of electrons between *S. oneidensis* and Hg^{II}

[68]. Evidently, more work is required to determine how this strain of *Shewanella* can reduce Hg^{II} and if this mode of action is shared with other anaerobic Hg^{II} reducers.

1.2.3.3 Oxygenic phototrophs

In oxic environments, where sunlight energy is typically strongest, abiotic photoreduction of Hg^{II} is a major pathway for Hg^0 production. However, field evidence suggests that oxygenic phototrophs (i.e. photosynthetic microorganisms that produce oxygen) also mediate Hg^{II} reduction [44,75–78]. Laboratory studies have shown that live diatoms and algae could reduce Hg^{II} [76,79–83]. There is only one report of a MerA-like enzyme in an oxygenic phototroph: the cyanobacteria *Synechocystis* PCC6803 can reduce Hg^{II} and U via an enzymatic system made up of a glutaredoxin and a putative MerA [84]. Though most of these studies have yet to provide conclusive mechanistic details for this phenomenon, it is suggested that perhaps components of their photosynthetic machinery [85], produced reductive metabolites [80], or biogenic organic exudates are facilitating abiotic Hg^{II} photoreduction [83,86,87].

1.2.3.4 Purple non-sulphur bacteria (anoxygenic phototrophs)

Few studies have explored whether anoxygenic phototrophs (photosynthetic organisms that do not produce oxygen) could play a role in Hg redox cycling. These photosynthetic bacteria live in anoxic environments that can also be inhabited by Hg methylators. Thus, they are poised to influence the Hg substrate available to methylators. The first detailed account of Hg^{II} reduction by anoxygenic phototrophs was observed in purple non-sulphur bacteria (PNSB) by members of my laboratory, Gregoire and Poulain [64]. In this study, the authors tested whether three model PNSB strains could reduce Hg^{II} during photoheterotrophy (i.e. anoxygenic photosynthesis coupled with organic carbon assimilation). In PNSB, photoheterotrophic growth has been associated with an accumulation of reduced redox cofactors in the form of NADPH that prevents efficient enzymatic

turnover and causes redox imbalance. PNSB can restore redox homeostasis by shuttling this excess reducing power onto exogenous electron acceptors such as dimethyl sulfoxide (DMSO) [88,89]. Redox cofactors are responsible for transferring electrons between proteins and enzymes of fundamental cellular processes such as photosynthesis and carbon metabolism and include but are not limited to; flavin adenine dinucleotide (FAD), nicotinamide adenine dinucleotide (NADH), quinones, and ferredoxins. The ability or potential to reduce a substance using reduced redox cofactors is hereafter referred to as 'reducing power'. The study by Gregoire and Poulain demonstrated that Hg^{II} could fulfill a similar role to DMSO as an electron acceptor and that Hg^{II} reduction was highest under conditions of excess reducing power [64]. During photoheterotrophy, they also observed increased growth rates with increasing Hg^{II} concentrations, and when alternative electron sinks were provided (HCO_3^- or DMSO), Hg^0 production decreased. The authors suggest that the site of Hg^{II} reduction may be similar to that of HCO_3^- and DMSO, namely the ubiquinone pool, which is an intramembrane redox cofactor of the electron transport chain, or that NAD(P)H could potentially reduce Hg^{II} via the activity of certain oxidoreductases. Interactions between Hg^{II} and ubiquinones have been reported in phototrophs as a target of Hg^{II} toxicity, but Hg^0 production was never reported [90]. Further mechanistic insights are required to identify both the source of reducing power and the site of Hg^{II} reduction in PNSB.

1.2.3.5 Heliobacteria and Clostridia (anoxygenic phototrophs and fermenters)

To determine if other anoxygenic phototrophs possess a similar mechanism, I, alongside another student, investigated whether *Heliomicrobium modesticaldum* Ice1 (Heliobacteria) is capable of reducing Hg^{II}. Heliobacteria, part of the Bacillota phylum (previously Firmicutes), are terrestrial obligate anaerobes [91]. Many have been isolated from rice paddies and, in the case of *H. modesticaldum*, from hot springs [92]. They can grow via photoheterotrophy or fermentation in the

absence of light by using pyruvate as a carbon source [93] and we found that *H. modesticaldum* could reduce Hg^{II} during both metabolisms [63]. **Figure 1.2** serves to illustrate which metabolic pathways compose the central energy metabolism of *H. modesticaldum* Ice1. Our mechanistic insights into Hg^{II} reduction by Heliobacteria have revealed that it is non-*mer* mediated, occurs during both anoxygenic photoheterotrophic and fermentative growth, and is suspected to be tied to the intracellular availability of reduced redox cofactors such as ferredoxins [63]. Under dark fermentation conditions, pyruvate oxidation is required for Hg^{II} reduction to occur, whereas under phototrophic conditions, cells can reduce Hg^{II} when grown on pyruvate, acetate, and even in the absence of a carbon source. We further investigated the role of pyruvate metabolism on Hg^{II} reduction. Pyruvate:ferredoxin oxidoreductase (PFOR) is one of the key enzymes involved in heliobacterial carbon metabolism: it couples the oxidation of pyruvate into acetyl-CoA to the reduction of ferredoxin. The heliobacterial photosynthetic electron transport chain also reduces ferredoxins to shuttle electrons from the photosynthetic reaction center to other complexes in the chain. We exposed *H. modesticaldum* Ice1 to a chemical inhibitor for PFOR, nitazoxanide, and found that Hg^{II} reduction during fermentation but not phototrophy was eliminated by exposure to this chemical. We also tested Hg^{II} reduction and PFOR inhibition in another fermentative, non-phototrophic Bacillota, *Clostridium acetobutylicum*, and found this strain could reduce Hg^{II} and that PFOR inhibition blocked this ability. These findings led us to hypothesize that reducing power, or reduced redox cofactors, generated by carbon fermentation or photosynthetic electron transport fuels Hg^{II} reduction in *H. modesticaldum* and *C. acetobutylicum*. Although we have identified a source of electrons used in the reduction of Hg^{II} to gaseous Hg^{0}, more work remains to identify specific enzymatic coupling points where this redox transformation occurs.

1.3 THESIS RATIONALE AND CHOICE OF PRIMARY MODEL ORGANISM

Hg contamination is a pressing global environmental issue with significant implications for human health and ecosystems. The conversion of inorganic Hg^{II} to MeHg by microbial processes in low-oxygen environments poses a substantial risk due to MeHg's toxic properties and its ability to biomagnify in food webs. Despite ongoing efforts to mitigate Hg pollution, gaps remain in our understanding of the microbial mechanisms governing Hg transformations, particularly the reduction of Hg^{II} to elemental Hg^0 by anaerobic microorganisms. The role these anaerobes play in Hg cycling is important to address as they occupy similar niches as Hg methylators. They are poised to compete for common nutrients like nitrogen and sulphur and for metals like Hg, thus influencing the formation of toxic Hg species and their environmental fate. *Heliomicrobium modesticaldum* Ice1, an anoxygenic phototroph, is a unique model organism for studying these processes due to its exceptional Hg^{II}-reducing capabilities [63]. The recent development of a CRISPR-based gene editing approach tailored to *H. modesticaldum* Ice1 is timely and pivotal for advancing our understanding of the mechanism catalyzing the reduction of Hg^{II} [94–97]. This innovative technique allows for precise gene deletions, enabling detailed physiological investigations that were previously not possible.

1.4 THESIS STRUCTURE AND OBJECTIVES

The goal of this thesis is to uncover physiological and environmental controls on anaerobic non-*mer* mediated Hg^{II} reduction. Each chapter of this thesis addresses one or more of the following three objectives:

1. To determine how nutrient availabilities and their associated metabolisms affect Hg^{II} reduction (**Chapters 2 and 3**)

2. To investigate genetic determinants and physiological controls involved in Hg^{II} reduction (**Chapters 4 and 5**)
3. To explore the possibility of anaerobic Hg^{II} reduction by other anoxygenic phototrophs (**Chapters 2 and 6**)

In **Chapter 2**, I investigated whether another representative of the Heliobacteria family could reduce Hg^{II} and the influence of sulphur assimilation pathways on phototrophic Hg^{II} reduction. I worked with *Heliobacillus mobilis,* a strain found in rice paddies, common hotspots of Hg contamination [15], that grows using a variety of sulphur sources [98]. I chose to focus on sulphur as it is both a ligand that can control the bioavailability of Hg in anoxic environments and is an essential nutrient to the Hg-methylating sulphate-reducing bacteria (SRB) [99]. I hypothesized that anaerobic Hg^{II} reduction depends on intracellular reducing power availability, and in turn, that assimilatory cellular pathways that draw upon reducing power can affect the amount of Hg^{II} reduced. I tested whether oxidized sulphur sources, requiring more reducing power to assimilate into biomass, would decrease the magnitude of Hg^{II} reduced compared to reduced sulphur sources.

In **Chapter 3,** I investigated whether other nutrients and their metabolism, specifically nitrogen, affect anaerobic Hg^{II} reduction. In this study, I chose to work with *H. modesticaldum* Ice1 for its well-characterized nitrogen metabolism. Heliobacteria, in the absence of bioavailable nitrogen sources, can fix $N_{2(g)}$ via nitrogenase enzyme activity. However, N_2 fixation into NH_3 requires significant inputs of reducing power. Similar to, my work in Chapter 2, I predicted that nitrogen sources that require more reducing power to be assimilated would decrease the magnitude of Hg^{II} reduced by *H. modesticaldum*.

In **Chapter 4,** I explored potential genetic determinants of anaerobic Hg^{II} reduction. The timely advent of a gene-editing technique tailored to *H. modesticaldum* and a collaboration with its

creators allowed us to test the involvement of certain genes in Hg^{II} reduction by *H. modesticaldum.* In this study, I tested seven gene-deletion mutants deficient for various genes involved in core metabolism and redox processes for their ability to reduce Hg^{II} under phototrophic and fermentative conditions.

My objective for **Chapter 5,** building upon the findings of previous chapters, was to provide further physiological insights into Hg^{II} reduction by *H. modesticaldum* using a chemical inhibitor approach. In this study, I tested the hypothesis that reduction depends on Hg^{II} interactions with cellular thiols. I tested Hg^{II} reduction during phototrophy and fermentation under a range of concentrations of the thiol-alkylating agent N-ethylmaleimide.

In my final data chapter, **Chapter 6**, I departed from studies with Heliobacteria to further explore the diversity of anoxygenic phototrophs that can catalyze the reduction of Hg^{II} to its elemental form. I tested whether the thermophilic filamentous anoxygenic phototroph, *Chloroflexus aurantiacus* J-10-fl, could reduce Hg^{II} under various metabolic conditions and carbon sources previously shown to support anaerobic Hg^{II} reducers.

I conclude this thesis in **Chapter 7** with a synthesis of my contributions to the field of mercury microbiology and recommendations for future avenues of research investigating this cryptic anaerobic Hg^{II} reduction pathway.

1.5 REFERENCES:

1. Obrist, D. *et al.* A review of global environmental mercury processes in response to human and natural perturbations: Changes of emissions, climate, and land use. *Ambio* **47**, 116–140 (2018).
2. Sonke, J. E. *et al.* Global change effects on biogeochemical mercury cycling. *Ambio* **52**, 853–876 (2023).
3. Ariya, P. A. *et al.* Mercury physicochemical and biogeochemical transformation in the atmosphere and at atmospheric interfaces: a review and future directions. *Chem Rev* **115**, 3760–802 (2015).
4. Streets, D. G. *et al.* Five hundred years of anthropogenic mercury: spatial and temporal release profiles. *Environ. Res. Lett.* **14**, 084004 (2019).
5. Selin, N. E. Global Biogeochemical Cycling of Mercury: A Review. *Annual Review of Environment and Resources* **34**, 43–63 (2009).
6. Rooney, J. P. The role of thiols, dithiols, nutritional factors and interacting ligands in the toxicology of mercury. *Toxicology* **234**, 145–56 (2007).
7. Antunes Dos Santos, A. *et al.* Methylmercury and brain development: A review of recent literature. *J Trace Elem Med Biol* **38**, 99–107 (2016).
8. Roman, H. A. *et al.* Evaluation of the Cardiovascular Effects of Methylmercury Exposures: Current Evidence Supports Development of a Dose–Response Function for Regulatory Benefits Analysis. *Environmental Health Perspectives* **119**, 607–614 (2011).
9. Zhang, Y. *et al.* Global health effects of future atmospheric mercury emissions. *Nat Commun* **12**, 3035 (2021).
10. Sunderland, E. M. Mercury exposure from domestic and imported estuarine and marine fish in the U.S. seafood market. *Environ Health Perspect* **115**, 235–42 (2007).
11. Pouilly, M. *et al.* Trophic Structure and Mercury Biomagnification in Tropical Fish Assemblages, Iténez River, Bolivia. *PLoS ONE* **8**, (2013).
12. Morel, F. M. M., Kraepiel, A. M. L. & Amyot, M. The Chemical Cycle and Bioaccumulation of Mercury. *Annual Review of Ecology and Systematics* **29**, 543–566 (1998).
13. Paterson, M. J. *et al.* Bioaccumulation of newly deposited mercury by fish and invertebrates: An enclosure study using stable mercury isotopes. *Can. J. Fish. Aquatic Sci.* **63**, 2213–2224 (2006).
14. Zhang, H., Feng, X., Larssen, T., Qiu, G. & Vogt, R. D. In inland China, rice, rather than fish, is the major pathway for methylmercury exposure. *Environ Health Perspect* **118**, 1183–8 (2010).
15. Rothenberg, S. E., Windham-Myers, L. & Creswell, J. E. Rice methylmercury exposure and mitigation: a comprehensive review. *Environ Res* **133**, 407–23 (2014).

16. UNEP. Minamata Convention on Mercury: Text and Annexes. *UNEP Chemicals Branch* 1–67 (2017).

17. UNEP. Global Mercury Assessment 2018. *UN Environment Programme, Chemicals and Health Branch* 1–62 (2019).

18. Choi, S. C., Chase Jr, T. & Bartha, R. Metabolic pathways leading to mercury methylation in Desulfovibrio desulfuricans LS. *Applied and Environmental Microbiology* **60**, 4072–4077 (//).

19. Fleming, E. J., Mack, E. E., Green, P. G. & Nelson, D. C. Mercury methylation from unexpected sources: molybdate-inhibited freshwater sediments and an iron-reducing bacterium. *Appl Environ Microbiol* **72**, 457–64 (2006).

20. Han, S. *et al.* Mercury speciation in marine sediments under sulfate-limited conditions. *Environ Sci Technol* **44**, 3752–7 (2010).

21. Gilmour, C. C. *et al.* Mercury methylation by novel microorganisms from new environments. *Environ Sci Technol* **47**, 11810–20 (2013).

22. Compeau, G. C. & Bartha, R. Sulfate-Reducing Bacteria: Principal Methylators of Mercury in Anoxic Estuarine Sediment. *Applied and Environmental Microbiology* **50**, 498–502 (1985).

23. Hamelin, S., Amyot, M., Barkay, T., Wang, Y. & Planas, D. Methanogens: Principal methylators of mercury in lake periphyton. *Environ. Sci. Technol.* **45**, 7693–7700 (2011).

24. Podar, M. *et al.* Global prevalence and distribution of genes and microorganisms involved in mercury methylation. *Sci Adv* **1**, e1500675 (2015).

25. Christensen, G. A. *et al.* Development and Validation of Broad-Range Qualitative and Clade-Specific Quantitative Molecular Probes for Assessing Mercury Methylation in the Environment. *Appl Environ Microbiol* **82**, 6068–78 (2016).

26. Yu, R. Q., Reinfelder, J. R., Hines, M. E. & Barkay, T. Syntrophic pathways for microbial mercury methylation. *ISME J* **12**, 1826–1835 (2018).

27. Hu, H. *et al.* Shifts in mercury methylation across a peatland chronosequence: From sulfate reduction to methanogenesis and syntrophy. *Journal of Hazardous Materials* **387**, 121967 (2020).

28. Parks, J. M. *et al.* The genetic basis for bacterial mercury methylation. *Science* **339**, 1332–5 (2013).

29. Date, S. S. *et al.* Kinetics of Enzymatic Mercury Methylation at Nanomolar Concentrations Catalyzed by HgcAB. *Applied and Environmental Microbiology* **85**, e00438-19 (2019).

30. Smith, S. D. *et al.* Site-Directed Mutagenesis of HgcA and HgcB Reveals Amino Acid Residues Important for Mercury Methylation. *Applied and Environmental Microbiology* **81**, 3205–3217 (2015).

31. Cooper, C. J. *et al.* Structure determination of the HgcAB complex using metagenome sequence data: insights into microbial mercury methylation. *Communications Biology* **3**, (2020).

32. Barkay, T. & Wagner-Döbler, I. Microbial Transformations of Mercury: Potentials, Challenges, and Achievements in Controlling Mercury Toxicity in the Environment. in *Advances in Applied Microbiology Volume 57* 1–52 (2005). doi:10.1016/s0065-2164(05)57001-1.

33. Gilmour, C. C. *et al.* Sulfate-reducing bacterium Desulfovibrio desulfuricans ND132 as a model for understanding bacterial mercury methylation. *Appl. Environ. Microbiol.* **77**, 3938–3951 (2011).

34. Qian, C. *et al.* Quantitative Proteomic Analysis of Biological Processes and Responses of the Bacterium Desulfovibrio desulfuricans ND132 upon Deletion of Its Mercury Methylation Genes. *PROTEOMICS* **18**, 1700479 (2018).

35. Hu, H. Y. *et al.* Oxidation and methylation of dissolved elemental mercury by anaerobic bacteria. *Nat Geosci* **6**, 751–754 (2013).

36. Grégoire, D. S. & Poulain, A. J. Shining light on recent advances in microbial mercury cycling. *Facets* **3**, 858–879 (2018).

37. Saouter, E., Gillman, M. & Barkay, T. An evaluation of mer-specified reduction of ionic mercury as a remedial tool of a mercury-contaminated freshwater pond. *Journal of Industrial Microbiology* **14**, 343–348 (1995).

38. Toribara, T. Y., Shields, C. P. & Koval, L. Behaviour of dilute solutions of mercury. *Talanta* **17**, 1025–1028 (1970).

39. Colombo, M. J., Ha, J. Y., Reinfelder, J. R., Barkay, T. & Yee, N. Anaerobic oxidation of Hg(0) and methylmercury formation by Desulfovibrio desulfuricans ND132. *Geochim Cosmochim Ac* **112**, 166–177 (2013).

40. Amyot, M., Mierle, G., Lean, D. R. S. & Mcqueen, D. J. Sunlight-Induced Formation of Dissolved Gaseous Mercury in Lake Waters. *Environ Sci Technol* **28**, 2366–2371 (1994).

41. O'Driscoll, N. J., Siciliano, S. D., Lean, D. R. & Amyot, M. Gross photoreduction kinetics of mercury in temperate freshwater lakes and rivers: application to a general model of DGM dynamics. *Environ Sci Technol* **40**, 837–43 (2006).

42. O'Driscoll, N. J. *et al.* Mercury photoreduction and photooxidation in lakes: Effects of filtration and dissolved organic carbon concentration. *J Environ Sci (China)* **68**, 151–159 (2018).

43. Nriagu, J. O. Mechanistic steps in the photoreduction of mercury in natural waters. *Science of The Total Environment* **154**, 1–8 (1994).

44. Poulain, A. J. *et al.* Biological and photochemical production of dissolved gaseous mercury in a boreal lake. *Limnol Oceanogr* **49**, 2265–2275 (2004).

45. O'Loughlin, E. J., Kelly, S. D., Kemner, K. M., Csencsits, R. & Cook, R. E. Reduction of AgI, AuIII, CuII, and HgII by FeII/FeIII hydroxysulfate green rust. *Chemosphere* **53**, 437–446 (2003).

46. Wiatrowski, H. A. *et al.* Reduction of Hg(II) to Hg(0) by magnetite. *Environ Sci Technol* **43**, 5307–13 (2009).

47. Liu, S. N. & Wiatrowski, H. A. Reduction of Hg(II) to Hg(0) by Biogenic Magnetite from two Magnetotactic Bacteria. *Geomicrobiol J* **35**, 198–208 (2018).

48. Allard, B. & Arsenie, I. Abiotic reduction of mercury by humic substances in aquatic system — an important process for the mercury cycle. *Water Air & Soil Pollution* **56**, 457–464 (1991).

49. Gu, B. *et al.* Mercury reduction and complexation by natural organic matter in anoxic environments. *Proc Natl Acad Sci U S A* **108**, 1479–83 (2011).

50. T. Barkay & B. Gu. Demethylation—The Other Side of the Mercury Methylation Coin: A Critical Review. *ACS Environmental Au* (2021) doi:10.1021/acsenvironau.1c00022.s001.

51. Barkay, T., Kritee, K., Boyd, E. & Geesey, G. A thermophilic bacterial origin and subsequent constraints by redox, light and salinity on the evolution of the microbial mercuric reductase. *Environ Microbiol* **12**, 2904–17 (2010).

52. Barkay, T., Miller, S. M. & Summers, A. O. Bacterial mercury resistance from atoms to ecosystems. *FEMS Microbiol Rev* **27**, 355–84 (2003).

53. Boyd, E. S. & Barkay, T. The mercury resistance operon: from an origin in a geothermal environment to an efficient detoxification machine. *Front Microbiol* **3**, 349 (2012).

54. Summers, A. O. & Sugarman, L. I. Cell-free mercury(II)-reducing activity in a plasmid-bearing strain of Escherichia coli. *J Bacteriol* **119**, 242–9 (1974).

55. Summers, A. O. Organization, expression, and evolution of genes for mercury resistance. *Annu Rev Microbiol* **40**, 607–34 (1986).

56. Furukawa, K. & Tonomura, K. Metallic Mercury-releasing Enzyme in Mercury-resistantPseudomonas. *Agricultural and Biological Chemistry* **36**, 217–226 (1972).

57. Varekamp, J. C. & Buseck, P. R. The speciation of mercury in hydrothermal systems, with applications to ore deposition. *Geochimica et Cosmochimica Acta* **48**, 177–185 (1984).

58. Christakis, C. A., Barkay, T. & Boyd, E. S. Expanded Diversity and Phylogeny of mer Genes Broadens Mercury Resistance Paradigms and Reveals an Origin for MerA Among Thermophilic Archaea. *Front. Microbiol.* **12**, (2021).

59. Dash, H. R., Sahu, M., Mallick, B. & Das, S. Functional efficiency of MerA protein among diverse mercury resistant bacteria for efficient use in bioremediation of inorganic mercury. *Biochimie* **142**, 207–215 (2017).

60. Vigneron, A., Cruaud, P., Aubé, J., Guyoneaud, R. & Goñi-Urriza, M. Transcriptomic evidence for versatile metabolic activities of mercury cycling microorganisms in brackish microbial mats. *npj Biofilms and Microbiomes* **7**, (2021).

61. Narita, M., Huang, C.-C., Koizumi, T. & Endo, G. Molecular Analysis of merA Gene Possessed by Anaerobic Mercury-Resistant Bacteria Isolated from Sediment of Minamata Bay. *Microbes and environments* **14**, 77–84 (1999).

62. Ní Chadhain, S. M., Schaefer, J. K., Crane, S., Zylstra, G. J. & Barkay, T. Analysis of mercuric reductase (merA) gene diversity in an anaerobic mercury-contaminated sediment enrichment. *Environmental Microbiology* **8**, 1746–1752 (2006).

63. Gregoire, D. S., Lavoie, N. C. & Poulain, A. J. Heliobacteria Reveal Fermentation As a Key Pathway for Mercury Reduction in Anoxic Environments. *Environ Sci Technol* **52**, 4145–4153 (2018).

64. Grégoire, D. S. & Poulain, A. J. A physiological role for HgII during phototrophic growth. *Nature Geoscience* **9**, 121–125 (2016).

65. Lavoie, N. C., Gregoire, D. S., Stenzler, B. R. & Poulain, A. J. Reduced sulphur sources favour Hg(II) reduction during anoxygenic photosynthesis by Heliobacteria. *Geobiology* (2019) doi:10.1111/gbi.12364.

66. Lin, H. *et al.* Unexpected Effects of Gene Deletion on Interactions of Mercury with the Methylation-Deficient Mutant ΔhgcAB. *Environmental Science & Technology Letters* **1**, 271–276 (2014).

67. Qian, C. *et al.* Global Proteome Response to Deletion of Genes Related to Mercury Methylation and Dissimilatory Metal Reduction Reveals Changes in Respiratory Metabolism in Geobacter sulfurreducens PCA. *J Proteome Res* **15**, 3540–3549 (2016).

68. Lee, S., Kim, D. H. & Kim, K. W. The enhancement and inhibition of mercury reduction by natural organic matter in the presence of Shewanella oneidensis MR-1. *Chemosphere* **194**, 515–522 (2018).

69. Wiatrowski, H. A., Ward, P. M. & Barkay, T. Novel reduction of mercury (II) by mercury-sensitive dissimilatory metal reducing bacteria. *Environ Sci Technol* **40**, 6690–6 (2006).

70. Hu, H. *et al.* Mercury reduction and cell-surface adsorption by Geobacter sulfurreducens PCA. *Environ Sci Technol* **47**, 10922–30 (2013).

71. Kerin, E. J. *et al.* Mercury methylation by dissimilatory iron-reducing bacteria. *Applied and Environmental Microbiology* **72**, 7919–7921 (2006).

72. Lu, X. *et al.* Anaerobic Mercury Methylation and Demethylation by Geobacter bemidjiensis Bem. *Environ Sci Technol* **50**, 4366–73 (2016).

73. Mehta, T., Coppi, M. V., Childers, S. E. & Lovley, D. R. Outer membrane c-type cytochromes required for Fe(III) and Mn(IV) oxide reduction in Geobacter sulfurreducens. *Appl Environ Microbiol* **71**, 8634–8641 (2005).

74. Estevez-Canales, M. *et al.* A severe reduction in the cytochrome C content of Geobacter sulfurreducens eliminates its capacity for extracellular electron transfer. *Environ Microbiol Rep* **7**, 219–226 (2015).

75. Amyot, M., Mierle, G., Lean, D. & McQueen, D. J. Effect of solar radiation on the formation of dissolved gaseous mercury in temperate lakes. *Geochimica et Cosmochimica Acta* **61**, 975–987 (1997).

76. Mason, R. P., Morel, F. M. M. & Hemond, H. F. The role of microorganisms in elemental mercury formation in natural waters. *Water, Air, & Soil Pollution* **80**, 775–787 (1995).

77. Zivkovic, I. *et al.* Relations between mercury fractions and microbial community components in seawater under the presence and absence of probable phosphorus limitation conditions. *J Environ Sci (China)* **75**, 145–162 (2019).

78. Vandal, G. M., Fitzgerald, W. F., Rolfhus, K. R. & Lamborg, C. H. Modeling the elemental mercury cycle in Pallette Lake, Wisconsin, USA. *Water, Air, & Soil Pollution* **80**, 529–538 (1995).

79. Ben-Bassat, D. & Mayer, A. M. Volatilization of Mercury by Algae. *Physiologia Plantarum* **33**, 128–132 (1975).

80. Ben-Bassat, D. & Mayer, A. M. Reduction of Mercury Chloride by Chlorella: Evidence for a Reducing Factor. *Physiologia Plantarum* **40**, 157–162 (1977).

81. Ben-Bassat, D., Shelef, G., Gruner, N. & Shuval, H. I. Growth of Chlamydomonas in a medium containing mercury. *Nature* **240**, 43–4 (1972).

82. Morelli, E. *et al.* Changes in the non-protein thiol pool and production of dissolved gaseous mercury in the marine diatom Thalassiosira weissflogii under mercury exposure. *Sci Total Environ* **408**, 286–93 (2009).

83. Liang, X. *et al.* Mercury Reduction, Uptake, and Species Transformation by Freshwater Alga Chlorella vulgaris under Sunlit and Dark Conditions. *Environmental Science & Technology* **56**, 4961–4969 (2022).

84. Marteyn, B. *et al.* The Synechocystis PCC6803 MerA-like enzyme operates in the reduction of both mercury and uranium under the control of the glutaredoxin 1 enzyme. *J Bacteriol* **195**, 4138–45 (2013).

85. Grégoire, D. S. & Poulain, A. J. A little bit of light goes a long way: the role of phototrophs on mercury cycling. *Metallomics* **6**, 396–407 (2014).

86. Lanzillotta, E. *et al.* Importance of the biogenic organic matter in photo-formation of dissolved gaseous mercury in a culture of the marine diatom Chaetoceros sp. *Science of The Total Environment* **318**, 211–221 (2004).

87. Deng, L., Deng, N., Mou, L. & Zhu, F. Photo-induced transformations of Hg(II) species in the presence of Nitzschia hantzschiana, ferric ion, and humic acid. *Journal of Environmental Sciences* **22**, 76–83 (2010).

88. McKinlay, J. B. & Harwood, C. S. Carbon dioxide fixation as a central redox cofactor recycling mechanism in bacteria. *Proceedings of the National Academy of Sciences* **107**, 11669–11675 (2010).

89. Richardson *et al.* The role of auxiliary oxidants in maintaining redox balance during phototrophic growth of Rhodobacter capsulatus on propionate or butyrate. *Archives of Microbiology* **150**, 131–137 (1988).

90. Asztalos, E., Sipka, G., Kis, M., Trotta, M. & Maroti, P. The reaction center is the sensitive target of the mercury(II) ion in intact cells of photosynthetic bacteria. *Photosynth Res* **112**, 129–40 (2012).

91. Amesz, J. The Heliobacteria, a New Group of Photosynthetic Bacteria. *J Photoch Photobio B* **30**, 89–96 (1995).

92. Asao, M. & Madigan, M. T. Taxonomy, phylogeny, and ecology of the heliobacteria. *Photosynth Res* **104**, 103–111 (2010).

93. Kimble, L. K., Mandelco, L., Woese, C. R. & Madigan, M. T. Heliobacterium modesticaldum, sp. nov., a thermophilic heliobacterium of hot springs and volcanic soils. *Archives of Microbiology* **163**, 259–267 (1995).

94. Baker, P. L. *et al.* Using the endogenous CRISPR-Cas system of Heliobacterium modesticaldum to delete the photochemical reaction center core subunit gene. *Appl Environ Microbiol* (2019) doi:10.1128/AEM.01644-19.

95. Baker, P. L. *et al.* A molecular biology toolkit for the phototrophic Firmicute, Heliobacterium modesticaldum. *Appl Environ Microbiol* (2019) doi:10.1128/AEM.01287-19.

96. Orf, G. S. & Redding, K. E. Expression and purification of affinity-tagged variants of the photochemical reaction center from Heliobacterium modesticaldum. *Photosynth Res* (2019) doi:10.1007/s11120-019-00672-3.

97. Layton, A. M. & Redding, K. E. Examination of Genetic Control Elements in the Phototrophic Firmicute Heliomicrobium modesticaldum. *Microorganisms* **10**, 876 (2022).

98. Beer-Romero, P. & Gest, H. Heliobacillus mobilis, a peritrichously flagellated anoxyphototroph containing bacteriochlorophyllg. *FEMS Microbiology Letters* **41**, 109–114 (1987).

99. Jeremiason, J. D. *et al.* Sulfate addition increases methylmercury production in an experimental wetland. *Environ Sci Technol* **40**, 3800–6 (2006).

1.6 FIGURES:

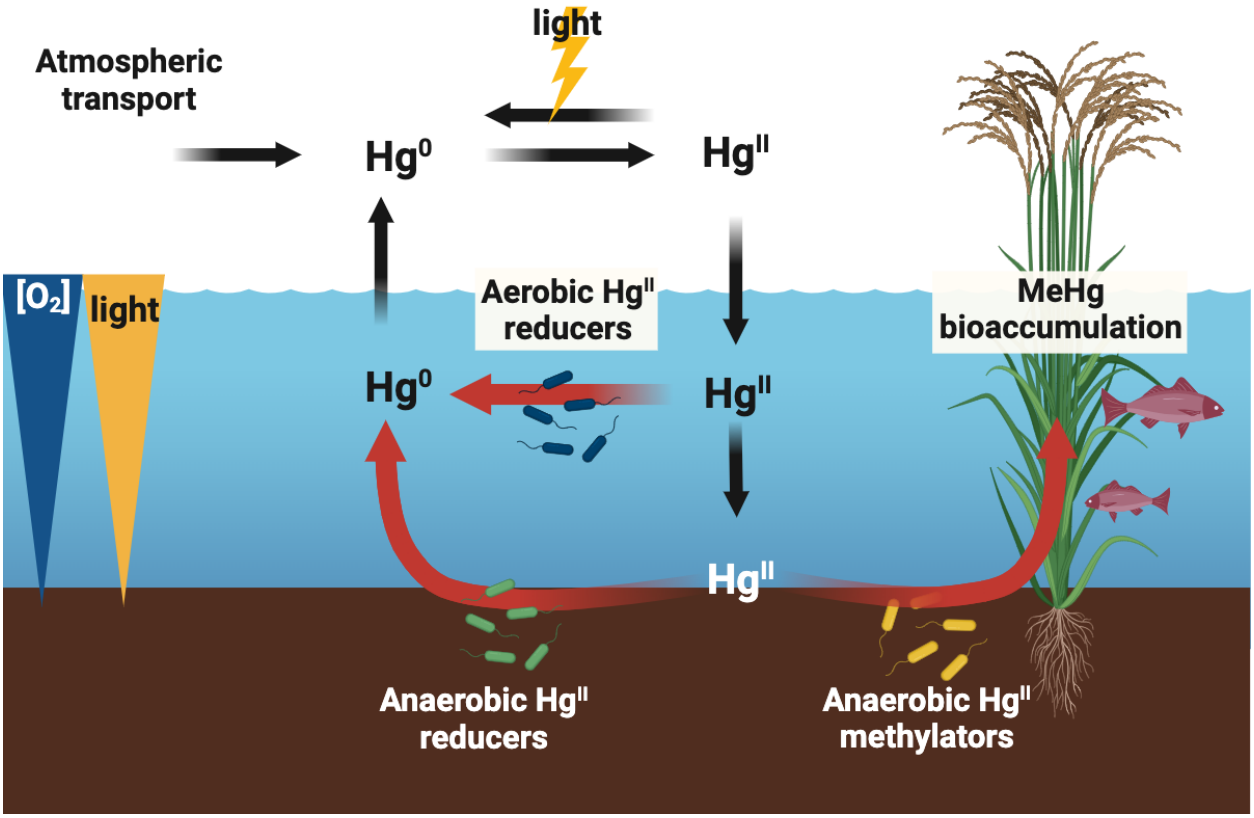

Figure 1.1: Conceptual summary of Hg transport and microbe-mediated transformations in the environment.
Three primary microbial pathways are represented with red arrows: aerobic Hg reduction via the mercuric reductase, anaerobic Hg methylation via *hgcAB*, and anaerobic Hg reduction which has no known genetic determinant. Arrows in black represent abiotic pathways of Hg transformation and transport.

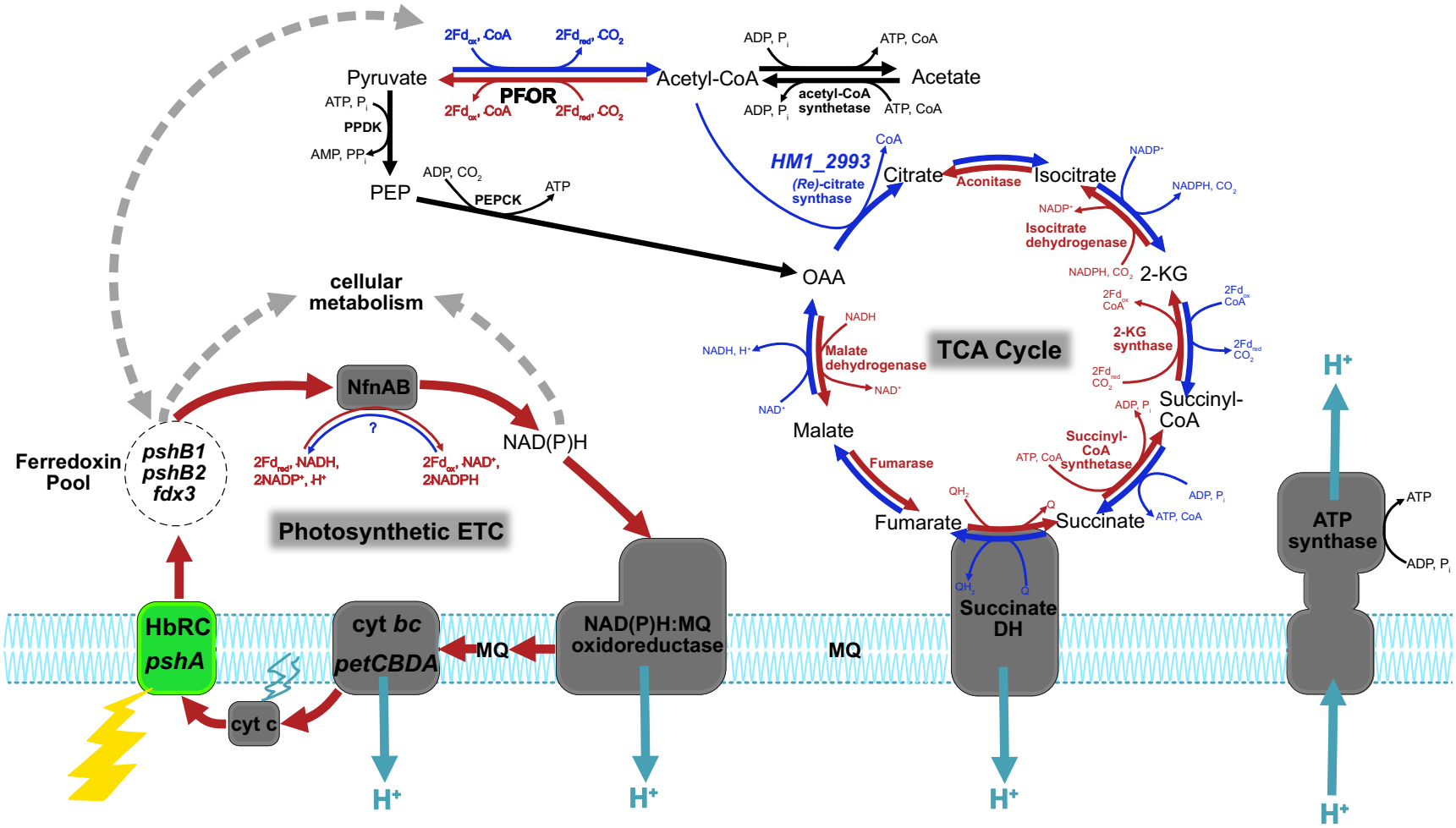
Pyruvate
PFOR
Acetyl-CoA
Acetate
acetyl-CoA synthetase
PPDK
PEP
PEPCK
OAA
HM1_2993
(Re)-citrate synthase
Citrate
Aconitase
Isocitrate
Isocitrate dehydrogenase
2-KG
2-KG synthase
Succinyl-CoA
Succinyl-CoA synthetase
Succinate
Fumarase
Fumarate
Malate
Malate dehydrogenase
TCA Cycle
cellular metabolism
NfnAB
NAD(P)H
Ferredoxin Pool
pshB1
pshB2
fdx3
Photosynthetic ETC
HbRC
pshA
cyt bc
petCBDA
cyt c
MQ
NAD(P)H:MQ oxidoreductase
Succinate DH
ATP synthase
H+

Figure 1.2: Central metabolic pathways in *H. modesticaldum* Ice1.
Heliobacterial reaction center = HbRC *pshA*; ferredoxin-encoding genes = *pshB1, pshB2,* and *fdx3;* cytochrome *bc* genes = *petCBDA*; and (*Re*)-citrate synthase encoding gene = HM1_2993. Arrows in red and blue are for enzymatic reactions operating in the reductive and oxidative directions, respectively. Pale blue arrows represent transmembrane proton movements. Non-redox enzymatic reactions are indicated with black arrows. Grey dashed arrows represent other destinations for the redox cofactors NAD(P)H and the ferredoxin pool. Abbreviations: Fd_{ox} = oxidized ferredoxin, Fd_{red} = reduced ferredoxin, HbRC = Heliobacterial photosynthetic reaction center, NfnAB = NADH-dependent ferredoxin:$NADP^+$ oxidoreductase, cyt *bc* = cytochrome *bc*, cyt c = cytochrome c_{553}, PPDK = pyruvate phosphate dikinase, PEPCK = phosphoenolpyruvate carboxykinase, PEP = phosphoenolpyruvate, OAA = oxaloacetate, 2-KG = 2-ketoglutarate, MQ = menaquinone, QH_2 = ubiquinol, Q = ubiquinone, Succinate DH = succinate dehydrogenase.

Chapter 2

Reduced sulphur sources favour Hg(II) reduction during anoxygenic photosynthesis by Heliobacteria

Noémie C. Lavoie [a], Daniel S. Grégoire [a], Benjamin R. Stenzler [a], Alexandre J. Poulain [a]

a - Biology Department, University of Ottawa, 30 Marie Curie, Ottawa, ON, K1N 6N5, Canada.

A modified version of this chapter was originally published as: **Lavoie, N.C**., Grégoire, D.S., Stenzler, B.R., Poulain, A.J., Reduced sulphur sources favour HgII reduction during anoxygenic photosynthesis by Heliobacteria. *Geobiology* **2020**, 18(1):70-79.

Direct link : https://onlinelibrary.wiley.com/doi/10.1111/gbi.12364

N.B. Supporting information for this chapter can be found in **Appendix A**

2.1 ABSTRACT

The consumption of rice has become a global food safety issue because rice paddies support the production of high levels of the potent neurotoxin, methylmercury. The production of methylmercury is carried out by chemotrophic anaerobes that rely on a diversity of terminal electron acceptors, namely sulphate. Sulphur can be a limiting nutrient in rice paddies and sulphate amendments are often used to stimulate crop production, which can increase methylmercury production. Mercury (Hg) redox cycling can affect Hg methylation by controlling the delivery of inorganic Hg substrates to methylators in anoxic habitats. Whereas sulphur is recognized as a key substrate controlling methylmercury production, the controls sulphur exerts on other microbe-mediated mercury transformations remain poorly understood. To explore the potential coupling between sulphur assimilation and anaerobic Hg^{II} reduction to Hg^0, we studied *Heliobacillus mobilis*, a mesophilic anoxygenic phototroph representative from the *Heliobacteriacea* family originally isolated from a rice paddy. Here, we tested whether the redox state of the sulphur sources available to *H. mobilis* would affect its ability to reduce Hg^{II}. By comparing Hg^0 production over a redox gradient of sulphur sources, we demonstrate that phototrophic Hg^{II} reduction is favoured in the presence of reduced sulphur sources such as thiosulphate and cysteine. We also show that cysteine exerts dynamic control on Hg cycling by affecting not only Hg bioavailability but also its abiotic photoreduction under low light conditions. Specifically, in the absence of cells we show that organic matter (as yeast extract) and cysteine are both required for photoreduction to occur. This study offers insights into how one of the most primitive forms of photosynthesis affects Hg redox transformations and frame Heliobacteria as key players in Hg cycling within paddy soils, forming a basis for management strategies to mitigate Hg accumulation in rice.

2.2 INTRODUCTION

Mercury (Hg) is a global contaminant that readily bioaccumulates in plant (Zhang, Feng, Larssen et al., 2010) and animal tissue (Sunderland, 2007) as neurotoxic methylmercury (MeHg). Rice paddies are frequently flooded and rich with nutrients that stimulate the anaerobic microbes responsible for Hg methylation (Rothenberg & Feng, 2012). The consumption of this contaminated rice has been identified as a route for Hg exposure in people (Zhang, Feng, Larssen et al., 2010, Rothenberg, Windham-Myers & Creswell, 2014). With rice being a staple food crop for over half of the world's population, MeHg accumulation in rice is becoming a global food safety issue (Rothenberg, Windham-Myers & Creswell, 2014).

In flooded anoxic rice paddies, Hg redox cycling can play a key role in determining the inorganic Hg available to Hg-methylators and MeHg that accumulates in the rice. Hg^{II} reduction can lead to Hg^0 evasion from the paddy soils (Kim, Kim, Kim et al., 2003, Wang, Lin, Yuan et al., 2016, Ao, Meng, Sapkota et al., 2017) and potentially affect its bioavailability to methylators (Colombo, Ha, Reinfelder et al., 2014). Hg^{II} reduction can occur through abiotic reactions with dissolved organic matter (Gu, Bian, Miller et al., 2011), iron-bearing minerals (Wiatrowski, Das, Kukkadapu et al., 2009, Bone, Bargar & Sposito, 2014), and by certain strains of anaerobic microbes (Schaefer, Letowski & Barkay, 2002, Wiatrowski, Ward & Barkay, 2006, Lin, Morrell-Falvey, Rao et al., 2014, Grégoire & Poulain, 2016, Lu, Liu, Johs et al., 2016, Zhao, Chen, Lu et al., 2017, Grégoire, Lavoie & Poulain, 2018, Liu & Wiatrowski, 2018).

Microbe-mediated Hg redox transformations that rely on dedicated detoxification strategies, such as those encoded by the *mer* operon, are largely absent in anaerobes (Barkay, Kritee, Boyd et al., 2010). Rather, anaerobic Hg^{II} reduction appears to be driven by core components of anaerobic respiration (Lin, Morrell-Falvey, Rao et al., 2014), fermentation

(Grégoire, Lavoie & Poulain, 2018), and anoxygenic photosynthesis (Grégoire & Poulain, 2016). Despite the evidence linking central metabolism to anaerobic Hg^{II} reduction, the contributions of anaerobes to Hg reduction in anoxic habitats remain largely overlooked.

Much of the evidence published to date suggests that Hg methylation is a cometabolic process linked to one-carbon compound metabolism (Choi, Chase & Bartha, 1994, Qian, Johs, Chen et al., 2016) in multiple clades of anaerobes (Parks, Johs, Podar et al., 2013, Podar, Gilmour, Brandt et al., 2015, Gionfriddo, Tate, Wick et al., 2016). However, the role that common pools of nutrients (e.g., C, N or S) play in controlling different cometabolic Hg transformations is rarely discussed. This is an important knowledge gap to address because anaerobic Hg^{II} reducers and Hg methylators occupy the same niche in the environment (Desrochers, Paulson, Ptacek et al., 2015) and likely compete for a common pool of Hg substrates and nutrients supporting anaerobic metabolisms. For instance, in rice paddies, sulphur can become a limiting nutrient and sulphate amendments are employed to maintain agricultural productivity (Blair & Lefroy, 1998). Such amendments would supply sulphate-reducing bacteria (SRB) that often dominate Hg methylation communities (Su, Chang, Hsi et al., 2016, Ma, Du, Wang et al., 2017, Vishnivetskaya, Hu, Van Nostrand et al., 2018) with ample substrates for anaerobic respiration, which can subsequently increase MeHg production (Jeremiason, Engstrom, Swain et al., 2006, Yu, Reinfelder, Hines et al., 2018). Reduced sulphur-bearing molecules such as sulphide (Pham, Morris, Zhang et al., 2014, Ticknor, Kucharzyk, Porter et al., 2015) and cysteine (Schaefer & Morel, 2009, Lin, Lu, Liang et al., 2015), generated by sulphur metabolism can also act as ligands affecting Hg bioavailability to Hg methylators.

In this study we used anoxygenic photosynthesis as a metabolic basis to explore coupling points between sulphur metabolism and anaerobic Hg^{II} reduction. Anoxygenic phototrophs such

as purple and green sulphur bacteria play key roles in the sulphur cycle of anoxic habitats by coupling sulphur oxidation to autotrophic growth (Zerkle, Kamyshny, Kump et al., 2010). Similarly, a wide diversity of anoxygenic phototrophs including purple non sulphur bacteria (PNSB) and Heliobacteria can influence sulphur cycling via assimilatory sulphur reduction pathways (Frigaard & Dahl, 2009). To date, no published study has delved into Heliobacteria's sulphur metabolism. Most information pertaining to Heliobacteria's sulphur metabolism can be gleaned from the annotated genome of *Heliobacterium modesticaldum* Ice1 indicating that the organism only has components of sulphur assimilatory reduction pathways (Sattley, Madigan, Swingley et al., 2008). Recent work with *H. modesticaldum* Ice1 showed that this strain was among the highest anaerobic Hg^{II} reducers on record (Grégoire, Lavoie & Poulain, 2018). Although *H. modesticaldum* is a thermophile (Kimble, Mandelco, Woese et al., 1995), this observation is noteworthy in the context of rice paddies because most Heliobacteria have been isolated from such environments (Ormerod, Kimble, Nesbakken et al., 1996, Stevenson, Kimble, Woese et al., 1997). In this study, we chose to work with the mesophile *Heliobacillus mobilis* (DSM-6151), a Heliobacterium originally isolated from a rice paddy in Thailand (Beer-Romero & Gest, 1987), to evaluate the potential for Heliobacteria to alter Hg's fate in rice paddies.

Heliobacteria are metabolically versatile terrestrial spore forming photoheterotrophs that also conduct one of the most primitive forms of photosynthesis. They are used to study the function of ancestral photochemical reaction centers, the key components in the energy conversion process of photosynthesis (Gisriel, Sarrou, Ferlez et al., 2017, Orf, Gisriel & Redding, 2018) . Determining their role on Hg redox transformations is not only relevant for contemporary environments, but may also provide insights into the chemistry of early Earth environments by

identifying conditions that may leave a redox-mediated signature in the rock record (Zheng, Gilleaudeau, Kah et al., 2018).

One general hypothesis that we are currently testing is that the magnitude of anaerobic Hg^{II} reduction to Hg^0, depends on the intracellular redox state of cells, which is coupled to the redox states of nutrients available during photoheterotrophic metabolism. Based on this hypothesis, we predicted that the redox state of the sulphur sources available to *Heliobacillus mobilis* would affect its ability to reduce Hg^{II}. Here, we show that the presence of cysteine, thiosulphate or sulphate, but not methionine, modulates the ability of Heliobacteria to reduce Hg^{II}.

2.3 MATERIALS AND METHODS

2.3.1 Anaerobic bioreporter assay and Hg speciation models

We used an *E. coli* biosensor to determine Hg bioavailability in the presence of various sulphur sources. The biosensor experiments were performed in minimal BMAA exposure medium (Stenzler, Hinz, Ruuskanen et al., 2017). The benefits of using a defined medium (BMAA) is two-fold. First, Hg speciation in solution can be predicted using thermodynamic binding constants between Hg and the various sulphur sources. Second, Hg-induced fluorescence can easily be measured.

We elected to work with an *E. coli* bioreporter because of the paucity of genetic tools currently available to work with Heliobacteria. We recognize that *E. coli* and Heliobacteria will likely exhibit different Hg uptake strategies due to their different cell walls and physiology and have adjusted our discussion accordingly. Furthermore, the application of the biosensor and modelling of Hg speciation was not possible in the complex DSMZ medium #370 (containing pyruvate and yeast extracts) in which bioreactor assays were performed because i) of the high

levels of autofluorescence originating from the medium which masked the Hg uptake signal and ii) the lack of thermodynamic data available for Hg binding with all components of yeast extracts. Note that we were unable to grow *H. mobilis* in minimal medium and this is the reason why we performed subsequent experiments in complex DSMZ #370 medium, as recommended by the culture collection. As such, the only bioavailability data presented here are for defined exposure medium. We recognize the caveat that Hg speciation in the more complex bioreactor assay medium will likely be altered. That being said, it was appropriate to discuss the role of sulphur sources on Hg bioavailability because it formed the basis of exposure conditions in the subsequent bioreactor assays.

Anaerobic bioassays were performed according to the methods outlined in previous work which we will summarize here (Stenzler, Hinz, Ruuskanen et al., 2017). Two *Escherichia coli* biosensors were used; one was a Hg inducible biosensor (*E. coli* NEB5α harboring the pUC57merR-Pp plasmid) where the production of a flavin based fluorescent protein (FbFP) was under the control of *merR* [the transcription regulator of the *mer* operon (Barkay, Miller & Summers, 2003)]. The other was a constitutive biosensor (*E. coli* NEB5α harbouring the pUC19AH206-Pp plasmid), which expressed the FbFP irrespective of the presence of Hg. Experiments with both biosensors were performed in parallel to control for the effect of the conditions tested on cell health. We observed that constitutive fluorescence production did not significantly decrease under any of the conditions tested compared to controls in minimal medium indicating that bioreporter cultures were healthy in all experiments (**Fig S1**). As part of the bioreporter assays, we modelled the speciation of Hg in BMAA across all sulphur treatments. All modelling for Hg chemical speciation was performed using PHREEQC v3.4.0. The distribution of

predicted Hg species for each sulphur treatment and thermodynamic constants employed are provided in **Table S1** and **Table S2**.

2.3.2 *Heliobacillus mobilis* cell culture growth conditions

All growth and experimental conditions are summarized in **Table S3**. For growth assays and bioreactor experiments we used the strain *Heliobacillus mobilis* from the DSMZ culture collection (strain number DSM-6151). Cell cultures were handled under anaerobic conditions in a Coy anaerobic glove box (atmosphere 97% $N_{2\,(g)}$ and 3% $H_{2\,(g)}$) or by using sterile anaerobic benchtop techniques where all equipment was sparged with 100% $N_{2\,(g)}$ prior to use. For all growth assays and bioreactor experiments, new cell cultures were revived in the anaerobic glovebox from cryostocks kept at -80°C by scraping frozen culture with a sterile pipette tip and discarding it into a Balch tube containing growth medium #370 from DSMZ amended with 20 mM pyruvate to improve cell growth. The medium #370 composition is: K_2HPO_4 1 g/L, yeast extract 10 g/L, Na-pyruvate 2.2 g/L, Na-ascorbate 0.5g/L, final pH adjusted to 6.8. For the sulphate treatment, we used $MgSO_4*7H_2O$ 1 g/L, for all other sulphur source treatments we substituted $MgSO_4$ with equimolar $MgCl_2*6H_2O$ to ensure cells were not deprived of Mg. Note that our attempts at reproducibly growing *H. mobilis* in a minimal medium have so far failed. All experiments were therefore performed in complex DSMZ #370 medium and results were interpreted accordingly. Cells were revived in the presence of the sulphur source to be tested in growth assays and bioreactor experiments (i.e. sulphate, thiosulphate, L-methionine, L-cysteine). Note that total sulphur content of the medium was normalized to 4 mM as per the culture collections recommendation except in experiments testing for the effect of cysteine concentration. Balch tubes were then crimped shut and the headspace was replaced with 100% $N_{2(g)}$. Cryostock revival cultures were incubated at 37°C with an incandescent light source emitting photoactive radiation

(PAR) at an intensity of 80 µmol photon m^{-2} s^{-1} until they reached mid-exponential stage. Cultures were then used to start new cultures with a 1% (v/v) inoculum into new Balch tubes containing 10 mL of the same growth medium. For bioreactor experiments, cells were harvested again after reaching mid-exponential to start cultures with a 1% inoculum in serum bottles containing 75 mL of the same growth medium. Upon reaching mid to late exponential phase, these cultures were used as a 10% (v/v) inoculum in bioreactor experiments containing the same growth medium.

Growth assays with *H. mobilis* were conducted to test for the effect of the different sulphur sources on cell growth. Cells were first revived and grown in medium #370 containing the sulphur source to be tested, upon reaching mid-exponential a 10% v/v cell inoculum was used to start a new series of cultures, and then upon reaching mid-late exponential a 1% v/v cell inoculum was taken to start the growth curves with either no sulphur, 4 mM sulphate, 4 mM thiosulphate, 4 mM L- methionine, ca. 300 µM L-cysteine or 4 mM L-cysteine. Cell growth was measured as the optical density at 600 nm (O.D. 600 nm) in individual Balch tubes using a spectrophotometer over at least 48 hours. Additional growth experiments in medium #370 + 4 mM sulphate were also performed at 20 µmol photon $m^{-2}s^{-1}$ vs 80 µmol photon $m^{-2}s^{-1}$ to test for the effects of light intensity (**Fig S2**), and in a sealed bioreactor to test the absence of $N_{2(g)}$ bubbling in the vessel on phototrophic growth.

2.3.3 Sulphur species concentrations in the bioreactor bioassay medium

To establish and determine the final concentrations of the various S species in the final bioreactor assay medium, we also took into consideration the carryover of sulphur sources added from the inocula. Furthermore, as per the manufacturer data, yeast extract contains ca. 0.09% sulphate, 0.2% cystine and 0.8% methionine, corresponding to final concentrations of 93 µM, 83 µM and 400 µM, respectively, prior to the addition of any new sulphur species. Furthermore, it is

likely that cystine was reduced to cysteine during the autoclaving step because DSMZ #370 medium contains the reducing agent ascorbate (Giustarini, Dalle-Donne, Colombo et al., 2008). Therefore, we performed bioreactor assays with a final concentration of sulphate (4.1 mM), thiosulphate (4 mM) and methionine (4.4 mM); we worked at two different cysteine concentrations corresponding to ca. 300 μM and 4.3 mM, referred to as "μM" and "mM" treatments, respectively. Working at μM levels cysteine was essential to maintain comparable bioavailability of Hg across all treatments, as described in the Results and Discussion section.

2.3.4 Hg^0 Bioreactor setup and sampling for cell density

All conditions tested in the bioreactor are summarized in **Table S3**. The bioreactor subsampling methodology is identical to that used in previous work (Grégoire & Poulain, 2016, Grégoire, Lavoie & Poulain, 2018). All bioreactor experiments were carried out at 37°C at a light intensity of 20 μmol photon m^{-2} s^{-1} to limit abiotic photoreduction of Hg (Grégoire & Poulain, 2016). All live cell bioreactor treatments were performed in triplicate with initial *H. mobilis* cell inoculums of 10% v/v from cultures grown until mid-late exponential phase, and abiotic controls were performed in duplicate. Each bioreactor experiment was spiked with 250 pM of $HgCl_2$ and ran for 48 hours to measure Hg^0 production using a Tekran 2537B CVAFS Analyzer.

2.3.5 Statistical analyses

One-way ANOVAs were used to test for the effect of sulphur source and cysteine concentration on Hg bioavailability, cell growth rates, and cumulative Hg^0 production. For the growth rates analysis, if the assumptions of normal distribution of residuals and/or constant variance were not passed, the data were transformed to their natural logarithm and reran to see if assumptions passed. For the Hg bioavailability and cumulative Hg^0 production analyses, in the

event that the assumptions of the normal distribution of residuals and constant variance were not fulfilled, non-parametric rank sum tests were employed. If the sample size differed across treatments, type III sum of squares were used to control for unbalanced designs. For all three analyses, treatments where a significant difference was observed were identified using a Tukey HSD *post hoc* test with the significance threshold set to $p<0.05$. All statistical analyses were performed in R v3.1.2 (CRAN Team, 2017). Detailed statistical results are provided in all figure legends.

2.4 RESULTS & DISCUSSION

2.4.1 Sulphur sources exert dynamic controls on Hg bioavailability

H. mobilis can grow phototrophically on a variety of oxidized and reduced sulphur sources (SO_4^{2-}, $S_2O_3^{2-}$, L-methionine, and L-cysteine) (Beer-Romero & Gest, 1987). This metabolic capability makes *H. mobilis* an ideal system in which to explore the effects of sulphur metabolism on anaerobic Hg redox cycling. We recognize that reduced sulphur species have high affinity for Hg^{II} and affect Hg bioavailability and therefore intracellular transformations. Bearing this in mind, our first objective was to control for the bioavailability of the Hg-sulphur complexes that were predicted to form in the presence of sulphate, thiosulphate, methionine and cysteine (**Fig 2.1** and **Table S2.1**). To achieve this, we measured and compared Hg bioavailability in the presence of these sulphur sources using an anaerobic *E. coli* Hg biosensor (Stenzler, Gaudet & Poulain, 2018), which expresses fluorescence proportionally to the concentration of intracellular Hg.

Sulphur source had a significant effect on Hg bioavailability (**Fig 2.1**; $p<0.001$). We observed that mM levels of thiosulphate slightly increased Hg bioavailability while mM levels of cysteine strongly and significantly decreased Hg bioavailability (**Fig 2.1A**; $p<0.001$). The results

from these experiments suggested that we had to alter cysteine concentrations from what was recommended in the DSMZ #370 medium, to maintain comparable Hg bioavailability across all treatments. Indeed, decreasing [cysteine] from mM to μM and nM ranges significantly increased Hg bioavailability (**Fig 2.1B;** $p<0.001$).

Using the *E. coli* bioreporter data, we designed exposure conditions under which Hg bioavailability was comparable across all treatments. Taking inocula carry over and sulphur species content of yeast extract into consideration, we performed bioreactor assays with a final concentration of sulphate (4.1 mM), thiosulphate (4 mM) and methionine (4.4 mM); we worked at two different cysteine concentrations corresponding to ca. 300 μM and 4.3 mM, referred to as "μM" and "mM", respectively.

2.4.2 Effect of sulphur sources on *H. mobilis* growth

Our second objective was to assess the effect of the various sulphur sources (i.e., SO_4^{2-}, $S_2O_3^{2-}$, L-methionine, and L-cysteine) added to DSMZ medium #370 on the growth of *H. mobilis*. The addition of different sulphur sources to DSMZ medium #370 did not affect the final cell density, which was comparable across sulphur treatments (**Fig 2.2A**). In contrast, we observed that added sulphur source had a significant effect ($p<0.05$) on growth rates (**Fig 2.2B**). Cells supplied with μM cysteine and mM thiosulphate displayed significantly ($p<0.05$) higher growth rates (0.122 ± 0.014 h^{-1} and 0.127 ± 0.004 h^{-1}, respectively) compared to the no sulphur added control (0.084 ± 0.004 h^{-1}). The growth rate of cells supplied with methionine (0.079 ± 0.005 h^{-1}) was not significantly different from the sulphate treatment (0.071 ± 0.010 h^{-1}) or the no sulphur added control (0.084 ± 0.004 h^{-1}). Cells supplied with mM levels of cysteine exhibited the slowest growth among all sulphur treatments (0.055 ± 0.002 h^{-1}) (**Fig 2.2A**).

The results obtained with μM levels of cysteine and mM levels of thiosulphate suggest there was a physiological advantage gained by consuming relatively more reduced sulphur sources; we noted a small physiological cost in having mM sulphate added to the growth medium (**Fig 2.2B**). We speculate that the slower growth rate observed in the presence of mM levels of cysteine may be due to the potentially toxic effect of cysteine (Shimada, Tanaka & Ishihama, 2016).

By understanding the ability of cells to grow in the presence of different sulphur sources added to DSMZ medium #370 and the bioavailability of different Hg-sulphur complexes, we estimated that we could reasonably compare Hg^0 production over a range of sulphur sources [sulphate (S redox state +6), thiosulphate [S redox states -1, +5 (Vairavamurthy, Manowitz, Luther et al., 1993)], methionine (S redox state -2) and cysteine (S redox state -2) in subsequent Hg reduction bioreactor experiments.

2.4.3 Growth is not required for phototrophic Hg reduction by *H. mobilis*

During our preliminary tests to optimize bioreactor assay conditions, we discovered that the continuous sparging of the bioreactor required for near-real time volatile Hg^0 quantification halted cell growth. Cells were unable to grow in the bioreactor under constant bubbling over a similar time frame (e.g. 48 hours) (**Table S2.3**) in contrast to sealed tubes which supported robust growth (**Fig 2.2A)**. We ruled out that low light intensity was inhibiting growth as the cells grew in sealed tubes and sealed non-sparging bioreactor (**Fig S2.2**). Despite the lack of growth in the bioreactor, we show that metabolically active *H. mobilis* cells were required for Hg^{II} reduction under conditions that support photoheterotrophic growth (**Fig 2.3A**) given that the no cell controls (except for mM levels of cysteine) (**Fig 2.3B**) and heat-killed controls (**Fig S2.3**) produced negligible amount of Hg^0.

We suspect that the continuous bubbling required to measure Hg^0 was inhibiting growth due to the removal of gaseous CO_2. Inorganic carbon (e.g. CO_2 or HCO_3^-) is an essential substrate used in anaplerotic reactions required for biosynthesis in *H. modesticaldum* and possibly other Heliobacteria (Tang, Feng, Zhuang et al., 2010). By removing endogenous CO_2 produced following organic carbon oxidation, *H. mobilis* would have been deprived of an essential nutrient to generate biomass (Beer-Romero & Gest, 1987, Richardson, King, Kelly et al., 1988). Photoheterotrophs can use inorganic carbon not only in anaplerotic reactions but also as an electron sink to maintain redox homeostasis and enable growth (Richardson, King, Kelly et al., 1988, McKinlay & Harwood, 2010). It is possible that the presence of HCO_3^- would have introduced a pathway that could compete for reducing power inside of the cell and confound the interpretation of our results. Therefore, we chose to not add HCO_3^- as an exogenous source of inorganic carbon and perform experiments as cell suspension rather than growth assays.

2.4.4 Reduced sulphur sources favour Hg^{II} reduction during anoxygenic photosynthesis

When comparing abiotic and biotic Hg^0 production, we observed that added sulphur source had a significant effect on cumulative Hg^0 production (**Fig 2.3**, $p<0.001$). Average Hg^0 production in the presence of live *H. mobilis* cells was highest when cells were provided with μM cysteine (56.60 ± 3.77 pmol Hg^0), followed by thiosulphate (40.62 ± 11.87 pmol Hg^0), methionine (27.06 ± 13.72 pmol Hg^0), no sulphur controls (27.05 ± 4.36 pmol Hg^0), sulphate (14.23 ± 11.30 pmol Hg^0), and the mM cysteine treatments (8.79 ± 5.00 pmol Hg^0) (**Fig 2.3A**). Hg^0 production in the presence of heat-killed cells and in the absence of cells was negligible, except for the mM cysteine no cell treatment (38.04 ± 14.50 pmol vs < 5 pmol Hg^0 for all other treatments) (**Fig S2.3** and **Fig 2.3B**); this observation is addressed in the following section.

The trends observed for biotic Hg^0 production were in line with our predictions. The most oxidized sulphur source, sulphate, led to lower Hg^0 production compared to the thiosulphate and μM cysteine treatments, which provided cells with relatively more reduced sulphur [e.g. S redox states for individual S atoms in thiosulphate are -1 and +5 (Vairavamurthy, Manowitz, Luther et al., 1993) and S redox state in cysteine is -2 vs. +6 in sulphate] (**Fig 3A**). Although cells did not grow in the bioreactor, we suspect that the higher Hg^0 production in the presence of thiosulphate and cysteine was tied to the lower metabolic costs of assimilating more reduced sulphur sources, as supported by our growth experiments (**Fig 2.2B**). Unfortunately, we were not able to fully address our hypothesis due to our inability to quantify intracellular reducing power available for Hg reduction because of the low cell density achieved in our bioreactor experiments. We can only speculate that excess reducing power generated by non growing cells was greater when cells were placed in the presence of cysteine and thiosulphate rather than sulphate, allowing for a greater amount of Hg^0 to be produced. Our results also suggest that Hg^{II} reduction is inhibited when Hg bioavailability is limited with high (mM) concentrations of cysteine (**Fig 2.3A** and **Fig 2.2B** respectively). This observation suggests that Hg^{II} reduction may occur intracellularly in *H. mobilis* as was previously suggested for *H. modesticaldum* (Grégoire, Lavoie & Poulain, 2018).

In the presence of added methionine, cells exhibited levels of Hg^0 production comparable to the no sulphur added control (**Fig 2.3A**). These results are in line with our preliminary experiments where the addition of methionine did not affect growth rate, yield or Hg bioavailability (**Fig 2.1** and **Fig 2.2**). Together, these findings support that addition of sulphur sources can affect Hg^{II} reduction during anoxygenic photosynthesis and highlight the complex interplay that exists between sulphur assimilation and cometabolic Hg^{II} reduction.

2.4.5 Cysteine and organic carbon catalyze Hg photoreduction at low light intensities

As previously shown, high levels of Hg^0 were produced under low light intensity in the presence of 4 mM of cysteine and the absence of cells (**Fig 2.3B**). Interestingly, under the same conditions, the mere addition of *H. mobilis* cells to the reactor inhibited Hg^0 production (**Fig 2.3A**). While there is precedence for Hg photoreduction in the presence of cysteine and UV light (Zheng & Hintelmann, 2010), to the best of our knowledge there is no evidence of cysteine catalyzing Hg photoreduction at the low visible light intensities employed in our experiments (20 µmol photon m^{-2} s^{-1}). We suspect that cysteine catalyzes the photoreduction of Hg^{II} using reduced components of the medium while the addition of cells shade and quench this photochemical reaction.

To further explore this potential mechanism supporting abiotic Hg^0 production under visible light; we controlled for the presence of light, organic carbon from yeast extract (YE) and cell shading. To test for the role of light, we repeated experiments in the dark, and in the light with formaldehyde-killed *H. mobilis* cells to create cell-induced shading in the reactor (**Table S2.3**). To test for the role of organic carbon, we irradiated the bioreactor while all sources of organic carbon (i.e., YE) were removed except for cysteine (**Table S2.3**).

All additional experimental treatments resulted in a strong inhibition of abiotic Hg^0 photoproduction which was comparable to the Hg^0 production observed in abiotic controls for sulphate, thiosulphate and methionine (**Fig 2.3B** and **Fig S2.4**). These results suggest that abiotic Hg^{II} photoreduction relies on the presence of high levels of cysteine and components of YE. Here, we can effectively rule out that Hg^{II} was photoreduced solely due to components of YE because all other abiotic sulphur treatments were supplied with the same amount of YE. By omitting all organic carbon except cysteine, we showed that the interaction between cysteine and organic compounds from YE is essential for Hg photoreduction. We recognize that the undefined nature of YE, similar to the undefined nature of dissolved organic matter, makes it difficult to provide a

detailed description of the pathway supporting abiotic Hg^{II} photoreduction under the conditions tested. As previously mentioned, we are currently developing a defined medium and plan to carry out new experiments to address this limitation.

2.4.6 Coupling sulphur cycling and cometabolic Hg transformations in the environment

In this work we show that *H. mobilis* can reduce Hg^{II} under conditions supporting phototrophic metabolism. We have demonstrated that after controlling for Hg bioavailability, phototrophic Hg^{II} reduction is favoured in the presence of reduced sulphur sources. Our study highlights the importance of sulphur as a nutrient driving anaerobic Hg^{II} reduction and provides the basis for exploring potential coupling points between sulphur assimilation, anaerobic Hg reduction and Hg methylation in anoxic habitats.

Sulphur can be a limiting nutrient in rice paddies requiring rice growers to use sulphate amendments (Blair & Lefroy, 1998) that can potentially increase Hg methylation (Gilmour, Henry & Mitchell, 1992). Under these conditions, our data suggest that Hg reduction and subsequent evasion could potentially be hampered. Although our study was prompted by increased concerns surrounding MeHg accumulation in rice paddies, our findings could apply to other habitats that support steep redox gradients, competition for nutrients and cometabolic Hg transformations. Nutrient cycling and cometabolic Hg transformations stand to be closely linked in Hg methylation hotspots such as periphytic microbial mats (Olsen, Brandt & Brooks, 2016), aquatic sediments (Fleming, Mack, Green et al., 2006, Correia & Guimarães, 2017) and waterlogged soils (Eklof, Bishop, Bertilsson et al., 2018). While our study makes a case for sulphur cycling as a coupling point for competing cometabolic Hg transformations, other nutrients such as iron (Sugio, Fujii, Takeuchi et al., 2003, Fleming, Mack, Green et al., 2006, Wiatrowski, Ward & Barkay, 2006, Bravo, Bouchet, Guedron et al., 2015) and organic carbon (Grégoire & Poulain, 2016, Christensen,

Somenahally, Moberly et al., 2018, Grégoire, Lavoie & Poulain, 2018) that are known to control Hg methylation and reduction, have the potential to fulfil a similar role. Curiously, the coupling between other macronutrients under strong microbial control such as nitrogen and Hg cycling remain unexplored despite the importance of nitrogen cycling in aquatic and terrestrial ecosystems.

By characterizing the environmental variables that drive different cometabolic Hg transformations in future work, we hope to better predict how nutrient availability and microbial activity will affect Hg mobility and toxicity in the environment. This knowledge could be used to hone predictive models and develop tractable Hg pollution management strategies that rely on supplying environmental conditions that stimulate favourable cometabolic Hg transformations (e.g. reduction or sequestration) rather than unfavourable ones (e.g. methylation). Strategies such as targeted nutrient amendments could then be applied *in situ* to limit the availability of the inorganic Hg and nutritional substrates that contribute to the accumulation of neurotoxic Hg in the environment.

Finally, further mechanistic information on the coupling between Hg redox chemistry and phototrophy would be useful in revealing the evolutionary and physiological context of how early life forms responded to Hg toxicity. Obtaining these details may reveal unsuspected information on the chemistry of primitive oceans supporting the evolution of early phototrophic metabolisms. Indeed, the absence of dedicated Hg resistance strategies such as the *mer* operon among anaerobes and phototrophs is puzzling. There appears to be a tight coupling between the presence of oxygen and the evolution of the *mer* operon (Barkay, Kritee, Boyd et al., 2010). Anaerobic and anoxygenic phototrophic metabolisms predate the rise of oxygen on planet Earth and cometabolic processes such as sequestration or the use of excess reducing power to catalyze Hg reduction may have been sufficient to cope with Hg toxicity in the absence of oxygen.

Author contributions

NCL, DSG, BRS and AJP designed the experiments, DSG, NCL and BRS carried them out, DG, NCL and BRS performed data analyses; DSG, NCL and AJP wrote the manuscript.

2.5 FIGURES AND CAPTIONS

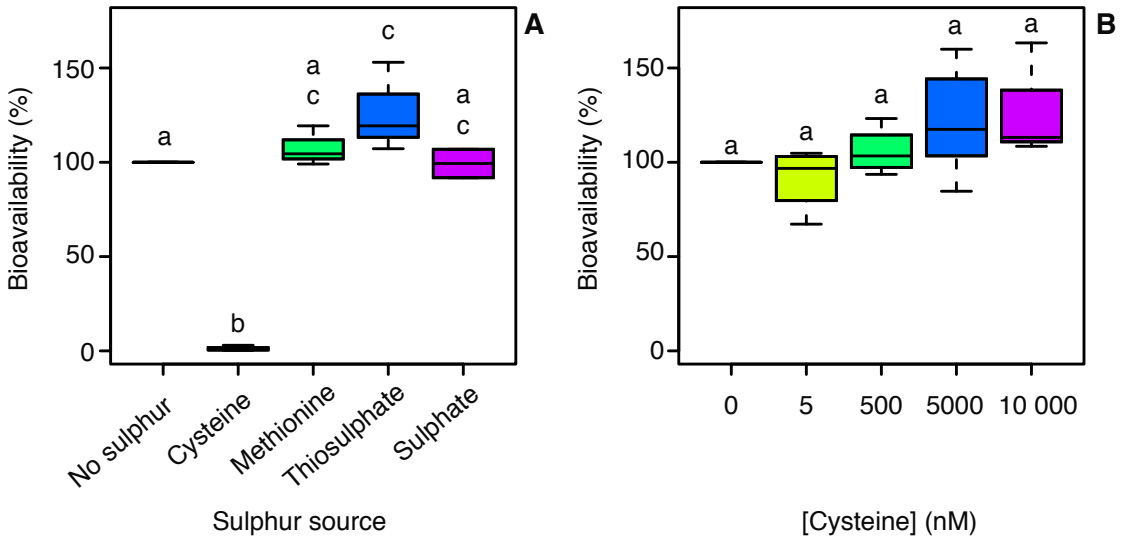

Figure 2.1: Bioavailability of 5 nM Hg in the presence of sulphur sources.
The bioavailability of 5 nM Hg was quantified in the presence of various sulphur sources with differing atom redox states measured with the *E. coli* bioreporter (A) and different concentrations of cysteine (B). Cells were exposed to Hg in BMAA minimal medium where [NO_3^-], the terminal electron acceptor, was set to 0.2 mM. For experiments comparing different sulphur sources total sulphur concentrations was normalized to 4 mM (A). The bottom and top of the boxes show the first and third quartiles respectively, the bar in the middle shows the median and the whiskers show the minimum and maximum for each treatment. The assumptions of normally distributed residuals and homoscedasticity required for parametric tests were not met, as such, rank sum tests were used to evaluate the effect of sulphur source and cysteine concentrations on Hg bioavailability. A one-way ANOVA with type III sum of squares was used to control for differing sample size across treatments when testing for the effect of sulphur source and cysteine on Hg bioavailability (n = 2 for sulphate; n =3 for cysteine, methionine and thiosulphate; n = 4 for 5 nM and 500 nM cysteine; n = 3 for 10 000 nM cysteine, n = 7 for 5000 nM cysteine and n = 9 for no sulphur controls). Sulphur source had a significant ($p<0.05$) effect on Hg bioavailability ($p=4.65 \times 10^{-7}$) (A) as did cysteine concentration ($p=6.78 \times 10^{-13}$) (B). The statistical conclusions for the non-parametric tests were identical to the parametric tests for sulphur source ($p=9.18 \times 10^{-10}$) and cysteine ($p=0.041$), as such multiple comparison results are included in the figure. Letters that are not shared between treatments indicate a significant difference according to the Tukey HSD test ($p < 0.05$).

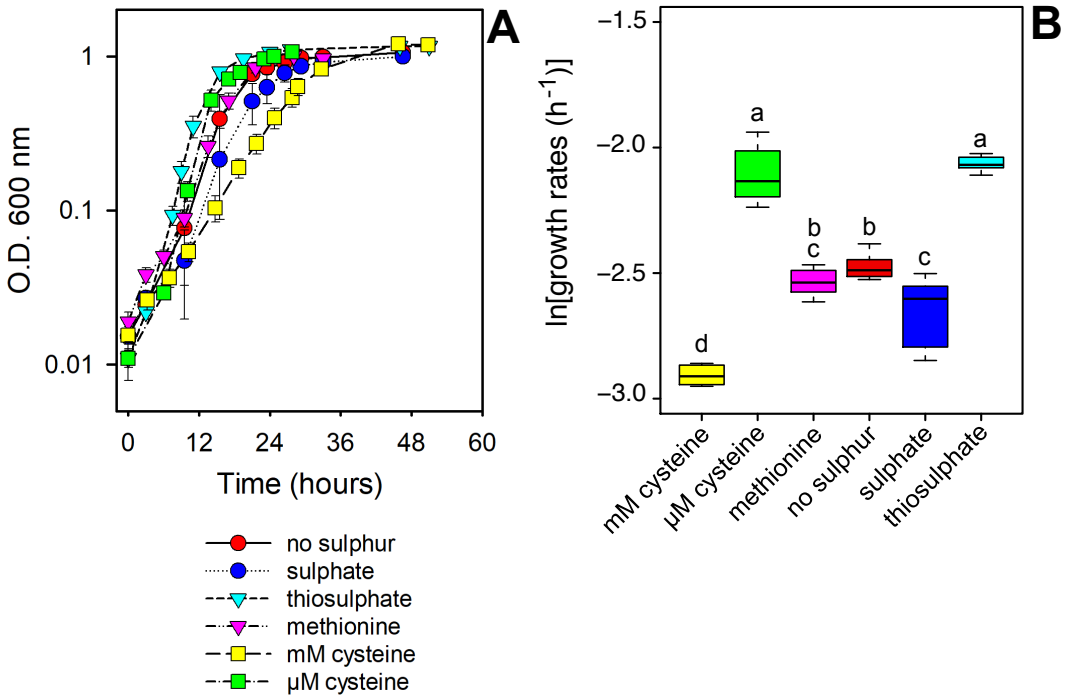

Figure 2.2: Phototrophic growth (A) and growth rates (B) of *H. mobilis* in the presence of different sulphur sources.

All cultures were grown in DSMZ medium #370 amended with 20 mM pyruvate and final concentrations of total sulphur were normalized to ca. 4 mM, except for the µM cysteine treatment. Results shown in panel (A) are shown as averages for n= 6 technical replicates in all cases except the methionine treatments where n = 5 and error bars represent standard deviations for each time point. The bottom and top of the boxes in panel (B) show the first and third quartiles respectively, the bar in the middle shows the median and the whiskers show the minimum and maximum for each treatment. The assumptions of normally distributed residuals were met ($p = 0.76$) but not homoscedasticity ($p = 0.038$) as required for parametric tests ($p > 0.05$ for rejection of null hypothesis). As such the growth rates were transformed to their natural logarithms to ensure the assumptions of normality ($p = 0.76$) and homoscedasticity ($p = 0.11$) were met for a parametric one-way ANOVA. That showed sulphur treatment had a significant effect on growth rate ($p = 2.2 \times 10^{-16}$). Letters that are not shared between treatments indicate a significant difference according to the Tukey HSD test ($p < 0.05$).

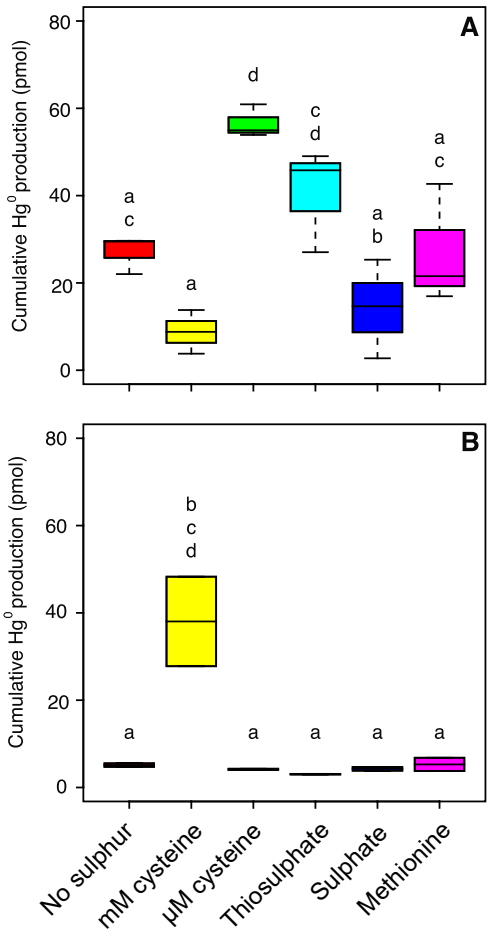

Figure 2.3:Cumulative Hg0 production for phototrophically grown *H. mobilis*.
Cumulative Hg^0 production for phototrophically grown *H. mobilis* (A) and no cell controls (B) amended with cysteine, thiosulphate, sulphate, methionine and no sulphur controls. All live cell experiments were performed in triplicate and no cell controls were performed in duplicate. $HgCl_2$ was added to a final concentration of 250 pM in all experiments. The bottom and top of the boxes respectively show the first and third quartiles, the bar in the middle shows the median and the whiskers show the minimum and maximum for each treatment. A one-way ANOVA with type III sum of squares showed that sulphur had a significant ($p<0.05$) effect on cumulative Hg^0 production ($p = 3.86 \times 10^{-6}$). Tests for constant variance ($p = 0.10$) and normal distribution ($p = 0.29$) were passed ($p > 0.05$ for rejection of null hypothesis). Letters that are not shared between treatments indicate a significant difference according to the Tukey HSD test ($p < 0.05$).

2.6 REFERENCES

Ao, M., B. Meng, A. Sapkota, Y. G. Wu, X. L. Qian, G. L. Qiu, S. Q. Zhong and L. H. Shang (2017). "The influence of atmospheric Hg on Hg contaminations in rice and paddy soil in the Xunyang Hg mining district, China." Acta Geochimica 36(2): 181-189.

Barkay, T., K. Kritee, E. Boyd and G. Geesey (2010). "A thermophilic bacterial origin and subsequent constraints by redox, light and salinity on the evolution of the microbial mercuric reductase." Environ Microbiol 12(11): 2904-2917.

Barkay, T., S. M. Miller and A. O. Summers (2003). "Bacterial mercury resistance from atoms to ecosystems." Fems Microbiology Reviews 27(2-3): 355-384.

Beer-Romero, P. and H. Gest (1987). "Heliobacillus mobilis, a peritrichously flagellated anoxyphototroph containing bacteriochlorophyllg." FEMS Microbiology Letters 41(2): 109-114.

Blair, G. and R. Lefroy (1998). "Sulfur and carbon research in rice production systems." Field Crops Research 56(1-2): 177-181.

Bone, S. E., J. R. Bargar and G. Sposito (2014). "Mackinawite (FeS) reduces mercury(II) under sulfidic conditions." Environ Sci Technol 48(18): 10681-10689.

Bravo, A. G., S. Bouchet, S. Guedron, D. Amouroux, J. Dominik and J. Zopfi (2015). "High methylmercury production under ferruginous conditions in sediments impacted by sewage treatment plant discharges." Water Res 80: 245-255.

Choi, S. C., T. Chase and R. Bartha (1994). "Metabolic Pathways Leading to Mercury Methylation in Desulfovibrio desulfuricans LS." Appl Environ Microbiol 60(11): 4072-4077.

Christensen, G. A., A. C. Somenahally, J. G. Moberly, C. M. Miller, A. J. King, C. C. Gilmour, S. D. Brown, M. Podar, C. C. Brandt, S. C. Brooks, A. V. Palumbo, J. D. Wall and D. A. Elias (2018). "Carbon Amendments Alter Microbial Community Structure and Net Mercury Methylation Potential in Sediments." Appl Environ Microbiol 84(3).

Colombo, M. J., J. Ha, J. R. Reinfelder, T. Barkay and N. Yee (2014). "Oxidation of Hg(0) to Hg(II) by diverse anaerobic bacteria." Chemical Geology 363: 334-340.

Correia, R. R. S. and J. R. D. Guimarães (2017). "Mercury methylation and sulfate reduction rates in mangrove sediments, Rio de Janeiro, Brazil: The role of different microorganism consortia." Chemosphere 167: 438-443.

Desrochers, K. A. N., K. M. A. Paulson, C. J. Ptacek, D. W. Blowes and W. D. Gould (2015). "Effect of Electron Donor to Sulfate Ratio on Mercury Methylation in Floodplain Sediments under Saturated Flow Conditions." Geomicrobiology Journal 32(10): 924-933.

Eklof, K., K. Bishop, S. Bertilsson, E. Bjorn, M. Buck, U. Skyllberg, O. A. Osman, R. M. Kronberg and A. G. Bravo (2018). "Formation of mercury methylation hotspots as a consequence of forestry operations." Sci Total Environ 613-614: 1069-1078.

Fleming, E. J., E. E. Mack, P. G. Green and D. C. Nelson (2006). "Mercury methylation from unexpected sources: molybdate-inhibited freshwater sediments and an iron-reducing bacterium." Appl Environ Microbiol 72(1): 457-464.

Frigaard, N. U. and C. Dahl (2009). Sulfur Metabolism in Phototrophic Sulfur Bacteria. Advances in Microbial Physiology, Vol 54. R. K. Poole. 54: 103-200.

Gilmour, C. C., E. A. Henry and R. Mitchell (1992). "Sulfate stimulation of mercury methylation in freshwater sediments." Environmental Science and Technology 26(11): 2281-2287.

Gionfriddo, C. M., M. T. Tate, R. R. Wick, M. B. Schultz, A. Zemla, M. P. Thelen, R. Schofield, D. P. Krabbenhoft, K. E. Holt and J. W. Moreau (2016). "Microbial mercury methylation in Antarctic sea ice." Nat Microbiol 1(10): 16127.

Gisriel, C., I. Sarrou, B. Ferlez, J. H. Golbeck, K. E. Redding and R. Fromme (2017). "Structure of a symmetric photosynthetic reaction center-photosystem." Science 357(6355): 1021-1025.

Giustarini, D., I. Dalle-Donne, R. Colombo, A. Milzani and R. Rossi (2008). "Is ascorbate able to reduce disulfide bridges? A cautionary note." Nitric Oxide 19(3): 252-258.

Grégoire, D. S., N. C. Lavoie and A. J. Poulain (2018). "Heliobacteria Reveal Fermentation As a Key Pathway for Mercury Reduction in Anoxic Environments." Environ Sci Technol 52(7): 4145-4153.

Grégoire, D. S. and A. J. Poulain (2016). "A physiological role for Hg-II during phototrophic growth." Nature Geoscience 9(2): 121-+.

Gu, B., Y. Bian, C. L. Miller, W. Dong, X. Jiang and L. Liang (2011). "Mercury reduction and complexation by natural organic matter in anoxic environments." Proc Natl Acad Sci U S A 108(4): 1479-1483.

Jeremiason, J. D., D. R. Engstrom, E. B. Swain, E. A. Nater, B. M. Johnson, J. E. Almendinger, B. A. Monson and R. K. Kolka (2006). "Sulfate addition increases methylmercury production in an experimental wetland." Environ Sci Technol 40(12): 3800-3806.

Kim, K. H., M. Y. Kim, J. Kim and G. Lee (2003). "Effects of changes in environmental conditions on atmospheric mercury exchange: Comparative analysis from a rice paddy field during the two spring periods of 2001 and 2002." Journal of Geophysical Research-Atmospheres 108(D19).

Kimble, L. K., L. Mandelco, C. R. Woese and M. T. Madigan (1995). "Heliobacterium Modesticaldum, Sp-Nov, a Thermophilic Heliobacterium of Hot-Springs and Volcanic Soils." Archives of Microbiology 163(4): 259-267.

Lin, H., X. Lu, L. Liang and B. Gu (2015). "Cysteine Inhibits Mercury Methylation by Geobacter sulfurreducens PCA Mutant ΔomcBESTZ." Environmental Science & Technology Letters 2(5): 144-148.

Lin, H., J. L. Morrell-Falvey, B. Rao, L. Liang and B. Gu (2014). "Coupled mercury-cell sorption, reduction, and oxidation on methylmercury production by Geobacter sulfurreducens PCA." Environ Sci Technol 48(20): 11969-11976.

Liu, S. N. and H. A. Wiatrowski (2018). "Reduction of Hg(II) to Hg(0) by Biogenic Magnetite from two Magnetotactic Bacteria." Geomicrobiology Journal 35(3): 198-208.

Lu, X., Y. Liu, A. Johs, L. Zhao, T. Wang, Z. Yang, H. Lin, D. A. Elias, E. M. Pierce, L. Liang, T. Barkay and B. Gu (2016). "Anaerobic Mercury Methylation and Demethylation by Geobacter bemidjiensis Bem." Environ Sci Technol 50(8): 4366-4373.

Ma, M., H. Du, D. Wang and T. Sun (2017). "Mercury methylation in the soils and sediments of Three Gorges Reservoir Region." Journal of Soils and Sediments 18(3): 1100-1109.

McKinlay, J. B. and C. S. Harwood (2010). "Carbon dioxide fixation as a central redox cofactor recycling mechanism in bacteria." Proc Natl Acad Sci U S A 107(26): 11669-11675.

Olsen, T. A., C. C. Brandt and S. C. Brooks (2016). "Periphyton Biofilms Influence Net Methylmercury Production in an Industrially Contaminated System." Environ Sci Technol 50(20): 10843-10850.

Orf, G. S., C. Gisriel and K. E. Redding (2018). "Evolution of photosynthetic reaction centers: insights from the structure of the heliobacterial reaction center." Photosynthesis Research 138(1): 11-37.

Ormerod, J. G., L. K. Kimble, T. Nesbakken, Y. A. Torgersen, C. R. Woese and M. T. Madigan (1996). "Heliophilum fasciatum gen. nov. sp. nov. and Heliobacterium gestii sp. nov.: endospore-forming heliobacteria from rice field soils." Arch Microbiol 165(4): 226-234.

Parks, J. M., A. Johs, M. Podar, R. Bridou, R. A. Hurt, Jr., S. D. Smith, S. J. Tomanicek, Y. Qian, S. D. Brown, C. C. Brandt, A. V. Palumbo, J. C. Smith, J. D. Wall, D. A. Elias and L. Liang (2013). "The genetic basis for bacterial mercury methylation." Science 339(6125): 1332-1335.

Pham, A. L. T., A. Morris, T. Zhang, J. Ticknor, C. Levard and H. Hsu-Kim (2014). "Precipitation of nanoscale mercuric sulfides in the presence of natural organic matter: Structural properties, aggregation, and biotransformation." Geochimica Et Cosmochimica Acta 133: 204-215.

Podar, M., C. C. Gilmour, C. C. Brandt, A. Soren, S. D. Brown, B. R. Crable, A. V. Palumbo, A. C. Somenahally and D. A. Elias (2015). "Global prevalence and distribution of genes and microorganisms involved in mercury methylation." Sci Adv 1(9): e1500675.

Qian, C., A. Johs, H. Chen, B. F. Mann, X. Lu, P. E. Abraham, R. L. Hettich and B. Gu (2016). "Global Proteome Response to Deletion of Genes Related to Mercury Methylation and Dissimilatory Metal Reduction Reveals Changes in Respiratory Metabolism in Geobacter sulfurreducens PCA." J Proteome Res 15(10): 3540-3549.

Richardson, D. J., G. F. King, D. J. Kelly, A. G. McEwan, S. J. Ferguson and J. B. Jackson (1988). "The role of auxiliary oxidants in maintaining redox balance during phototrophic growth of Rhodobacter capsulatus on propionate or butyrate." Archives of Microbiology 150(2): 131-137.

Rothenberg, S. E. and X. B. Feng (2012). "Mercury cycling in a flooded rice paddy." Journal of Geophysical Research-Biogeosciences 117: 1-16.

Rothenberg, S. E., L. Windham-Myers and J. E. Creswell (2014). "Rice methylmercury exposure and mitigation: a comprehensive review." Environ Res 133: 407-423.

Sattley, W. M., Madigan, M. T., Swingley, W. D., Cheung, P. C., Clocksin, K. M., Conrad, A. L., . . . Touchman, J. W. (2008). "The genome of Heliobacterium modesticaldum, a phototrophic representative of the Firmicutes containing the simplest photosynthetic apparatus." Journal of Bacteriology, 190(13), 4687-4696.

Schaefer, J. K., J. Letowski and T. Barkay (2002). "mer-mediated resistance and Volatilization of Hg(II) under anaerobic conditions." Geomicrobiology Journal 19(1): 87-102.

Schaefer, J. K. and F. M. M. Morel (2009). "High methylation rates of mercury bound to cysteine by Geobacter sulfurreducens." Nature Geoscience 2(2): 123-126.

Shimada, T., K. Tanaka and A. Ishihama (2016). "Transcription factor DecR (YbaO) controls detoxification of L-cysteine in Escherichia coli." Microbiology 162(9): 1698-1707.

Stenzler, B., A. Hinz, M. Ruuskanen and A. J. Poulain (2017). "Ionic Strength Differentially Affects the Bioavailability of Neutral and Negatively Charged Inorganic Hg Complexes." Environmental Science & Technology 51(17): 9653-9662.

Stenzler, B. R., J. Gaudet and A. J. Poulain (2018). "An Anaerobic Biosensor Assay for the Detection of Mercury and Cadmium." J Vis Exp(142).

Stevenson, A. K., L. K. Kimble, C. R. Woese and M. T. Madigan (1997). "Characterization of new phototrophic heliobacteria and their habitats." Photosynthesis Research 53(1): 1-11.

Su, Y. B., W. C. Chang, H. C. Hsi and C. C. Lin (2016). "Investigation of biogeochemical controls on the formation, uptake and accumulation of methylmercury in rice paddies in the vicinity of a coal-fired power plant and a municipal solid waste incinerator in Taiwan." Chemosphere 154: 375-384.

Sugio, T., M. Fujii, F. Takeuchi, A. Negishi, T. Maeda and K. Kamimura (2003). "Volatilization of mercury by an iron oxidation enzyme system in a highly mercury-resistant

Acidithiobacillus ferrooxidans strain MON-1." Biosci Biotechnol Biochem 67(7): 1537-1544.

Sunderland, E. M. (2007). "Mercury exposure from domestic and imported estuarine and marine fish in the U.S. seafood market." Environ Health Perspect 115(2): 235-242.

Tang, K. H., X. Feng, W. Q. Zhuang, L. Alvarez-Cohen, R. E. Blankenship and Y. J. Tang (2010). "Carbon flow of heliobacteria is related more to clostridia than to the green sulfur bacteria." J Biol Chem 285(45): 35104-35112.

CRAN Team. (2017). "Changes in R From version 3.4.2 to version 3.4.3." R Journal 9(2): 568-570.

Ticknor, J. L., K. H. Kucharzyk, K. A. Porter, M. A. Deshusses and H. Hsu-Kim (2015). "Thiol-Based Selective Extraction Assay to Comparatively Assess Bioavailable Mercury in Sediments." Environ Eng Sci 32(7): 564-573.

Vairavamurthy, A., B. Manowitz, G. W. Luther and Y. Jeon (1993). "Oxidation state of sulfur in thiosulfate and implications for anaerobic energy metabolism." Geochimica et Cosmochimica Acta 57(7): 1619-1623.

Vishnivetskaya, T. A., H. Hu, J. D. Van Nostrand, A. M. Wymore, X. Xu, G. Qiu, X. Feng, J. Zhou, S. D. Brown, C. C. Brandt, M. Podar, B. Gu and D. A. Elias (2018). "Microbial community structure with trends in methylation gene diversity and abundance in mercury-contaminated rice paddy soils in Guizhou, China." Environ Sci Process Impacts 20(4): 673-685.

Wang, X., C. J. Lin, W. Yuan, J. Sommar, W. Zhu and X. B. Feng (2016). "Emission-dominated gas exchange of elemental mercury vapor over natural surfaces in China." Atmospheric Chemistry and Physics 16(17): 11125-11143.

Wiatrowski, H. A., S. Das, R. Kukkadapu, E. S. Ilton, T. Barkay and N. Yee (2009). "Reduction of Hg(II) to Hg(0) by magnetite." Environ Sci Technol 43(14): 5307-5313.

Wiatrowski, H. A., P. M. Ward and T. Barkay (2006). "Novel reduction of mercury (II) by mercury-sensitive dissimilatory metal reducing bacteria." Environ Sci Technol 40(21): 6690-6696.

Yu, R. Q., J. R. Reinfelder, M. E. Hines and T. Barkay (2018). "Syntrophic pathways for microbial mercury methylation." ISME J 12(7): 1826-1835.

Zerkle, A. L., A. Kamyshny, L. R. Kump, J. Farquhar, H. Oduro and M. A. Arthur (2010). "Sulfur cycling in a stratified euxinic lake with moderately high sulfate: Constraints from quadruple S isotopes." Geochimica Et Cosmochimica Acta 74(17): 4953-4970.

Zhang, H., X. Feng, T. Larssen, G. Qiu and R. D. Vogt (2010). "In inland China, rice, rather than fish, is the major pathway for methylmercury exposure." Environ Health Perspect 118(9): 1183-1188.

Zhao, L., H. Chen, X. Lu, H. Lin, G. A. Christensen, E. M. Pierce and B. Gu (2017). "Contrasting Effects of Dissolved Organic Matter on Mercury Methylation by Geobacter sulfurreducens PCA and Desulfovibrio desulfuricans ND132." Environ Sci Technol 51(18): 10468-10475.

Zheng, W., G. J. Gilleaudeau, L. C. Kah and A. D. Anbar (2018). "Mercury isotope signatures record photic zone euxinia in the Mesoproterozoic ocean." Proc Natl Acad Sci U S A.

Zheng, W. and H. Hintelmann (2010). "Isotope fractionation of mercury during its photochemical reduction by low-molecular-weight organic compounds." J Phys Chem A 114(12): 4246-4253.

Chapter 3

Reducing power consumption by nitrogen fixation does not affect Hg reduction by the anoxygenic phototroph *Heliomicrobium modesticaldum*

Noémie C. Lavoie [a], Alexandre J. Poulain [a]

a - Biology Department, University of Ottawa, 30 Marie Curie, Ottawa, ON, K1N 6N5, Canada.

This chapter has been submitted to *Geobiology*.

N.B. Supporting information for this chapter can be found in **Appendix B**

3.1 ABSTRACT

The production of neurotoxic methylmercury (MeHg) in flooded anoxic rice paddy fields and its subsequent bioaccumulation in rice grains has become a global food safety issue. MeHg is produced by anaerobic microbes that rely on diverse terminal electron acceptors and nutrients, namely nitrogen. In rice paddies, nitrogen (N) fertilizers have been widely applied as an essential nutrient to grow rice. However, depending on the N species used in fertilizers this may inadvertently stimulate the microbial metabolisms involved in Hg methylation. Mercury (Hg) reduction to gaseous elemental Hg^0 by other anaerobic microbes can increase Hg mobility in anoxic sediments and affect Hg methylation by controlling the availability of inorganic Hg^{II}. Nitrogen amendments that supply N in its most oxidized form (ex: nitrate, dinitrogen) can inhibit MeHg production, whereas amendments supplying more reduced N (ex: ammonium & urea) increase MeHg production. Our prior work demonstrated that more reduced sulphur sources increased anaerobic Hg^{II} reduction, a possible consequence of a more reduced cytoplasm. However, little is known on the coupling of nitrogen, whether oxidized or reduced species, and anaerobic Hg^{II} reduction. To explore the potential influence of nitrogen availability and metabolism on anaerobic Hg^{II} reduction, we studied *Heliomicrobium modesticaldum* Ice1, an anoxygenic phototroph from the Heliobacteria family capable of ammonium uptake and nitrogen fixation. In this study, we tested how nitrogen fixation and ammonium uptake influenced the magnitude of Hg^{II} reduced to $Hg^0_{(g)}$. Here, we found that nitrogen species and availability did not appreciably influence the magnitude of Hg^{II} reduction. Findings from this study offer valuable insights into the yet-understood mechanism of Hg^{II} reduction by nitrogen-fixing photoheterotrophs. Furthermore, our results offer insights into how this microbial family, with

multiple isolates from rice paddy fields, stands to affect Hg cycling and limit the production of MeHg.

3.2 INTRODUCTION

Anthropogenic human activities have led to increased organic and inorganic mercury release into the environment. Airborne inorganic Hg pollution can travel long distances before being deposited in aquatic and terrestrial ecosystems including agricultural land [1]. Rice plants are well-known for their ability to hyperaccumulate metals [2,3] from the soil into their seeds. Rice paddies are frequently flooded leading to anoxia, and rich with substrates that stimulate the activity of anaerobic microbes responsible for transforming inorganic Hg^{II} into methylmercury (MeHg) such as sulphate reducers, fermenters, and methanogenic archaea [4]. As a result, rice paddies can be hotspots for MeHg production [5] and accumulation in rice grains [6]. Consequently, the consumption of rice has become an emerging pathway of neurotoxic MeHg exposure in people [7]. Given that rice is a staple food crop for over half of the world's population, it has become a global food safety issue [8,9]. Thus, investigating factors that influence the cycling of Hg in rice paddies and similar environments is vital to developing measures to mitigate Hg exposure to people.

Within flooded rice paddies, Hg redox cycling is one of the factors that can control the availability of inorganic Hg to methylators and MeHg accumulation in rice. Of particular interest is Hg^{II} reduction as it leads to the evasion of gaseous elemental Hg^0 from soils and water [10–12] and affects the bioavailability of inorganic Hg to methylators [13]. Abiotically, reduction can be catalyzed by dissolved organic matter [14] and iron minerals like mackinawite and magnetite [15,16]. Biotically-mediated Hg^{II} reduction can occur via the activity of aerobic [17] and anaerobic microorganisms [18–26] and is understood to serve as a detoxification mechanism or a way to maintain redox homeostasis [21]. In oxic environments, Hg^{II} reduction is catalyzed by aerobic microorganisms harbouring the

genetically encoded mercuric reductase [27]. This Hg^{II} reduction enzyme is, however, mainly absent in anaerobes [28]. Instead, anaerobic Hg^{II} reduction appears to be driven by core components of anaerobic respiration [22], fermentation [19] and anoxygenic phototrophy [20,21].

The connection between central energy metabolism and anaerobic Hg^{II} reduction gives rise to the question of how the microbial production of volatile Hg^0 is affected by the availability of nutrients such as nitrogen, carbon, or sulphur. Knowledge of this issue would further our understanding of how a common nutrient can influence anaerobic Hg^{II} reduction and Hg methylation. This issue is critical because anaerobic Hg^{II} reducers and Hg methylators can occur in the same anoxic environments and compete for the same pool of Hg substrates and nutrients that support anaerobic metabolisms. In addition, targeted nutrient amendments could form the basis for Hg pollution mitigation strategies to limit undesired microbial Hg cycling activity.

There is growing concern over how the disruption of nutrient cycling due to global changes and human activities may affect the rate and magnitude of microbial Hg transformations [29], particularly so within agricultural production systems susceptible to Hg contamination [30].
Of all nutrient amendments in rice paddies, nitrogen (N) is by far the most abundantly added, with an estimated 2.2 X 10^7 t N/km^2 applied to grow rice in 2010 globally [31]. Nitrogen amendments, such as ammonia, urea, and nitrate, are applied to enhance rice productivity as these systems are often N-limited [32]. These N additions, not only essential to plants, undergo a series of reactions as consortia of microorganisms vie for their use.

Chief among these nitrogen reactions, nitrification (from NH_4^+ to NO_3^-), denitrification (from NO_3^- to N_2), dissimilatory nitrate reduction (from NO_3^- to NH_4^+), nitrite oxidation (NO_2^- to NO_3^-), anaerobic ammonia oxidation (from NH_4^+ to N_2), and nitrogen fixation (from N_2 to NH_3) are mediated by certain microorganisms also suspected to be involved in the biogeochemical

cycling of mercury (**SI Table 1)**. Multiple pathways involved in nitrogen cycling have been found in putative Hg methylators from the Hg-MATE database [29]. Over 42% of putative methylators were capable of nitrogen fixation, 11% capable of dissimilatory nitrate reduction, 10% capable of some steps of denitrification, and 7% capable of nitrite oxidation. This highlights the genetic potential for the coupling of nitrogen and microbial MeHg production. Additionally, some studies have brought to light the impact of N amendments on Hg transformations in agricultural and other ecosystems. For example, urea addition, a source of NH_4^+, enhanced Hg bioavailability and abundance of Hg methylators which in turn increased the concentrations of MeHg in rice fields [33] but also in rice grains [34–36]. Conversely, nitrate fertilization in rice paddies caused a shift in Hg methylating microbial communities and decreased production of MeHg [37]. Nitrate addition to rice paddies was also found to inhibit Hg^{II} reduction (likely by microbes not harbouring the *mer* operon), Hg methylation, and MeHg demethylation via competition between nitrate and other electron acceptors [30]. The same study found that NH_4^+ and urea additions promoted Hg^0 production, suggested to be via an annamox-coupled metal reduction by unidentified anaerobes. The inhibitory effects of nitrate on Hg methylation have also been observed in aquatic ecosystems and are believed to be linked to the inhibition of sulphate-reducing bacteria by promoting the activity of dissimilatory nitrate reducers [38–42]. Nitrate being a more energetically favourable terminal electron acceptor than sulphate, its addition to ecosystems would have conferred an advantage to microbes capable of dissimilatory nitrate reduction. Interestingly, Hg demethylation, a potential microbial detoxification pathway, has also been observed to be partly inhibited by nitrate [43]. Lastly, nitrous oxide, a potent greenhouse gas that is emitted from agricultural soils [44], was experimentally shown to inhibit MeHg formation by methanogenic archaea and sulphate-reducing bacteria in Arctic tundra soils [45].

Despite the many recent studies uncovering links between N species and microbial Hg cycling, critical knowledge gaps remain. Specifically, as others have also mentioned [30], the roles different N species and metabolism play in anaerobic Hg^{II} reduction have seldom been reported and require further study. To address this knowledge gap, we investigated the influence of ammonium (NH_4^+) and dinitrogen (N_2) on anaerobic Hg^{II} reduction using a model microorganism from the *Heliobacteriacea*, *Heliomicrobium modesticaldum* Ice1, one of the best-studied members of this family, capable of the highest anaerobic Hg^{II} reduction recorded to date [19]. This family is characterized as metabolically versatile, terrestrial, spore-forming anoxygenic photoheterotrophs capable of growing in the absence of light via fermentation. We elected to work with the Heliobacteria as many representatives are commonly found in rice paddies [46]. Thus, further characterizing the factors that influence their ability to reduce Hg^{II} will inform us of their likely ecological role within rice paddy Hg cycling. In addition, since many Heliobacteria are capable of biological nitrogen fixation [47–50] this provides us the opportunity to investigate how nitrogen source availability and metabolism influence the magnitude of Hg^{II} reduction. *H. modesticaldum* Ice1 can acquire nitrogen either via NH_4^+ uptake or via $N_{2(g)}$ fixation into NH_3 [51]. In bacteria, NH_4^+ uptake from the environment is believed to occur mainly via passive diffusion at concentrations >1 mM [52]. Under lower or depleted NH_4^+ concentrations, *amt* gene expression encoding ammonium transporters, is upregulated as cells attempt to scavenge any easily available nitrogen from their environment [49]. The glutamine synthetase/glutamate synthase (GS/GOGAT) pathway then serves as the major means of incorporating exogenous ammonium or ammonium fixed from N_2 [48]. This pathway is essential for growth as glutamine is the main nitrogen donor for purine and pyrimidine synthesis. In Heliobacteria, N_2 fixation relies on the nitrogenase complex, encoded by *nifHDK* [47], to break the triple bond in N_2 and form NH_3. Under conditions of insufficient bioavailable nitrogen

sources, diazotrophs like Heliobacteria transform one molecule of N_2 into 2 molecules of NH_3. This process requires 16 ATP molecules as a source of chemical energy and 8 molecules of reduced ferredoxin (Fd_{red}) as a source of reducing power: $N_2 + 8\ H^+ + 8\ Fd_{red} + 16\ ATP = 2\ NH_3 + H_2 + 8\ Fd_{ox} + 16\ ADP + 16\ P_i$ [53]. As this process is quite costly to cells, it lowers growth yield in phototrophic and chemotrophic cultures of *Heliobacterium mobile* [48] and *Heliomicrobium modesticaldum* Ice1 [49,50] compared to growth on NH_4^+. Due to such a high cost of fixing N_2, nitrogenase activity is "switched-off" and its transcription is repressed by the presence of NH_4^+ [48,49,54].

Mechanistic insights into Hg^{II} reduction by Heliobacteria have revealed that it is non-*mer* mediated, occurs during both anoxygenic photoheterotrophic and fermentative growth, and is suspected to be tied to the intracellular availability of reduced redox cofactors such as ferredoxins [19,20]. A general hypothesis that we are currently investigating is that the magnitude of anaerobic Hg^{II} reduction to Hg^0 depends on the intracellular availability of reduced redox cofactors, or reducing power, which is also drawn upon to assimilate certain nutrients into biomass. Based on this hypothesis, we predicted that fixing N_2 would decrease the magnitude of Hg^{II} reduction compared to the less energy and reducing power-intensive uptake of NH_4^+. In this study, the effects of N_2 and NH_4^+ on anaerobic Hg^{II} reduction were elucidated by tracking the production of gaseous elemental Hg^0 by phototrophic cultures of *Heliomicrobium modesticaldum* Ice1 grown in controlled-conditions bioreactors. Here, we show that despite differences in growth and N source, the magnitude of Hg^{II} reduced by *H. modesticaldum* Ice1 did not appreciably vary between N_2 fixation and NH_4^+ assimilation. We further discuss the role of Heliobacteria as nitrogen fixers and Hg^{II} reducers within the context of competing substrate availability and Hg methylation.

3.3 METHODS

3.3.1 Microbial culturing

All experiments were conducted using the strain *Heliomicrobium modesticaldum* Ice1 from the DSMZ culture collection (DSM-9504). Cell cultures were handled under anaerobic conditions in a Coy anaerobic glove box (atmosphere 97% $N_{2(g)}$ and 3% $H_{2(g)}$) or by using sterile anaerobic benchtop techniques where all equipment was sparged with 100% $N_{2(g)}$ prior to use. For all growth assays and bioreactor experiments, new cell cultures were revived in the anaerobic glovebox from cryostocks kept at −80°C by scraping frozen culture with a sterile pipette tip and discarding it into a Balch tube containing either growth medium PYE devoid of ammonium (PYE-N_2) or PYE with 15mM ammonium (PYE-NH_4^+), where the headspace of the tubes was then sparged to contain 100% $N_{2(g)}$ for PYE-N_2 and 100% $Ar_{(g)}$ for PYE-NH_4^+. We estimated that the $N_{2(g)}$ concentration in a 10mL Balch tube and a 75mL serum bottle added at a gauge pressure of 0.54atm and incubated at 50°C is 58.2mM.

The medium composition of PYE-NH_4^+ is Na-pyruvate 2.2 g/L, yeast extract 0.2 g/L, K_2HPO_4 1 g/L, $MgSO_4*7H_2O$ 0.2 g/L, $Na_2S_2O_3$ 1 mM, $CaCl_2*2H_2O$ 0.02 g/L, $(NH_4)_2SO_4$ 1 g/L (15.1 mM of NH_4^+), anoxic $FeSO_4$ 20 µM, D-biotin 0.015 µg/mL, vitamin B12 as cyanocobalamin 0.02 µg/mL, and 1 mL of trace element solution SL6. Trace elements SL6 contained: $ZnSO_4*7$ H_2O 0.1 g/L, $MnCl_2*4$ H_2O 0.3 g/L, H_3BO_3 0.3 g/L, $CoCl_2*6H_2O$ 0.2 g/L, $CuCl_2*2H_2O$ 0.01 g/L, $NiCl_2*6H_2O$ 0.02 g/L, $Na_2MoO_4*2H_2O$ 0.03 g/L. The medium composition of PYE-N_2 is the same as PYE-NH_4^+ except for the omission of $(NH_4)_2SO_4$. The only source of nitrogen is gaseous $N_{2(g)}$ provided in the headspace of culturing vessels and bubbled in bioreactors.

Yeast extract could be not completely omitted because while it contains nitrogen sources primarily in the form of glutamate there are also other essential yet unknown trace nutrients for *H.*

modesticaldum Ice1. All of our efforts to create a growth medium devoid of yeast extract have failed to support growth during NH_4^+ uptake and N_2 fixation. Therefore, the compromise was to keep a low but consistent amount of yeast extract in both versions of the growth medium. Furthermore, we tested whether 0.2g/L of yeast extract alone could supply sufficient nitrogen to support growth in PYE-N_2. We compared *H. modesticaldum* Ice1 growth in PYE-N_2 with $Ar_{(g)}$ in the headspace versus with $N_{2(g)}$ in the headspace. No growth was observed over the course of 72 hours if $Ar_{(g)}$ was the headspace gas, confirming that the 0.2 g/L of yeast extract did not supply enough nitrogen on its own to support growth (**SI Figure 3.1)**. As such, we included 0.2 g/L of yeast extract in both growth media.

Cultures were incubated at 50 °C with an incandescent light source emitting photoactive radiation (PAR) at an intensity of 80 μmol photon m^{-2} s^{-1} until they reached mid-exponential stage. Cultures were then used to start new cultures with a 10% (v/v) inoculum into new Balch tubes containing 10 mL of the same growth medium.

For bioreactor experiments, cells were harvested again after reaching mid-exponential to start cultures with a 10% (v/v) inoculum in serum bottles containing 75 mL of the same growth medium. Upon reaching mid- to late-exponential phase, these cultures were used as a 10% (v/v) inoculum in bioreactor experiments containing the same growth medium.

3.3.2 Bioreactor experiments

All conditions tested in the bioreactor are summarized in **SI Table 3.2** For experiments testing the influence of N_2 fixation in medium PYE-N_2, bioreactor vessels were bubbled with 100% $N_{2(g)}$ at a rate of 0.5 L/min. The estimated concentration of $N_{2(g)}$ in the bioreactor is 37.7 mM. The bioreactor set-up and subsampling methodologies are identical to those validated and used in previous work [19,21] except for the following modification. For all live cell bioreactors, cultures

were inoculated into the bioreactor and incubated sealed shut for approximately 24 hours in the absence of Hg until an O.D. 600nm of ~0.1-0.15 was reached. Once the desired O.D. was reached, bioreactor gas bubbling resumed, and Hg was spiked. All bioreactor experiments were carried out at 50°C at a light intensity of 20 μmol photon m^{-2} s^{-1} to limit abiotic photoreduction of Hg^{II} [21]. All live cell bioreactor treatments were performed in duplicates with initial *H. modesticaldum* Ice1 cell inoculum of 10% (v/v) from cultures grown until mid- to late-exponential phase, and abiotic controls were performed once. Each bioreactor experiment was spiked with 250 pM of $HgCl_2$ and ran for 48 hr to measure cumulative Hg^0 production using a Tekran 2537B CVAFS Analyzer.

3.3.3 Statistical analyses

It was important to us to determine a threshold at which changes in cumulative Hg^0 production could be deemed biologically meaningful. We set this threshold to at least 50% decrease in Hg^0 production between treatments because our past experiments have highlighted that innate biological variability between replicates can lead to up to 25% differences in cumulative Hg^0 produced. Given the lengthy nature of the experiments, 7 days of culturing and 48 hours to run one replicate experiment, we prioritized replicating experiments if they met our threshold for biologically meaningful decreases in Hg^0 production. Thus, due to the lack of biologically meaningful decrease in Hg^0 production between the treatments, bioreactor experiments were repeated only in duplicates. All essential statistical information is provided in the figure captions. Given n = 2 and the lack of difference in Hg^{II} reduction between treatments, we did not perform additional statistical tests.

3.4 RESULTS AND DISCUSSION

3.4.1 Growth on N_2 or NH_4^+ is supported during anoxygenic photoheterotrophy

In this work, our first objective was to establish and validate the growth media and conditions that would support *H. modesticaldum* Ice1 growth on both nitrogen sources and whether growth was possible during N_2 fixation by phototrophic and fermenting cultures. *H. modesticaldum* Ice1 could not reliably grow on N_2 in the dark via fermentation in the same growth medium that supported phototrophic N_2 fixation (**Figure 3.1)**, and cell growth rates and yields were not compatible with our bioreactor methodology. As such, we omitted testing fermentative Hg^{II} reduction in the present work, focusing rather on comparing phototrophic Hg^{II} reduction under different nitrogen treatments. The chemical composition of both growth media used in this study only differed in their nitrogen source. Here, phototrophic NH_4^+ uptake and assimilation were supported in growth medium PYE-NH_4^+, which contained $(NH_4)_2SO_4$. Additionally, phototrophic N_2 fixation was supported in growth medium PYE-N_2, where the sole source of nitrogen that supported growth was $N_{2(g)}$ (**SI Fig. 3. 1**).

3.4.2 Nitrogen source and availability does not influence Hg^{II} reduction during phototrophy

The trends observed for biotic Hg^0 production were not in line with our hypothesis and predictions as the magnitude of Hg^0 produced did not vary considerably between N_2 fixation (74.26 pmol, 85.08 pmol) and NH_4^+ uptake (79.00 pmol, 80.07 pmol) despite, even, differences in growth yield (**Figure. 3.2A-B)**. Hg^0 production in the absence of cells in both sterile growth media was negligible (<10 pmol) (**SI Figure 3.2**).

Next, we tested whether the absence of exogenous nitrogen sources can affect Heliobacteria's ability to reduce Hg^{II} by placing cultures in medium PYE-N_2 devoid of nitrogen sources and replacing the bioreactor gas phase with Argon. We found that photoheterotrophic Hg^{II} reduction in medium PYE-N_2 under nitrogen-limited conditions with Argon gas (90.35 pmol, 91.11 pmol) (**Figure 3.3A**) was comparable to Hg^{II} reduction in the presence of nitrogen gas (74.26 pmol, 85.08 pmol) (**Figure 3.2A**) even though cultures did not appreciably grow in the bioreactor (**Figure 3.3B**). These results corroborate our multiple observations that photoheterotrophic Hg^{II} reduction by Heliobacteria can occur in metabolically active but non-significantly growing cultures [19,20].

3.4.3 Exposure to oxygen inhibits Hg^0 production

We further sought to test the limits of Hg^{II} reduction by *H. modesticaldum* Ice1 by determining whether reduction may occur when cultures are exposed to room air. Exposure to O_2 is known to irreversibly oxidize heliobacterial bacteriochlorophyll *g* pigments and cause cell lysis [46,55]. Additionally, nitrogenases are extremely sensitive to O_2, which causes irreversible destruction of these enzymes [56]. As such, we expected these conditions to inhibit Hg^{II} reduction via: 1) fully disrupting metabolism and 2) molecular oxygen re-oxidizing any produced Hg^0 to Hg^{II} [57]. We found that exposure to room air during bioreactor assays did indeed inhibit Hg^{II} reduction and caused cell lysis, marked by a decreasing O.D. 600nm (**SI Figure 3.3. A-B)**. Though strict anaerobes, Heliobacteria are exposed to oxygen occasionally in their native terrestrial environments. Flooded anoxic soils like rice paddies may drain or mix and re-introduce O_2, and hot spring biofilms may seasonally produce O_2 as overlying cyanobacterial mats bloom. Heliobacteria likely survive seasonal O_2 exposure by sporulation [46,58]; during that time of desiccation and O_2 exposure, cells remain dormant, awaiting favourable conditions. These results

provide further clarification on the role of Heliobacteria as Hg^{II} reducers strictly during periods of anoxia in rice paddy ecosystems or in hot spring microbial mats where they likely co-exist with anaerobic Hg methylators.

3.4.4 Insights into the Hg^{II} reduction mechanism of Heliobacteria

In this study, we found that *H. modesticaldum* Ice1 readily reduces Hg^{II} even in the absence of added nitrogen, but that ability strictly occurs under anoxic conditions. The accumulating weight of evidence suggests that in Heliobacteria, photoheterotrophic reduction does not require active cell growth and can occur in certain nutrient-limited conditions. By contrast, our previous research established that fermentative Hg^{II} reduction by Heliobacteria requires the oxidizable carbon source, pyruvate, and that the magnitude of Hg^{II} reduced depends on the concentration of pyruvate provided [19].

Our previous insights into the mechanism of Heliobacterial Hg^{II} reduction suggest that the redox transformation depends in part on the availability of reducing power [19]. In Heliobacteria, reducing power, or the availability of reduced redox cofactors such as the one-electron-carrying ferredoxins, is generated through pyruvate oxidation during fermentation or through photo-induced electron transfer reactions during phototrophy [50,59,60]. Interestingly, our results show that even in conditions where significant amounts of reducing power are expected to be used by a costly metabolic process, N_2 fixation, photoheterotrophic Hg^{II} reduction still occurs. This is in stark contrast to our prior findings studying the influence of sulphur sources and metabolism on Hg^{II} reduction by *Heliobacterium mobile* [20]. The magnitude of Hg^{II} reduction increased when *H. mobile* grew on more reduced sulphur sources like thiosulphate & cysteine. We proposed that assimilating more reduced sulphur sources was less “costly” in terms of reducing power, thus increasing the potential source of electrons for the reduction of Hg^{II}. In the present study, however, we do not

observe any relation between Hg^{II} reduction and the assimilation of more or less costly N substrates. We further discuss potential causes for the lack of observed differences between Hg^{II} reduction during photoheterotrophic growth on NH_4^+, N_2, or in nitrogen-depleted conditions.

3.4.5 Possibility #1 for lack of differences: No meaningful differences in reducing power availability

We cannot currently determine if photo-induced electron transfer and pyruvate oxidation can generate comparable amounts of reducing power, whether in the form of ferredoxins or NAD(P)H, during N_2 fixation, NH_4^+ uptake, and N-limited conditions. Further investigations of this possibility would require a method amenable to quantifying the concentrations of reduced versus oxidized redox cofactors like NAD(P)H and ferredoxins in our bioreactor experiments with Heliobacteria. In our hands, existing redox cofactor quantification protocols have required more biomass than what Heliobacteria can achieve in bioreactor experiments. In addition, to the best of our knowledge, there are no published methods to measure concentrations of oxidized versus reduced ferredoxins. We can, however, make a few inferences on the differences in reducing power requirements for N_2 fixation and Hg^{II} reduction. Eight electrons are required to reduce N_2 to NH_3, whereas 2 electrons are required to reduce Hg^{II} to Hg^0. Considering the physiological needs of cells, micro to millimolar concentrations of N_2 need to be reduced into biologically available NH_3. One can thus estimate that for 1 mM of N_2 to be fixed, approximately 8 mM of reducing equivalents must be used by the cell. By comparison, Hg^{II} reduction by Heliobacteria occurs at 250 pM concentrations of Hg^{II} and would thus require ~500 pM of reducing equivalents. It is therefore possible we observed no difference in Hg^{II} reduction due to N_2 fixation because 250 pM of Hg^{II} to Hg^0 requires very little reducing power. It is possible that sufficient amounts of reducing power remain available despite the nitrogenase consuming mM amounts of reduced ferredoxins.

3.4.6 Possibility #2: Dedicated source of reducing power for nitrogen fixation

Another possible explanation for the lack of differences between treatments is whether the ferredoxins used as reducing power by the nitrogenase are also a source of reducing power for Hg^{II} reduction. *H. modesticaldum* Ice1's genome contains multiple mobile dicluster [4Fe-4S] ferredoxin-encoding genes, some with experimentally verified enzymatic partners (i.e. HM1_1462, HM1_1461, HM1_2505 [60–62]*)* and some with unknown or putative partners (i.e.: HM1_0869, HM1_1043, HM1_0357, HM1_2767). This knowledge gap makes it unclear whether all these ferredoxins behave as part of a common and interchangeable pool of "available" reducing power or if some genes encode for ferredoxins with enzymatic specificity to the nitrogenase. Studies using other microbial models have found evidence in support of ferredoxins having a certain degree of enzyme coupling specificity. Some have argued that, by virtue of being genetically encoded electron carriers, ferredoxins can tune their reduction potentials and partner specificity through mutations [63]. This would allow ferredoxins to selectively shuttle electrons to specific pathways [64,65]. According to the annotated genome of *H. modesticaldum* Ice1, there is a ferredoxin gene (HM1_0869) in the *nif* nitrogenase operon, which, by its proximity, may imply the existence of a ferredoxin that supplies reducing power only to this nitrogenase [66]. Comparisons of the transcriptomes of *H. modesticaldum* Ice1 during N_2 fixation versus NH_4^+ uptake reveal that in the absence of NH_4^+, all genes involved in fixing N_2 are upregulated by ~25 fold, including HM1_0869 [49]. By contrast, expression of the two ferredoxins, HM1_1462, HM1_1461, known to accept electrons from the photosynthetic reaction center and pyruvate oxidation [60–62] was somewhat reduced in the absence of NH_4^+. This may be evidence in favour of a pool of ferredoxins, encoded by HM1_0869, that primarily or strictly transfers electrons to the nitrogenase. However,

further enzymatic assays specifically investigating the interaction of different ferredoxins with the nitrogenase would be required to shed more light on this matter.

At the time of writing this, a timely study by colleagues was published on the topic of ferredoxin specificity in *H. modesticaldum* Ice1 [60]. Authors identified which of the small mobile dicluster ferredoxins encoded by the *H. modesticaldum* genome are capable of accepting electrons from the heliobacterial photosynthetic reaction center (HbRC) and pyruvate:ferredoxin oxidoreductase (PFOR). They found that only ferredoxins encoded by HM1_1462, HM1_1461, and HM1_2505 could accept electrons from HbRC and PFOR. By contrast, HM1_0869 and the other putative ferredoxins were not found to interact with either enzymatic complex. Proteomic analyses of all 7 ferredoxins detected the production of all ferredoxins except for HM1_1043 and HM1_2767 by the wild-type strain under nitrogen-depleted conditions. In studying HM1_0869, the putative ferredoxin within the *nif* operon, they found that it was always expressed under nitrogen-depleted conditions and never expressed in the presence of NH_4^+. However, counterintuitively, gene deletion mutants without HM1_0869 could grow readily in nitrogen-depleted conditions via N_2 fixation. Findings on HM1_0869 indicate it is non-necessary for diazotrophic growth, but it is expressed nonetheless, perhaps serving a supportive role in supplying additional reducing power or a yet unknown function.

By drawing on experimental evidence acquired both in the present work and by others studying Heliobacteria transcriptomes and ferredoxin expression and specificity, we deem there is evidence in favour of the following conclusion. The pool of reduced ferredoxins the nitrogenase draws on, which may or may not be a separate pool encoded by HM1_0869, does not influence photoheterotrophic Hg^{II} reduction by *H. modesticaldum* Ice1. It is also possible that the concentration of reduced ferredoxins is not appreciably different between our treatments (i.e.

NH_4^+, N_2, no nitrogen) to affect the cell's ability to reduce trace concentrations of Hg^{II}. Furthermore, though it may be a small step towards elucidating the mechanism of Hg^{II} reduction by Heliobacteria, we can confidently assert that the nitrogenase, an enzyme that catalyzes oxidation-reduction reactions, does not play a role in Hg^{II} reduction. This is substantiated by the observation that Hg^{II} reduction occurs in the presence of NH_4^+, a condition that shuts down all nitrogenase activity, and in the presence of N_2 fixation.

Ultimately, though the lack of a known cellular Hg^{II} reduction mechanism hampers further interpretations of this study's results, they highlight that perhaps not all nutrients and their metabolic pathways influence the magnitude of Hg^{II} reduction by Heliobacteria. To further investigate the mechanism of Hg^{II} reduction in Heliobacteria, we have begun using a targeted-gene deletion approach. Our future work seeks to identify genetically encoded elements that enable Heliobacteria to reduce Hg^{II} to its less toxic gaseous form Hg^0.

3.5 ENVIRONMENTAL IMPLICATIONS

In the environment, whether it be rice paddies or hot spring microbial mats, microbial cells are rarely growing at the exponential rates observed in laboratories due in part to frequent nutrient limitations. *H. modesticaldum* Ice1's ability to photoreduce Hg^{II} under growth- and nutrient-limited laboratory conditions suggests it may be able to do so readily in environments where it is found. Heliobacteria are abundantly found in flooded rice paddy soils, can fix nitrogen and grow using simple organic carbon sources. It has thus been proposed that they may have a mutually beneficial relationship with plants such as rice, where they provide biologically available nitrogen to plants and, in exchange, receive organic carbon [46]. Given Heliobacteria's ability to reduce Hg^{II}, it would be of great interest to uncover how their close association influences mercury uptake by rice plants. Overall, our study's findings highlight the possibility that in anoxic environments where

Heliobacteria and Hg methylators cohabitate, Heliobacteria could likely reduce Hg^{II} while using N_2, NH_4^+, and even while being N-limited. This positions Heliobacteria as resilient anaerobic microbes that could have a competing advantage against Hg methylators and thus influence the fate of mercury pollution.

Finally, our research aims to enhance our understanding of the impact changes in nutrient availability have on microbial activity and, in turn, on the mobility and toxicity of Hg in the environment. This is a particularly crucial area of research as Hg pollution in agricultural settings poses an increasing threat to human health. Further investigation into anaerobic microbial Hg^{II} reduction is imperative for refining global Hg cycling models and developing viable strategies to mitigate Hg pollution. We emphasize the importance of carefully tailored nitrogen amendments that consider their potential impacts not only on crop productivity but also on microbial Hg transformations.

ACKNOWLEDGMENETS

Our work was funded by NSERC Discovery and Accelerator grants, CFI funding to AJP and NSERC graduate scholarships to NCL.

AUTHOR CONTRIBUTIONS

N.C.L and A.J.P. designed experiments, N.C.L. carried them out and performed data analysis, and N.C.L. and A.J.P. wrote the manuscript.

3.6 FIGURES AND CAPTIONS

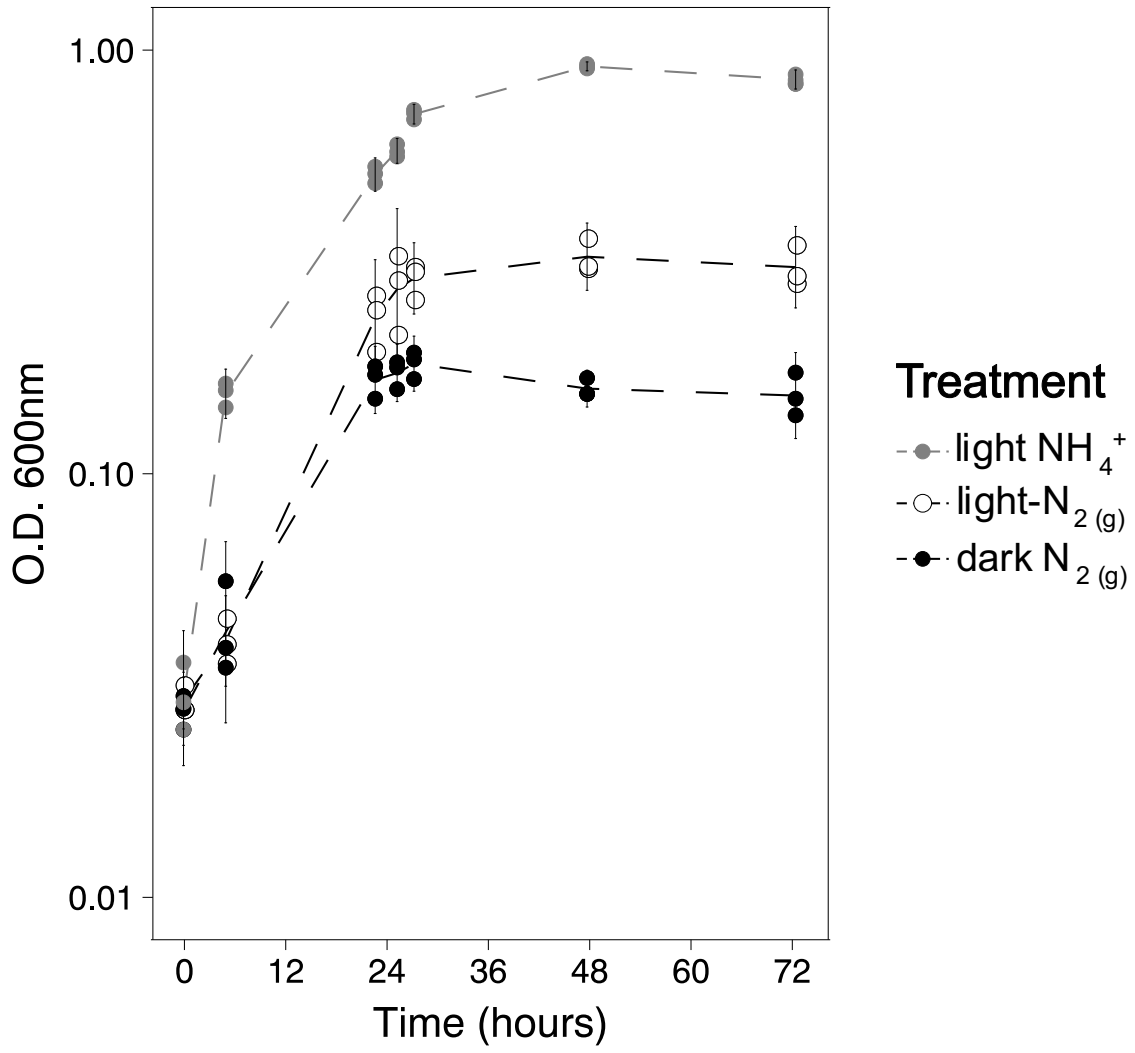

Figure 3.1: Phototrophic and chemotrophic growth of *H. modesticaldum* Ice1 in the presence of either $N_{2(g)}$ or NH_4^+ nitrogen sources.
Cultures were grown in either PYE-N_2 ($N_{2(g)}$) or PYE-NH_4^+ (NH_4^+). Results are shown for n = 3 biological replicates (circles), and error bars represent standard deviations for each time point. Note that fermentative growth in PYE-NH_4^+ was omitted from testing upon discovering that fermentative growth in PYE-N_2 would not be successful in later bioreactor experiments.

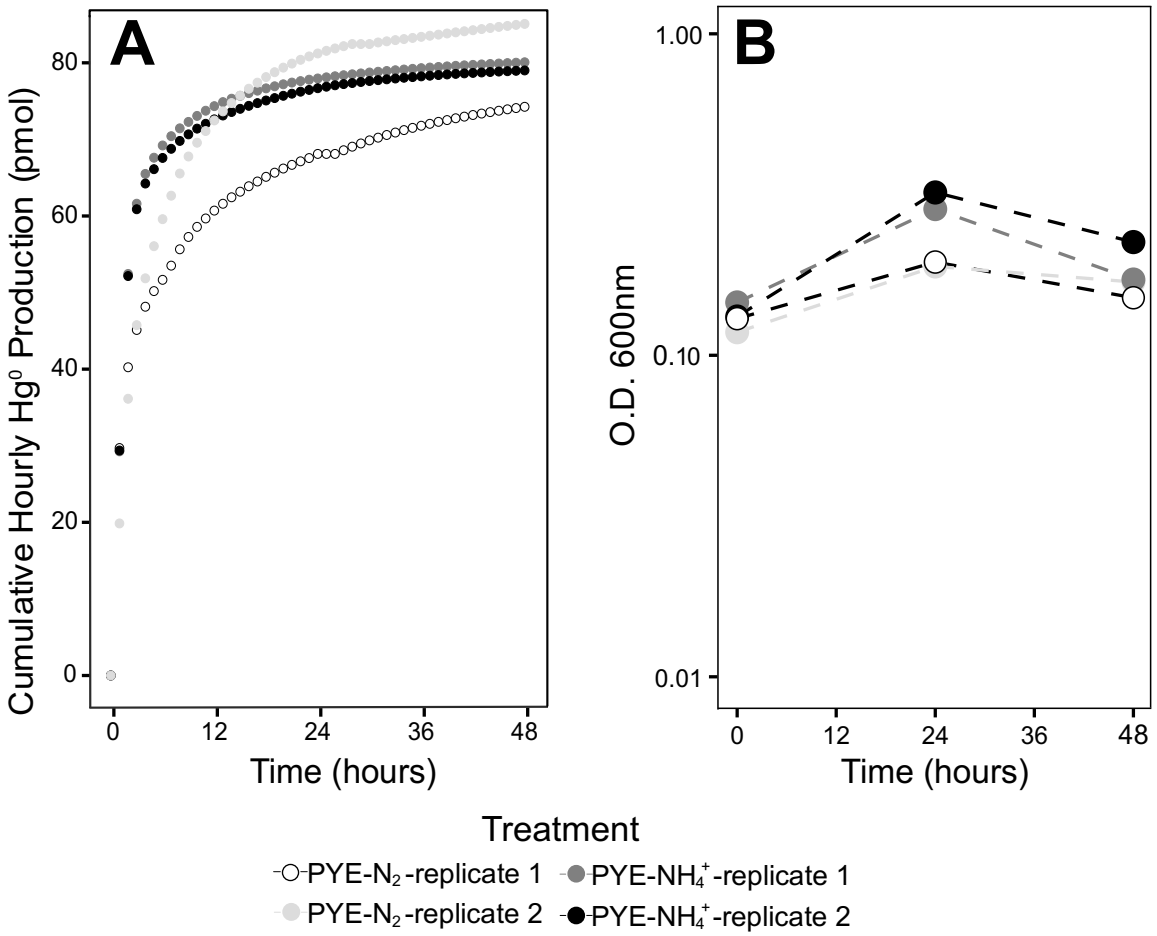

Figure 3.2: Hg^0 production by *H. modesticaldum* Ice1 grown phototrophically in media PYE-N_2 and PYE-NH_4^+.

(A) Cumulative hourly Hg^0 production and (B) cell growth (as measured by O.D. 600 nm) during bioreactor experiments. Results are representative cases of biological replicates (n = 2). Each cumulative Hg^0 data point was recorded once per time step by the instrument, as such no error bars were included. Hg was added to a final concentration of 250 pM. The gas source bubbled for PYE-N_2 experiments was 100% $N_{2(g)}$ and for PYE-NH_4^+ was 100% $Ar_{(g)}$.

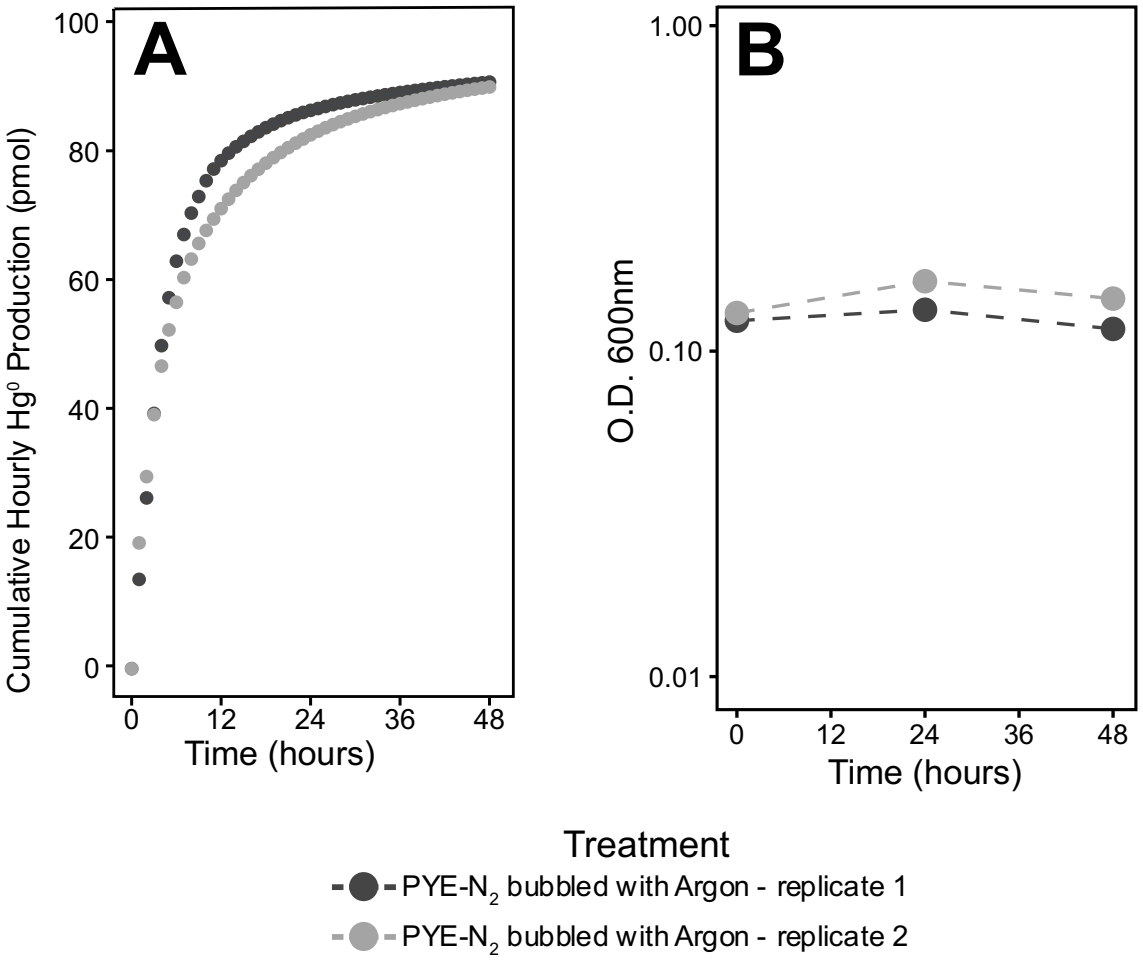

Figure 3.3: Hg^0 production by *H. modesticaldum* Ice1 grown phototrophically in media PYE-N_2 supplied with Argon gas.
(A) Cumulative hourly Hg^0 production and (B) cell growth (as measured by O.D. 600 nm) during bioreactor experiments. Results are representative cases of biological replicates (n = 2). Each cumulative Hg^0 data point was recorded once per time step by the instrument, as such no error bars were included. Hg was added to a final concentration of 250 pM.

3.7 REFERENCES

1. Fitzgerald, W. F., Engstrom, D. R., Mason, R. P. & Nater, E. A. The Case for Atmospheric Mercury Contamination in Remote Areas. *Environ. Sci. Technol.* **32**, 1–7 (1998).

2. Peralta-Videa, J. R., Lopez, M. L., Narayan, M., Saupe, G. & Gardea-Torresdey, J. The biochemistry of environmental heavy metal uptake by plants: Implications for the food chain. *Int. J. Biochem. Cell Biol.* **41**, 1665–1677 (2009).

3. McLaughlin, M. J., Parker, D. R. & Clarke, J. M. Metals and micronutrients – food safety issues. *Field Crops Res.* **60**, 143–163 (1999).

4. Parks, J. M. *et al.* The genetic basis for bacterial mercury methylation. *Science* **339**, 1332–5 (2013).

5. Rothenberg, S. E. & Feng, X. Mercury cycling in a flooded rice paddy. *J. Geophys. Res. Biogeosciences* **117**, n/a-n/a (2012).

6. Liu, J., Meng, B., Poulain, A. J., Meng, Q. & Feng, X. Stable isotope tracers identify sources and transformations of mercury in rice (Oryza sativa L.) growing in a mercury mining area. *Fundam. Res.* **1**, 259–268 (2021).

7. Zhang, H., Feng, X., Larssen, T., Qiu, G. & Vogt, R. D. In inland China, rice, rather than fish, is the major pathway for methylmercury exposure. *Env. Health Perspect* **118**, 1183–8 (2010).

8. Rothenberg, S. E., Windham-Myers, L. & Creswell, J. E. Rice methylmercury exposure and mitigation: a comprehensive review. *Env. Res* **133**, 407–23 (2014).

9. Liu, M. *et al.* Rice life cycle-based global mercury biotransport and human methylmercury exposure. *Nat. Commun.* **10**, (2019).

10. Ao, M. *et al.* The influence of atmospheric Hg on Hg contaminations in rice and paddy soil in the Xunyang Hg mining district, China. *Acta Geochim.* **36**, 181–189 (2017).

11. Kim, K. H., Kim, M. Y., Kim, J. & Lee, G. Effects of changes in environmental conditions on atmospheric mercury exchange: Comparative analysis from a rice paddy field during the two spring periods of 2001 and 2002. *J. Geophys. Res.-Atmospheres* **108**, (2003).

12. Wang, X. *et al.* Emission-dominated gas exchange of elemental mercury vapor over natural surfaces in China. *Atmospheric Chem. Phys.* **16**, 11125–11143 (2016).

13. Colombo, M. J., Ha, J. Y., Reinfelder, J. R., Barkay, T. & Yee, N. Anaerobic oxidation of Hg(0) and methylmercury formation by Desulfovibrio desulfuricans ND132. *Geochim. Cosmochim. Acta* **112**, 166–177 (2013).

14. Gu, B. *et al.* Mercury reduction and complexation by natural organic matter in anoxic environments. *Proc Natl Acad Sci U A* **108**, 1479–83 (2011).

15. Bone, S. E., Bargar, J. R. & Sposito, G. Mackinawite (FeS) reduces mercury(II) under sulfidic conditions. *Env. Sci Technol* **48**, 10681–9 (2014).

16. Wiatrowski, H. A. *et al.* Reduction of Hg(II) to Hg(0) by magnetite. *Env. Sci Technol* **43**, 5307–13 (2009).

17. Christakis, C. A., Barkay, T. & Boyd, E. S. Expanded Diversity and Phylogeny of mer Genes Broadens Mercury Resistance Paradigms and Reveals an Origin for MerA Among Thermophilic Archaea. *Front. Microbiol.* **12**, (2021).

18. Liu, S. N. & Wiatrowski, H. A. Reduction of Hg(II) to Hg(0) by Biogenic Magnetite from two Magnetotactic Bacteria. *Geomicrobiol. J.* **35**, 198–208 (2018).

19. Gregoire, D. S., Lavoie, N. C. & Poulain, A. J. Heliobacteria Reveal Fermentation As a Key Pathway for Mercury Reduction in Anoxic Environments. *Env. Sci Technol* **52**, 4145–4153 (2018).

20. Lavoie, N. C., Gregoire, D. S., Stenzler, B. R. & Poulain, A. J. Reduced sulphur sources favour Hg(II) reduction during anoxygenic photosynthesis by Heliobacteria. *Geobiology* (2019) doi:10.1111/gbi.12364.

21. Grégoire, D. S. & Poulain, A. J. A physiological role for HgII during phototrophic growth. *Nat. Geosci.* **9**, 121–125 (2016).

22. Lin, H., Morrell-Falvey, J. L., Rao, B., Liang, L. & Gu, B. Coupled mercury-cell sorption, reduction, and oxidation on methylmercury production by Geobacter sulfurreducens PCA. *Env. Sci Technol* **48**, 11969–76 (2014).

23. Schaefer, J. K., Letowski, J. & Barkay, T. mer-mediated resistance and Volatilization of Hg(II) under anaerobic conditions. *Geomicrobiol. J.* **19**, 87–102 (2002).

24. Wiatrowski, H. A., Ward, P. M. & Barkay, T. Novel reduction of mercury (II) by mercury-sensitive dissimilatory metal reducing bacteria. *Env. Sci Technol* **40**, 6690–6 (2006).

25. Zhao, L. D. *et al.* Contrasting effects of dissolved organic matter on mercury methylation by Geobacter sulfurreducens PCA and Desulfovibrio desulfuricans ND132. *Environ. Sci. Technol.* **51**, 10468–10475 (2017).

26. Lu, X. *et al.* Anaerobic Mercury Methylation and Demethylation by Geobacter bemidjiensis Bem. *Env. Sci Technol* **50**, 4366–73 (2016).

27. Osborn, A. M., Bruce, K. D., Strike, P. & Ritchie, D. A. Distribution, diversity and evolution of the bacterial mercury resistance (mer) operon. *FEMS Microbiol. Rev.* **19**, 239–262 (1997).

28. Barkay, T., K. Kritee, Kritee, K., Boyd, E. S. & Geesey, G. G. A thermophilic bacterial origin and subsequent constraints by redox, light and salinity on the evolution of the microbial mercuric reductase. *Environ. Microbiol.* **12**, 2904–2917 (2010).

29. Sonke, J. E. *et al.* Global change effects on biogeochemical mercury cycling. *Ambio* **52**, 853–876 (2023).

30. Chen, J. *et al.* The divergent effects of nitrate and ammonium application on mercury methylation, demethylation, and reduction in flooded paddy slurries. *J. Hazard. Mater.* **460**, 132457 (2023).

31. Zhang, X. *et al.* Managing nitrogen for sustainable development. *Nature* **528**, 51–59 (2015).

32. Linquist, B. A., Liu, L., van Kessel, C. & van Groenigen, K. J. Enhanced efficiency nitrogen fertilizers for rice systems: Meta-analysis of yield and nitrogen uptake. *Field Crops Res.* **154**, 246–254 (2013).

33. Sun, T. *et al.* Inorganic versus organic fertilizers: How do they lead to methylmercury accumulation in rice grains. *Environ. Pollut.* **314**, 120341 (2022).

34. Tang, Z. *et al.* Mercury in rice (Oryza sativa L.) and rice-paddy soils under long-term fertilizer and organic amendment. *Ecotoxicol. Environ. Saf.* **150**, 116–122 (2018).

35. Tang, Z., Fan, F., Deng, S. & Wang, D. Mercury in rice paddy fields and how does some agricultural activities affect the translocation and transformation of mercury - A critical review. *Ecotoxicol. Environ. Saf.* **202**, 110950 (2020).

36. Tang, Z., Fan, F., Wang, X., Shi, X. & Wang, D. Understanding the effects of long-term different fertilizer applications on methylmercury accumulation in rice (Oryza sativa L.) plants. *Sci. Total Environ.* **777**, 146125 (2021).

37. Li, Y. *et al.* Amendments of nitrogen and sulfur mitigate carbon-promoting effect on microbial mercury methylation in paddy soils. *J. Hazard. Mater.* **448**, (2023).

38. Effler, S. W. & Matthews, D. A. Implications of redox processes for the rehabilitation of an urban lake, onondaga lake, New York. *Lake Reserv. Manag.* **24**, 122–138 (2008).

39. Matthews, D. A. *et al.* Whole-lake nitrate addition for control of methylmercury in mercury-contaminated Onondaga Lake, NY. *Environ. Res.* **125**, 52–60 (2013).

40. Shih, R., Robertson, W. D., Schiff, S. L. & Rudolph, D. L. Nitrate controls methyl mercury production in a streambed bioreactor. *J. Environ. Qual.* **40**, 1586–1592 (2011).

41. Strickman, R. J. & Mitchell, C. P. J. Mercury methylation in stormwater retention ponds at different stages in the management lifecycle. *Environ. Sci. Process. Impacts* **20**, 595–606 (2018).

42. Todorova, S. *et al.* Evidence for regulation of monomethyl mercury by nitrate in a seasonally stratified, eutrophic lake. *Environ. Sci. Technol.* **43**, 6572–6578 (2009).

43. Marvin-DiPasquale, M. C. & Oremland, R. S. Bacterial Methylmercury Degradation in Florida Everglades Peat Sediment. *Environ. Sci. Technol.* **32**, 2556–2563 (1998).

44. Linquist, B., van Groenigen, K. J., Adviento-Borbe, M. A., Pittelkow, C. & van Kessel, C. An agronomic assessment of greenhouse gas emissions from major cereal crops. *Glob. Change Biol.* **18**, 194–209 (2012).

45. Zhang, L. *et al.* Inhibition of Methylmercury and Methane Formation by Nitrous Oxide in Arctic Tundra Soil Microcosms. *Environ. Sci. Technol.* **57**, 5655–5665 (2023).

46. Asao, M. & Madigan, M. T. Taxonomy, phylogeny, and ecology of the heliobacteria. *Photosynth. Res.* **104**, 103–111 (2010).

47. Enkh-Amgalan, J., Kawasaki, H. & Seki, T. NifH and NifD sequences of heliobacteria: a new lineage in the nitrogenase phylogeny. *Fems Microbiol. Lett.* **243**, 73–79 (2005).

48. Kimble, L. K. & Madigan, M. T. Nitrogen-Fixation and Nitrogen-Metabolism in Heliobacteria. *Arch. Microbiol.* **158**, 155–161 (1992).

49. Sheehy, D. *et al.* Genome-wide Transcriptional Response during the Shift to N2-fixing Conditions in Heliobacterium modesticaldum. *J. Proteomics Bioinform.* **11**, (2018).

50. Tang, K. H., Yue, H. & Blankenship, R. E. Energy metabolism of Heliobacterium modesticaldum during phototrophic and chemotrophic growth. *Bmc Microbiol.* **10**, (2010).

51. Kimble, L. K., Mandelco, L., Woese, C. R. & Madigan, M. T. Heliobacterium Modesticaldum, Sp-Nov, a Thermophilic Heliobacterium of Hot-Springs and Volcanic Soils. *Arch. Microbiol.* **163**, 259–267 (1995).

52. Kleiner, D. Bacterial ammonium transport. *FEMS Microbiol. Lett.* **32**, 87–100 (1985).

53. Howard, J. B. & Rees, D. C. Structural Basis of Biological Nitrogen Fixation. *Chem Rev* **96**, 2965–2982 (1996).

54. Kimble, L. K. & Madigan, M. T. Evidence for an Alternative Nitrogenase in Heliobacterium-Gestii. *Fems Microbiol. Lett.* **100**, 255–260 (1992).

55. Ferlez, B. *et al.* The Effect of Bacteriochlorophyll g Oxidation on Energy and Electron Transfer in Reaction Centers from Heliobacterium modesticaldum. *J. Phys. Chem. B* **119**, 13714–13725 (2015).

56. Gallon, J. R. The oxygen sensitivity of nitrogenase: a problem for biochemists and micro-organisms. *Trends Biochem. Sci.* **6**, 19–23 (1981).

57. Amyot, M., Morel, F. M. M. & Ariya, P. A. Dark Oxidation of Dissolved and Liquid Elemental Mercury in Aquatic Environments. *Environ. Sci. Technol.* **39**, 110–114 (2005).

58. Kimble-Long, L. K. & Madigan, M. T. Molecular evidence that the capacity for endosporulation is universal among phototrophic heliobacteria. *Fems Microbiol. Lett.* **199**, 191–195 (2001).

59. Tang, K. H. *et al.* Carbon Flow of Heliobacteria Is Related More to Clostridia than to the Green Sulfur Bacteria. *J. Biol. Chem.* **285**, 35104–35112 (2010).

60. Walters, K. A., Redding, K. E. & Golbeck, J. H. Identification and characterization of the low molecular mass ferredoxins involved in central metabolism in Heliomicrobium modesticaldum. *Photosynth. Res.* (2024) doi:10.1007/s11120-023-01069-z.

61. Heinnickel, M., Shen, G. Z. & Golbeck, J. H. Identification and characterization of PshB, the dicluster ferredoxin that harbors the terminal electron acceptors F-A and F-B in Heliobacterium modesticaldum. *Biochemistry* **46**, 2530–2536 (2007).

62. Romberger, S. P., Castro, C., Sun, Y. L. & Golbeck, J. H. Identification and characterization of PshBII, a second F-A/F-B-containing polypeptide in the photosynthetic reaction center of Heliobacterium modesticaldum. *Photosynth. Res.* **104**, 293–303 (2010).

63. Battistuzzi, G. *et al.* Redox thermodynamics of low-potential iron-sulfur proteins. *JBIC J. Biol. Inorg. Chem.* **5**, 748–760 (2000).

64. Campbell, I. J., Bennett, G. N. & Silberg, J. J. Evolutionary Relationships Between Low Potential Ferredoxin and Flavodoxin Electron Carriers. *Front. Energy Res.* **7**, (2019).

65. Atkinson, J. T., Campbell, I., Bennett, G. N. & Silberg, J. J. Cellular Assays for Ferredoxins: A Strategy for Understanding Electron Flow through Protein Carriers That Link Metabolic Pathways. *Biochemistry* **55**, 7047–7064 (2016).

66. Sattley, W. M. *et al.* The genome of Heliobacterium modesticaldum, a phototrophic representative of the Firmicutes containing the simplest photosynthetic apparatus. *J. Bacteriol.* **190**, 4687–4696 (2008).

Chapter 4

Ferredoxin functional redundancy directly controls Hg^{II} reduction in *Heliomicrobium modesticaldum*

N. C. Lavoie[1], P. L. Baker[2], K. E. Redding[2], A. J. Poulain[1]

Affiliations: [1] University of Ottawa, 30 Marie Curie, Ottawa, Ontario K1N 6N5, Canada
[2] Arizona State University, 1711 S Rural Rd, Tempe, AZ 85287-1604, USA

N.B. Supporting information for this chapter can be found in **Appendix C**

4.1 ABSTRACT

Microorganisms play key roles in controlling the fate of mercury (Hg) in the environment. While some microbes are responsible for producing the most toxic form, methylmercury, in the absence of oxygen, others can limit its production by altering its redox state, namely by catalyzing the production of the volatile Hg^0. *Heliomicrobium modesticaldum* Ice1, an anoxygenic phototroph, can reduce Hg^{II} to Hg^0; however, the underlying mechanism of this process remains unknown. In this study, a CRISPR-Cas-based gene deletion approach was used to test the ability of seven gene-deletion mutants to reduce Hg^{II} compared to the wild-type. Deletion of genes encoding ferredoxins, photosynthetic electron transport complexes, and a TCA cycle enzyme were investigated for their potential role in catalyzing Hg^{II} reduction. These genes were targeted because of their involvement in cellular redox processes. We observed that all mutants retained the ability to produce Hg^0 during phototrophic and fermentative growth. Our findings confirm that the source of reducing power used to reduce Hg^{II} to Hg^0 is generated via either photosynthetic electron transport or pyruvate fermentation. Though an enzymatic coupling site remains to be identified, we discuss potential targets for future investigations.

4.2 INTRODUCTION

Mercury, a toxic heavy metal, is a globally distributed environmental contaminant emitted from natural and anthropogenic activities [1]. Elemental Hg^0, its volatile form, can travel long distances in the atmosphere before depositing in terrestrial and aquatic ecosystems as oxidized Hg^{II} [2]. Within these ecosystems, abiotic reactions and microbe-mediated transformations largely determine the fate and toxicity of mercury. In anoxic environments, anaerobic microbes possessing the *hgcAB* genes methylate inorganic mercury into methylmercury (MeHg), its most toxic form [3]. MeHg bioaccumulates in certain terrestrial food crops like rice [4] and biomagnifies in aquatic food

webs thus posing a threat to human health [5,6]. To mitigate the risks of Hg pollution in these environments, it is important to characterize the processes that control the availability of inorganic Hg substrates for methylation.

Redox transformations of Hg in anoxic environments play key roles in determining the speciation and availability of inorganic Hg^{II} and Hg^0 to Hg-methylating microbes [7,8]. At interfaces close to the atmosphere, reduction of dissolved Hg^{II}, typically catalyzed by photochemical reactions, can lead to the evasion of gaseous elemental Hg^0 [7]. Deeper in the water column or in sediments, Hg redox cycling is catalyzed by iron-bearing minerals [9–11], reactive dissolved organic matter [12], and anaerobic microbes [11,13–20]. Aerobic microorganisms containing the genetically encoded Hg detoxification enzyme, mercuric reductase (MerA), catalyze the reduction of Hg^{II} to its less toxic and volatile form, Hg^0 [21,22]. Hg^{II} reduction by anaerobes that do not harbour MerA has also been observed and is associated with anaerobic respiration [15,18,23,24], fermentation [13], or anoxygenic photosynthesis [13,14,20]. While Hg^0 is a dominant chemical species in anoxic environments [25,26], mechanisms driving anaerobic Hg^{II} reduction remain elusive and challenging to identify in the environment due to the lack of molecular targets. In this study, we aimed to gain insights into the mechanisms by which Heliobacteria, metabolically versatile photoheterotrophic anaerobes, reduce Hg^{II}.

We previously showed that the anoxygenic phototroph *Heliomicrobium modesticaldum* Ice1 was among the highest anaerobic Hg^{II} reducers on record [13]. Heliobacteria are strict anaerobes found in diverse terrestrial ecosystems, from hot spring microbial mats to flooded anoxic soils [27]. Much of what is known of the cellular physiology of Heliobacteria is derived from studies with *H. modesticaldum* Ice1. This thermophilic microbe, capable of anoxygenic photoheterotrophy in the presence of light, can also ferment in the dark [28]. Photoheterotrophic growth requires either

pyruvate, acetate + HCO_3^-, lactate, D-ribose, D-fructose or D-glucose, whereas fermentative growth is only supported by pyruvate oxidation [28,29]. Our mechanistic insights into Hg^{II} reduction by Heliobacteria have revealed that it is non-*mer* mediated, occurs during both anoxygenic photoheterotrophic and fermentative growth, and is suspected to be tied to the intracellular availability of reduced redox cofactors such as ferredoxins [13,20].

Pyruvate:ferredoxin oxidoreductase (PFOR) is one of Heliobacteria's key carbon metabolism enzymes, active during both fermentative and photoheterotrophic growth [29,30]. PFOR couples the oxidation of pyruvate to acetyl-CoA and CO_2 with the reduction of ferredoxins, small one-electron-carrying redox cofactors. PFOR is thus one of the primary generators of reducing power during pyruvate fermentation. During photoheterotrophy, cells can generate reducing power via PFOR activity but also via the photosynthetic electron transport chain (pETC). Both PFOR and the photosynthetic reaction center (HbRC) transfer electrons to ferredoxins; subsequently ferredoxins are used as reduced redox cofactor for other pathways (**Figure 4.1**), some of which may be associated with Hg^{II} reduction [31]. Under dark fermentation conditions, pyruvate oxidation is required for Hg^{II} reduction to occur, while under phototrophic conditions, cells can reduce Hg^{II} when grown on pyruvate, acetate, and even in the absence of a carbon source [13]. We further investigated the role of pyruvate metabolism on Hg^{II} reduction by exposing *H. modesticaldum* Ice1 to a chemical inhibitor for PFOR; nitazoxanide. We found that Hg^{II} reduction during fermentation, but not photoheterotrophy, was eliminated by exposure to nitazoxanide. These findings led us to propose that reducing power, or reduced redox cofactors, generated by pyruvate fermentation or photosynthetic electron transport, fuels Hg^{II} reduction.

Although we have identified a source of electrons used in the reduction of Hg^{II} to gaseous Hg^0, we have yet to identify enzymatic coupling points where the redox transformation occurs.

The recent development of a Heliobacteria-tailored CRISPR-based genome editing technique [32,33] has allowed us to create mutants deficient in their ability to catalyze certain redox transformations. We evaluated their Hg^{II} reduction phenotype. Specifically, we targeted genes encoding cytosolic ferredoxins, components of the photosynthetic electron transport chain, and carbon metabolism enzymes (**Table 4.1**). Hg^{II} reduction phenotypes of seven mutants were determined using anaerobic bioreactor assays under phototrophic and fermentative conditions. Here, we report that none of the mutants tested lost the ability to reduce Hg^{II} to Hg^0. Overall, these negative results provide valuable mechanistic details, which we further discuss along with additional genetic targets to be investigated in future work.

4.3 METHODS

4.3.1 Generation of gene deletion strains

The gene knockouts were made using a two-step procedure based on the endogenous CRISPR-Cas system in *H. modesticaldum* Ice1 [33,34]. Δ*fdx3,* Δ*pshB1,* Δ*pshB2,* and Δ*pshB1pshB2* were most recently characterized in Walters *et al.* 2024 [31], Δ*petCBDA* was created and described in Leung *et al.* 2021 [35], Δ*pshA* was created and characterized in detail in Baker *et al.* 2019 [32], and Δ*HM1_2993* was created for this study (**Table 4.1**).

Briefly, two plasmids are transformed sequentially in *H. modesticaldum*. A non-replicating step 1 plasmid containing a template for homologous recombination to delete the target gene(s) was created and introduced into wild-type *H. modesticaldum* via conjugation, and successful integrants were selected using antibiotic resistance. The step 2 plasmid contained a CRISPR array directing the native Type 1-A CRISPR-Cas system to target the desired gene(s) to delete. Successful knockout strains were selected for by acquisition of a new antibiotic resistance and loss

of the previous one. PCR amplification of the target gene locus was then performed to confirm gene deletion.

4.3.2 Microbial culturing

Bioreactor experiments were conducted using the wild type strain *Heliomicrobium modesticaldum* Ice1 from DSMZ culture collection (DSM-9504), and gene deletion strains Δ*fdx3,* Δ*pshB1,* Δ*pshB2,* Δ*pshB1pshB2,* Δ*petCBDA,* Δ*pshA,* and Δ*HM1_2993* (**Table 4.1**). All cell cultures were handled under anaerobic conditions in a Coy anaerobic glove box (atmosphere 97% $N_{2(g)}$ and 3% $H_{2(g)}$) or by using sterile anaerobic benchtop techniques where all equipment was sparged with 100% $N_{2(g)}$ prior to use. For each bioreactor assay, new cell cultures were revived from frozen stocks preserved at −80°C by scraping frozen culture with a sterile pipette tip and dropping it into a Balch tube containing growth medium PYE where the headspace of the tubes was then sparged to contain 100% $N_{2(g)}$.

The medium composition for 1 L of PYE is Na-pyruvate 2.2 g/L, yeast extract 0.2 g/L, K_2HPO_4 1 g/L, $MgSO_4*7H_2O$ 0.2 g/L, $Na_2S_2O_3$ 1 mM, $CaCl_2*2H_2O$ 0.02 g/L, $(NH_4)_2SO_4$ 1 g/L (15.1 mM of NH_4^+), anoxic $FeSO_4$ 20 µM, D-biotin 0.015 µg/mL, vitamin B12 as cyanocobalamin 0.02 µg/mL, and 1 mL of trace element solution SL6. Trace elements SL6 contained: $ZnSO_4*7$ H_2O 0.1 g/L, $MnCl_2*4$ H_2O 0.3 g/L, H_3BO_3 0.3 g/L, $CoCl_2*6H_2O$ 0.2 g/L, $CuCl_2*2H_2O$ 0.01 g/L, $NiCl_2*6H_2O$ 0.02 g/L, $Na_2MoO_4*2H_2O$ 0.03 g/L.

Cultures were incubated at 50 °C with an incandescent light source emitting photoactive radiation (PAR) at an intensity of 80 µmol photon m^{-2} s^{-1} until they reached mid-exponential phase. Cultures were then used to start new cultures with a 10% (v/v) inoculum into new Balch tubes containing 10 ml of the same growth medium and the appropriate selection antibiotic for gene deletion strains. Briefly, 50 µg/mL of kanamycin was used to select for mutant Δ*HM1_2993,*

Δ*pshA* and 10 μg/mL erythromycin for Δ*pshB1,* Δ*pshB2,* Δ*pshB1pshB2,* Δ*fdx3,* Δ*petCBDA*. Depending on the metabolic conditions desired, these re-inoculations and all subsequent ones were either kept in front of the light for photoheterotrophic growth or wrapped in foil and kept in the dark for fermentative growth.

Cells were harvested again after reaching mid-exponential in Balch tubes to start cultures with a 10% (v/v) inoculum in serum bottles containing 75 ml of the same growth medium and without antibiotics. Upon reaching mid- to late-exponential phase, these cultures were used as a 10% (v/v) inoculum in bioreactor experiments containing approximately 500 mL of the same growth medium.

4.3.3 Bioreactor experiments

This study's bioreactor setup and subsampling methodology are identical to those validated and used in prior research [13,14]. All bioreactor experiments were conducted at 50°C in ~ 500 mL of growth medium PYE. For fermentatively growing cultures, bioreactors were kept in complete darkness, whereas for photoheterotrophically growing cultures, the bioreactors were continuously exposed to a light intensity of 20 μmol photon m^{-2} s^{-1} to limit abiotic photoreduction of Hg^{II} [13]. Additionally, prior experiments with medium PYE found little to no abiotic Hg^0 production in sterile medium devoid of cell cultures exposed to light or in the dark [13]. Live cell bioreactors were performed for each gene deletion mutant and wild-type *H. modesticaldum* Ice1. Every bioreactor experiment was spiked with 250 pM of $HgCl_2$ into approximately 500 mL of bioreactor PYE media and ran for 48 hours to measure cumulative and hourly Hg^0 production using a Tekran 2537B CVAFS Analyzer.

4.4 RESULTS & DISCUSSION

4.4.1 Bioreactors for enzyme gene deletion mutants

We first set out to test whether the loss of core enzymes and protein complexes involved in photosynthetic electron transfer (encoded by *petCBDA*, and *pshA*) or a key step of the oxidative TCA cycle (*(Re)*-citrate synthase encoded by *HM1_2993)* would result in the loss of the Hg^{II} reduction phenotype normally observed in wild-type *H. modesticaldum* Ice1.

When grown fermentatively in growth media containing pyruvate, the wild-type produced between 108.4 to 124.6 pmol of Hg^0 (**Figure 4.2A**) (reducing on average 92.7% of the Hg^{II} present). The mutant deficient for *(Re)*-citrate synthase, Δ*HM1_2993*, produced 94.5 pmol of Hg^0 when growing in the dark via pyruvate fermentation (**Figure 4.2A**). Without the gene for *(Re)*-citrate synthase, *H. modesticaldum* cannot carry out its oxidative tricarboxylic acid cycle (TCA) because the citrate synthase is responsible for the production of citrate from oxaloacetate and acetyl-CoA (**Figure 4.1**). Furthermore, wild-type *H modesticaldum* cannot run its TCA cycle fully in reverse because it lacks the citrate lyase that converts citrate into acetyl-CoA and oxaloacetate. As such, Δ*HM1_2993* is unable to rely on enzymes of its TCA cycle in any direction to maintain redox homeostasis or fix CO_2, and none of these enzymes appear to be directly coupled to Hg^{II} reduction. Furthermore, fermentation of mM amounts of pyruvate by PFOR may generate sufficient reducing power to fuel the reduction of ~125 pmol of Hg^{II} to Hg^0. Note that oxaloacetate can be produced from PEP (**Figure 4.1**) and possibly allow for a few steps of the reductive TCA to be performed, leading to the accumulation of citrate, but this does not appear to affect Hg^{II} reduction.

When grown photoheterotrophically in growth media containing pyruvate, wild-type *H. modesticaldum* produced between 80.4 to 91.0 pmol of Hg^0 (reducing on average 67.2% of the

Hg^{II} present) (**Figure 4.2B**). We found that the mutant deficient for the core subunit of the Heliobacterial photosynthetic reaction center, Δ*pshA*, could produce 84.3 pmol Hg^0 when exposed to light (**Figure 4.2B**). Given that deleting *pshA* renders this mutant non-phototrophic and thus entirely reliant on fermentative growth [32], we expected Hg^{II} reduction would still occur as it did. The mutant Δ*petCBDA*, devoid of cytochrome *bc*, produced 104.5 pmol of Hg^0 when exposed to light in the bioreactor (**Figure 4.2B**). Similar to Δ*pshA*, deleting the genes for cytochrome *bc* renders this mutant non-phototrophic as the protein complex is only required during photosynthetic electron transport [35]. We further tested whether Hg^{II} reduction by Δ*petCBDA* was only fueled by pyruvate fermentation by assaying the mutant in the light in culture media devoid of any carbon source. We found, as we expected, that little to no Hg^0 was produced when carbon sources were absent (14.7 pmol). Overall, in the absence of functional photosynthetic electron transport, our results show that pyruvate fermentation is the primary source of reducing power fueling Hg^{II} reduction by yet-unidentified protein(s). These data also clearly show that abiotic Hg^{II} photoreduction does not occur in our system.

4.4.2 Bioreactors for ferredoxin gene deletion mutants

Next, we tested whether the loss of genes encoding for the cytosolic redox cofactors, ferredoxins, would result in mutants incapable of reducing Hg^{II}. As ferredoxins are the primary electron-carrying cofactors for pETC and pyruvate fermentation via PFOR, we predicted that mutants deficient in ferredoxins would exhibit a decreased ability to reduce Hg^{II}. Our work focused on genes encoding three ferredoxins, *fdx3*, *pshB1* and *pshB2*. All three ferredoxins are predicted to interact directly with components of the reaction center (HbRC), as well as with PFOR [31].

In the dark, Δ*fdx3* produced 75.3 and 80.0 pmol of Hg^0 (**Figure 4.3A**) while not growing significantly in the bioreactor (**SI Table 4.1**). This is contrary to our past experiments with wild-

type *H. modesticaldum*, where significant cell growth was required for elevated fermentative Hg^0 production [13]. Though not a lethal gene deletion, it is possible that the absence of Fdx3 affects multiple metabolic steps beyond PFOR, namely if Fdx3 is used as a redox cofactor within the TCA cycle. While *H. modesticaldum* Ice1 is incapable of autotrophic CO_2 fixation, it does rely on anaplerotic CO_2 fixation via two key enzymes, PEP carboxykinase (PEPCK) and pyruvate:ferredoxin oxidoreductase (PFOR) when it operates in the reductive direction to produce pyruvate from acetyl-CoA and CO_2 [29,30]. The CO_2 produced as part of the oxidative TCA cycle can be used for such anaplerotic reactions. However, due to the absence of Fdx3, there may be limitations in the TCA cycle's ability to produce CO_2. Additionally, our bioreactor assays are constantly bubbled with Argon, leading to a rapid loss of biologically produced CO_2. Thus, in these conditions, Δ*fdx3* may become CO_2-limited. We attempted to restore this mutant's ability to grow by providing 1 mM HCO_3^- in the growth medium, but to no avail (**SI Table 4.1**); however, it could still produce 76.7 pmol of Hg^0. To further test whether the continued production of Hg^0 in the absence of growth was associated with pyruvate fermentation, we exposed Δ*fdx3* in the bioreactor to media devoid of any carbon source. As expected, the mutant could only produce 14.9 pmol of Hg^0 in the absence of fermentable carbon substrates (**Figure 4.3A**). Unexpectedly, deleting *fdx3* yielded a mutant capable of high levels of fermentative Hg^{II} reduction in the absence of meaningful growth, which was not rescued by the addition of exogenous inorganic carbon. Individual deletion-mutants for Δ*pshB1* and Δ*pshB2*, ferredoxins known to accept electrons from the HbRC [36,37] and grown fermentatively produced 90.6 and 99.0 pmol of Hg^0, respectively (**Figure 4.3A**). On the other hand, the double deletion-mutant Δ*pshB1pshB2* yielded extremely variable cumulative Hg^0 production (28.1, 71.2, and 100.8 pmol), directly associated with its variable ability to grow in the bioreactor (**SI Table 4.1**). Similar to Δ*fdx3*, Δ*pshB1pshB2* may

struggle with efficient enzymatic turnover for fermentative growth when these two essential ferredoxins are absent. Unlike our previous work with the wild-type strain where Hg^{II} reduction during fermentation requires growth, these mutant experiments suggest that in the absence of certain ferredoxins, namely Fdx3, *H. modesticaldum* can, in fact, reduce Hg^{II} without significant fermentative growth. This is a surprising result that remains unexplained.

When grown phototrophically, ferredoxin gene-deletion mutant Δ*fdx3* produced 97.1 and 105.6 pmol of Hg^0, Δ*pshB1* produced 100.5 pmol, and Δ*pshB1pshB2* produced 105.6 pmol (**Figure 4.3B**). Unlike for dark bioreactors, in the light Δ*pshB1pshB2* and Δ*fdx3* reliably grew and reduced Hg^{II} (**SI Table 4.1**). This suggests that deleting certain ferredoxin genes may affect fermentative but not photoheterotrophic growth. Δ*pshB2* exhibited a marked decrease in its ability to reduce Hg^{II} when growing phototrophically, only producing 22.6 pmol and 47.5 pmol of Hg^0 (**Figure 4.3B**). Δ*pshB2* also struggled to grow in the bioreactor assays (**SI Table 4.1**). To determine whether the low Hg^{II} reduction phenotype was due to the lack of growth, we amended bioreactors with HCO_3^-, similarly to what was attempted with Δ*fdx3*. Adding 20mM HCO_3^- did not enable growth nor did it stimulate Hg^{II} reduction. However, adding 20 mM HCO_3^- increased the pH to 7.66, a tenfold increase in $[H^+]$, a pH increase that *H. modesticaldum* could not tolerate. We then tested Δ*pshB2* in the presence of 1mM HCO_3^- added to the bioreactor. We found that the mutant regained the ability to grow (**SI Table 4.1**) and produce high levels of Hg^0; 103.1 and 104.6 pmol (**Figure 4.3B**). As the addition of HCO_3^- restores growth for this mutant, this suggests that cells suffered from issues with enzymatic turnover linked to anaplerotic CO_2 fixation. Thus, for Δ*pshB2*, phototrophic Hg^{II} reduction required active growth in the bioreactor, which could be restored by HCO_3^- addition.

Overall, as all ferredoxin mutants retain the capacity to produce Hg^0, there is no evidence supporting the involvement of certain ferredoxins over others in Hg^{II} reduction. It is important to note, however, that there are other putative ferredoxins encoded in the genome of *H. modesticaldum* Ice1 that we did not investigate, and thus, we cannot discount their potential involvement in Hg^{II} reduction.

4.4.3 Ferredoxin gene redundancy & lack of evidence for loss of Hg reduction associated to specific Fd genes

As briefly mentioned above, one of the long-standing questions in heliobacterial physiology has been whether there is functional redundancy between the various ferredoxin-encoding genes. The annotated *H. modesticaldum* Ice1 genome contains seven genes that code for known and hypothetical low molecular weight [4Fe-4S] ferredoxins [31]. These genes are HM1_1462 (PshB1), HM1_1461 (PshB2), HM1_2505 (Fdx3), HM1_0869, HM1_1043, HM1_0357, and HM1_2767. PshB1 and PshB2 are the most well-studied ferredoxins, having been identified as the primary electron acceptors for the HbRC [36,37]. Recent work by Walters *et al*. investigated whether some of these small mobile dicluster ferredoxins are capable of accepting electrons from the HbRC and PFOR [31]. They identified functional redundancy for three ferredoxins; PshB1, PshB2, and Fdx3 can accept electrons from the HbRC and PFOR. However, HM1_0357, HM1_1043, HM1_2767, and HM1_0869 could not serve as electron acceptors for either protein in *in vitro* assays, and they do not yet have a known role. These timely findings reveal that within our own experiments with gene-deletion mutants Δ*pshB1,* Δ*pshB2,* Δ*pshB1pshB2,* and Δ*fdx3* (for which deletion did not affect Hg^{II} reduction when controlling for growth) there always remains at least one ferredoxin permitting electron transfer to the HbRC and/or PFOR.

Walters *et al*. identified that the only mutants that produce Fdx3 are Δ*pshB1pshB2* and Δ*pshB2*, therefore suggesting that Fdx3 substitutes for PshB2 in its absence. Δ*pshB1pshB2* struggled to consistently grow fermentatively and, by association, consistently reduce Hg^{II}. This suggests that Fdx3, the only available ferredoxin for this mutant, is either: 1) not always produced in sufficient concentration during fermentation or 2) has a lower substrate affinity for carbon metabolism enzymes than PshB1 or PshB2. Although we did not test for this, it is also possible that Δ*pshB1pshB2* lacks the ability to produce enough endogenous CO_2 for anaplerotic fixation (as previously tested and described for Δ*pshB2)*. It remains to be determined why the reliance on anaplerotic CO_2 fixation is greater during phototrophy than fermentation for Δ*pshB2*.

To date, no viable mutant has been made devoid of all three genes, suggesting cells must have at least one of these ferredoxins to live. The redundant yet essential function of these three ferredoxins ultimately complicates using a gene-deletion approach to test their role in Hg^{II} reduction. We can conclusively state that no single ferredoxin-encoding gene is solely necessary for Hg^{II} reduction to occur during either phototrophy or fermentation. However, we cannot rule out whether a pool of reduced ferredoxin, composed of interchangeable Fdx3, PshB1, and PshB2, is the direct electron donor for Hg^{II} reduction.

4.4.4 Insights into anaerobic Hg^{II} reduction mechanism

Overall, our findings illustrate that none of the tested genes are solely responsible for the Hg^{II} reduction phenotype in *H. modesticaldum* Ice1. The observation that gene-deletion mutants deficient for the pETC complexes, *petCBDA* and *pshA*, readily reduce Hg^{II} in the light validates our prior findings that reducing power generated by pyruvate fermentation or pETC fuels the reduction of Hg^{II} [13]. Additionally, mutants lacking one or two of the three primary ferredoxins retained their ability to reduce Hg^{II} once controlled for growth deficiencies. This suggests, when

taken into account with their known functional redundancy [31], that no single ferredoxin is involved in Hg^{II} reduction, but rather a pool of reduced ferredoxins, encoded by multiple genes, may be involved. It remains unknown whether ferredoxins directly transport electrons to a site that reduces Hg^{II}, act as intermediate carriers transferring electrons to other redox cofactors such as NAD(P)H, which may be more directly involved in Hg^{II} reduction, or can transfer electrons directly to Hg^{II} one at a time.

Electrons carried by ferredoxins can be used by an electron-bifurcating enzyme, the NADH-dependent ferredoxin:NADP+ oxidoreductase (NfnAB). This enzyme couples the exergonic reduction of $NADP^+$ by ferredoxin with the endergonic reduction of $NADP^+$ by NADH in a reversible reaction [38]. NfnAB plays a central role in interconverting ferredoxins and NAD(P)H generated from pETC and carbon metabolism [29]. As such, NfnAB may be involved in Hg^{II} reduction either as the next downstream receiver of reducing power from central metabolism or it may be the catalytic site of Hg^{II} reduction. Given its central role in metabolism, NfnAB may not be successfully deleted from *H. modesticaldum.* However, NfnAB, its cofactors, and Hg^{II} could be assayed *in vitro* for the production of Hg^0 similar to the work Walters *et al.* did with PFOR and ferredoxins [31]. *In vivo* heterologous expression of NfnAB in a non-reducing microbial strain could also be a potential avenue to determine if the Hg^{II} reduction phenotype is acquired when certain genes and proteins are present.

4.5 CONCLUSION

One of the challenging aspects of investigating non-*mer* Hg^{II} reduction in anaerobes is testing the role of cellular machinery on Hg^{II} reduction without confounding effects from a cascade of interconnected cellular pathways. Using a gene-deletion approach may one day yield a growing mutant Heliobacteria incapable of reducing Hg^{II}. In addition to a gene-deletion approach, future

work should also incorporate proteomics or transcriptomics to quantify the effect of gene deletions on the expression and synthesis of cellular components and Hg^{II} reduction. Such an approach has been successfully carried out with *Geobacter sulfurreducens* PCA to investigate its ability to reduce Hg^{II} [24] but has yet to be applied to phototrophic or fermentative Hg^{II} reduction. Developing a greater understanding of the physiological and genetic controls on anaerobic Hg^{II} reduction will be essential to future work tracking the contributions of these anaerobes to Hg cycling in the environment.

Acknowledgments

Our work was funded by NSERC Discovery and Accelerator grants, CFI funding to AJP and NSERC graduate scholarships to NCL.

Author contributions

N.C.L and A.J.P. designed experiments, N.C.L. carried them out and performed data analysis, and N.C.L. and A.J.P. wrote the manuscript. P. L. B. and K. E. R. provided gene deletion mutants created at their laboratory and insights into Heliobacterial metabolism.

4.6 FIGURES AND TABLE

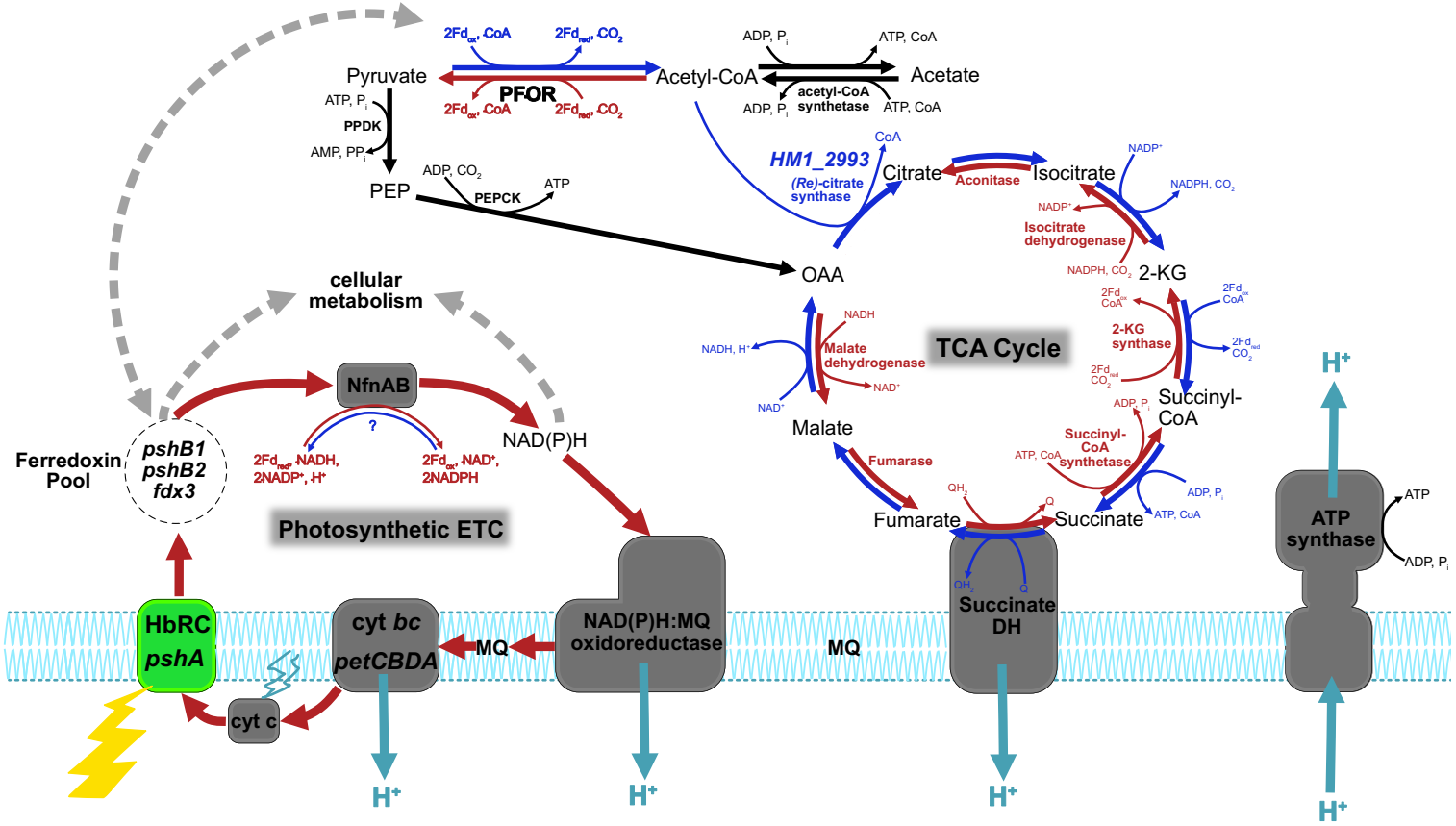

Figure 4.1: Metabolic pathways in which *pshA*, *pshB1*, *pshB2*, *fdx3*, *petCBDA*, and HM1_2993 participate in.

Names in italics represent specific genes that were deleted in the present study: Heliobacterial reaction center = pshA; ferredoxin-encoding genes = *pshB1, pshB2,* and *fdx3;* cytochrome *bc* genes = *petCBDA*; and (*Re*)-citrate synthase encoding gene = HM1_2993. Arrows in red and blue are for enzymatic reactions operating in the reductive and oxidative directions, respectively. Pale blue arrows represent transmembrane proton movements. Non-redox enzymatic reactions are indicated with black arrows. Grey dashed arrows represent other destinations for the redox cofactors NAD(P)H and the ferredoxin pool. Abbreviations: Fd_{ox} = oxidized ferredoxin, Fd_{red} = reduced ferredoxin, HbRC = Heliobacterial photosynthetic reaction center, NfnAB = NADH-dependent ferredoxin:$NADP^+$ oxidoreductase, cyt *bc* = cytochrome *bc*, cyt c = cytochrome c_{553}, PPDK = pyruvate phosphate dikinase, PEPCK = phosphoenolpyruvate carboxykinase, PEP = phosphoenolpyruvate, OAA = oxaloacetate, 2-KG = 2-ketoglutarate, MQ = menaquinone, QH_2 = ubiquinol, Q = ubiquinone, Succinate DH = succinate dehydrogenase.

Table 4.1: Summary of the gene deletion *H. modesticaldum* Ice1 mutants tested in this study, their associated proteins, known roles in cellular metabolism, and reference to the original creation and characterization of the mutant.

Gene deletion(s)	Locus ID	Protein(s)	Known roles	References
fdx3	HM1_2505	low molecular weight [4Fe-4S] ferredoxin	redox cofactor, interacts with PFOR and HbRC	Walters *et al.* 2024
pshB1	HM1_1462	low molecular weight [4Fe-4S] ferredoxin	redox cofactor, interacts with PFOR and HbRC	Walters *et al.* 2024
pshB2	HM1_1461	low molecular weight [4Fe-4S] ferredoxin	redox cofactor, interacts with PFOR and HbRC	Walters *et al.* 2024
pshB1pshB2	HM1_1461, 1462	low molecular weight [4Fe-4S] ferredoxins	redox cofactors, interacts with PFOR and HbRC	Walters *et al.* 2024
HM1_2993	HM1_2993	*(Re)*-citrate synthase	convert oxaloacetate to citrate, part of oTCA cycle	Sattley *et al.* 2008
petCBDA	HM1_0696, 0697, 0698, 0699	four cytochrome *bc* complex subunits	core component of photosynthetic electron transport chain	Sattley *et al.* 2008
pshA	HM1_0690	HbRC core polypeptide PshA	core component of photosynthetic electron transport chain	Sattley *et al.* 2008

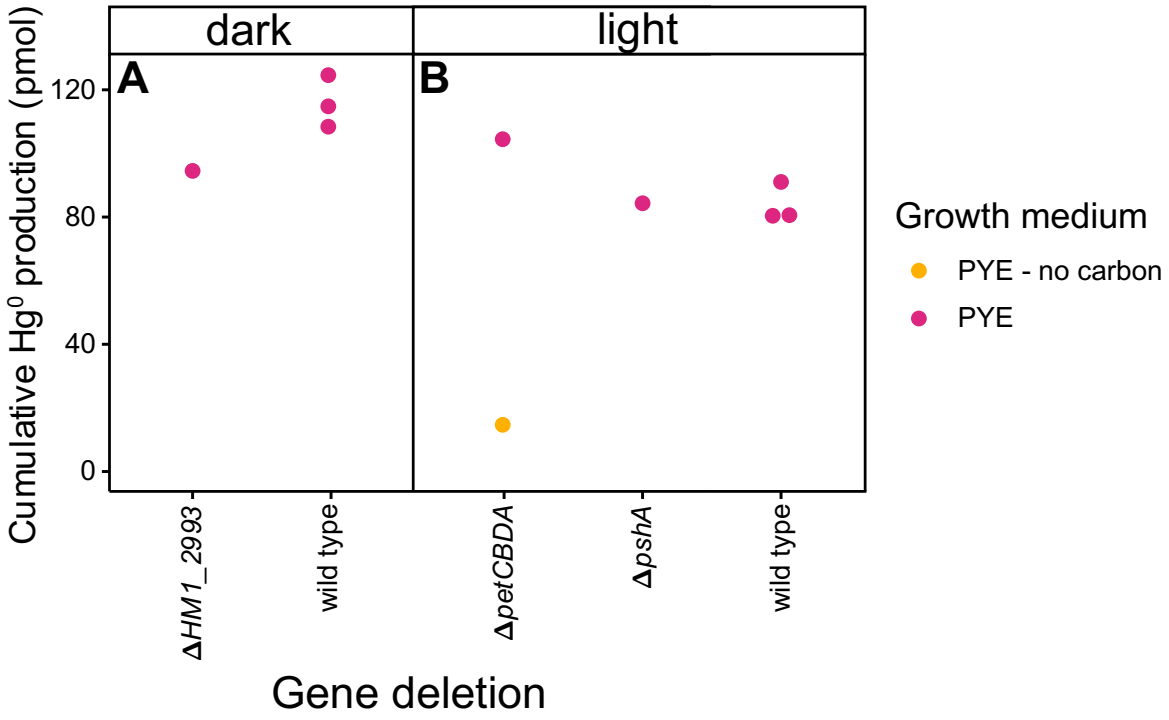

Figure 4.2: Cumulative Hg^0 produced in bioreactors with *H. modesticaldum* wild-type and gene-deletion mutants
exposed to A) dark growth conditions and B) light growth conditions. All bioreactors contained medium PYE except for one experiment with Δ*petCBDA* where all carbon sources were omitted. For the wild type strain and key gene deletion mutants, experiments were repeated as biological replicates.

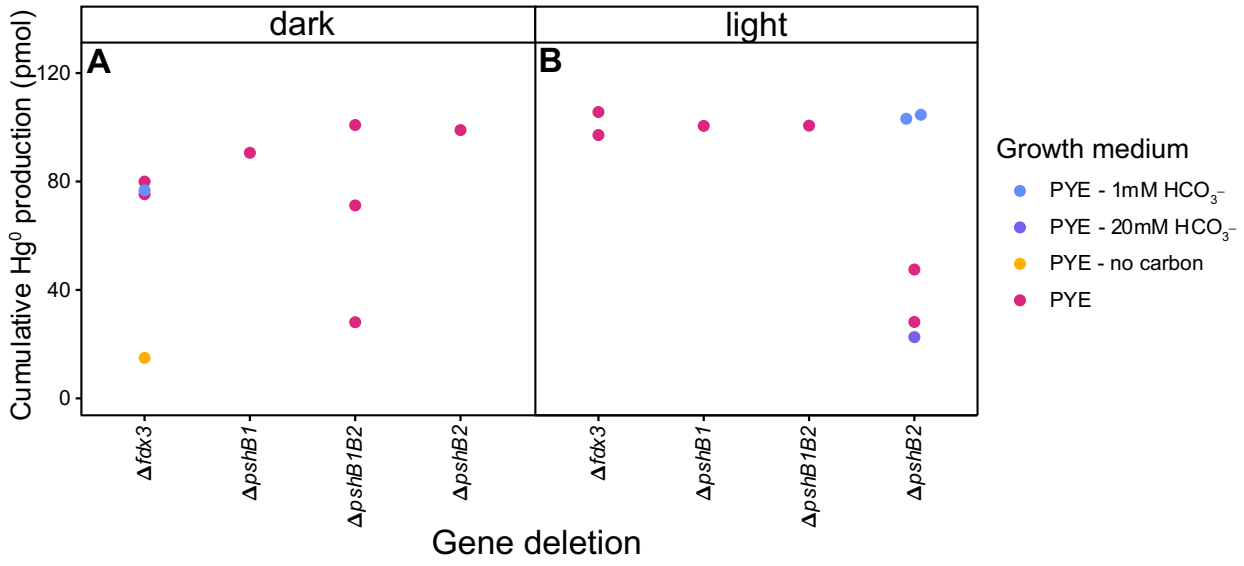

Figure 4.3: Cumulative Hg^0 produced in bioreactors with *H. modesticaldum* ferredoxin gene-deletion mutants
exposed to A) dark fermenting growth conditions and B) light photoheterotrophic growth conditions. Bioreactors contained growth medium PYE, and for certain assays, HCO_3^- was added, or all carbon sources were omitted. For key gene deletion mutants, experiments were repeated as biological replicates.

4.7 REFERENCES

1. Obrist, D. *et al.* A review of global environmental mercury processes in response to human and natural perturbations: Changes of emissions, climate, and land use. *Ambio* **47**, 116–140 (2018).
2. Selin, N. E. *et al.* Chemical cycling and deposition of atmospheric mercury: Global constraints from observations. *Journal of Geophysical Research: Atmospheres* **112**, (2007).
3. Parks, J. M. *et al.* The genetic basis for bacterial mercury methylation. *Science* **339**, 1332–5 (2013).
4. Zhang, H., Feng, X., Larssen, T., Qiu, G. & Vogt, R. D. In inland China, rice, rather than fish, is the major pathway for methylmercury exposure. *Environ Health Perspect* **118**, 1183–8 (2010).
5. Sunderland, E. M. Mercury exposure from domestic and imported estuarine and marine fish in the U.S. seafood market. *Environ Health Perspect* **115**, 235–42 (2007).
6. Paterson, M. J. *et al.* Bioaccumulation of newly deposited mercury by fish and invertebrates: An enclosure study using stable mercury isotopes. *Can. J. Fish. Aquatic Sci.* **63**, 2213–2224 (2006).
7. Fitzgerald, W. F., Lamborg, C. H. & Hammerschmidt, C. R. Marine Biogeochemical Cycling of Mercury. *Chem. Rev.* **107**, 641–662 (2007).
8. Amyot, M., Mierle, G., Lean, D. & McQueen, D. J. Effect of solar radiation on the formation of dissolved gaseous mercury in temperate lakes. *Geochimica et Cosmochimica Acta* **61**, 975–987 (1997).
9. Wiatrowski, H. A. *et al.* Reduction of Hg(II) to Hg(0) by magnetite. *Environ Sci Technol* **43**, 5307–13 (2009).
10. Bone, S. E., Bargar, J. R. & Sposito, G. Mackinawite (FeS) reduces mercury(II) under sulfidic conditions. *Environ Sci Technol* **48**, 10681–9 (2014).
11. Liu, S. N. & Wiatrowski, H. A. Reduction of Hg(II) to Hg(0) by Biogenic Magnetite from two Magnetotactic Bacteria. *Geomicrobiol J* **35**, 198–208 (2018).
12. Gu, B. *et al.* Mercury reduction and complexation by natural organic matter in anoxic environments. *Proc Natl Acad Sci U S A* **108**, 1479–83 (2011).
13. Gregoire, D. S., Lavoie, N. C. & Poulain, A. J. Heliobacteria Reveal Fermentation As a Key Pathway for Mercury Reduction in Anoxic Environments. *Environ Sci Technol* **52**, 4145–4153 (2018).
14. Grégoire, D. S. & Poulain, A. J. A physiological role for HgII during phototrophic growth. *Nature Geoscience* **9**, 121–125 (2016).

15. Lin, H., Morrell-Falvey, J. L., Rao, B., Liang, L. & Gu, B. Coupled mercury-cell sorption, reduction, and oxidation on methylmercury production by Geobacter sulfurreducens PCA. *Environ Sci Technol* **48**, 11969–76 (2014).

16. Lu, X. *et al.* Anaerobic Mercury Methylation and Demethylation by Geobacter bemidjiensis Bem. *Environ Sci Technol* **50**, 4366–73 (2016).

17. Schaefer, J. K., Letowski, J. & Barkay, T. mer-mediated resistance and Volatilization of Hg(II) under anaerobic conditions. *Geomicrobiol J* **19**, 87–102 (2002).

18. Wiatrowski, H. A., Ward, P. M. & Barkay, T. Novel reduction of mercury (II) by mercury-sensitive dissimilatory metal reducing bacteria. *Environ Sci Technol* **40**, 6690–6 (2006).

19. Zhao, L. D. *et al.* Contrasting effects of dissolved organic matter on mercury methylation by Geobacter sulfurreducens PCA and Desulfovibrio desulfuricans ND132. *Environmental Science & Technology* **51**, 10468–10475 (2017).

20. Lavoie, N. C., Gregoire, D. S., Stenzler, B. R. & Poulain, A. J. Reduced sulphur sources favour Hg(II) reduction during anoxygenic photosynthesis by Heliobacteria. *Geobiology* (2019) doi:10.1111/gbi.12364.

21. Barkay, T., Kritee, K., Boyd, E. & Geesey, G. A thermophilic bacterial origin and subsequent constraints by redox, light and salinity on the evolution of the microbial mercuric reductase. *Environ Microbiol* **12**, 2904–17 (2010).

22. Christakis, C. A., Barkay, T. & Boyd, E. S. Expanded Diversity and Phylogeny of mer Genes Broadens Mercury Resistance Paradigms and Reveals an Origin for MerA Among Thermophilic Archaea. *Front. Microbiol.* **12**, (2021).

23. Lee, S., Kim, D. H. & Kim, K. W. The enhancement and inhibition of mercury reduction by natural organic matter in the presence of Shewanella oneidensis MR-1. *Chemosphere* **194**, 515–522 (2018).

24. Qian, C. *et al.* Global Proteome Response to Deletion of Genes Related to Mercury Methylation and Dissimilatory Metal Reduction Reveals Changes in Respiratory Metabolism in Geobacter sulfurreducens PCA. *J Proteome Res* **15**, 3540–3549 (2016).

25. Poulin, B. A. *et al.* Mercury transformation and release differs with depth and time in a contaminated riparian soil during simulated flooding. *Geochimica et Cosmochimica Acta* **176**, 118–138 (2016).

26. Bouffard, A. & Amyot, M. Importance of elemental mercury in lake sediments. *Chemosphere* **74**, 1098–1103 (2009).

27. Asao, M. & Madigan, M. T. Taxonomy, phylogeny, and ecology of the heliobacteria. *Photosynth Res* **104**, 103–111 (2010).

28. Kimble, L. K., Mandelco, L., Woese, C. R. & Madigan, M. T. Heliobacterium Modesticaldum, Sp-Nov, a Thermophilic Heliobacterium of Hot-Springs and Volcanic Soils. *Arch Microbiol* **163**, 259–267 (1995).

29. Tang, K. H., Yue, H. & Blankenship, R. E. Energy metabolism of Heliobacterium modesticaldum during phototrophic and chemotrophic growth. *Bmc Microbiol* **10**, (2010).

30. Tang, K. H. *et al.* Carbon Flow of Heliobacteria Is Related More to Clostridia than to the Green Sulfur Bacteria. *J Biol Chem* **285**, 35104–35112 (2010).

31. Walters, K. A., Redding, K. E. & Golbeck, J. H. Identification and characterization of the low molecular mass ferredoxins involved in central metabolism in Heliomicrobium modesticaldum. *Photosynth Res* (2024) doi:10.1007/s11120-023-01069-z.

32. Baker, P. L. *et al.* Using the endogenous CRISPR-Cas system of Heliobacterium modesticaldum to delete the photochemical reaction center core subunit gene. *Appl Environ Microbiol* (2019) doi:10.1128/AEM.01644-19.

33. Baker, P. L. *et al.* A molecular biology toolkit for the phototrophic Firmicute, Heliobacterium modesticaldum. *Appl Environ Microbiol* (2019) doi:10.1128/AEM.01287-19.

34. Orf, G. S., Gisriel, C. J., Granstrom, J., Baker, P. L. & Redding, K. E. The PshX subunit of the photochemical reaction center from Heliobacterium modesticaldum acts as a low-energy antenna. *Photosynthesis Research* **151**, 11–30 (2022).

35. Leung, S. W., Baker, P. L. & Redding, K. E. Deletion of the cytochrome bc complex from Heliobacterium modesticaldum results in viable but non-phototrophic cells. *Photosynth Res* **148**, 137–152 (2021).

36. Heinnickel, M., Shen, G. Z. & Golbeck, J. H. Identification and characterization of PshB, the dicluster ferredoxin that harbors the terminal electron acceptors F-A and F-B in Heliobacterium modesticaldum. *Biochemistry-Us* **46**, 2530–2536 (2007).

37. Romberger, S. P., Castro, C., Sun, Y. L. & Golbeck, J. H. Identification and characterization of PshBII, a second F-A/F-B-containing polypeptide in the photosynthetic reaction center of Heliobacterium modesticaldum. *Photosynth Res* **104**, 293–303 (2010).

38. Buckel, W. & Thauer, R. K. Flavin-Based Electron Bifurcation, Ferredoxin, Flavodoxin, and Anaerobic Respiration With Protons (Ech) or NAD(+) (Rnf) as Electron Acceptors: A Historical Review. *Front Microbiol* **9**, 401 (2018).

Chapter 5

Anaerobic Hg^{II} reduction is driven by cellular Hg^{II}-thiol interactions

Noémie C. Lavoie [a], Alexandre J. Poulain [a]

a - Biology Department, University of Ottawa, 30 Marie Curie, Ottawa, ON, K1N 6N5, Canada.

This chapter has been submitted to *Access Microbiology*.

N.B. Supporting information for this chapter can be found in **Appendix D**

5.1 ABSTRACT

Redox reactions determine the availability of mercury species, Hg^{II} and Hg^{0}, to anaerobic microbes responsible for the methylation of inorganic Hg into toxic methylmercury. Certain anaerobes also play an important role in Hg cycling in methylation hot spots by reducing Hg^{II} to its gaseous elemental form Hg^{0}, yet their contributions remain unquantified due to a paucity of mechanistic information or genetic targets. In this work, we sought to uncover further mechanistic details on anaerobic Hg^{II} reduction by the versatile anoxygenic photoheterotroph and fermenter *Heliomicrobium modesticaldum* Ice1. Due to Hg^{II}'s electrophilic attraction to thiols, we hypothesized that cellular thiol groups are likely interaction sites involved in Hg^{II} reduction. We exposed *H. modesticaldum* to the thiol-alkylating agent N-ethylmaleimide to irreversibly bind to thiols and found a concentration-dependent inhibition of Hg^{0} production during anoxygenic photoheterotrophy and fermentation. We propose updated insights into Heliobacterial Hg^{II} reduction where Hg^{II}-thiol interactions are a key step of the mechanism and discuss potential enzymatic coupling sites that merit further investigation.

5.2 DATA SUMMARY

The authors confirm all supporting data are provided in the paper and in the supplementary data files "SI_figures.docx" and "SI_raw_data.xlsx".

5.3 INTRODUCTION

Mercury, a toxic heavy metal, is globally distributed via atmospheric transport and can bioaccumulate and biomagnify in food webs, particularly in its methylated form, methylmercury (MeHg) [1]. Microbial processes heavily regulate much of Hg's fate [2]. Its most neurotoxic form, MeHg, is produced from inorganic Hg by anaerobic microorganisms in terrestrial and aquatic environments [3–7]. Within these anoxic environments, microbially-mediated redox cycling can

affect the speciation and availability of Hg substrate to methylators [8]. Its role is 2-fold: Hg^0 oxidation supplies dissolved Hg^{II} required for methylation, and Hg^{II} reduction can lead to evasion of gaseous Hg^0. Anoxygenic phototrophs and anaerobes thrive in low light anoxic conditions also inhabited by Hg methylators. In these environments, abiotic Hg^{II} photoreduction is nearly absent; thus, anoxygenic phototrophs requiring low light intensity to thrive and anaerobes stand to be critical drivers of Hg^{II} reduction [9–11] and influence MeHg formation.

Unlike many aerobes that reduce Hg via dedicated enzymatic machinery as part of a detoxification strategy encoded by the *mer* operon [12,13], genetic determinants have yet to be found for anaerobic Hg^{II} reducers [9–11,14–19]. The information currently available suggests that core components of anaerobic respiration [15], fermentation [9] or anoxygenic phototrophy [10] are driving Hg^{II} reduction. However, without detailed mechanisms or genetic targets, it remains challenging to assess the contribution of anaerobic Hg^{II} reduction to global Hg cycling. The purpose of our study was to gain insights into the mechanisms allowing Heliobacteria, a type of metabolically versatile anaerobe, to reduce Hg^{II} to its gaseous elemental form, Hg^0.

Heliobacteria are terrestrial, spore-forming, strictly anaerobic bacteria capable of photoheterotrophy in the presence of light and fermentation in the dark [20]. They are the only known family of phototrophs from the Bacillota phylum, formerly Firmicutes. They conduct a primitive form of photosynthesis characterized by a unique photosynthetic pigment, bacteriochlorophyll g [21,22]. Its most well-studied representative, the type strain *Heliomicrobium modesticaldum* Ice1, originates from hot spring soils in Iceland and has also been found in hot spring microbial mats in Yellowstone [23].

In an early effort to investigate the diversity of phototrophs capable of anaerobic Hg^{II} reduction, we tested *H. modesticaldum* Ice1 and found that it could reduce over 80% of Hg^{II} to

Hg^0 [9]. We then discovered that another member of this family, *Heliobacterium mobile*, shared this ability [11] and that the magnitude of Hg^{II} reduced by *H. mobile* could be increased by growing it on more reduced sulphur sources such as thiosulphate. No apparent dedicated Hg^{II} reduction machinery (i.e. *mer* operon genes) was found in either of these strains. We pursued experiments with *H. modesticaldum* to further investigate the mechanism at play. In the absence of any oxidizable carbon source in the growth media, phototrophic cells could reduce Hg^{II} but fermentative cells could not. This indicates a connection between intracellular availability of reduced redox cofactors and Hg^{II} reduction and led us to further investigate the role of reducing power- generating enzymes on Hg^{II} reduction. Pyruvate: ferredoxin oxidoreductase (PFOR) is one of the key carbon metabolism enzymes in Heliobacteria, active during both fermentative and photoheterotrophic growth [24]. It couples the oxidation of the organic carbon source pyruvate into acetyl-CoA to the reduction of ferredoxins, small one-electron-carrying redox cofactors. PFOR is thus one of the primary generators of reducing power during Heliobacterial fermentation. During phototrophy, cells can generate reducing power via PFOR activity but also via the photosynthetic electron transport chain. Both PFOR and the photosynthetic reaction center transfer electrons to ferredoxins which then shuttle electrons to other enzymes [24–28]. We inhibited PFOR activity in fermentative cells using the chemical nitazoxanide (NTZ) which eliminated fermentative Hg^{II} reduction completely. We made the same observation in another fermentative but non-phototrophic Bacillota, *Clostridium acetobutylicum*. Importantly, PFOR inhibition did not affect Hg^{II} reduction under phototrophic conditions. These findings led us to propose that Hg^{II} reduction is dependent on the cells' ability to generate reducing power, i.e. to reduce redox cofactors through the photosynthetic electron transport chain or organic carbon oxidation via PFOR. Although these findings suggest a source of electrons fueling Hg^{II} reduction, we did not identify specific enzymatic

coupling points. We suspect thiol-bearing intracellular proteins or low molecular mass molecules as probable sites involved in Hg^{II} reduction on the basis of the following: 1) the reduction of Hg^{II} by Heliobacteria appears to be cytosolic [9,11,29], 2) Hg^{II} is highly electrophilic and binds preferentially to SH- cysteine residues on protein surfaces [30], and 3) as reducing power availability appears to dictate the magnitude of Hg^{II} reduced [9,10] , enzymes in the oxidoreductase class and their electron carriers may be involved in this metal reduction reaction.

We hypothesize that SH- are likely binding sites involved in Hg^{II} reduction. We predict that blocking Hg^{II} access to SH- groups will decrease Hg^{II} reduction. We thus searched for potential chemical inhibitors with specificity to SH- groups. N-ethylmaleimide (NEM) is an organic compound that is reactive towards thiols and is commonly used to modify cysteine residues in proteins. The thiolate anion (RS^-) of cysteine attacks the electrophilic center of the C=C bond of the maleimide group to form a thioether bond (R-S-R) between the thiol and the maleimide [31,32]. This reaction with thiols occurs near pH 6.5-7.5, and the resulting thioether bond is virtually irreversible [31]. In the early days of discovering the mercuric reductase enzyme (MerA), researchers used NEM on a Hg^{II} reducing *E. coli* strain to determine if the reduction mechanism required interaction with thiol groups for the activity to occur [33]. In their work, NEM bound to cell thiols and resulted in the inhibition of the Hg^{II} reduction phenotype in a concentration-dependent manner. It was later confirmed that the reduction activity was attributable to MerA, a flavin disulphide oxidoreductase [33–35]. NEM has also been used in studies investigating the protein complexes that make up the photosynthetic electron transport chain (pETC) in plant chloroplasts. *In vitro* assays with purified pETC proteins demonstrated that NEM reacts with thiol ligands on ferredoxin: $NADP^+$ oxidoreductase (FNR), causing it to lose its catalytic activity by preventing electron transfer from ferredoxins to FNR [36].

In the present work, we show that exposing *H. modesticaldum* Ice1 to sub-lethal concentrations of NEM inhibits anaerobic Hg^{II} reduction in a concentration-dependent manner during both photoheterotrophic and fermentative metabolisms. Hg mass balance assays further suggest that the inhibition of Hg^{II} reduction by NEM is not caused by differences in Hg^{II}-cell partitioning. Our findings implicate interactions between Hg^{II} and cell thiols as an important part of anaerobic Hg^{II} reduction. We further discuss mechanistic insights into possible enzymatic partners and propose avenues of future investigation for this cryptic microbial Hg transformation.

5.4 MATERIAL AND METHODS

5.4.1 Microbial Culturing

***Heliomicrobium modesticaldum* Ice1:**

MIC assays with NEM and bioreactor experiments were conducted using the strain *Heliomicrobium modesticaldum* Ice1 from the DSMZ culture collection (DSM-9504). Cell cultures were handled under anaerobic conditions in a Coy anaerobic glove box (atmosphere 97% $N_{2(g)}$ and 3% $H_{2(g)}$) or by using sterile anaerobic benchtop techniques where all equipment was sparged with 100% $N_{2(g)}$ prior to use. For all growth assays and bioreactor experiments, new cell cultures were revived in the anaerobic glovebox from cryostocks kept at −80°C by scraping frozen culture with a sterile pipette tip and discarding it into a Balch tube containing growth medium PYE where the headspace of the tubes was then sparged to contain 100% $N_{2(g)}$.

The medium composition of PYE is Na-pyruvate 2.2 g/L, yeast extract 0.2 g/L, K_2HPO_4 1 g/L, $MgSO_4*7H_2O$ 0.2 g/L, $Na_2S_2O_3$ 1 mM, $CaCl_2*2H_2O$ 0.02 g/L, $(NH_4)_2SO_4$ 1 g/L (15.1 mM of NH_4^+), anoxic $FeSO_4$ 20 µM, D-biotin 0.015 µg/mL, vitamin B12 as cyanocobalamin 0.02 µg/mL, and 1 mL of trace element solution SL6. Trace elements SL6 contained: $ZnSO_4*7\ H_2O$ 0.1 g/L,

$MnCl_2$*4 H_2O 0.3 g/L, H_3BO_3 0.3 g/L, $CoCl_2$*6H_2O 0.2 g/L, $CuCl_2$*2H_2O 0.01 g/L, $NiCl_2$*6H_2O 0.02 g/L, Na_2MoO_4*2H_2O 0.03 g/L.

Cultures were incubated at 50 °C with an incandescent light source emitting photoactive radiation (PAR) at an intensity of 80 μmol photon m^{-2} s^{-1} until they reached mid-exponential phase. Cultures were then used to start new cultures with a 10% (v/v) inoculum into Balch tubes containing 10 mL of the same growth medium. Depending on the metabolic conditions desired, these re-inoculations and all subsequent ones were either kept in front of light for photoheterotrophic growth or wrapped in foil and kept in the dark for fermentative growth.

For bioreactor experiments, cells were harvested again after reaching mid-exponential to start cultures with a 10% (v/v) inoculum in serum bottles containing 75 mL of the same growth medium. Upon reaching mid- to late-exponential phase, these cultures were used as a 10% (v/v) inoculum in bioreactor experiments containing the same growth medium. For MIC experiments, cells were transferred again after reaching mid-exponential to start the MIC assay in 10 mL Balch tubes.

***Escherichia coli* NEB5α:**

NEM-Hg partitioning assays were conducted with *E. coli* NEB5α (DH5α derivative of the K12 strain). Cultures were prepared under anaerobic conditions in a Coy anaerobic glove box. Cultures were revived from -80°C cryostocks onto fumarate-GMM plates [37] and incubated at 37 °C in anaerobic jars. A single colony was then picked and added to liquid GMM medium [37] in an anaerobic Balch tube and grown overnight. The following day, cultures were used for NEM-Hg partitioning assays.

5.4.2 NEM minimum inhibitory concentration assays

We conducted minimum inhibitory concentration assays with *H. modesticaldum* Ice1 to identify NEM concentrations to work at for later Hg partitioning assays and bioreactor experiments. Effectively, we monitored growth curves with NEM added at different concentrations. N-ethylmaleimide powdered reagent (99+%, Thermo Scientific Chemicals) was used to prepare working solutions and were kept away from bright light sources to prevent photodegradation per the manufacturer's MSDS documentation. *H. modesticaldum* Ice1 was cultured as previously described and mid-exponential photoheterotrophic and fermentative cultures were added to separate Balch tubes containing PYE growth media to a final O.D. 600nm of ~ 0.2, which is the same cell density used for bioreactor experiments. To these Balch tubes, NEM solution was added to a final concentration of 0, 100 µM, and 200 µM. Each condition was prepared in biological triplicates. Balch tubes were then incubated at 50 °C in the light or dark, and cell growth was measured as the optical density at 600 nm (O.D. 600nm) in individual Balch tubes using a spectrophotometer over the course of 48 hours. Additional experiments were also later included for photoheterotrophic cultures at an NEM concentration of 1000 µM after the initial assays showed cultures tolerated lower concentrations quite well.

5.4.3 NEM-Hg partitioning assays with *E. coli*, a non-reducing strain

We developed a Hg partitioning assay to quantify THg associated to different fractions (cell, media, and glass associated) under NEM exposure. *E. coli* NEB5α, rather than *H. modesticaldum*, was used to test the effect of NEM on Hg partitioning because it does not reduce Hg^{II} to Hg^{0} [9]. As the *E. coli* O.D. 600nm required to retrieve a sizable pellet was ~0.4, yet the bioreactor assays are conducted at an O.D. 600nm of ~0.2, we doubled the concentration of Hg and NEM that *E. coli* was exposed to compared to the concentrations used for bioreactors. Thus,

we maintained equal ratios of cell O.D.600nm: Hg: NEM between the partitioning assays and bioreactor experiments, i.e. 0.400 O.D.: 500 pM Hg: 400 μM NEM for *E.coli* assays & 0.200: 250 pM: 200 μM for *H.modesticaldum* bioreactors.

In preparation for these assays, all material was acid-washed for 24 hours in 10% HCl to remove traces of Hg bound to glass Balch tubes, 5 mL Teflon vials, or plastic 2 mL microcentrifuge tubes. All material was brought into a Coy anaerobic glovebox to deoxygenate for 48 hours prior to the start of assays. Additionally, all assay steps were performed inside the anaerobic chamber.

E. coli was cultured as previously described. Three Balch tube cultures of similar O.D. 600nm were chosen for the assay. Cultures were gently centrifuged to form pellets and resuspended twice in medium PYE to remove traces of GMM medium. In six Balch tubes with PYE medium, sufficient resuspended *E.* coli was added to reach an O.D. 600nm of ~0.4 in a final volume of 10 mL. Six sterile controls containing only medium PYE were also prepared. To half of all assay Balch tubes, 400 μM of NEM solution was added; to the no NEM controls, the same volume of anoxic water was added. Tubes were wrapped in foil and then placed to incubate in a shaking incubator at 37 °C for one hour to allow NEM to saturate cells. After one hour, 500 pM of $HgCl_2$ was added to every tube. 1 mL was subsampled from each Balch tube into microcentrifuge tubes to quantify the total Hg added at the start of the experiment. Balch tubes were then incubated for three hours at 37 °C. We chose an assay duration of three hours because of two lines of reasoning: 1) *E. coli*-based Hg biosensors reveal that within the first three hours of exposure the vast majority of Hg^{II} added can be detected intracellularly [38,39], and 2) in our anaerobic Hg^{II} reduction bioreactor assays the first 0 to 12 hours have consistently high rates of Hg^0 production [9].

At the end of the three-hour exposure time, samples were then prepared to extract and quantify Hg associated to different fractions. To begin, we subsampled 2 mL of each live culture Balch tube into centrifuge tubes and gently spun down at 3000 rpm for 10 minutes. After spinning down the samples, the supernatant was removed and filter-sterilized through a 0.2 μm syringe filter to remove residual cells. The filtrated liquid was kept as it represents the media-associated Hg fraction. Additionally, we prepared the following blanks in Teflon tubes to quantify any background Hg from reagents: PBS buffer blank, PYE medium blank, and milliQ blank. Next, we washed the remaining cell pellets once with 1 mL PBS buffer to remove any residual media-associated Hg, gently spun at 3000 rpm for 10 minutes, and put the discarded PBS supernatant into a microcentrifuge tube labelled "PBS wash".

All microcentrifuge tubes and Balch tubes were brought to a trace metal clean lab for the next steps of the extraction. We resuspended the cell pellet with 1 mL of 70% HNO_3, transferred the liquid to a Teflon vial, and rinsed the Eppendorf tube with another 1 mL HNO_3 to retrieve any leftover Hg. We also added the samples taken at the start of the experiment into Teflon tubes and rinsed the microcentrifuge tubes with 1 mL of 70% HNO_3. We then put these Teflon vials in an incubator set to 55 °C to digest for one hour. The purpose of this digestion is to break down cells and free any intracellular Hg.

Balch tubes were thoroughly emptied, and their insides were soaked for 15 minutes three times with 10 mL of 10% HCl to remove any Hg bound to glass, keeping 1 mL of each wash in clean Teflon tubes. Lastly, we added 1% v/v of 70% concentrated HNO_3 to all Teflon vial samples not previously prepared with HNO_3 to preserve them prior to analysis. We then prepared samples for CVAFS according to the EPA Method 1631 and quantified total Hg in samples on a Tekran® 2600 Automated Sample Analysis System.

Though we tried, we could not successfully obtain consistent intracellular vs cell-surface THg results with the *E.coli* Hg partitioning assay (data not included). The original chemical agent we used to remove cell-surface Hg, DMSA, caused the cell pellet to lose integrity. We suspect that DMSA was destabilizing the outer membrane of *E.coli,* as reported by others [40].

5.4.4 Bioreactor experiments with *H. modesticaldum* Ice1

The bioreactor setup and subsampling methods used in this study were identical to those validated and used in prior research [9,10]. All bioreactor experiments were conducted at 50 °C in growth medium PYE. Fermentative bioreactor experiments were conducted in complete darkness and phototrophic bioreactors were placed under a light intensity of 20 μmol photon m^{-2} s^{-1} to limit abiotic photoreduction of Hg^{II} [10]. Live cell bioreactors were performed in triplicates for each condition tested and with initial *H. modesticaldum* Ice1 cell inocula of 10% (v/v) from cultures grown until mid- to late-exponential phase. An abiotic bioreactor experiment exposed to light and containing sterile PYE growth media with 100 μM NEM was performed once to confirm the absence of any NEM-mediated photoreduction of Hg^{II}. For every bioreactor experiment, a fresh NEM solution was prepared by dissolving its powdered form in sterile anoxic water to a thousand-fold higher concentration than the desired final concentration of NEM in the bioreactor. For example, a 200 mM stock was prepared to spike into a bioreactor for a final concentration of 200 μM. Every bioreactor experiment was spiked with 250 pM of $HgCl_2$ and ran for 48 hours to measure cumulative hourly Hg^0 production using a Tekran 2537B CVAFS Analyzer. NEM solutions were always added to the bioreactor prior to spiking with Hg^{II} to allow NEM to saturate cells. Briefly, the overall order of operation for bioreactors is: 1) set up bioreactor with anoxic growth media, 2) add cell culture, 3) spike NEM stock solution into the bioreactor to reach desired final concentration, 4) After one hour, spike $HgCl_2$ to a final concentration of 250 pM.

5.4.5 Statistical analyses

Two-way parametric ANOVAs were used to test for the effect of NEM addition on total Hg partitioning to different fractions and on cumulative Hg^0 production during phototrophic and fermentative bioreactors. Tests for assumptions of normal distribution of residuals and constant variance were passed. For both analyses, treatments where significant differences were observed were identified using a Tukey HSD *post hoc* test with the significance threshold set to $p<0.05$. All statistical analyses were performed in R version 4.2.2 (R Core Team) with "multcomp" [41] and "car" [42] packages. Detailed statistical results are provided in the figure captions.

5.5 RESULTS

5.5.1 MIC identifies tolerable range of NEM concentration

Due to N-ethylmaleimide's strong cellular inhibitory potential, we first conducted minimum inhibitory concentration assays on phototrophic and fermentative cultures of *H. modesticaldum* Ice1 to identify a range of NEM concentrations to work with for subsequent experiments. In these assays, we used the same starting cell O.D. 600nm as used in Hg^{II} bioreactor experiments to accurately identify a cell-to-NEM ratio to use in later bioreactor experiments. We determined that concentrations from 0 to 1000 μM of NEM had none to severe effects on growth rate and cellular yield for photoheterotrophic and fermentative cultures (**SI Figure 5.1**). Having identified a range of NEM concentrations at the cusp of causing adverse effects, we performed Hg partitioning assays at an equivalent 200 μM and bioreactor assays at 0, 100, and 200 μM.

5.5.2 NEM does not affect Hg partitioning

Considering that Hg^{II} cellular bioavailability is in part influenced by interactions with cell-surface thiol groups [15,43–47], we also aimed to verify if NEM prevented Hg^{II} from associating to cells. To test this, we exposed a non-reducing strain of *E. coli* to Hg^{II} and NEM and analyzed to

which fractions Hg^{II} was associated after a 3-hour incubation. To be consistent with later bioreactor experiments, we used equivalent ratios of cell O.D. 600nm: Hg concentration: NEM concentration. As we needed higher cellular biomass to successfully extract cell-bound Hg we doubled cell O.D., Hg, and NEM concentrations compared to bioreactors, i.e. for an O.D. 600nm of 0.400 we added 500 pM Hg (1 ng in 10 mL) and 400 μM of NEM to these assays.

Here we report no significant effect of 400 μM NEM addition on the partitioning of Hg to different fractions (p=0.77) (**Figure 5.1**). Mean cell-associated total Hg was not different between cells exposed to 0 μM NEM and to 400 μM (0.21 ± 0.07 ng and 0.31 ± 0.04 ng, respectively). Mirroring these results, there were no significant differences between Hg concentrations remaining in the growth media at 0 μM and 400 μM NEM (0.28 ± 0.13 ng and 0.16 ± 0.06 ng, respectively). The percent mean total Hg recovered was 91± 2% across all treatments when comparing the sum of cell, glass, and media-associated Hg fractions to the Hg initially added to the assays. Our results highlight that pM concentrations of Hg^{II} can still partition to cells exposed to 400 μM of NEM. With these results in hand, we proceeded to test the effect of NEM on Hg^{II} reduction by *H. modesticaldum*.

5.5.3 NEM differentially inhibits Hg^0 production during photoheterotrophy and fermentation

To test whether NEM addition prevented anaerobic Hg^{II} reduction by *H. modesticaldum* Ice1, we compared cumulative Hg^0 production over the course of 48 hours under both photoheterotrophic and fermentative growth conditions at NEM concentrations of 0 μM, 100 μM, and 200 μM. Here, we added 250 pM of $HgCl_2$ to bioreactor cultures containing an equivalent cell density measured as O.D. 600nm of 0.2. The sterile growth media bioreactor shows there is negligible abiotic photoreduction of Hg^{II} in the presence of 100 μM NEM (**SI Figure 5.2B**).

We found that there was a significant concentration-dependent effect of NEM on cumulative Hg^0 production by *H. modesticaldum* ($p=2.5 * 10^{-8}$) (**Figure 5.2**). Within the first few hours of bioreactor assays, NEM treatments displayed a large drop in hourly Hg^0 produced. This drop was most pronounced under fermentative conditions and maximum at 200 μM NEM (**Figure 5.3**). Unlike in Balch tubes, photoheterotrophic and fermentative cultures did not grow in bioreactors exposed to 100 μM and 200 μM (**SI Figure 5.3**). We do not attribute the decrease in Hg^0 production specifically to the lack of growth. Our previous work highlights that Heliobacterial Hg^{II} reduction under phototrophic conditions occurs even in the absence of quantifiable growth or an oxidizable carbon source [9,11]. However, under fermentative conditions, the availability of a carbon source directly impacts the magnitude of Hg^0 produced [9].

Typically, in the absence of NEM, the magnitude of Hg^{II} reduction is greater for fermentative cultures than for phototrophic ones. To take this difference into account when considering the effect of NEM on Hg^0 production, we compared the mean percent difference in Hg^0 produced between no NEM and NEM-added bioreactors. The phototrophic bioreactors with 200 μM of NEM showed a mean decrease in cumulative Hg^0 production compared to bioreactors without NEM of 85 ± 2.2% (mean percent difference ± standard error of the mean percent). On the other hand, the fermentative bioreactors with 200 μM of NEM exhibited a lower mean decrease of 68.4 ± 4.5%. Interestingly, this effect is inversed at a concentration of 100μM where we observe a greater mean decrease in fermentative Hg^0 production (36 ± 7.6%) than phototrophic Hg^0 production 14.8 ± 22.8%.

5.6 DISCUSSION

5.6.1 Hg partitioning assay suggests NEM inhibition of Hg^{II} reduction is not due to preventing Hg from partitioning to cells.

The high affinity of Hg^{II} for thiol ligands means that on a typical cell surface with ligands such as thiols, carboxyls, and phosphates, Hg^{II} will first bind to thiol groups, often in a two or more thiol coordination [37]. There are both passive [48,49] and active [44,50] Hg^{II} uptake mechanisms; some entail interactions with cell-surface thiols, while others do not. Bacterial surface thiol concentrations can range from 16 to 33 mmol per gram of wet cell weight [51]. Furthermore, estimated intracellular thiol concentrations for anaerobes range from 10 to 200 mM [52]. As we did not observe significant differences in Hg partitioning in the presence of μM-levels of NEM, we do not expect all cell-surface and intracellular thiols to be irreversibly bound to this chemical inhibitor, likely leaving mM amounts of thiols available for potential Hg^{II} interaction. Therefore, in bioreactor assays with *H. modesticaldum*, it is very unlikely that NEM inhibition of Hg^{II} reduction is caused by binding to all cellular thiols and preventing uptake. However, as we used the Gram-negative *E. coli* for Hg partitioning assays, we worked under the assumption that Hg^{II} bioavailability and cell-surface interactions are comparable to those with the Gram-positive Heliobacteria. We chose to work with *E. coli* instead of Heliobacteria for this assay because of the risk of results being skewed by Hg^0 evasion and loss during the multiple steps of the partitioning assays. We cannot discount that their dissimilarities in cell membrane structures may cause differences in interactions between Hg^{II} and cells, and between NEM and cell-surface thiols. However, some of these differences may be negligible as cell-surface thiols concentrations of Gram-positive and Gram-negative bacteria and between mesophilic and thermophilic strains are similar [51].

At the onset of the development of Hg partitioning assays with *E. coli*, we sought to quantify intracellular versus cell-surface Hg^{II}. Our initial attempt at the assay used the powerful Hg chelator DMSA[30] to remove cell-surface Hg but it caused the cell pellet to lose integrity and shrink in size after successive cell washing and re-pelleting steps. We suspect that DMSA was destabilizing the outer membranes of *E.coli* and causing cell lysis, an effect reported by others [40]. Ultimately, we could not successfully extract membrane-associated Hg and intracellular-associated Hg. Therefore, we cannot further substantiate whether the concentration-dependent inhibition of NEM on Heliobacterial Hg^{II} reduction is linked to greater extracellular or intracellular Hg partitioning. An alternative chemical inhibitor approach may be used to test if irreversible binding to cell-surface thiols blocks all Hg^{II} reduction. Monobromo(trimethylammonio)bimane (mBBr) binds irreversibly to thiols while being too large to penetrate cell membranes [53,54], unlike NEM, which can reach the cytosol [55,56]. In future work, we plan to test Hg^{II} reduction by *H. modesticaldum* under mBBr exposure.

5.6.2 NEM may inhibit essential enzymatic pathways

NEM that enters the cytosol and irreversibly binds to thiol groups may prevent multiple cellular pathways from operating normally, including those linked to Hg^{II} reduction. Research using NEM as an alkylating agent has highlighted its inhibitory effect on multiple proteins and intracellular thiol-bearing molecules. For those relevant to Heliobacteria, we discuss their potential role in Hg^{II} reduction.

In *H. modesticaldum*, the photosynthetic reaction center and PFOR reduce ferredoxins; one-electron cytosolic redox cofactors [25]. Ferredoxins carry electrons to other oxidoreductases, namely to the NADH-dependent ferredoxin:$NADP^+$ oxidoreductase (NfnAB) [25]. This type of oxidoreductase, first characterized in *Clostridium kluyveri*, shares sequence and functional

similarity with plant ferredoxin:$NADP^+$ oxidoreductases (FNR) [57]. NfnAB is an electron-bifurcating enzyme that couples the exergonic reduction of $NADP^+$ with ferredoxin and the endergonic reduction of $NADP^+$ with NADH in a reversible reaction [58]. As such, it plays a crucial role in maintaining redox homeostasis by balancing the ratio of oxidized and reduced pyridines (i.e. NAD(H) and NADP(H)) and ferredoxin pools [59]. Considering that electron flow, or reducing power, from fermentation and phototrophy both interface via NfnAB and the enzyme catalyzes 2-electron transfer reactions, it may be of interest for future investigations. NfnAB may either be the enzymatic site of Hg^{II} reduction or the next oxidoreductase controlling electron flow towards a yet unidentified cellular site of Hg^{II} reduction. Though Hg^{II}'s affinity for bacterial NfnAB is not documented, there is precedent to suspect Hg^{II}-thiol interactions on this protein. A study investigating cadmium inhibition of spinach FNR activity found that cadmium was binding to cysteine residues on FNR, which was further confirmed by showing decreased binding of Cd^{II} to FNR upon addition of N-ethylmaleimide [60,61]. Authors further suggest that cadmium's inhibition of FNR may cause conformational changes that disturb ferredoxin binding and thus electron transfer. As Hg^{II} and Cd^{II} share chemical properties (e.g., cationic soft metals having an affinity for sulphur and the ability to displace Zn and Fe in metalloproteins [62]) and plant FNR and prokaryotic NfnAB share sequence similarity, Hg^{II} may be able to interact with Heliobacterial NfnAB and perhaps intercept electrons. Our current methodology cannot verify whether NEM inhibited NfnAB activity and whether this, in turn, inhibited Hg^{II} reduction. Given the central role of NfnAB in *H. modesticaldum,* no gene deletion attempt has been successful to date. A deletion approach may thus not be an achievable way to test the role of this enzyme in Hg^{II} reduction. Gene insertions into non-reducing anaerobes or *in vitro* purified protein assays may be alternative options to test whether NfnAB and its cofactors can catalyze Hg^{II} reduction.

5.6.3 NEM may affect cytosolic thiol-based redox buffers

Strong irreversible binding of NEM to thiols may stop the proper functioning of cytosolic low molecular mass (LMM) redox buffers like free-cysteine, glutathione [56], and bacillithiols which *H. modesticaldum* uses in lieu of glutathione [63]. Upon entering the cytosol, Hg^{II} will likely interact with intracellular thiol-based redox buffers such as bacillithiols and free-cysteines and quench or possibly oxidize them [64,65]. Redox buffers offer intracellular protection against the oxidative stress of Hg by being themselves a target for oxidation [66]. Thiol-based redox homeostasis systems, such as thioredoxins/thioredoxin reductases and bacilliredoxins/bacillithiol disulfide reductases work to re-reduce oxidized protein thiols and bacillithiols respectively [67–69]. We propose the reduction to Hg^0 may happen via cellular re-reduction of Hg^{II} bound to thiols via such thiol-based redox regulating machinery. A similar mechanism has been proposed but not verified in *Thermus thermophilus* HB27 wherein thioredoxins might directly reduce or sequester Hg^{II}, or that thioredoxin reductases may reduce thioredoxin-Hg^{II} complexes thus leading to detoxification by evasion of Hg^0 [70]. Future experiments targeting these proteins via either inhibitory or gene deletion approaches may serve to elucidate whether there is a coupling between thiol-based redox homeostasis systems and anaerobic Hg^{II} reduction.

5.7 CONCLUSION

There is little doubt that NEM lacks enzymatic specificity due to its irreversible binding mechanism to thiols. However, our findings support a reduction pathway where Hg^{II} interacts with thiol-bearing cell machinery. It is yet to be confirmed whether this interaction occurs with cell-surface thiols or thiol-bearing intracellular proteins and LMM molecules. With the recent advent of a reliable CRISPR-based molecular biology toolkit for *H. modesticaldum* [25,71–74], it is now possible to delete or insert specific genes of interest to resolve mechanistic details for anaerobic

Hg^{II} reduction. These experiments will be important for identifying genetic controls in Heliobacteria and can eventually be used to develop genetic targets to track anaerobic Hg^{II} reduction in the environment.

Author contributions

N.C.L and A.J.P. designed experiments, N.C.L. carried them out and performed data analysis, and N.C.L. and A.J.P. wrote the manuscript.

Conflict of interest

The authors declare that there are no conflicts of interest.

Funding information

Our work was funded by NSERC Discovery and Accelerator grants, CFI funding to AJP and NSERC graduate scholarships to NCL.

5.8 FIGURES AND CAPTIONS

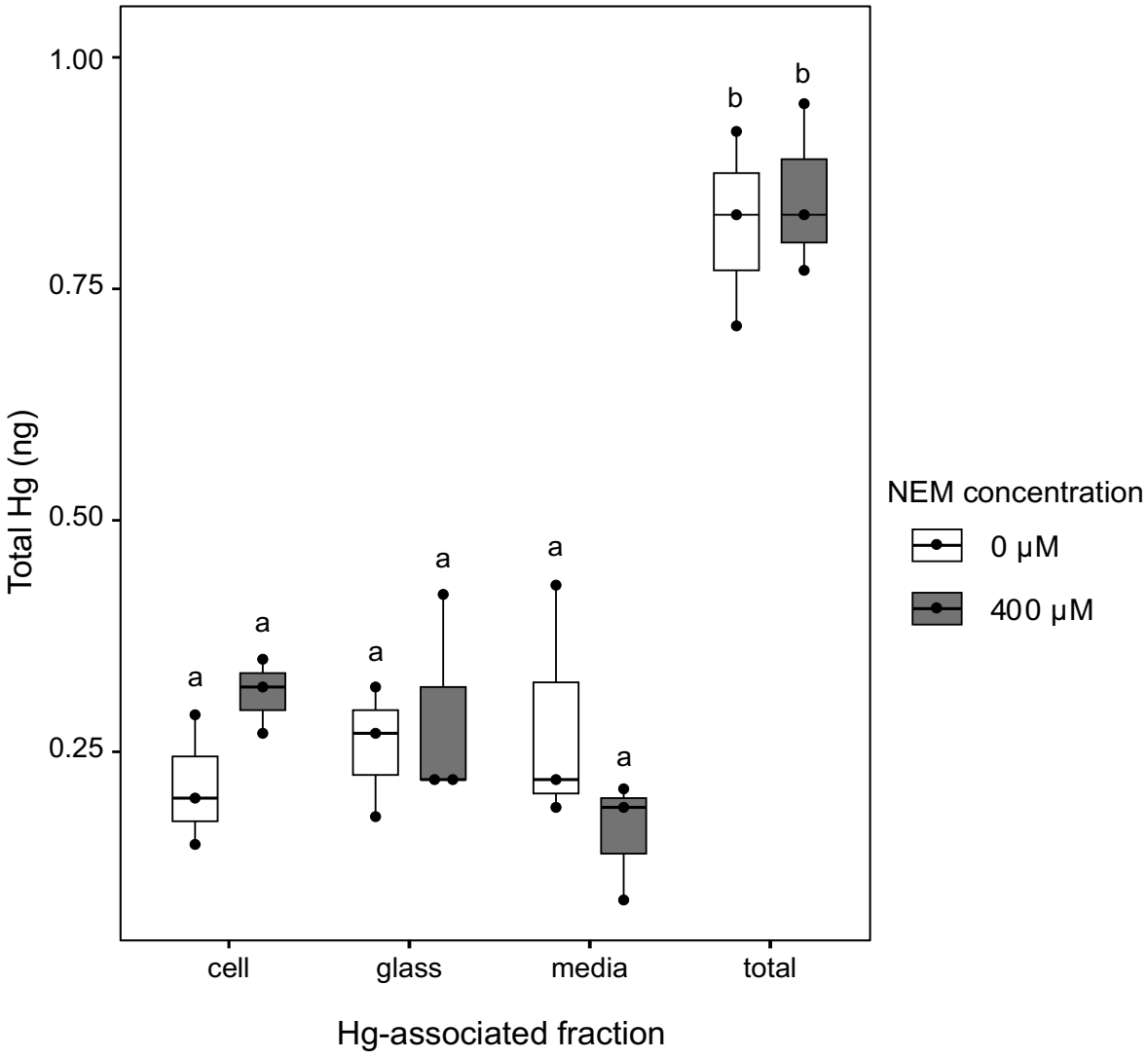

Figure 5.1: Total Hg quantified from partitioning assays of *E. coli* cultures in medium PYE and exposed to NEM for 3 hours. Hg-associated fractions represent in order from left to right: *E. coli* cell-pellet associated Hg, glass-bound Hg from Balch tubes, Hg remaining in 0.2 µm-filtered spent growth media, and the total Hg initially present in the exposure assay. We maintained equal ratios of cell O.D.600nm : Hg : NEM between the exposure assay and bioreactor experiments, i.e. 0.400 O.D.: 500pM Hg: 400µM NEM for these *E.coli* assays & 0.200: 250pM: 200µM for *H.modesticaldum* bioreactors. At the start of the exposure, approximately [Hg^{II}] = 500 pM or 1 ng in 10 mL of culture was added. The bottom and top of the boxes show the first and third quartiles, respectively; the bar in the middle shows the median, and the whiskers show the minimum and maximum for each treatment. The black circles overlain represent the individual sample measurements for n = 3 *E. coli* biological replicates. Assumptions of normally distributed residuals (p = 0.16) and homoscedasticity (p = 0.99) were met for a two-way parametric ANOVA,

which showed there was a significant difference between Hg-associated fractions ($p = 4.8 * 10^{-9}$) but not between NEM concentrations ($p = 0.77$) or their interaction ($p = 0.248$). Letters that are not shared between fractions indicate a significant difference according to the Tukey HSD test ($p < 0.05$).

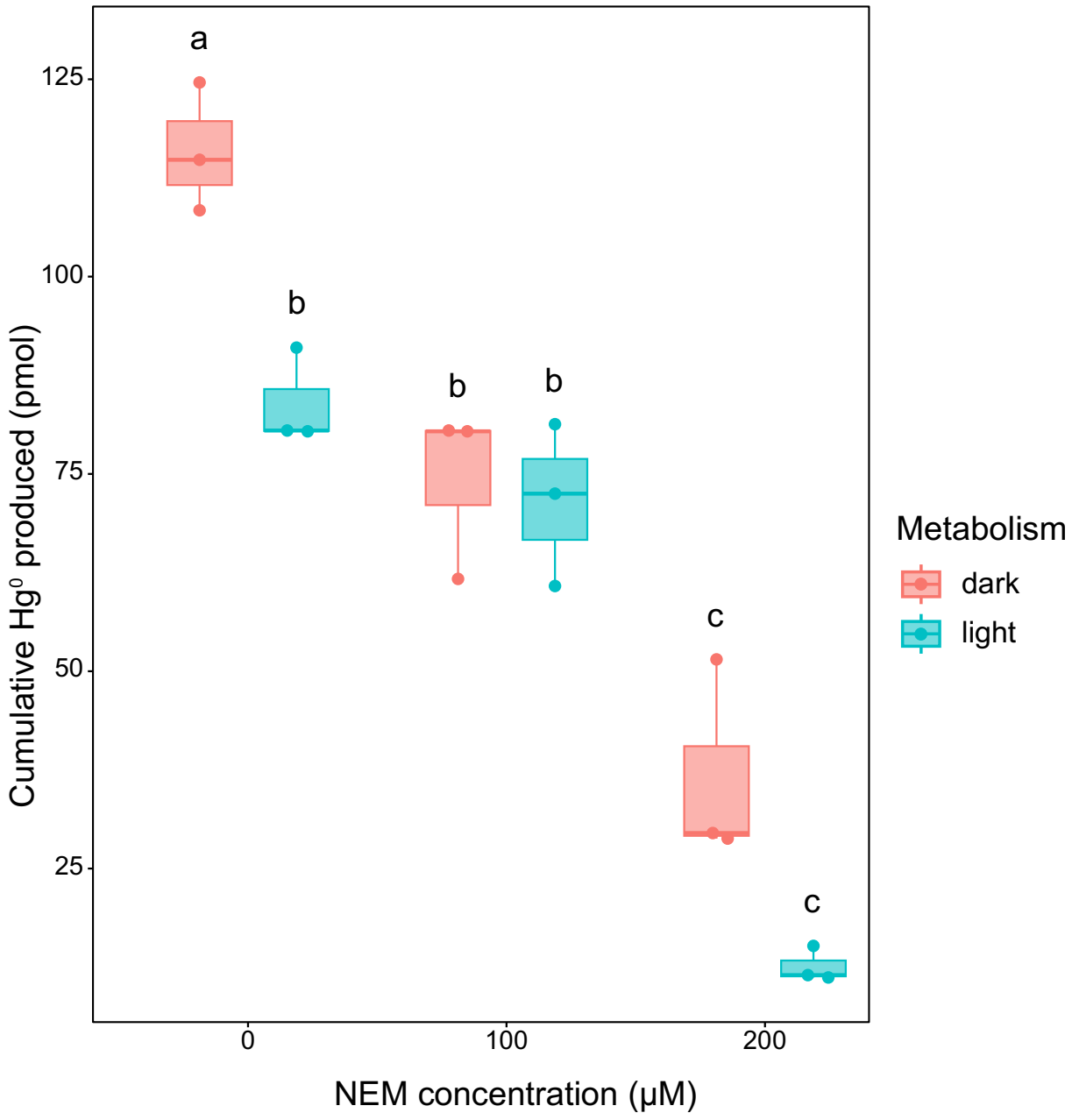

Figure 5.2: Cumulative Hg^0 produced during bioreactor experiments with *H. modesticaldum* Ice1

grown photoheterotrophically (light) and fermentatively (dark) in medium PYE exposed to NEM concentrations ranging from 0 to 200 μM. The bottom and top of the boxes show the first and third quartiles, respectively; the bar in the middle shows the median, and the whiskers show the minimum and maximum for each treatment. The circles overlain represent the individual bioreactor experiments (n = 3) as biological replicates. Assumptions of normally distributed

residuals ($p = 0.85$) and homoscedasticity ($p = 0.93$) were met for a two-way parametric ANOVA, which showed there was a significant effect of NEM addition and Metabolism on cumulative Hg^0 production ($p = 2.5 * 10^{-8}$ and $p = 6.7 * 10^{-4}$ respectively) and a significant effect of their interaction ($p = 0.043$). Letters that are not shared between fractions indicate a significant difference according to the Tukey HSD test ($p < 0.05$).

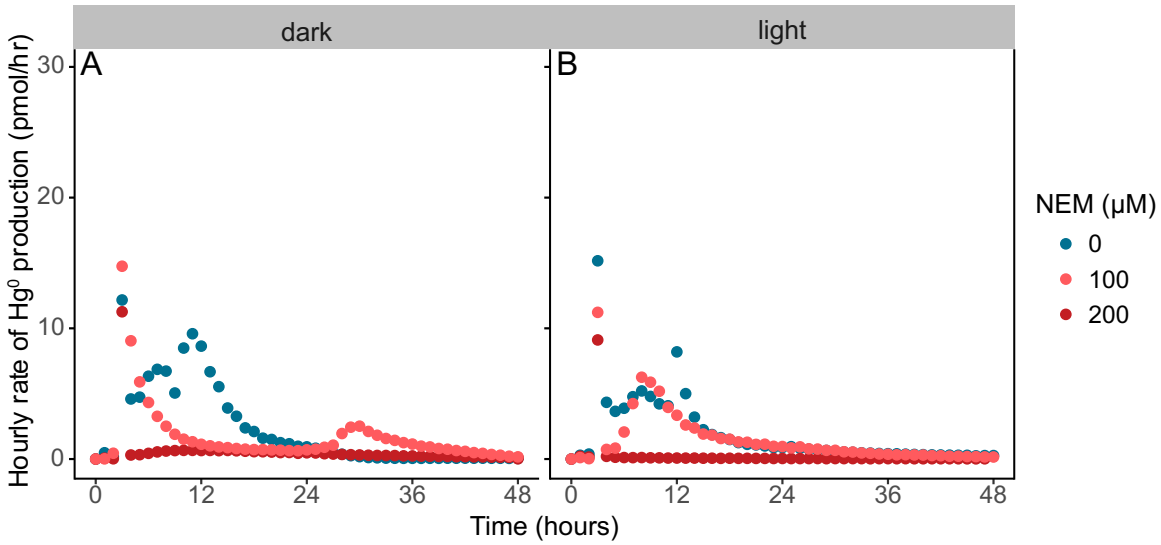

Figure 5.3: Hourly rate of Hg^0 production for individual representative bioreactor assays with *H. modesticaldum* Ice1 in medium PYE during A) dark (fermentative) and B) light (photoheterotrophic) exposure to NEM.

5.9 REFERENCES

1. Morel, F. M. M., Kraepiel, A. M. L. & Amyot, M. The Chemical Cycle and Bioaccumulation of Mercury. *Annual Review of Ecology and Systematics* **29**, 543–566 (1998).

2. Selin, N. E. Global Biogeochemical Cycling of Mercury: A Review. *Annual Review of Environment and Resources* **34**, 43–63 (2009).

3. Fleming, E. J., Mack, E. E., Green, P. G. & Nelson, D. C. Mercury methylation from unexpected sources: molybdate-inhibited freshwater sediments and an iron-reducing bacterium. *Appl Environ Microbiol* **72**, 457–64 (2006).

4. Han, S. *et al.* Mercury speciation in marine sediments under sulfate-limited conditions. *Environ Sci Technol* **44**, 3752–7 (2010).

5. Podar, M. *et al.* Global prevalence and distribution of genes and microorganisms involved in mercury methylation. *Sci Adv* **1**, e1500675 (2015).

6. Schartup, A. T. *et al.* Freshwater discharges drive high levels of methylmercury in Arctic marine biota. *Proc Natl Acad Sci U S A* **112**, 11789–94 (2015).

7. Parks, J. M. *et al.* The genetic basis for bacterial mercury methylation. *Science* **339**, 1332–5 (2013).

8. Hsu-Kim, H., Kucharzyk, K. H., Zhang, T. & Deshusses, M. A. Mechanisms regulating mercury bioavailability for methylating microorganisms in the aquatic environment: a critical review. *Environ Sci Technol* **47**, 2441–56 (2013).

9. Gregoire, D. S., Lavoie, N. C. & Poulain, A. J. Heliobacteria Reveal Fermentation As a Key Pathway for Mercury Reduction in Anoxic Environments. *Environ Sci Technol* **52**, 4145–4153 (2018).

10. Grégoire, D. S. & Poulain, A. J. A physiological role for HgII during phototrophic growth. *Nature Geoscience* **9**, 121–125 (2016).

11. Lavoie, N. C., Gregoire, D. S., Stenzler, B. R. & Poulain, A. J. Reduced sulphur sources favour Hg(II) reduction during anoxygenic photosynthesis by Heliobacteria. *Geobiology* (2019) doi:10.1111/gbi.12364.

12. Barkay, T., K. Kritee, Kritee, K., Boyd, E. S. & Geesey, G. G. A thermophilic bacterial origin and subsequent constraints by redox, light and salinity on the evolution of the microbial mercuric reductase. *Environmental Microbiology* **12**, 2904–2917 (2010).

13. Christakis, C. A., Barkay, T. & Boyd, E. S. Expanded Diversity and Phylogeny of mer Genes Broadens Mercury Resistance Paradigms and Reveals an Origin for MerA Among Thermophilic Archaea. *Front. Microbiol.* **12**, (2021).

14. Liu, S. N. & Wiatrowski, H. A. Reduction of Hg(II) to Hg(0) by Biogenic Magnetite from two Magnetotactic Bacteria. *Geomicrobiol J* **35**, 198–208 (2018).

15. Lin, H., Morrell-Falvey, J. L., Rao, B., Liang, L. & Gu, B. Coupled mercury-cell sorption, reduction, and oxidation on methylmercury production by Geobacter sulfurreducens PCA. *Environ Sci Technol* **48**, 11969–76 (2014).

16. Schaefer, J. K., Letowski, J. & Barkay, T. mer-mediated resistance and Volatilization of Hg(II) under anaerobic conditions. *Geomicrobiol J* **19**, 87–102 (2002).

17. Wiatrowski, H. A., Ward, P. M. & Barkay, T. Novel reduction of mercury (II) by mercury-sensitive dissimilatory metal reducing bacteria. *Environ Sci Technol* **40**, 6690–6 (2006).

18. Zhao, L. D. *et al.* Contrasting effects of dissolved organic matter on mercury methylation by Geobacter sulfurreducens PCA and Desulfovibrio desulfuricans ND132. *Environmental Science & Technology* **51**, 10468–10475 (2017).

19. Lu, X. *et al.* Anaerobic Mercury Methylation and Demethylation by Geobacter bemidjiensis Bem. *Environ Sci Technol* **50**, 4366–73 (2016).

20. Asao, M. & Madigan, M. T. Taxonomy, phylogeny, and ecology of the heliobacteria. *Photosynth Res* **104**, 103–111 (2010).

21. Brockmann, H. & Lipinski, A. Bacteriochlorophyll g. A new bacteriochlorophyll from Heliobacterium chlorum. *Arch. Microbiol.* **136**, 17–19 (1983).

22. Gest, H. & Favinger, J. L. Heliobacterium chlorum, an anoxygenic brownish-green photosynthetic bacterium containing a “new” form of bacteriochlorophyll. *Arch. Microbiol.* **136**, 11–16 (1983).

23. Kimble, L. K., Mandelco, L., Woese, C. R. & Madigan, M. T. Heliobacterium modesticaldum, sp. nov., a thermophilic heliobacterium of hot springs and volcanic soils. *Archives of Microbiology* **163**, 259–267 (1995).

24. Tang, K. H., Yue, H. & Blankenship, R. E. Energy metabolism of Heliobacterium modesticaldum during phototrophic and chemotrophic growth. *Bmc Microbiol* **10**, (2010).

25. Walters, K. A., Redding, K. E. & Golbeck, J. H. Identification and characterization of the low molecular mass ferredoxins involved in central metabolism in Heliomicrobium modesticaldum. *Photosynth Res* (2024) doi:10.1007/s11120-023-01069-z.

26. Heinnickel, M., Shen, G. Z. & Golbeck, J. H. Identification and characterization of PshB, the dicluster ferredoxin that harbors the terminal electron acceptors F-A and F-B in Heliobacterium modesticaldum. *Biochemistry-Us* **46**, 2530–2536 (2007).

27. Romberger, S. P., Castro, C., Sun, Y. L. & Golbeck, J. H. Identification and characterization of PshBII, a second F-A/F-B-containing polypeptide in the photosynthetic reaction center of Heliobacterium modesticaldum. *Photosynth Res* **104**, 293–303 (2010).

28. Tang, K. H. *et al.* Carbon Flow of Heliobacteria Is Related More to Clostridia than to the Green Sulfur Bacteria. *J Biol Chem* **285**, 35104–35112 (2010).

29. Grégoire, D. S., Janssen, S. E., Lavoie, N. C., Tate, M. T. & Poulain, A. J. Stable Isotope Fractionation Reveals Similar Atomic-Level Controls during Aerobic and Anaerobic Microbial Hg Transformation Pathways. *Applied and Environmental Microbiology* **87**, e00678-21 (2021).

30. Rooney, J. P. The role of thiols, dithiols, nutritional factors and interacting ligands in the toxicology of mercury. *Toxicology* **234**, 145–56 (2007).

31. Gregory, J. D. The Stability of N-Ethylmaleimide and its Reaction with Sulfhydryl Groups. *J. Am. Chem. Soc.* **77**, 3922–3923 (1955).

32. Smyth, D., Blumenfeld, O. & Konigsberg, W. Reactions of N-ethylmaleimide with peptides and amino acids. *Biochemical Journal* **91**, 589–595 (1964).

33. Summers, A. O. & Sugarman, L. I. Cell-Free Mercury(II)-Reducing Activity in a Plasmid-Bearing Strain of Escherichia coli. *Journal of Bacteriology* **119**, 242–249 (1974).

34. Fox, B. & Walsh, C. T. Mercuric reductase. Purification and characterization of a transposon-encoded flavoprotein containing an oxidation-reduction-active disulfide. *Journal of Biological Chemistry* **257**, 2498–2503 (1982).

35. Fox, B. S. & Walsh, C. T. Mercuric reductase: homology to glutathione reductase and lipoamide dehydrogenase. Iodoacetamide alkylation and sequence of the active site peptide. *Biochemistry* **22**, 4082–4088 (1983).

36. Shahak, Y., Crowther, D. & Hind, G. The involvement of ferredoxin-NADP+ reductase in cyclic electron transport in chloroplasts. *Biochimica et Biophysica Acta (BBA) - Bioenergetics* **636**, 234–243 (1981).

37. Stenzler, B. R., Zhang, R., Semrau, J. D., DiSpirito, A. A. & Poulain, A. J. Diffusion of H2S from anaerobic thiolated ligand biodegradation rapidly generates bioavailable mercury. *Environmental Microbiology* **24**, 3212–3228 (2022).

38. Stenzler, B. R., Gaudet, J. & Poulain, A. J. An Anaerobic Biosensor Assay for the Detection of Mercury and Cadmium. *J Vis Exp* (2018) doi:10.3791/58324.

39. Stenzler, B., Hinz, A., Ruuskanen, M. & Poulain, A. J. Ionic Strength Differentially Affects the Bioavailability of Neutral and Negatively Charged Inorganic Hg Complexes. *Environ. Sci. Technol.* **51**, 9653–9662 (2017).

40. Alakomi, H.-L., Paananen, A., Suihko, M.-L., Helander, I. M. & Saarela, M. Weakening Effect of Cell Permeabilizers on Gram-Negative Bacteria Causing Biodeterioration. *Applied and Environmental Microbiology* **72**, 4695–4703 (2006).

41. Hothorn, T., Bretz, F. & Westfall, P. Simultaneous Inference in General Parametric Models. *Biometrical Journal* **50**, 346–363 (2008).

42. Weisberg, Fox J. *An R Companion to Applied Regression*. (Sage, Thousand Oaks CA, 2019).

43. Mareike Gutensohn, J. Schaefer, E. Yunda, U. Skyllberg, & E. Björn. The Combined Effect of Hg(II) Speciation, Thiol Metabolism, and Cell Physiology on Methylmercury Formation by Geobacter sulfurreducens. *Environmental Science and Technology* (2023) doi:10.1021/acs.est.3c00226.

44. Schaefer, J. K. *et al.* Active transport, substrate specificity, and methylation of Hg(II) in anaerobic bacteria. *Proc Natl Acad Sci U S A* **108**, 8714–9 (2011).

45. Schaefer, J. K. & Morel, F. M. M. High methylation rates of mercury bound to cysteine by Geobacter sulfurreducens. *Nat Geosci* **2**, 123–126 (2009).

46. Hu, H. *et al.* Mercury reduction and cell-surface adsorption by Geobacter sulfurreducens PCA. *Environ Sci Technol* **47**, 10922–30 (2013).

47. Liu, Y. R. *et al.* Effects of Cellular Sorption on Mercury Bioavailability and Methylmercury Production by Desulfovibrio desulfuricans ND132. *Environ Sci Technol* **50**, 13335–13341 (2016).

48. Benoit, J. M., Gilmour, C. C. & Mason, R. P. Aspects of Bioavailability of Mercury for Methylation in Pure Cultures of Desulfobulbus propionicus (1pr3). *Applied and Environmental Microbiology* **67**, 51–58 (2001).

49. Mason, R. P., Reinfelder, J. R. & Morel, F. M. M. Uptake, toxicity, and trophic transfer of mercury in a coastal diatom. *Environ Sci Technol* **30**, 1835–1845 (1996).

50. Schaefer, J. K., Szczuka, A. & Morel, F. M. M. Effect of divalent metals on Hg(II) uptake and methylation by bacteria. *Environmental Science and Technology* **48**, 3007–3013 (2014).

51. Yu, Q., Szymanowski, J., Myneni, S. C. B. & Fein, J. B. Characterization of sulfhydryl sites within bacterial cell envelopes using selective site-blocking and potentiometric titrations. *Chemical Geology* **373**, 50–58 (2014).

52. Gutensohn, M., Schaefer, J. K., Maas, T. J., Skyllberg, U. & Björn, E. Metabolic turnover of cysteine-related thiol compounds at environmentally relevant concentrations by Geobacter sulfurreducens. *Front. Microbiol.* **13**, (2023).

53. Joe-Wong, C., Shoenfelt, E., Hauser, E. J., Crompton, N. & Myneni, S. C. B. Estimation of Reactive Thiol Concentrations in Dissolved Organic Matter and Bacterial Cell Membranes in Aquatic Systems. *Environ. Sci. Technol.* **46**, 9854–9861 (2012).

54. Thomas, S. A., Mishra, B. & Myneni, S. C. B. Cellular Mercury Coordination Environment, and Not Cell Surface Ligands, Influence Bacterial Methylmercury Production. *Environ. Sci. Technol.* **54**, 3960–3968 (2020).

55. D. McLaggan *et al.* Glutathione-dependent conversion of N-ethylmaleimide to the maleamic acid by Escherichia coli: an intracellular detoxification process. *Applied and Environmental Microbiology* **66**, 1393–1399 (2000).

56. Mojica, E.-R. E., Kim, S. & Aga, D. S. Formation of N-Ethylmaleimide (NEM)-Glutathione Conjugate and N-Ethylmaleamic Acid Revealed by Mass Spectral Characterization of Intracellular and Extracellular Microbial Metabolites of NEM. *Applied and Environmental Microbiology* **74**, 323–326 (2008).

57. Seedorf, H. *et al.* The genome of Clostridium kluyveri, a strict anaerobe with unique metabolic features. *Proceedings of the National Academy of Sciences* **105**, 2128–2133 (2008).

58. Buckel, W. & Thauer, R. K. Flavin-Based Electron Bifurcation, Ferredoxin, Flavodoxin, and Anaerobic Respiration With Protons (Ech) or NAD(+) (Rnf) as Electron Acceptors: A Historical Review. *Front Microbiol* **9**, 401 (2018).

59. Poudel, S. *et al.* Origin and Evolution of Flavin-Based Electron Bifurcating Enzymes. *Front Microbiol* **9**, 1762 (2018).

60. Grzyb, J., Bojko, M., Waloszek, A. & Strzałka, K. Ferredoxin:NADP+ oxidoreductase as a target of Cd2+ inhibitory action – Biochemical studies. *Phytochemistry* **72**, 14–20 (2011).

61. Grzyb, J., Waloszek, A., Latowski, D. & Więckowski, S. Effect of cadmium on ferredoxin:NADP+ oxidoreductase activity. *Journal of Inorganic Biochemistry* **98**, 1338–1346 (2004).

62. Parks, J. M. & Smith, J. C. Chapter Five - Modeling Mercury in Proteins. in *Methods in Enzymology* (ed. Voth, G. A.) vol. 578 103–122 (Academic Press, 2016).

63. Sattley, W. M. *et al.* The genome of Heliobacterium modesticaldum, a phototrophic representative of the Firmicutes containing the simplest photosynthetic apparatus. *J Bacteriol* **190**, 4687–4696 (2008).

64. Hansen, J. M., Zhang, H. & Jones, D. P. Differential oxidation of thioredoxin-1, thioredoxin-2, and glutathione by metal ions*. *Free Radical Biology and Medicine* **40**, 138–145 (2006).

65. Wang, Y., Robison, T. & Wiatrowski, H. The impact of ionic mercury on antioxidant defenses in two mercury-sensitive anaerobic bacteria. *Biometals* **26**, 1023–1031 (2013).

66. Meyer, A. J. & Hell, R. Glutathione homeostasis and redox-regulation by sulfhydryl groups. *Photosynth Res* **86**, 435–57 (2005).

67. Fassler, R., Zuily, L., Lahrach, N., Ilbert, M. & Reichmann, D. The Central Role of Redox-Regulated Switch Proteins in Bacteria. *Front. Mol. Biosci.* **8**, (2021).

68. Chandrangsu, P., Loi, V. V., Antelmann, H. & Helmann, J. D. The Role of Bacillithiol in Gram-Positive Firmicutes. *Antioxid Redox Signal* **28**, 445–462 (2018).

69. Ma, Z. *et al.* Bacillithiol is a major buffer of the labile zinc pool in Bacillus subtilis. *Molecular Microbiology* **94**, 756–770 (2014).

70. Norambuena, J., Wang, Y., Hanson, T., Boyd, J. M. & Barkay, T. Low molecular weight thiols and thioredoxins are important players in Hg(II) resistance in Thermus thermophilus HB27. *Appl Environ Microbiol* (2018) doi:10.1128/AEM.01931-17.

71. Baker, P. L. *et al.* A molecular biology toolkit for the phototrophic Firmicute, Heliobacterium modesticaldum. *Appl Environ Microbiol* (2019) doi:10.1128/AEM.01287-19.

72. Baker, P. L. *et al.* Using the endogenous CRISPR-Cas system of Heliobacterium modesticaldum to delete the photochemical reaction center core subunit gene. *Appl Environ Microbiol* (2019) doi:10.1128/AEM.01644-19.

73. Layton, A. M. & Redding, K. E. Examination of Genetic Control Elements in the Phototrophic Firmicute Heliomicrobium modesticaldum. *Microorganisms* **10**, 876 (2022).

74. Orf, G. S., Gisriel, C. J., Granstrom, J., Baker, P. L. & Redding, K. E. The PshX subunit of the photochemical reaction center from Heliobacterium modesticaldum acts as a low-energy antenna. *Photosynthesis Research* **151**, 11–30 (2022).

Chapter 6

The anoxygenic phototroph *Chloroflexus aurantiacus* J-10-fl does not reduce Hg^{II} to Hg^{0}

Noémie C. Lavoie [a], Alexandre J. Poulain [a]

a - Biology Department, University of Ottawa, 30 Marie Curie, Ottawa, ON, K1N 6N5, Canada.

N.B. Supporting information for this chapter can be found in **Appendix E**

6.1 ABSTRACT

Mercury (Hg) is a pervasive environmental pollutant whose toxicity is amplified through microbial methylation processes, leading to neurotoxic methylmercury (MeHg) formation. In anoxic environments, the microbial reduction of Hg^{II} to elemental Hg^{0} plays a crucial role in mercury cycling, controlling the pool of inorganic Hg available for methylation. This study explores the Hg^{II} reduction potential of the filamentous anoxygenic phototroph *Chloroflexus aurantiacus* J-10-fl, a model organism from the Chloroflexota phylum. Despite shared metabolic and environmental characteristics with known anoxygenic phototrophs capable of Hg^{II} reduction, such as *Rhodobacter capsulatus* and *Heliomicrobium modesticaldum*, C. aurantiacus J-10-fl was found incapable of reducing Hg^{II} under various growth conditions, including anoxygenic photoheterotrophy and aerobic chemoheterotrophy on different carbon substrates (acetate, pyruvate, butyrate, and glucose) and photoautotrophy. Bioreactor experiments demonstrated that Hg^{0} production in cultures was comparable to abiotic controls, indicating minimal microbial contribution to Hg^{II} reduction. These findings demonstrate that the mechanisms underlying microbial Hg^{II} reduction are not universally present among anoxygenic phototrophs. Conducting detailed mechanistic studies with Hg^{II}-reducers and non-reducers to identify the factors that enable microbial Hg^{II} reduction will offer deeper insights into the ecological roles and evolutionary adaptations of microorganisms in mercury cycling.

6.2 INTRODUCTION

The heavy metal mercury (Hg) is a globally distributed pollutant whose fate is heavily regulated by microbial processes [1]. In terrestrial and aquatic environments, its most neurotoxic form, methylmercury (MeHg), is produced from inorganic Hg by anaerobic microorganisms [2–5]. Within these anoxic environments, Hg redox cycling is one of the key factors controlling the

availability of inorganic Hg to methylators [6]. Hg^{II} reduction leads to the formation of elemental gaseous Hg^0, which can volatilize from water and soils [7–9] and thus affect the remaining fraction of inorganic Hg available to Hg methylators.

In low-light anoxic environments, dissolved organic matter and iron minerals such as mackinawite and magnetite can abiotically catalyze the reduction of Hg^{II} [10–12]. Biotically, certain aerobic [13] and anaerobic microorganisms [14–22] can also reduce Hg^{II}. Aerobes containing the genetically encoded mercuric reductase (MerA) [23] reduce Hg^{II} as part of a detoxification strategy [24]. Unlike *mer*-mediated Hg^{II} reduction, dedicated genetic determinants for anaerobic Hg^{II} reduction have yet to be identified, making it challenging to measure the contribution of these pathways to Hg cycling in the environment. Research findings suggest that for these bacteria, core components of cellular respiration [20,25], fermentation, [15] or anoxygenic phototrophy [15,17] are driving anaerobic Hg^{II} reduction.

To date, anaerobic Hg^{II} reduction has been identified in a wide range of bacteria belonging to the Bacillota, Pseudomonadota, and Thermodesulfobacteriota phyla (**SI Figure 6.1**). Two dissimilatory metal-reducing bacteria (DMRB), *Geobacter sulfurreducens* PCA and *Shewanella oneidensis* MR-1, are reported to reduce Hg^{II} via non-*mer* mediated mechanisms. These DMRB perform extracellular electron transfer where outer membrane cytochromes transfer electrons from intracellular processes to an extracellular electron acceptor [26]. In *G. sulfurreducens* PCA, the ability to reduce Hg^{II} to Hg^0 is greatly affected by the abundance of outer membrane c-type cytochromes [18,27]. In *S. oneidensis* MR-1, the reduction of Hg^{II} is linked to the availability of electron acceptors and donors for respiration [20,28]. In recent work with an engineered *S. oneidensis* mutant deficient for OmcA, an outer-membrane cytochrome c, Hg^{II} reduction was significantly

decreased [29]. Thus, for these DMRB, though the mechanism is not fully known, Hg^{II} is reduced extracellularly and outer-membrane cytochromes are involved as electron carriers.

In the environment, increased Hg^0 production has been associated with blooms of phototrophic microorganisms both in freshwater [30,30–33] and marine [34] ecosystems. To further investigate the potential roles of phototrophs in Hg cycling, we tested whether purple non-sulphur bacteria (PNSB), commonly found in such ecosystems, could reduce Hg^{II}. We found that three different species reduced Hg^{II} during anoxygenic photoheterotrophy when grown on the reduced carbon source and that under those conditions, exposure to sublethal concentrations of Hg^{II} enhanced growth [17]. Members of the PNSB are known to accrue excess reducing power as NAD(P)H while growing photoheterotrophically on reduced carbon sources such as butyrate, and to maintain redox homeostasis, these microbes can shuttle excess reducing power onto electron sinks such as inorganic carbon ions (HCO_3^-) or dimethylsulfoxide (DMSO) [35,36]. It was thus demonstrated that PNSB could use Hg^{II} as an electron sink to maintain redox homeostasis.

Lastly, we identified novel anaerobic Hg^{II} reducers in the Bacillota phylum (formerly Firmicutes): two anoxygenic photoheterotrophs from the *Heliobacteriaceae* and a fermenting *Clostridium* [15,16]. Though not well resolved, the mechanism does not appear to be directly linked to the redox state of the carbon source but tied to cells' ability to generate reducing power from photosynthetic electron transport or fermentation of organic carbon sources. Searching for new anaerobic Hg^{II} reducers is essential for uncovering the evolutionary and physiological contexts that shape this response to inorganic Hg among phylogenetically distinct microorganisms. While mechanistic details can be resolved by studying individual strains, further insights may also be gained from comparisons of reduction capabilities across different genetic and environmental backgrounds.

In this work, we chose to further investigate the potential for phylogenetically distant anoxygenic phototrophs to catalyze Hg^{II} reduction. Bacteria capable of anoxygenic phototrophy are denoted by the presence of a photosynthetic reaction center. Type II reaction centers employ quinones as terminal electron acceptors and are found in PNSB, purple sulphur bacteria, and Chloroflexi. Type I uses ferredoxins as its electron acceptors and are characteristic of the Heliobacteria and green sulphur bacteria. The ability to reduce Hg^{II} is thus found among anoxygenic phototrophs harbouring both types of reaction centers. In addition, Hg^{II} is a potent toxicant to photosynthetic machinery due to its electrophilic nature. In PNSB, Hg^{II} exposure damages reaction centers and light-harvesting complexes and can react with quinones and cytochromes [37,38], thus impeding cyclic electron transport. Given the high affinity of Hg^{II} for photosynthetic machinery, reducing Hg^{II} to gaseous elemental Hg^0 may serve as a detoxification mechanism.

We selected a model filamentous anoxygenic phototroph from the Chloroflexota phylum, *Chloroflexus aurantiacus* J-10-fl. Quite cosmopolitan, strains of *C. aurantiacus* have been found in hot spring microbial mats in the United States, Guatemala, Iceland, Japan, and New Zealand [39]. Early characterization efforts revealed that this filamentous anoxygenic phototroph has a mixotrophic lifestyle, able to grow as an aerobic chemoheterotroph or anoxygenic photoheterotroph in the presence of a variety of organic carbon sources likely derived from cyanobacteria present in microbial mats [39,40]. A novel CO_2 fixation pathway was first discovered in *C. aurantiacus;* enabling it to grow photoautotrophically via the 3-hydroxypropionate bi-cycle (3-OHP) [41–43]. *C. aurantiacus* J-10-fl, though phylogenetically distant from the Heliobacteriaceae and purple non-sulphur bacteria, shares environmental and cellular similarities with both microbial groups. Like the Hg^{II}-reducing PNSB, *C. aurantiacus* J-10-fl can grow mixotrophically aerobically

and anaerobically using diverse organic carbon sources [40], and both use a type II quinone-based photosynthetic reaction center [44]. Like *Heliomicrobium modesticaldum* Ice1, *C. aurantiacus* J-10-fl is a thermophile capable of growing at 50-60°C and originates from hot spring microbial mats [39].

We aimed to assess whether *C. aurantiacus* could reduce Hg^{II} while growing on the same organic carbon substrates that have supported Hg^{II} reduction in other known anaerobic Hg^{II} reducers (**Table 6.1**). As the 3-OHP bi-cycle is a carbon metabolic pathway not found in other known Hg^{II} reducers, we also tested whether Hg^{II} reduction occurred during photoautotrophy. Additionally, we share our reliable culturing approach, which we hope will aid other researchers working with *C. aurantiacus* as a model organism. We have adapted culture media and conditions to support the vigorous growth of *C. aurantiacus* during aerobic chemoheterotrophy, anoxygenic photoheterotrophy, and anoxygenic photoautotrophy. Here, we report the extensive inability of *C. aurantiacus* J-10-fl to reduce Hg^{II} and further discuss metabolic insights this provides on the reduction mechanism(s) in other known anaerobic Hg^{II} reducers.

6.3 MATERIAL AND METHODS

6.3.1 Microbial culturing

All experiments were conducted using the strain *Chloroflexus aurantiacus* J-10-fl from the DSMZ culture collection (DSM-635). Cell cultures were handled under anaerobic conditions in a Coy anaerobic glove box (atmosphere 97% N_2 (g) and 3% H_2 (g)) or by using sterile anaerobic benchtop techniques where all equipment was sparged with 100% N_2 (g) prior to use. For all growth assays and bioreactor experiments, new cell cultures were revived in the anaerobic glovebox from cryostocks kept at −80 °C by scraping frozen culture with a sterile pipette tip and

discarding it into a Balch tube containing the optimal revival growth medium, which was a modified PE medium based on the Hanada *et al.* 1995 [45] recipe that contains acetate as the primary carbon source and a pH of 7.5. Revival cultures were flushed with 100% $N_{2(g)}$ and incubated at 50 °C with an incandescent light source emitting photoactive radiation (PAR) at an intensity of 80 µmol photon m^{-2} s^{-1} until they reached mid-exponential stage. Revival cultures were then used to start new cultures with a 10% (v/v) inoculum into Balch tubes or 100 mL serum bottles containing fresh modified PE medium.

6.3.2 Growth media recipes for different metabolisms

Given the mixotrophic capabilities of *C. aurantiacus,* we developed variations of the PE medium and growth conditions to permit anoxygenic photoheterotrophy, aerobic chemoheterotrophy, and anoxygenic photoautotrophy. Our base modified PE medium contained the following in 1 L: sodium acetate 0.5 g, sodium-succinate 0.5 g, sodium-glutamate 0.5 g, casamino acids 0.5 g, $Na_2S_2O_3$ 0.5 g, KH_2PO_4 0.38 g, K_2HPO_4 0.39 g, $(NH_4)_2SO_4$ 0.5 g, $CaCl_2*2H_2O$ 0.015 g, NaCl 0.117 g, vitamin solution 1 mL, trace metals solution 1 mL, $FeSO_4*7H_2O$ 1 mL from a 20 mM anoxic stock solution. The vitamin solution contained the following in 100 mL of 50% v/v DMSO/H_2O: thiamin hydrochloride 0.1 g, riboflavin 0.002 g, D-biotin 0.01 g, folic acid 0.05 g, para-aminobenzoic acid 0.01 g, cyanocobalamine 0.0015 g. The trace metals solution contained in 1 L: $MgSO_4*4H_2O$ 0.111 g, $ZnSO_4*7H_2O$ 0.0288 g, $Co(NO_3)_2*6H_2O$ 0.0292 g, $CuSO_4*5H_2O$ 0.0252 g, $Na_2MoO_4*2H_2O$ 0.0242 g, H_3BO_3 0.031 g, Na_2-EDTA 3 g. Variations of the heterotrophic growth medium were made by substituting sodium acetate in the modified PE medium for equimolar (6.1 mM) concentrations of either sodium butyrate, sodium pyruvate, or D-glucose. An autotrophic growth medium was made by removing

all organic matter from the modified PE medium (remove acetate, succinate, glutamate, and casamino acids) and providing 50 mM of $NaHCO_3$ in the growth medium.

6.3.3 Anaerobic culturing modifications

Growing *C. aurantiacus* in the autotrophic modified PE medium was initially very slow until we sparged the Balch tube headspace with a gas mix containing 10% H_2: 10% CO_2: 80% N_2. Indeed, others experimenting with *Chlorofexi* and photoautotrophy report that supplementing H_2 gas in the headspace was necessary to achieve significant cell growth [43]. Briefly, our culturing protocol involved reviving *C. aurantiacus* in modified PE medium containing acetate, then upon reaching mid-exponential phase, 1 mL of culture per new inoculum was gently centrifuged, pelleted, and washed with autotrophic modified PE medium 3 times to remove traces of organic carbon. Cultures were incubated with an incandescent light source and upon reaching mid-exponential phase they were re-inoculated 10% (v/v) into fresh autotrophic medium. This step was repeated once more, for a total of three rotation to ensure vigorous autotrophic growth prior to starting experiments. During the whole growth curve period, we sparged the Balch tubes once a day with fresh gas mix containing 10% H_2: 10% CO_2: 80% N_2.

6.3.4 Aerobic modifications

Growing *C. aurantiacus* aerobically required a modified set-up to overcome the challenges of rapid water evaporation at 50 °C and consistent Hg-free O_2 supply. We used a Tekran® Model 1100 Zero Air Generator to pump filtered and Hg-free room air into microbial cultures grown in 250 mL glass bottles fitted with a 2-port screw-top cap. The Zero Air Generator was connected to Tygon tubing, followed by a Y-shaped tube connector, 2 pieces of tubing, then 2 gas flow meters, 2 pieces of tubing, 2 more Y-shaped tube connectors, 4 pieces of tubing, 4 in-line 0.2 mm Teflon

gas filters, 4 pieces of autoclaved Teflon tubing inserted into the inlet ports of 4 glass bottles containing microbial cultures. These bottles were inside an incubator set to 50 °C. A small piece of foil was kept on top of the outlet port of the bottles to minimize water loss to evaporation. Effectively, from one pump box, we were able to grow 4 cultures simultaneously. With this set-up we were able to greatly minimize evaporative loss (less than 5% of the total volume).

6.3.5 Bioreactor methodology

For anaerobic bioreactor experiments, cells were harvested from Balch tube-grown cultures after reaching mid-exponential to start cultures with a 10% (v/v) inoculum in serum bottles containing 75 mL of the same growth medium. Upon reaching mid- to late-exponential phase, one of these cultures was used as an inoculum in a bioreactor experiment containing the same growth medium. Enough culture inoculum was added to reach an initial O.D. 600nm of ~0.2 in a 0.5 L bioreactor. For aerobic bioreactor experiments, cells were harvested from 250 mL glass bottles containing 125 mL of culture and growth media and re-inoculated at 10% (v/v) into new 250 mL glass bottles with fresh media. Upon reaching mid- to late- exponential phase, one of these cultures was used as an inoculum in a bioreactor experiment containing the same growth medium.

The bioreactor set-up and subsampling methodologies are identical to those validated and used in previous work [15,17] except for the following modification. For all aerobic bioreactors, room air was the source of gas and was pumped into the bioreactor by a Tekran® Model 1100 Zero Air Generator. All bioreactor experiments were carried out at 50 °C, and for phototrophic experiments at a light intensity of 20 μmol photon m^{-2} s^{-1} to limit abiotic photoreduction of Hg^{II} [17]. All live cell bioreactor treatments were performed in triplicates with initial *C. aurantiacus* J-10-fl cell inocula grown until mid- to late-exponential phase, and abiotic controls were performed once. Each

bioreactor experiment was spiked with 250 pM of $HgCl_2$ and ran for 48 hours to measure cumulative Hg^0 production using a Tekran 2537B CVAFS Analyzer.

6.4 RESULTS

6.4.1 Growth is possible on carbon substrates used by known Hg^{II} reducers

Our first goal was to investigate the growth of *C. aurantiacus* J-10-fl on carbon sources that support high Hg^{II} reduction by known anaerobic Hg^{II} reducers. The modified PE growth medium sustained anoxygenic photoheterotrophy when substituted with acetate, pyruvate, or butyrate (**Figure 6.1A**). Pyruvate-grown cultures exhibited faster growth and reached stationary phase earlier than those grown on acetate or butyrate. However, all three carbon sources produced comparable final cellular yields. Aerobic chemoheterotrophic growth on acetate, pyruvate, or glucose was well supported (**Figure 6.1B**). Aerobic glucose cultures grew the fastest and had the highest cellular yield, likely due to the high energy yield of glycolysis. Generally, cellular yields were higher for cultures grown photoheterotrophically than chemoheterotrophically, a finding that aligns with Pierson & Castenholtz's original isolation and characterization of strain J-10-fl as a faster grower under phototrophic conditions [39]. Lastly, we report slow but consistent growth in autotrophic modified PE medium (**Figure 6.1C**). Interestingly, the photoautotrophic cultures continued growing much longer than their heterotrophic counterparts. It is likely that daily sparging of culture tubes with a gas mix containing 10% H_2: 10% CO_2: 80% N_2 provided a fresh supply of growth substrates. Others. have also observed that during photoautotrophy, *C. aurantiacus* J-10-fl continues to grow slowly but at a relatively consistent rate for weeks [43].

6.4.2 *Chloroflexus aurantiacus* does not reduce Hg in any of the tested conditions

With established culturing conditions, we proceeded to investigate whether *C. aurantiacus* J-10-fl could reduce Hg^{II} to Hg^0 while growing on carbon sources that fuel Hg^{II} reduction by microorganisms. We conducted bioreactor experiments to assess whether significant Hg^{II} reduction occurred under a range of carbon sources and metabolic conditions. In this context, significant reduction refers to live cell treatments that generate more Hg^0 compared to sterile growth media controls. Our previous studies highlight that interactions between Hg^{II} and growth media components typically contribute up to 10% of total Hg^0 production [15,16].

After extensive investigations, we report no meaningful Hg^{II} reduction during anoxygenic phototrophy and aerobic chemotrophy (**Table 6.1)**. The lack of Hg^{II} reduction is not associated with a lack of cellular activity, as all cultures grew significantly in the bioreactors (**SI Figure 6.2**). We observed similar levels of Hg^0 production for live cell bioreactors (0.1 to 6.2 pmol of Hg^0) (**Table 6.1**) and sterile growth medium bioreactors (2.2 to 4.5 pmol of Hg^0) (**SI Table 6.1)**, confirming that what little Hg^0 was detected originated primarily from abiotic reactions. Carbon substrate availability and metabolism did not affect the cumulative Hg^0 produced by cultures. Despite some shared physiological and environmental similarities with known anaerobic Hg^{II} reducers, *Chloroflexus aurantiacus* J-10-fl does not share their ability to reduce Hg^{II}.

6.5 DISCUSSION

6.5.1 Common metabolic pathways and environmental conditions are not associated with the ability to reduce Hg^{II}

In the absence of a fully detailed anaerobic Hg^{II} reduction mechanism, we can only speculate why *C. aurantiacus* does not reduce Hg^{II}. It may be that the unknown reduction

mechanism is absent in this Chloroflexi or that due to cellular differences such as cell membrane composition or production of extracellular polymeric substance (EPS) [46], Hg^{II} is not bioavailable for intracellular reduction to Hg^0. However, by comparing known non-*mer* Hg^{II} reducers to other microbes incapable of Hg^{II} reduction, like *E. coli* K12 and now *C. aurantiacus*, we can shed some light on this elusive microbially mediated redox reaction.

Our results with *C. aurantiacus* J-10-fl highlight that not all thermophiles from hot springs can reduce Hg^{II}. Hot springs can vary widely in mercury concentrations, with values ranging from 8 pM to 120μM [47]. Microbial communities inhabiting geothermal environments high in Hg have had to adapt to this toxicity challenge [47]. Consequently, mercuric reductases (MerA) are commonly found in Bacteria and Archaea taxa in present-day hot springs [24]. Indeed, MerA is hypothesized to have originated from thermophilic bacteria in geothermal environments, and while some *merA* homologues have been identified in hot spring *Chloroflexi*, none have been found in phototrophic strains [13]. *H. modesticaldum* Ice1, also found in hot spring microbial mats, can reduce Hg^{II} in the absence of *merA*. Perhaps, in *C. aurantiacus'* immediate environment, there is little to no pressure from toxic Hg species, whether from naturally low concentrations or from protection conferred by microbial mat neighbours capable of Hg^{II} reduction.

While evidence to date shows that reducing power in the form of reduced ferredoxins generated by pyruvate:ferredoxin oxidoreductase (PFOR) is essential for fermentative Hg^{II} reduction by *Heliomicrobium modesticaldum* and *Clostridium acetobutylicum* [15], the presence of PFOR and ferredoxins in a genome does not correlate with the capacity to reduce Hg^{II}. *C. aurantiacus* and *E. coli* have genes for PFOR and ferredoxin synthesis and yet do not reduce Hg^{II} [15,48,49]. Though further mechanistic investigations are needed, this suggests the presence of PFOR

and ferredoxins are not sufficient for the reduction of $Hg^{II,}$ and there may be additional, yet unknown, cellular components or conditions required for reduction to be favourable.

This study reveals that not all anoxygenic phototrophs can reduce Hg^{II}. While PNSB and Heliobacteria reduce Hg^{II} during anoxygenic photoheterotrophy [15–17], *C. aurantiacus* conclusively cannot do so when grown photoautotrophically or photoheterotrophically. Furthermore, our findings show that photoheterotrophic growth on reduced carbon sources like butyrate does not create conditions conducive to Hg^{II} reduction in all photoheterotrophs. When grown phototrophically on butyrate, PNSB accrue excess reducing power in the form of NAD(P)H, causing a redox imbalance and stunting growth [35]. To maintain redox homeostasis, PNSB offload excess electrons onto DMSO or CO_2 /HCO_3^- via the activity of certain Calvin Cycle enzymes [35,36,50]. PNSB have been shown to reduce Hg^{II} only when grown on butyrate because Hg^{II} can act as an electron sink to maintain redox homeostasis [17]. *C. aurantiacus* cannot reduce Hg^{II} photoheterotrophically on butyrate; it is possible that growth on butyrate does not create a redox imbalance in this microorganism. Indeed, it has been suggested that in *C. aurantiacus*, the 3-OHP bi-cycle contributes to redox homeostasis during photoheterotrophic growth by using excess reducing power to fix CO_2 into larger organic molecules [51]. In other words, *C. aurantiacus* generates reducing power via photosynthetic electron transport and oxidative TCA cycle activity, which is then consumed by the 3-OHP bi-cycle to synthesize larger metabolites. Therefore, redox imbalance may not occur in *C. aurantiacus* cells, and thus, Hg^{II} reduction may not be a favourable process as it is in PNSB. Anoxygenic phototrophy is found across multiple phyla, and as this study demonstrates, although not all can reduce Hg^{II}, in time, we may uncover more than can.

6.5.2 Non-*mer* Hg^{II} reduction may be more common among strict anaerobes

Facultative aerobes like *Shewanella oneidensis* MR-1 and *Rhodobacter capsulatus,* are known Hg^{II} reducers. In *R. capsulatus*, this reduction occurs exclusively under anaerobic conditions [17], while *S. oneidensis* can reduce Hg^{II} during aerobic and anaerobic respiration [20]. *S. oneidensis* stands out as being the only known facultative aerobe capable of non-*mer* reduction in the presence of O_2. Other facultative aerobes, such as *E. coli* K12 and *C. aurantiacus*, do not reduce Hg^{II} under either aerobic or anaerobic conditions [15]. Although only a handful of microorganisms have been extensively studied for non-*mer* Hg^{II} reduction, all but *S. oneidensis* can only do so in anaerobic conditions. Determining if other microorganisms can reduce Hg^{II} may reveal whether anaerobic non-*mer* reduction is the rule or the exception and, from a mechanistic standpoint, whether the ability to reduce O_2 generally impedes this microbial transformation.

We have long questioned whether anaerobic Hg^{II} reduction may be an accidental consequence of a more reduced cytoplasm, where non-specific Hg^{II} reduction is occurring rather than a specific enzymatic reaction with Hg^{II}. In this version of a hypothesized mechanism, Hg^{II} may be able to scavenge electrons from multiple intracellular components if the redox potential strongly favours its reduction to Hg^0. A more reduced cytoplasm is generally linked to the absence of strong oxidizing agents such as oxygen [52]. Cell components that contribute to a more electronegative cytosolic redox potential include protein and non-protein reduced redox cofactors and functional groups such as thiols. While quantifying intracellular ratios of reduced to oxidized redox cofactors can be challenging and varies significantly depending on culturing conditions, it is possible to estimate how oxidized or reduced proteins or proteomes are based on their amino acid sequences. *Zc*, the carbon oxidation state of molecules, is a calculation of the average charge on carbon atoms given charges of all other surrounding atoms. The *Zc* of proteins is a particularly

informative metric as thermodynamics predict that more oxidized molecules are more stable in more oxidizing environments [53]. For microbes, this metric is linked with the redox conditions of their surrounding environment, where more negative *Zc* correlates with more electronegative environmental redox potentials [54–60].

We queried results from Dick & Tan (2023) for reference proteome *Zc* at the phylum, class, and, if available, order levels for microbes we tested for their ability or inability to reduce Hg^{II} (**SI Table 6.2**). These results highlight that of all microbial strains tested, Heliobacteria and Clostridia have the most negative *Zc* at the phylum and class level. However, the ability or inability to reduce Hg^{II} is not apparently linked to a trend in proteome *Zc* as some non-Hg reducers have a more negative *Zc* than Hg^{II} reducers. It is important to reiterate that a more reduced cytoplasm is not only a consequence of more reduced proteins but also of reduced non-protein components such as redox cofactors which cannot be accounted for solely by *Zc* [53]. Though this is a preliminary high-level search, there appears to be no clear relation between proteome *Zc* and Hg^{II} reduction ability, limiting, for now, the potential of *Zc* to be used as a screening tool to identify potential Hg reducers. To further investigate whether Hg^{II} reduction is a consequence of a more reduced cytoplasm, future endeavours should calculate *Zc* only for cytosolic protein components and develop or modify methods to quantify intracellular redox potential in a more direct manner.

6.6 CONCLUSION

Overall, our study highlights that the ability to reduce Hg^{II} is not necessarily shared by microorganisms that occupy similar environmental niches, consume common substrates, or operate related cellular machinery. Continued investigations into potential novel Hg^{II} reducers, like this present work, are needed to elucidate the apparent link between an anaerobic lifestyle and the ability to reduce Hg^{II} in the absence of *merA*. Anaerobic and anoxygenic phototrophic

metabolisms predate the rise of oxygen on Earth. As such, uncovering both the diversity of non-*mer*-based reducers and the mechanism(s) at play may one day reveal how ancient microorganisms coped with Hg toxicity in the absence of oxygen. Given the cryptic nature of the anaerobic Hg^{II} reduction mechanism found in anaerobes like Heliobacteria and PNSB, future work would gain fundamental insights from comparing their response to Hg^{II} to that of microbes incapable of reduction. Analyzing the transcriptomes of both Hg^{II}-reducing and non-reducing anoxygenic phototrophs may identify differences in expression responses to Hg^{II} exposure, which could, in turn, provide deeper insights into the mechanism of Hg^{II} reduction.

Funding info

Our work was funded by NSERC Discovery and Accelerator grants, CFI funding to AJP and NSERC graduate scholarships to NCL.

Author contributions

N.C.L and A.J.P. designed experiments, N.C.L. carried them out and performed data analysis, and N.C.L. and A.J.P. wrote the manuscript.

6.7 FIGURES AND TABLES

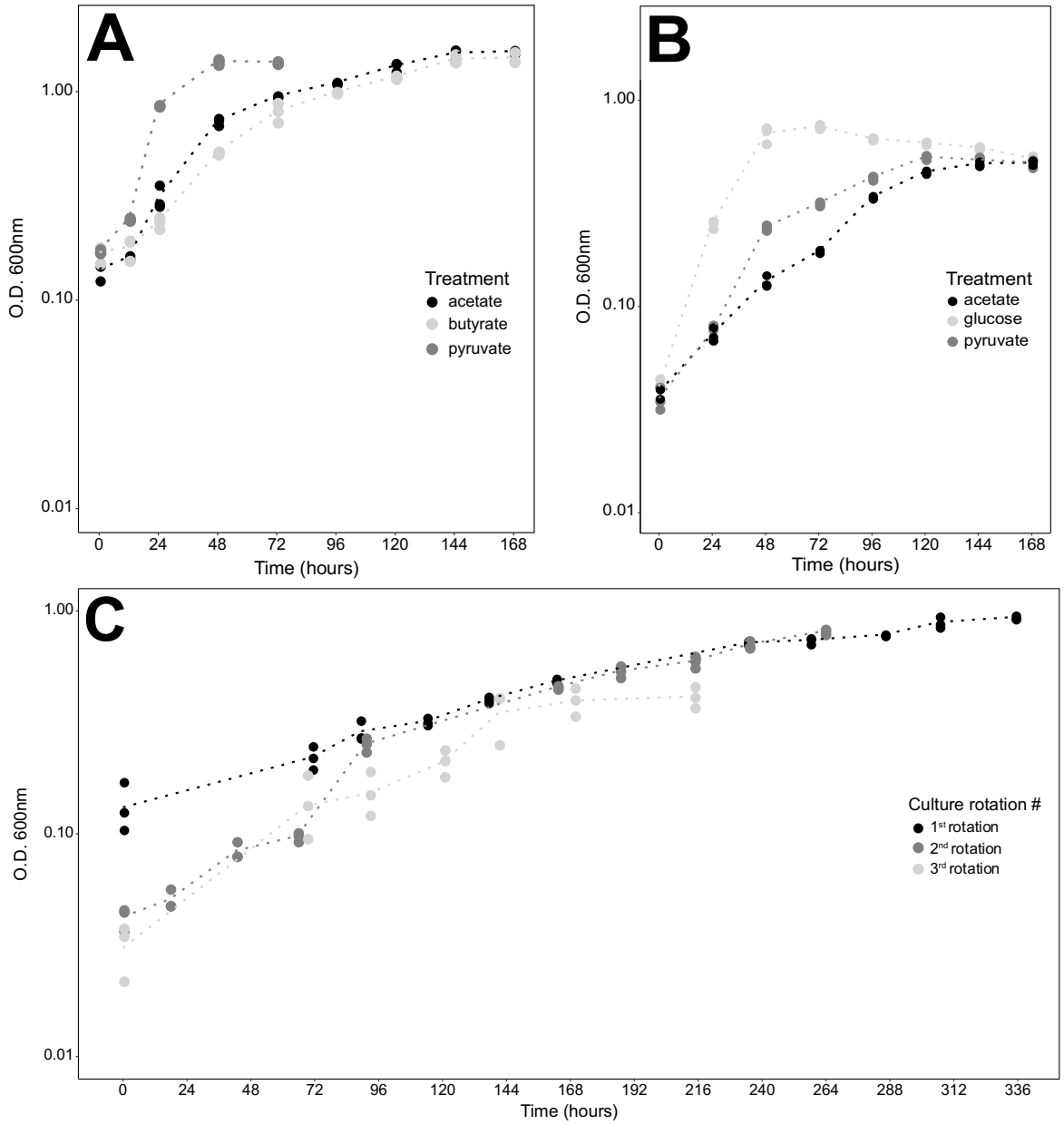

Figure 6.1: Growth curves for *Chloroflexus aurantiacus* J10-fl
Biological triplicates were monitored over time for cultures grown A) photoheterotrophically, B) chemoheterotrophically in the presence of $O_{2(g)}$, and C) photoautotrophically. Note that for photoautotrophy, the three growth curves presented show the 1st culture rotation into photoautotrophic conditions, a 2nd subsequent rotation, and a 3rd rotation to illustrate the adaptation of *C. aurantiacus* to CO_2 fixation.

Table 6.1: Bioreactor results for *Chloroflexus aurantiacus* J10-fl grown phototrophically and chemotrophically on various carbon sources and for other strains we previously tested.

Model organism	Metabolism	Carbon source	# of replicates	Mean cumulative Hg^0 production (pmol)	Relative Hg^0 production (%)	Reference
Chloroflexus aurantiacus J-10-fl	aerobic chemoheterotrophy	acetate	3	0.4 ± 0.5	0	Present work
Chloroflexus aurantiacus J-10-fl	anoxygenic photoheterotrophy	acetate	3	3.0 ± 2.0	2	Present work
Chloroflexus aurantiacus J-10-fl	aerobic chemoheterotrophy	pyruvate	3	0.2 ± 0.2	0	Present work
Chloroflexus aurantiacus J-10-fl	anoxygenic photoheterotrophy	pyruvate	3	2.1 ± 0.1	2	Present work
Chloroflexus aurantiacus J-10-fl	aerobic chemoheterotrophy	glucose	3	0.1 ± 0.1	0	Present work
Chloroflexus aurantiacus J-10-fl	anoxygenic photoheterotrophy	butyrate	3	4.5 ± 1.7	4	Present work
Chloroflexus aurantiacus J-10-fl	anoxygenic photoautotrophy	bicarbonate	1	6	5	Present work
Clostridium acetobutylicum	anaerobic chemoheterotrophy	pyruvate	1	41	33	*Gregoire et al.* 2018
Clostridium acetobutylicum	anaerobic chemoheterotrophy	glucose	1	52	42	*Gregoire et al.* 2018
Escherischia coli K-12	anaerobic chemoheterotrophy	pyruvate	1	4	3	*Gregoire et al.* 2018
Geobacter sulfurreducens PCA	anaerobic chemoheterotrophy	acetate	2	21 ± 1	17	*Gregoire et al.* 2018
Heliobacterium mobile	anoxygenic photoheterotrophy	pyruvate	3	57 ± 4	45	*Lavoie et al.* 2019
Heliomicrobium modesticaldum Ice1	anoxygenic photoheterotrophy	acetate	2	52 ± 9	42	*Gregoire et al.* 2018
Heliomicrobium modesticaldum Ice1	anaerobic chemoheterotrophy	acetate	2	12 ± 10	10	*Gregoire et al.* 2018
Heliomicrobium modesticaldum Ice1	anoxygenic photoheterotrophy	pyruvate	2	100 ± 3	80	*Gregoire et al.* 2018
Heliomicrobium modesticaldum Ice1	anaerobic chemoheterotrophy	pyruvate	3	124 ± 6	100	*Gregoire et al.* 2018
Rhodobacter capsulatus SB1003	anoxygenic photoheterotrophy	acetate	1	6	5	*Gregoire & Poulain* 2016
Rhodobacter capsulatus SB1003	anoxygenic photoheterotrophy	butyrate	1	25	20	*Gregoire & Poulain* 2016

6.8 REFERENCES

1. Selin, N. E. Global Biogeochemical Cycling of Mercury: A Review. *Annual Review of Environment and Resources* **34**, 43–63 (2009).

2. Fleming, E. J., Mack, E. E., Green, P. G. & Nelson, D. C. Mercury methylation from unexpected sources: molybdate-inhibited freshwater sediments and an iron-reducing bacterium. *Appl Environ Microbiol* **72**, 457–64 (2006).

3. Han, S. *et al.* Mercury speciation in marine sediments under sulfate-limited conditions. *Environ Sci Technol* **44**, 3752–7 (2010).

4. Podar, M. *et al.* Global prevalence and distribution of genes and microorganisms involved in mercury methylation. *Sci Adv* **1**, e1500675 (2015).

5. Schartup, A. T. *et al.* Freshwater discharges drive high levels of methylmercury in Arctic marine biota. *Proc Natl Acad Sci U S A* **112**, 11789–94 (2015).

6. Hsu-Kim, H., Kucharzyk, K. H., Zhang, T. & Deshusses, M. A. Mechanisms regulating mercury bioavailability for methylating microorganisms in the aquatic environment: a critical review. *Environ Sci Technol* **47**, 2441–56 (2013).

7. Ao, M. *et al.* The influence of atmospheric Hg on Hg contaminations in rice and paddy soil in the Xunyang Hg mining district, China. *Acta Geochimica* **36**, 181–189 (2017).

8. Kim, K. H., Kim, M. Y., Kim, J. & Lee, G. Effects of changes in environmental conditions on atmospheric mercury exchange: Comparative analysis from a rice paddy field during the two spring periods of 2001 and 2002. *Journal of Geophysical Research-Atmospheres* **108**, (2003).

9. Wang, X. *et al.* Emission-dominated gas exchange of elemental mercury vapor over natural surfaces in China. *Atmospheric Chemistry and Physics* **16**, 11125–11143 (2016).

10. Bone, S. E., Bargar, J. R. & Sposito, G. Mackinawite (FeS) reduces mercury(II) under sulfidic conditions. *Environ Sci Technol* **48**, 10681–9 (2014).

11. Wiatrowski, H. A. *et al.* Reduction of Hg(II) to Hg(0) by magnetite. *Environ Sci Technol* **43**, 5307–13 (2009).

12. Gu, B. *et al.* Mercury reduction and complexation by natural organic matter in anoxic environments. *Proc Natl Acad Sci U S A* **108**, 1479–83 (2011).

13. Christakis, C. A., Barkay, T. & Boyd, E. S. Expanded Diversity and Phylogeny of mer Genes Broadens Mercury Resistance Paradigms and Reveals an Origin for MerA Among Thermophilic Archaea. *Frontiers in Microbiology* **12**, (2021).

14. Liu, S. N. & Wiatrowski, H. A. Reduction of Hg(II) to Hg(0) by Biogenic Magnetite from two Magnetotactic Bacteria. *Geomicrobiol J* **35**, 198–208 (2018).

15. Gregoire, D. S., Lavoie, N. C. & Poulain, A. J. Heliobacteria Reveal Fermentation As a Key Pathway for Mercury Reduction in Anoxic Environments. *Environ Sci Technol* **52**, 4145–4153 (2018).

16. Lavoie, N. C., Gregoire, D. S., Stenzler, B. R. & Poulain, A. J. Reduced sulphur sources favour Hg(II) reduction during anoxygenic photosynthesis by Heliobacteria. *Geobiology* (2019) doi:10.1111/gbi.12364.

17. Grégoire, D. S. & Poulain, A. J. A physiological role for HgII during phototrophic growth. *Nature Geoscience* **9**, 121–125 (2016).

18. Lin, H., Morrell-Falvey, J. L., Rao, B., Liang, L. & Gu, B. Coupled mercury-cell sorption, reduction, and oxidation on methylmercury production by Geobacter sulfurreducens PCA. *Environ Sci Technol* **48**, 11969–76 (2014).

19. Schaefer, J. K., Letowski, J. & Barkay, T. mer-mediated resistance and Volatilization of Hg(II) under anaerobic conditions. *Geomicrobiol J* **19**, 87–102 (2002).

20. Wiatrowski, H. A., Ward, P. M. & Barkay, T. Novel reduction of mercury (II) by mercury-sensitive dissimilatory metal reducing bacteria. *Environ Sci Technol* **40**, 6690–6 (2006).

21. Zhao, L. D. *et al.* Contrasting effects of dissolved organic matter on mercury methylation by Geobacter sulfurreducens PCA and Desulfovibrio desulfuricans ND132. *Environmental Science & Technology* **51**, 10468–10475 (2017).

22. Lu, X. *et al.* Anaerobic Mercury Methylation and Demethylation by Geobacter bemidjiensis Bem. *Environ Sci Technol* **50**, 4366–73 (2016).

23. Osborn, A. M., Bruce, K. D., Strike, P. & Ritchie, D. A. Distribution, diversity and evolution of the bacterial mercury resistance (mer) operon. *FEMS Microbiology Reviews* **19**, 239–262 (1997).

24. Barkay, T., K. Kritee, Kritee, K., Boyd, E. S. & Geesey, G. G. A thermophilic bacterial origin and subsequent constraints by redox, light and salinity on the evolution of the microbial mercuric reductase. *Environmental Microbiology* **12**, 2904–2917 (2010).

25. Lin, H. *et al.* Unexpected Effects of Gene Deletion on Interactions of Mercury with the Methylation-Deficient Mutant ΔhgcAB. *Environmental Science & Technology Letters* **1**, 271–276 (2014).

26. Estevez-Canales, M. *et al.* A severe reduction in the cytochrome C content of Geobacter sulfurreducens eliminates its capacity for extracellular electron transfer. *Environ Microbiol Rep* **7**, 219–226 (2015).

27. Qian, C. *et al.* Global Proteome Response to Deletion of Genes Related to Mercury Methylation and Dissimilatory Metal Reduction Reveals Changes in Respiratory Metabolism in Geobacter sulfurreducens PCA. *J Proteome Res* **15**, 3540–3549 (2016).

28. Lee, S., Kim, D. H. & Kim, K. W. The enhancement and inhibition of mercury reduction by natural organic matter in the presence of Shewanella oneidensis MR-1. *Chemosphere* **194**, 515–522 (2018).

29. Fang, Y. *et al.* A promotion strategy of enhancing the mercury removal in *Shewanella oneidensis* MR-1 based on the mercury absorption and electronic consumption via mer operon. *Journal of Environmental Chemical Engineering* **12**, 112993 (2024).

30. Mason, R. P., Morel, F. M. M. & Hemond, H. F. The role of microorganisms in elemental mercury formation in natural waters. *Water, Air, & Soil Pollution* **80**, 775–787 (1995).

31. Poulain, A. J. *et al.* Biological and photochemical production of dissolved gaseous mercury in a boreal lake. *Limnol Oceanogr* **49**, 2265–2275 (2004).

32. Amyot, M., Mierle, G., Lean, D. & McQueen, D. J. Effect of solar radiation on the formation of dissolved gaseous mercury in temperate lakes. *Geochimica et Cosmochimica Acta* **61**, 975–987 (1997).

33. Vandal, G. M., Fitzgerald, W. F., Rolfhus, K. R. & Lamborg, C. H. Modeling the elemental mercury cycle in Pallette Lake, Wisconsin, USA. *Water, Air, & Soil Pollution* **80**, 529–538 (1995).

34. Baeyens, W. & Leermakers, M. Elemental mercury concentrations and formation rates in the Scheldt estuary and the North Sea. *Marine Chemistry* **60**, 257–266 (1998).

35. McKinlay, J. B. & Harwood, C. S. Carbon dioxide fixation as a central redox cofactor recycling mechanism in bacteria. *Proceedings of the National Academy of Sciences* **107**, 11669–11675 (2010).

36. Richardson *et al.* The role of auxiliary oxidants in maintaining redox balance during phototrophic growth of Rhodobacter capsulatus on propionate or butyrate. *Archives of Microbiology* **150**, 131–137 (1988).

37. Asztalos, E., Sipka, G., Kis, M., Trotta, M. & Maróti, P. The reaction center is the sensitive target of the mercury(II) ion in intact cells of photosynthetic bacteria. *Photosynthesis Research* **112**, 129–140 (2012).

38. Asztalos, E., Italiano, F., Milano, F., Maróti, P. & Trotta, M. Early detection of mercury contamination by fluorescence induction of photosynthetic bacteria. *Photochem Photobiol Sci* **9**, 1218–1223 (2010).

39. Pierson, B. K. & Castenholz, R. W. A phototrophic gliding filamentous bacterium of hot springs, Chloroflexus aurantiacus, gen. and sp. nov. *Arch. Microbiol.* **100**, 5–24 (1974).

40. Madigan, M. T., Petersen, S. R. & Brock, T. D. Nutritional studies on Chloroflexus, a filamentous photosynthetic, gliding bacterium. *Arch. Microbiol.* **100**, 97–103 (1974).

41. Eisenreich, W., Strauss, G., Werz, U., Fuchs, G. & Bacher, A. Retrobiosynthetic analysis of carbon fixation in the phototrophic eubacterium Chloroflexus aurantiacus. *European Journal of Biochemistry* **215**, 619–632 (1993).

42. Zarzycki, J., Brecht, V., Müller, M. & Fuchs, G. Identifying the missing steps of the autotrophic 3-hydroxypropionate CO2 fixation cycle in Chloroflexus aurantiacus. *Proceedings of the National Academy of Sciences of the United States of America* **106**, 21317–21322 (2009).

43. Kawai, S., Nishihara, A., Matsuura, K. & Haruta, S. Hydrogen-dependent autotrophic growth in phototrophic and chemolithotrophic cultures of thermophilic bacteria, Chloroflexus aggregans and Chloroflexus aurantiacus, isolated from Nakabusa hot springs. *FEMS Microbiology Letters* **366**, fnz122 (2019).

44. Tang, K.-H., Urban, V. S., Wen, J., Xin, Y. & Blankenship, R. E. SANS Investigation of the Photosynthetic Machinery of *Chloroflexus aurantiacus*. *Biophysical Journal* **99**, 2398–2407 (2010).

45. Hanada, S., Hiraishi, A., Shimada, K. & Matsuura, K. Isolation of Chloroflexus aurantiacus and related thermophilic phototrophic bacteria from Japanese hot springs using an improved isolation procedure. *The Journal of General and Applied Microbiology* **41**, 119–130 (1995).

46. Cruz, K., Guezennec, J. & Barkay, T. Binding of Hg by bacterial extracellular polysaccharide: a possible role in Hg tolerance. *Appl Microbiol Biotechnol* **101**, 5493–5503 (2017).

47. Geesey, G. G., Barkay, T. & King, S. Microbes in mercury-enriched geothermal springs in western North America. *Sci Total Environ* **569–570**, 321–331 (2016).

48. Tang, K.-H. *et al.* Complete genome sequence of the filamentous anoxygenic phototrophic bacterium Chloroflexus aurantiacus. *BMC Genomics* **12**, 334–334 (2011).

49. Blattner, F. R. *et al.* The Complete Genome Sequence of Escherichia coli K-12. *Science* **277**, 1453–1462 (1997).

50. Rizk, M. L., Laguna, R., Smith, K. M., Tabita, F. R. & Liao, J. C. Redox homeostasis phenotypes in RubisCO-deficient Rhodobacter sphaeroides via ensemble modeling. *Biotechnol Prog* **27**, 15–22 (2011).

51. Kawai, S., Shimamura, S., Shimane, Y. & Tsukatani, Y. Proteomic Time-Course Analysis of the Filamentous Anoxygenic Phototrophic Bacterium, Chloroflexus aurantiacus, during the Transition from Respiration to Phototrophy. *Microorganisms* **10**, 1288 (2022).

52. Green, J. & Paget, M. S. Bacterial redox sensors. *Nat Rev Microbiol* **2**, 954–966 (2004).

53. Dick, J. M. Average oxidation state of carbon in proteins. *Journal of The Royal Society Interface* **11**, 20131095 (2014).

54. Dick, J. M., Yu, M. & Tan, J. Uncovering chemical signatures of salinity gradients through compositional analysis of protein sequences. *Biogeosciences* **17**, 6145–6162 (2020).

55. Dick, J. M. & Tan, J. Chemical Links Between Redox Conditions and Estimated Community Proteomes from 16S rRNA and Reference Protein Sequences. *Microb Ecol* **85**, 1338–1355 (2023).

56. Dick, J. M., Yu, M., Tan, J. & Lu, A. Changes in Carbon Oxidation State of Metagenomes Along Geochemical Redox Gradients. *Front. Microbiol.* **10**, (2019).

57. Fones, E. M. *et al.* Physiological adaptations to serpentinization in the Samail Ophiolite, Oman. *ISME J* **13**, 1750–1762 (2019).

58. Boyer, G. M., Schubotz, F., Summons, R. E., Woods, J. & Shock, E. L. Carbon Oxidation State in Microbial Polar Lipids Suggests Adaptation to Hot Spring Temperature and Redox Gradients. *Frontiers in Microbiology* **11**, (2020).

59. Dick, J. M., Boyer, G. M., Canovas III, P. A. & Shock, E. L. Using thermodynamics to obtain geochemical information from genomes. *Geobiology* **21**, 262–273 (2023).

60. Flamholz, A. I., Goyal, A., Fischer, W. W., Newman, D. K. & Phillips, R. The proteome is a terminal electron acceptor. *bioRxiv* (2024).

Chapter 7

Synthesis of current insights into anaerobic Hg^{II} reduction by the anoxygenic phototrophs and fermenters Heliobacteria

7.1 SUMMARY OF RESEARCH OUTCOMES & CONTRIBUTIONS

The central objective of my thesis was to provide new mechanistic details on environmental and physiological factors that drive Hg^{II} reduction by anoxygenic phototrophs and fermenters. I accomplished this by using a combination of microbial physiology, molecular biology, and trace Hg analytical techniques. I outlined how central machinery involved in anoxygenic photosynthesis, carbon, sulphur, and nitrogen metabolisms control the ability of Heliobacteria to reduce Hg^{II}. I also further expanded on the known diversity of anaerobic reducers. My thesis makes significant progress toward uncovering the cellular mechanism responsible for anaerobic Hg^{II} reduction.

In **Chapter 2**, I investigated whether a yet-tested Heliobacteria, *Heliobacillus mobilis* now *Heliobacterium mobile*, could reduce Hg^{II}, and I tested if assimilatory metabolism that consumes reducing power could control the magnitude of Hg^0 produced during anoxygenic phototrophy. I hypothesized that assimilatory metabolisms that require reduced redox cofactors draw on the same pool of reducing power that fuels Hg^{II} reduction. I specifically tested whether oxidized sulphur sources that required more reducing power to be assimilated into biomass would limit Hg^{II} reduction compared to more reduced sulphur sources. Given that the affinity of reduced sulphur and Hg often dictates its bioavailability, I also employed biosensor assays with *E. coli*. I found no significant differences in Hg bioavailability to cells in growth media supplemented with these different sulphur sources. Ultimately, I showed that assimilating more reduced sulphur sources like cysteine and thiosulphate does indeed support higher levels of Hg^0 production by *H. mobilis*. My findings positioned Heliobacteria as key players in rice paddy Hg and S cycling. One of the challenges faced in my work at the time was the lack of a publicly available sequenced genome for *H. mobilis;*I had to make assumptions about *H. mobilis* gene content based on the genome of

H. modesticaldum, which indicated that some, but not all, genes involved in assimilatory sulphur reduction were present. Ironically, an annotation of the *H. mobilis* genome was released shortly after our work was published in 2019 (NCBI Taxonomic ID 28064). Its annotation reveals a complete set of genes for assimilatory sulphur reduction, confirming its observed ability to grow on sulphate, thiosulphate, cysteine, and methionine.

Overall, in this chapter, I expand on the known diversity of known anaerobic Hg^{II} reducers, adding *H. mobilis* to the growing list, and advance our knowledge of how nutrient availability affects microbial Hg transformations. Agricultural environments like rice paddies can become sulphur-limited, and as such, S-containing fertilizer usage is already common and increasing in application [1]. The effects of such amendments on rice paddy Hg cycling has gained attention in recent years and appears to stimulate most microbial Hg transformation pathways, including Hg methylation and anaerobic Hg^{II} reduction [2]. My findings pave the way for future research investigating whether resource competition for common nutrients and Hg substrates between anaerobic Hg^{II} reducers and methylators is a mechanism that limits or worsens MeHg production in the environment; co-culture studies would be an excellent place to start. These insights may lead to the development of Hg pollution mitigation strategies that rely on targeted nutrient amendments to limit undesired microbial Hg cycling activity.

In **Chapter 3,** I investigated how nitrogen availability and metabolism in *Heliomicrobium modesticaldum* Ice1 affect the magnitude of Hg^{II} reduction during phototrophy. Like my work in Chapter 2, I sought to test the overarching hypothesis that assimilatory metabolisms that consume reducing power affect the magnitude of Hg^{II} that can be reduced. *H. modesticaldum* Ice1 can switch to N_2 fixation when there is insufficient NH_4^+ in its environment. However, it is an incredibly costly process, requiring large amounts of ATP and reducing power in the form of

ferredoxins. I thus compared phototrophic Hg^0 production in cultures of *H. modesticaldum* grown on N_2 to those grown on NH_4^+, predicting that N_2 fixation would yield significantly lower cumulative Hg^0. Much to my surprise, I found that nitrogen availability and species had no effect on Hg^{II} reduction, as cultures could reduce Hg^{II} even in the absence of any nitrogen source. This discovery was in sharp contrast with my results from Chapter 2 and did not support my overarching hypothesis, instead suggesting that the pool of ferredoxins drawn upon for N_2 fixation does not influence photoheterotrophic Hg^{II} reduction. It remains to be tested whether this is due to separate pools of reduced redox cofactors fueling N_2 fixation and Hg^{II} reduction or if there is no appreciable difference in reducing power availability between nitrogen treatments. Our study highlights that even in environmental conditions limited in nitrogen, *H. modesticaldum* could continue to produce significant amounts of Hg^0. Hg methylation potential co-occurs with a variety of nitrogen metabolisms, including N_2 fixation and ammonium uptake [3]. Competition for key nutrients like nitrogen and Hg^{II} between anaerobic reducers and methylators may be a key mechanism limiting the production of toxic MeHg. Co-culture or field studies will be beneficial in uncovering the effects of nutrient and Hg substrate competition on anaerobic microbial Hg transformations.

In **Chapter 4,** I used a gene-deletion approach to further investigate the Hg^{II} reduction mechanism in *Heliomicrobium modesticaldum* Ice1. Given the suspected central role played by reducing power-generating pathways, I tested Hg^{II} reduction by mutants deficient for ferredoxins, photosynthetic electron transfer complexes (pETC), and a carbon metabolism protein. My research showed that no single gene tested was responsible for Hg^{II} reduction in *H. modesticaldum* Ice1. Mutants lacking pETC complexes could reduce Hg^{II} in the light only in the presence of a carbon source, supporting our previous discovery that pETC or, in its absence, pyruvate fermentation fuels Hg^{II} reduction in Heliobacteria [4]. Much to my surprise, single or double ferredoxin gene-deletion

mutants could still reduce Hg^{II}. When these experiments were initially conducted, it was unknown whether PshB1, PshB2, and Fdx3 could all interact with PFOR and the Heliobacterial photosynthetic reaction center (HbRC) or whether there was some enzyme specificity. This unknown made it difficult to predict whether there would be differences in Hg^0 production during phototrophy versus fermentation. Furthermore, it made it difficult to reconcile my ferredoxin mutant results with my hypotheses implicating ferredoxins as primary sources of reducing power for Hg^{II} reduction. Three years after these experiments, colleagues published an experiment identifying PshB1, PshB2, and Fdx3 as the only ferredoxins capable of interacting with PFOR and HbRC [5]. Their findings confirmed that there is a pool of interchangeable but essential ferredoxins connecting phototrophic and fermentative pathways in *H. modesticaldum*. Thus, in my own work, I could conclusively state that no single tested ferredoxin-encoding gene is solely necessary for Hg^{II} reduction to occur. Rather, it is more likely that a pool of reduced ferredoxins, composed of PshB1, PshB2, and Fdx3, provides electrons from central metabolism, either pETC or pyruvate fermentation, to the unknown site of Hg^{II} reduction. There have been attempts to create a mutant deficient for all three ferredoxins, but, to date, none have been viable. A different approach than gene-deletion alone will therefore be needed to elucidate the role of ferredoxins in Heliobacterial Hg^{II} reduction.

In **Chapter 5**, I tested the hypothesis that cellular thiol groups are likely binding sites involved in Hg^{II} reduction. Thiols are abundant functional groups found on cell membranes, in the cytosol as part of low molecular weight thiol redox buffers, and in proteins. Hg^{II}, being extremely electrophilic, is known to preferentially bind to thiol groups over other cellular functional groups [6–11]. I exposed *H. modesticaldum* to a range of sublethal concentrations of a thiol-alkylating agent, N-ethylmaleimide (NEM), to test whether Hg^{II} reduction is inhibited when a certain portion of

cellular thiol sites are blocked. My results identified concentration-dependent inhibition of Hg^{II} reduction by NEM during phototrophy and fermentation, suggesting indeed that part of the Hg^{II} reduction mechanism requires Hg^{II} and thiol interactions. I proposed potential enzymatic coupling sites for Hg^{II} reduction that involve thiols and redox cofactors. The findings from my work imply the possibility of a reduction mechanism involving oxidoreductases with active site thiol residues, like NfnAB, or thiol-based redox homeostasis systems. Future work investigating this cryptic Hg^{II} reduction pathway should target these cellular systems next.

In my final **Chapter 6**, I explored whether other anoxygenic phototrophs could catalyze Hg^{II} reduction. Prior work had identified purple non sulphur bacteria and Heliobacteria as Hg^{II}-reducing anoxygenic phototrophs. Thus, it raised the possibility that other phylogenetically distant anoxygenic phototrophs could also reduce Hg^{II}. I thoroughly investigated whether the filamentous anoxygenic phototroph *Chloroflexus aurantiacus* J-10-fl could reduce Hg^{II} when grown both as a phototroph and as an aerobic chemotroph on a diverse range of carbon sources previously shown to support anaerobic Hg^{II} reducers. Conclusively, this bacterium has no capacity to reduce Hg^{II}, suggesting that shared metabolic lifestyles and environmental niches do not necessarily translate to shared Hg^{II} reduction abilities. It is indeed puzzling why some anaerobes can reduce such low pM levels of Hg^{II} when others clearly cannot. The secret to Hg^{II} reduction may lie within common physiological adaptations to a strict anaerobic lifestyle.

7.2 UPDATED INSIGHTS INTO MECHANISM OF HG^{II} REDUCTION BY ANAEROBES

Our prior findings [4] and those of **Chapter 4** support that catabolic processes involved in reducing power generation, like photosynthetic electron transport and pyruvate fermentation, provide electrons to an unknown site of Hg^{II} reduction. Insights into anaerobic Hg^{II} reduction by

Shewanella oneidensis MR-1 and *Geobacter sulfurreducens* PCA also suggest anaerobic electron transport chains provide a source of electrons for the reduction of Hg^{II} [12–14]. Further investigation is warranted to determine whether common cellular components are catalyzing the two-electron reduction of Hg^{II} in all anaerobic reducers.

One of the outstanding questions of this thesis is how far downstream from catabolic reactions does Hg^{II} reduction occur? Is it occurring at an enzymatic complex directly involved in catabolism, like NfnAB in Heliobacteria, or is it occurring further downstream in a cellular pathway involved in redox homeostasis, anabolism, or other cellular processes? **Figure 7.1** serves to illustrate the coupling between reducing power-consuming and -generating pathways to potential downstream sites of Hg^{II} reduction. In **Chapter 5,** my findings suggest a role for cellular thiols in Hg^{II} reduction. I proposed that other than NfnAB, thiol-based redox homeostasis systems such as the thioredoxin/thioredoxin reductase (Trx) and bacillithiol/bacillithiol disulphide reductase systems (BSH), both of which are present in *H. modesticaldum*, are likely targets for Hg^{II} given their role in providing protection against thiol- oxidizing agents [15–17]. Microbiological studies with *mer*-based aerobic reducers showed that low molecular weight thiols and thioredoxins further confer Hg^{II} resistance [17]. Therefore, priority for future work should be to investigate if such thiol systems can catalyze the anaerobic reduction of Hg^{II}.

The findings of **Chapter 2** but not **Chapter 3** supported my hypothesis that reducing power-consuming anabolic pathways and their substrate availability can control the magnitude of Hg^{II} reduced to Hg^{0}. In retrospect, a potential effect that I never accounted for in **Chapter 2** is whether assimilating reduced sulphur increased the synthesis and concentration of thiol-bearing cell components. Such effects have been reported for numerous bacterial strains where the assimilation of various sulphur sources affects the synthesis and thiol content of cells [18–21].

Differences in cellular thiol synthesis and content could, in turn, affect Hg^{II} reduction by favouring Hg-thiol interactions, a suspected key part of the reduction mechanism according to my findings in **Chapter 5**. Further testing of this hypothesis will require a robust method to quantify intracellular ratios of redox cofactors and cellular thiols under various treatment conditions.

7.3 RECOMMENDATIONS FOR FUTURE METHODS

Much of my work suggests reduced redox cofactors, possibly ferredoxins, are the primary source of reducing power for Hg^{II} reduction. I have frequently searched for and have yet to find existing methods to quantify reduced versus oxidized cytosolic ferredoxins. Given the role of NfnAB in interconverting ferredoxins and NAD(P)H, quantifying the ratios of these cofactors may be an acceptable proxy. However, in practice, a method previously used to quantify NADH/NAD+ in purple non-sulphur bacteria [22] proved frustratingly difficult with Heliobacteria experiments. In bioreactor assays, cultures often did not yield sufficient biomass for effective redox cofactor extraction [4]. Future experiments should strive to adopt or refine redox cofactor quantification techniques, such as genetically encoded fluorescent biosensors for $NADH/NAD^+$ [23,24] and metabolomics [25], as part of our toolkit to further investigate anaerobic Hg^{II} reduction.

Chapter 3 represents the first use of a genetic approach to study Hg^{II} reduction by anoxygenic phototrophs and fermenters. Future work should continue to use these tools to resolve mechanistic details of this microbial Hg transformation. Proteomic or transcriptomic analyses with a well-studied organism like *H. modesticaldum* could further elucidate the metabolic response to such trace-level Hg^{II} exposure. While my work only investigated the effects of gene deletions, examining the effect of gene insertions into non-reducers may prove essential in identifying cellular machinery that confers the ability to reduce Hg^{II}. Recent advances in the artificial intelligence program Alphafold now permit the modelling of biomolecular interactions between

proteins and ions [26]. Such a tool could be used to pre-screen for proteins that have the potential to interact with Hg prior to genetic investigations.

7.4 ENVIRONMENTAL SIGNIFICANCE

Despite significant global concerted efforts to decrease Hg releases to the environment, past pollution continues to be a pathway of Hg exposure to people with the re-emission of legacy Hg from soils and oceans being two-fold larger than new anthropogenic emissions [27–29]. Anaerobic microbes play a key role in the re-emission process by accessing and remobilizing sequestered mercury deposited at the sediment-water interface [30]. Their activity can lead to either new MeHg production or increased availability of mobile Hg^{II} and Hg^{0} species by redox transformations [31,32]. General climate change trends are increasing eutrophication and water stratification, thereby expanding oxygen minimum zones [33]. This, in turn, is expected to favour the rise of anaerobic microbial metabolisms in new environments and will likely lead to an increase in microbial Hg methylation and anaerobic redox cycling [33,34].

The work presented in my thesis contributes essential knowledge for the development of Hg pollution management strategies, a key goal set by the Minamata Convention. **Chapters 2 and 3** highlight that fertilizing strategies should carefully consider the effects of amendments on microbial Hg transformations. By focusing on physiological controls of Hg^{II} reduction by anoxygenic phototrophs and fermenters, I was able to identify how the availability of essential nutrients such as sulphur, carbon, and nitrogen, and the presence of oxygen can influence the magnitude of anaerobic Hg^{II} reduction. Investigating how these variables also exert control on Hg^{II} reduction in the environment will be vital in identifying habitats that support this microbial transformation process. Additionally, by studying *in situ* co-occurring Hg methylation and anaerobic Hg^{II} reduction activity, we will develop a greater understanding of the role, or niche, of

anaerobic Hg^{II} reducers within Hg cycling at the environmental scale and to what extent they may truly limit the production of MeHg.

7.5 CONCLUSION

My thesis makes valuable contributions to our growing knowledge of the roles microorganisms play in Hg biogeochemical cycling. I determined how sulphur but not nitrogen nutrient availabilities and their associated metabolisms affect Hg^{II} reduction. Furthermore, I explored the diversity of anaerobic Hg^{II} reducers, identifying that other Heliobacteria but not Chloroflexi are capable of this redox transformation. Lastly, I investigated genetic determinants and physiological controls involved in Hg^{II} reduction, eliminating multiple candidate genes thought to be involved in the process and uncovering that Hg-thiol interactions are a vital part of the mechanism. Through this thesis, my positive and negative results have built a strong foundation of knowledge upon which future scientists can continue to explore anaerobic Hg^{II} reduction. By applying my findings and recommendations, future research may, at last, fully uncover the cellular machinery responsible for reducing Hg^{II} to its gaseous form in the absence of the *mer* operon. Such a discovery will undoubtedly yield invaluable insights into the origin and evolution of this metal transformation pathway, facilitate field studies investigating the roles of anaerobic Hg^{II} reducers in the environment, and perhaps even lead to the creation of bioremediation technologies that harness the power of microbes to alleviate Hg pollution.

7.6 MAIN FIGURE

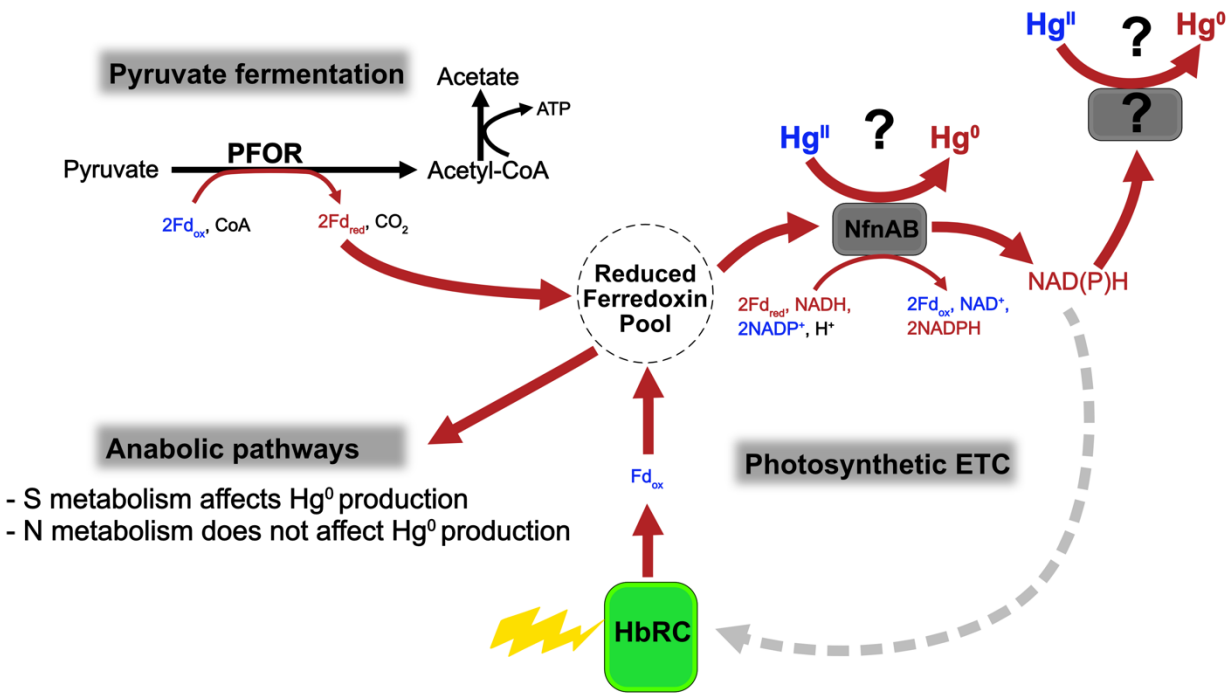

Figure 7.1: Updated insights into the potential mechanism of Hg^{II} reduction by Heliobacteria.
This figure outlines the flow of reducing power, represented as red arrows, from pyruvate fermentation and photosynthetic ETC into anabolic pathways and to proposed potential catalytic sites of Hg^{II} reduction. Red font represents reduced molecules and blue font represents their oxidized form. HbRC = Heliobacterial photosynthetic reaction center, PFOR = pyruvate:ferredoxin oxidoreductase, NfnAB = NADH-dependent ferredoxin:NADP+ oxidoreductase, Fd_{ox} = oxidized ferredoxin, Fd_{red} = reduced ferredoxin.

7.7 REFERENCES

1. Hinckley, E.-L. S., Crawford, J. T., Fakhraei, H. & Driscoll, C. T. A shift in sulfur-cycle manipulation from atmospheric emissions to agricultural additions. *Nat. Geosci.* **13**, 597–604 (2020).

2. Liu, J. *et al.* Mercury and Sulfur Redox Cycling Affect Methylmercury Levels in Rice Paddy Soils across a Contamination Gradient. *Environ. Sci. Technol.* **57**, 8149–8160 (2023).

3. Chen, J. *et al.* The divergent effects of nitrate and ammonium application on mercury methylation, demethylation, and reduction in flooded paddy slurries. *Journal of Hazardous Materials* **460**, 132457 (2023).

4. Gregoire, D. S., Lavoie, N. C. & Poulain, A. J. Heliobacteria Reveal Fermentation As a Key Pathway for Mercury Reduction in Anoxic Environments. *Environ Sci Technol* **52**, 4145–4153 (2018).

5. Walters, K. A., Redding, K. E. & Golbeck, J. H. Identification and characterization of the low molecular mass ferredoxins involved in central metabolism in Heliomicrobium modesticaldum. *Photosynth Res* (2024) doi:10.1007/s11120-023-01069-z.

6. Hsu-Kim, H., Kucharzyk, K. H., Zhang, T. & Deshusses, M. A. Mechanisms regulating mercury bioavailability for methylating microorganisms in the aquatic environment: a critical review. *Environ Sci Technol* **47**, 2441–56 (2013).

7. Delnomdedieu, M. & Allis, J. W. Interaction of inorganic mercury salts with model and red cell membranes: Importance of lipid binding sites. *Chemico-Biological Interactions* **88**, 71–87 (1993).

8. Delnomdedieu, M., Boudou, A., Georgescauld, D. & Dufourc, E. J. Specific interactions of mercury chloride with membranes and other ligands as revealed by mercury-NMR. *Chemico-Biological Interactions* **81**, 243–269 (1992).

9. Dunham-Cheatham, S., Farrell, B., Mishra, B., Myneni, S. & Fein, J. B. The effect of chloride on the adsorption of Hg onto three bacterial species. *Chemical Geology* **373**, 106–114 (2014).

10. Mangal, V., Stenzler, B. R., Poulain, A. J. & Gueguen, C. Aerobic and Anaerobic Bacterial Mercury Uptake is Driven by Algal Organic Matter Composition and Molecular Weight. *Environ Sci Technol* (2018) doi:10.1021/acs.est.8b04909.

11. Regnell, O. & Watras, Carl. J. Microbial Mercury Methylation in Aquatic Environments: A Critical Review of Published Field and Laboratory Studies. *Environ. Sci. Technol.* **53**, 4–19 (2019).

12. Lin, H., Morrell-Falvey, J. L., Rao, B., Liang, L. & Gu, B. Coupled mercury-cell sorption, reduction, and oxidation on methylmercury production by Geobacter sulfurreducens PCA. *Environ Sci Technol* **48**, 11969–76 (2014).

13. Qian, C. *et al.* Global Proteome Response to Deletion of Genes Related to Mercury Methylation and Dissimilatory Metal Reduction Reveals Changes in Respiratory Metabolism in Geobacter sulfurreducens PCA. *J Proteome Res* **15**, 3540–3549 (2016).

14. Fang, Y. *et al.* A promotion strategy of enhancing the mercury removal in *Shewanella oneidensis* MR-1 based on the mercury absorption and electronic consumption via mer operon. *Journal of Environmental Chemical Engineering* **12**, 112993 (2024).

15. Ma, Z. *et al.* Bacillithiol is a major buffer of the labile zinc pool in Bacillus subtilis. *Molecular Microbiology* **94**, 756–770 (2014).

16. Helmann, J. D. Bacillithiol, a New Player in Bacterial Redox Homeostasis. *Antioxidants & Redox Signaling* **15**, 123–133 (2011).

17. Norambuena, J., Wang, Y., Hanson, T., Boyd, J. M. & Barkay, T. Low molecular weight thiols and thioredoxins are important players in Hg(II) resistance in Thermus thermophilus HB27. *Appl Environ Microbiol* (2018) doi:10.1128/AEM.01931-17.

18. Anderson, M. T., Mitchell, L. A., Sintsova, A., Rice, K. A. & Mobley, H. L. T. Sulfur Assimilation Alters Flagellar Function and Modulates the Gene Expression Landscape of Serratia marcescens. *mSystems* **4**, e00285-19 (2019).

19. Scott, C. *et al.* A global response to sulfur starvation in Pseudomonas putida and its relationship to the expression of low-sulfur-content proteins. *FEMS Microbiology Letters* **267**, 184–193 (2007).

20. Forquin, M.-P. *et al.* Global Regulation of the Response to Sulfur Availability in the Cheese-Related Bacterium Brevibacterium aurantiacum. *Applied and Environmental Microbiology* **77**, 1449–1459 (2011).

21. Gutensohn, M., Schaefer, J. K., Maas, T. J., Skyllberg, U. & Björn, E. Metabolic turnover of cysteine-related thiol compounds at environmentally relevant concentrations by Geobacter sulfurreducens. *Front. Microbiol.* **13**, (2023).

22. Grégoire, D. S. & Poulain, A. J. A physiological role for HgII during phototrophic growth. *Nature Geoscience* **9**, 121–125 (2016).

23. Knudsen, J. D., Carlquist, M. & Gorwa-Grauslund, M. NADH-dependent biosensor in Saccharomyces cerevisiae: principle and validation at the single cell level. *AMB Express* **4**, 81 (2014).

24. Wilkening, S. *et al.* Discriminating changes in intracellular NADH/NAD+ levels due to anoxicity and H2 supply in *R. eutropha* cells using the Frex fluorescence sensor. *Biochimica et Biophysica Acta (BBA) - Bioenergetics* **1860**, 148062 (2019).

25. Sander, K. *et al.* Targeted redox and energy cofactor metabolomics in Clostridium thermocellum and Thermoanaerobacterium saccharolyticum. *Biotechnol Biofuels* **10**, 270 (2017).

26. Abramson, J. *et al.* Accurate structure prediction of biomolecular interactions with AlphaFold 3. *Nature* **630**, 493–500 (2024).

27. Obrist, D. *et al.* A review of global environmental mercury processes in response to human and natural perturbations: Changes of emissions, climate, and land use. *Ambio* **47**, 116–140 (2018).

28. UNEP. Global Mercury Assessment 2018. *UN Environment Programme, Chemicals and Health Branch* 1–62 (2019).

29. Amos, H. M., Jacob, D. J., Streets, D. G. & Sunderland, E. M. Legacy impacts of all-time anthropogenic emissions on the global mercury cycle. *Global Biogeochemical Cycles* **27**, 410–421 (2013).

30. Poulin, B. A. *et al.* Mercury transformation and release differs with depth and time in a contaminated riparian soil during simulated flooding. *Geochimica et Cosmochimica Acta* **176**, 118–138 (2016).

31. Colombo, M. J., Ha, J. Y., Reinfelder, J. R., Barkay, T. & Yee, N. Anaerobic oxidation of Hg(0) and methylmercury formation by Desulfovibrio desulfuricans ND132. *Geochim Cosmochim Ac* **112**, 166–177 (2013).

32. Hu, H. Y. *et al.* Oxidation and methylation of dissolved elemental mercury by anaerobic bacteria. *Nat Geosci* **6**, 751–754 (2013).

33. Sonke, J. E. *et al.* Global change effects on biogeochemical mercury cycling. *Ambio* **52**, 853–876 (2023).

34. Grégoire, D. S. & Poulain, A. J. A little bit of light goes a long way: the role of phototrophs on mercury cycling. *Metallomics* **6**, 396–407 (2014).

Appendix A

Supporting information for Chapter 2

Noémie C. Lavoie [a], Daniel S. Grégoire [a], Benjamin R. Stenzler [a], Alexandre J. Poulain [a]

a - Biology Department, University of Ottawa, 30 Marie Curie, Ottawa, ON, K1N 6N5, Canada.

A modified version of this chapter was originally published as: **Lavoie, N.C**., Grégoire, D.S., Stenzler, B.R., Poulain, A.J., Reduced sulphur sources favour HgII reduction during anoxygenic photosynthesis by Heliobacteria. *Geobiology* **2020**, 18(1):70-79.

Direct link : https://onlinelibrary.wiley.com/doi/10.1111/gbi.12364

SUPPLEMENTARY FIGURES

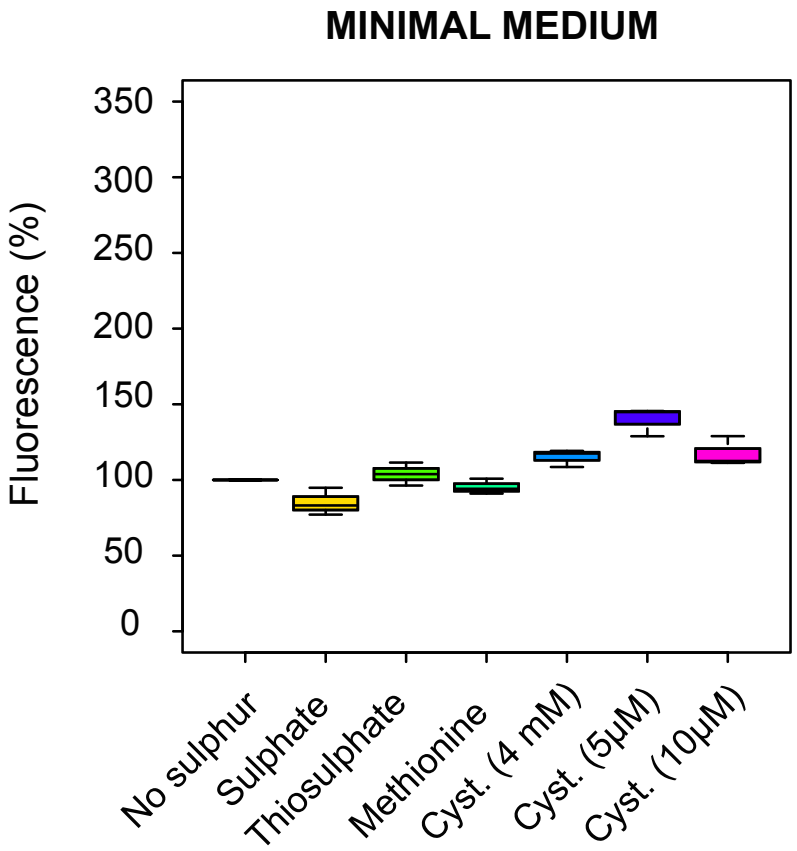

Figure S2.1 Fluorescence in the presence of 5 nM Hg, sulphate, thiosulphate, methionine and different concentrations of cysteine for constitutive bioreporter cells. Cells were exposed to Hg in BMAA exposure medium where [NO_3^-] was set to 0.2 mM. Data presented here are from technical triplicates. For experiments comparing different sulphur sources total sulphur concentrations was normalized to 4 mM. The bottom and top of the boxes show the first and third quartiles respectively, the bar in the middle shows the median and the whiskers show the minimum and maximum for each treatment.

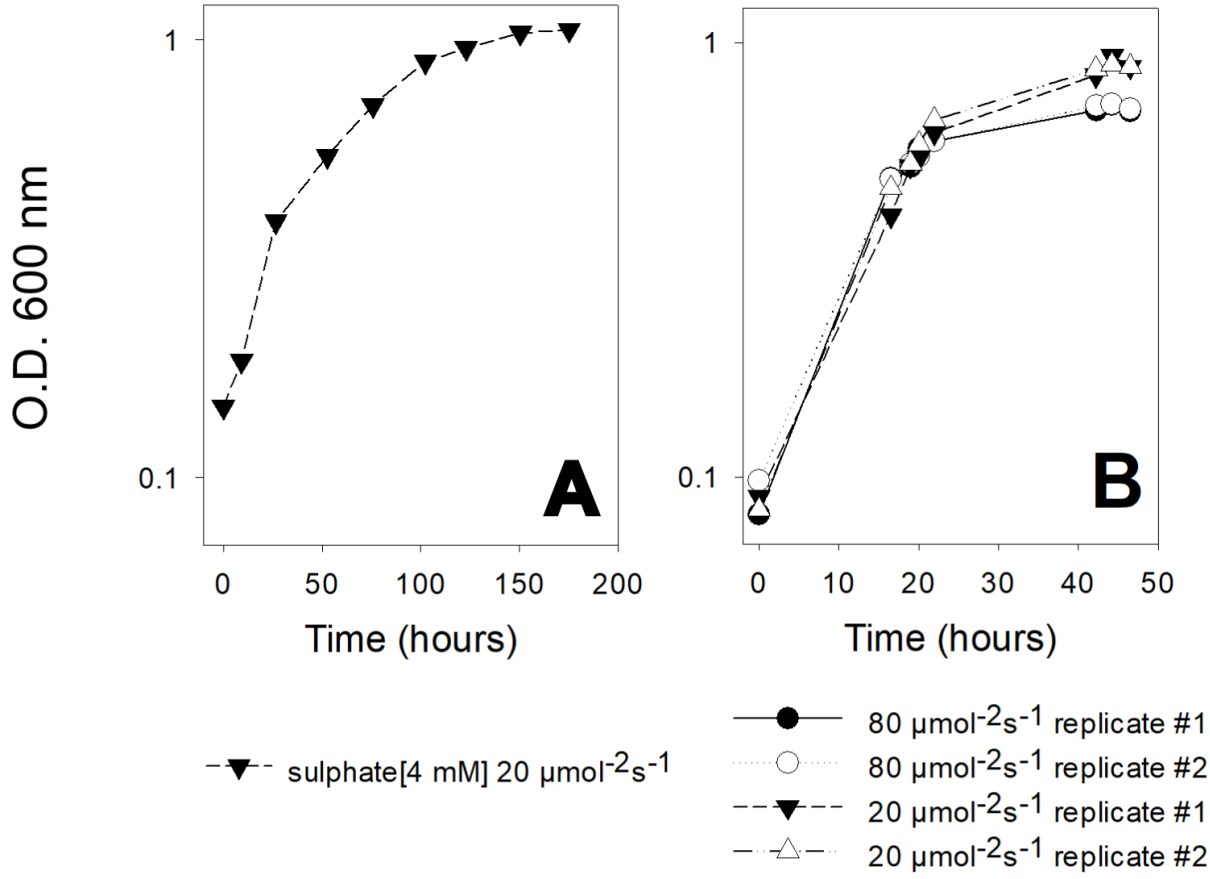

Figure S2.2 Phototrophic growth of *H. mobilis* in DSMZ medium #370 (A) 4 mM sulphate supplied with low light intensity (µmol photon m^{-2} s^{-1}) in a closed non-bubbling bioreactor (e.g. not connected to the Hg^0 analyzer) n =1, and (B) 4 mM sulphate in the presence of different light intensities in sealed Balch tubes.

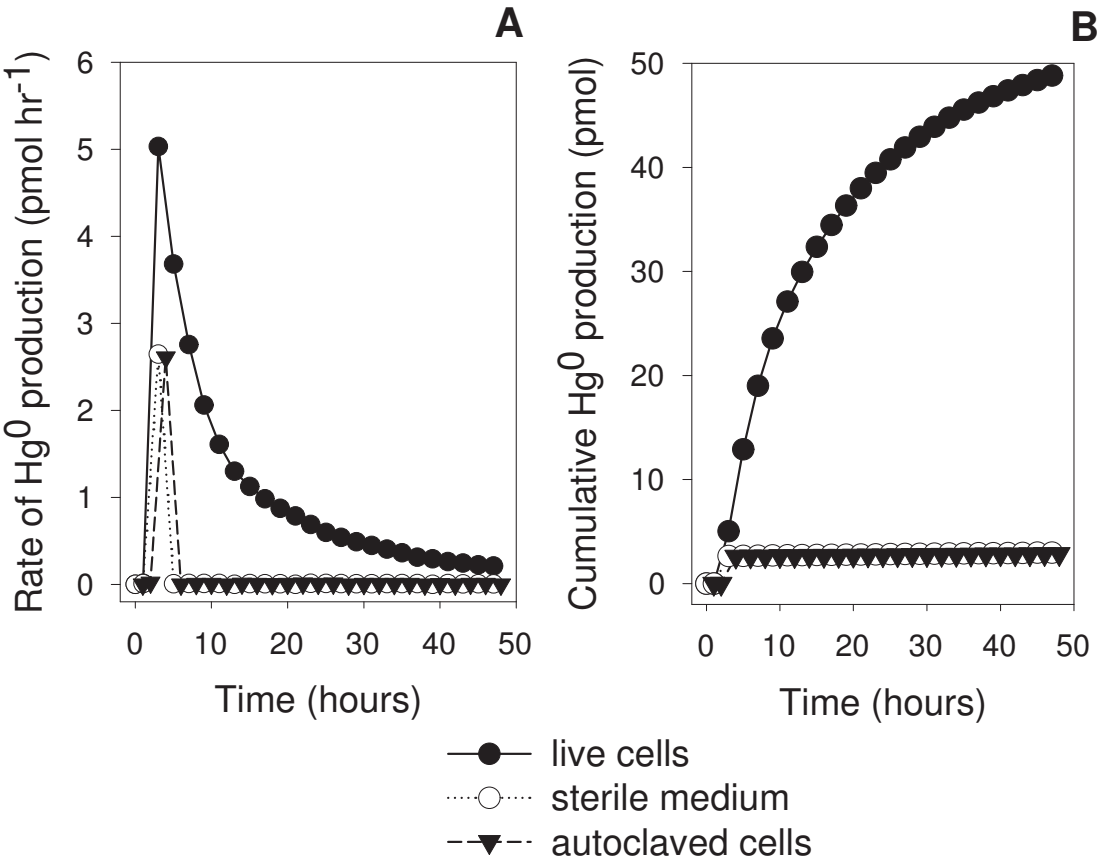

Figure S2.3 Hg^0 production by *H. mobilis* grown phototrophically with 2 mM thiosulphate as a sulphur source. Rate of Hg^0 production (A) and cumulative Hg^0 production (B) for live cells, sterile medium without cells and autoclaved cells. $HgCl_2$ was added to a final concentration of 250 pM in all experiments. Results are representative cases of replicated experiments but each data point was recorded once by the instrument as such no error bars are included.

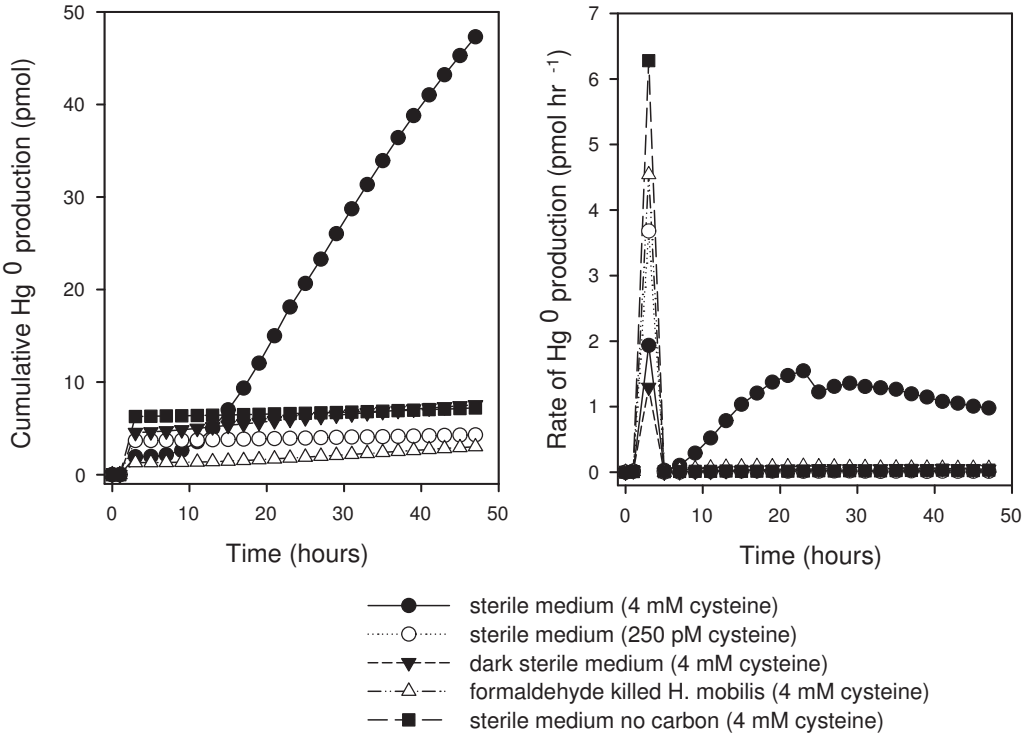

Figure S2.4 Abiotic Hg^0 production in the bioreactor amended with cysteine. All experiments were performed in the presence of light except for the dark treatment. (A) Cumulative Hg^0 production for sterile medium containing no cells and 4 mM cysteine or 250 pM cysteine. (B) Cumulative Hg^0 production for sterile medium with no cells and 4 mM cysteine in the dark, formaldehyde-killed *H. mobilis* with 4 mM cysteine, and sterile medium with no cells devoid of all organic carbon sources except 4 mM cysteine. $HgCl_2$ was added to a final concentration of 250 pM in all experiments.

SUPPLEMENTARY TABLES

Table S2.1 Thermodynamic modeling data predicting dominant Hg species formed in the presence of sulphate (SO_4^{-2}), thiosulphate ($S_2O_3^{-2}$), methionine (met) and cysteine (cys) in BMAA media at 37 ˚C. All sulphur sources were calculated at 4 mM unless otherwise stated.

Sulphur source	$Hg(OH)_2$	$Hg(S_2O_3)_2^{-2}$	$Hg(S_2O_3)_3^{-4}$	$Hg(NH_3)_2^{+2}$	$HgH_2(Cys)_2$	$HgH(Cys)_2^{-}$	$HgHCys^{+}$	$Hg(Met)_2$	$HgMet^{+}$
No sulphur	97.0	0	0	3.0	0	0	0	0	0
Sulphate	97.0	0	0	3.0	0	0	0	0	0
Thiosulphate	0	89.3	10.7	0	0	0	0	0	0
Methionine	1.2	0	0	0	0	0	0	97.4	1.4
Cysteine (4 mM)	0	0	0	0	90.7	9.2	0	0	0
Cysteine (5 µM)	0	0	0	0	62.6	5.4	30.4	0	0
Cysteine (10 µM)	0	0	0	0	74.6	6.4	18.0	0	0

Table S2.2: Equilibrium formation constants ($log_{10}K$, T = 25°C) for all aqueous Hg species considered in the speciation calculations. Activity corrections for ionic strength were made using the B-dot Equation if the ion-specific hard core diameter (å) was present, otherwise activity corrections were made according to the Davies equation. Temperature corrections to $log_{10}K$ were made using the Van't Hoff equation but if a temperature dependent analytical expression was present, $log_{10}K$ was calculated using the expression from Parkhurst et al., (2013) (2) with values A_1, A_2, A_3, A_4, A_5, A_6 and temperature in Kelvin:

Formula	å	$log_{10}K$	ΔH(KJ/mol)	$A_1, A_2, A_3, A_4, A_5, A_6$	Reference
$Hg^{2+} + 2H_2O = Hg(OH)_2 + 2H^+$	3.4			2.971E+2, 4.096E-2, -1.797E+4, -1.066E+2, 7.724E+5, 0	(3)
$NH_3 + H^+ = NH_4^+$	2.5			3.749E+1, -1.545E-3, -6.956E+2, -1.149E+1, 2.655E+5, 0	(4)
$Hg^{2+} + NH_3 = HgNH_3^{2+}$		8.8			(5)
$Hg^{2+} + 2NH_3 = Hg(NH_3)_2^{2+}$		17.8	-311		(5)
$Hg^{2+} + 3NH3 = Hg(NH_3)_3^{2+}$		18.156	-429		(5)
$Hg^{2+} + 4NH_3 = Hg(NH_3)_4^{2+}$		19.3	-548		(5)
$2Hg^{2+} + H_2O = Hg_2(OH)^{3+} + H^+$	8.2			6.069E+2, 9.088E-2, -3.232E+4, -2.212E+2, 1.650E+6, 0	(3)
$Hg^{2+} + H_2O = HgOH^+ + H^+$	4.1			2.785E+2, 4.231E-2, -1.780E+4, -9.968E+1, 1.056E+6, 0	(4)
$Hg^{2+} + SO_4^{2-} = HgSO_4$		2.535			(5)
$Hg^{2+} + NO_3^- = HgNO_3^+$		-0.3157			(5)
$Hg^{2+} + 2NO_3^- = Hg(NO_3)_2$		-0.697			(5)
$MOPS^- + H^+ = HMOPS$		7.184	-21.1		(6)
β-Gylcerophosphate^{2-} + H^+ = Hβ-Gylcerophosphate$^-$		6.65	1.85		(6)
Hβ-Gylcerophosphate$^-$ + H^+ = H_2β-Gylcerophosphate		1.329	12.2		(6)
$H^+ + Cysteine^{2-} = HCysteine^-$		10.87			(7)

$2H^+ + Cysteine^{2-} = H_2Cysteine$	19.38		(7)
$3H^+ + Cysteine^{2-} = H_3Cysteine^+$	21.67		(7)
$Hg^{2+} + Cysteine^{2-} = HgCysteine$	35.73		(7)
$Hg^{2+} + H^+ + Cysteine^{2-} = HgHCysteine^+$	43.83		(7)
$Hg^{2+} + 2H^+ + Cysteine^{2-} = HgH_2Cysteine^{2+}$	46.12		(7)
$Hg^{2+} + 2Cysteine^{2-} = Hg(Cysteine)_2^{2-}$	44.55		(7)
$Hg^{2+} + H^+ + 2Cysteine^{2-} = HgH(Cysteine)_2^-$	53.97		(7)
$Hg^{2+} + 2H^+ + 2Cysteine^{2-} = HgH_2(Cysteine)_2$	62.04		(7)
$H^+ + Methionine^- = HMethionine$	9.26		(8)
$2H^+ + Methionine^- = H_2Methionine+$	11.56		(8)
$Hg^{2+} + Methionine^- = HgMethionine^+$	12.8		(9)
$Hg^{2+} + 2Methionine^- = Hg(Methionine)_2$	19.5		(9)
$Hg^{2+} + S_2O_3^{2-} = Hg(S_2O_3)_2^{2-}$	29.18		(10)
$Hg^{2+} + 3S_2O_3^{2-} = Hg(S_2O_3)_3^{4-}$	30.3		(10)
$S_2O_3^{2-} + 2H^+ = H_2S_2O_3$	3.4	1.497E+3, 2.381E-1, -8.404E+4, -5.420E+2, 5.037E+6, 0	(4)

$S_2O_3^{2-} + H^+ = HS_2O_3^-$	3.6	7.637E+2, 1.228E-1, -4.334E+4, 2.762E+2, 2.691E+6, 0	- (4)
$Na^+ + S_2O_3^{2-} = NaS_2O_3^-$	3.6	1.604E+3, 2.468E-1, -8.865E+4, 5.815E+2, 5.218E+6, 0	- (11)

SUPPLEMENTARY REFERENCES

1. Rodionov DA, Vitreschak AG, Mironov AA, Gelfand MS. 2004. Comparative genomics of the methionine metabolism in Gram-positive bacteria: A variety of regulatory systems. Nucleic Acids Research 32:3340-3353.

2. Parkhurst DLa. 2013. Description of input and examples for PHREEQC version 3--a computer program for speciation, batch-reaction, one-dimensional transport, and inverse geochemical calculations. Reston, Virginia : U.S. Department of the Interior, U.S. Geological Survey, 2013.

3. Blanc P. 2012. Mercury associated physical and chemical constants: updating of the THERMODDEM database. IMaHg project rapport BRGM RP-61299-FR:32p.

4. Shock EL, Sassani DC, Willis M, Sverjensky DA. 1997. Inorganic species in geologic fluids: correlations among standard molal thermodynamic properties of aqueous ions and hydroxide complexes. Geochimica et Cosmochimica Acta 61:907-950.

5. Smith R, Martell A, Motekaitis R. 2004. NIST standard reference database 46. NIST Critically Selected Stability Constants of Metal Complexes Database Ver 2.

6. Goldberg RN, Kishore N, Lennen RM. 2002. Thermodynamic quantities for the ionization reactions of buffers. Journal of physical and chemical reference data 31:231-370.

7. Cardiano P, Falcone G, Foti C, Sammartano S. 2011. Sequestration of Hg2+ by some biologically important thiols. Journal of Chemical & Engineering Data 56:4741-4750.

8. Pettit LD, Powell K. 2006. The IUPAC stability constants database. Chemistry international.

9. Van Der Linden W, Beers C. 1974. Determination of the composition and the stability constants of complexes of mercury (II) with amino acids. Analytica chimica acta 68:143-154.

10. Nyman C, Salazar T. 1961. Complex ion formation of mercury (II) and thiosulfate ion. Analytical Chemistry 33:1467-1469.

11. Wagman DD, Evans WH, Parker VB, Schumm RH, Halow I. 1982. The NBS tables of chemical thermodynamic properties. Selected values for inorganic and C1 and C2 organic substances in SI units. National Standard Reference Data System,

Appendix B

Supporting Information for Chapter 3

Noémie C. Lavoie [a], Alexandre J. Poulain [a]

a - Biology Department, University of Ottawa, 30 Marie Curie, Ottawa, ON, K1N 6N5, Canada.

SUPPLEMENTARY TABLES

SI Table 3.1: Microorganisms capable of Hg transformations and their nitrogen metabolisms.

Strain	Nitrogen metabolism	Hg transformation	Studies
Geobacter spp.	dissimilatory nitrate reduction	Hg methylation*	Kerin *et al.* 2006
Pseudomonas spp.	denitrification	merA Hg reduction*	Harada *et al.* 2019
Nitrosomonas europaea	nitrification	merA Hg reduction*	Park and Ely 2008
hypothesized anaerobes	anammox	cometabolic Hg reduction	Chen *et al.* 2023
Acidobacteria, *Actinobacteria*, *Deltaproteobacteria*, *Euryarchaeota*, *Firmicutes*, *Nitrospirae*, *Spirochaetes*	nitrogen fixation	Hg methylation	McDaniel *et al.* 2020, Sonke *et al.* 2023, Zheng *et al.* 2022
Beijerinckia mobilis KDr_2, *Azotobacter* spp., *Ensifer medicae, Rhizobium leguminosarum*	nitrogen fixation	merA Hg reduction*	Ray *et al.* 1993, Ghosh *et al.* 1996, Arregui *et al.* 2021
Nitrospinae	nitrite oxidation	Hg methylation	Tada *et al.* 2020

* symbol represents experimental validation of the Hg transformation pathway

SI Table 3.2: Summary of culturing and bioreactor conditions tested in Hg^{II} reduction experiments.

Growth medium	Nitrogen source (mM)	Carbon sources (mM or g/L)	$HgCl_2$ spike (pM)	Reactor gas source	Cumulative Hg^0 production (pmol)	Special condition
PYE-N_2	N_2 (37.7)	Pyruvate (20 mM) + Yeast extract (0.2 g/L)	250	N_2	9.96	sterile control, no cells
PYE-NH_4^+	NH_4 (15.1)	Pyruvate (20 mM) + Yeast extract (0.2 g/L)	250	Argon	6.96	sterile control, no cells
PYE-N_2	N_2 (37.7)	Pyruvate (20 mM) + Yeast extract (0.2 g/L)	250	N_2	74.26	initial 24h sealed incubation N_2
PYE-N_2	N_2 (37.7)	Pyruvate (20 mM) + Yeast extract (0.2 g/L)	250	N_2	85.08	initial 24h sealed incubation N_2
PYE-N_2	NA	Pyruvate (20 mM) + Yeast extract (0.2 g/L)	250	Argon	91.11	initial 24h sealed incubation N_2
PYE-N_2	NA	Pyruvate (20 mM) + Yeast extract (0.2 g/L)	250	Argon	90.35	initial 24h sealed incubation N_2
PYE-NH_4^+	NH_4 (15.1)	Pyruvate (20 mM) + Yeast extract (0.2 g/L)	250	Argon	80.07	initial 24h sealed incubation Ar
PYE-NH_4^+	NH_4 (15.1)	Pyruvate (20 mM) + Yeast extract (0.2 g/L)	250	Argon	79.00	initial 24h sealed incubation Ar
PYE-N_2	NA	Pyruvate (20 mM) + Yeast extract (0.2 g/L)	250	room O_2	9.33	initial 24h sealed incubation N_2
PYE-NH_4^+	NH_4 (15.1)	Pyruvate (20 mM) + Yeast extract (0.2 g/L)	250	room O_2	10.15	initial 24h sealed incubation Ar

SUPPLEMENTARY FIGURES:

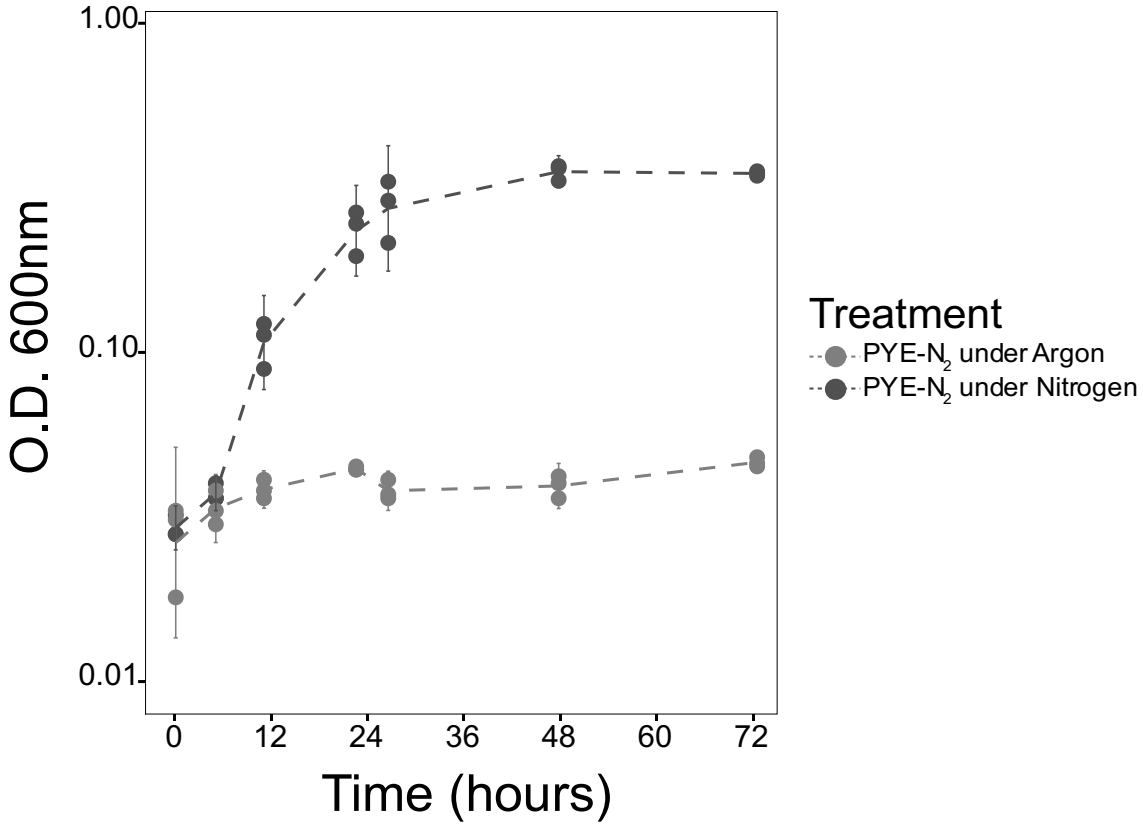

SI Figure 3.1: Phototrophic growth of *H. modesticaldum* Ice1 in medium PYE-N_2 in the presence of either $N_{2(g)}$ (dark grey circles) or $Ar_{(g)}$ (pale grey circles). Results are shown for n = 3 biological replicates, and error bars represent standard deviations for each time point.

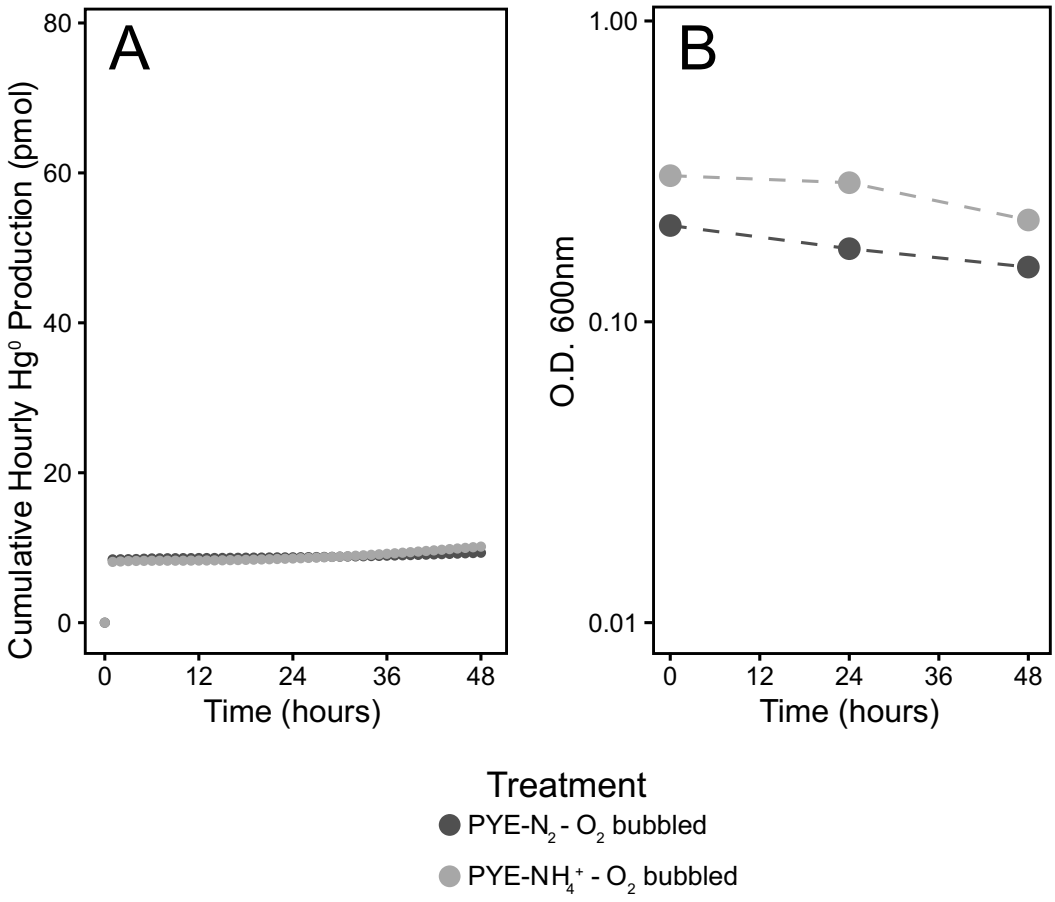

SI Figure 3.2: Cumulative hourly Hg^0 production by autoclave-sterilized and cell-free media PYE-N_2 (white circles) and PYE-NH_4^+ (black circles). Each cumulative Hg^0 data point was recorded once per time step by the instrument, as such no error bars were included. Hg was added to a final concentration of 250 pM. The gas source bubbled for PYE-N_2 experiments was 100% $N_{2(g)}$ and for PYE-NH_4^+ was 100% $Ar_{(g)}$.

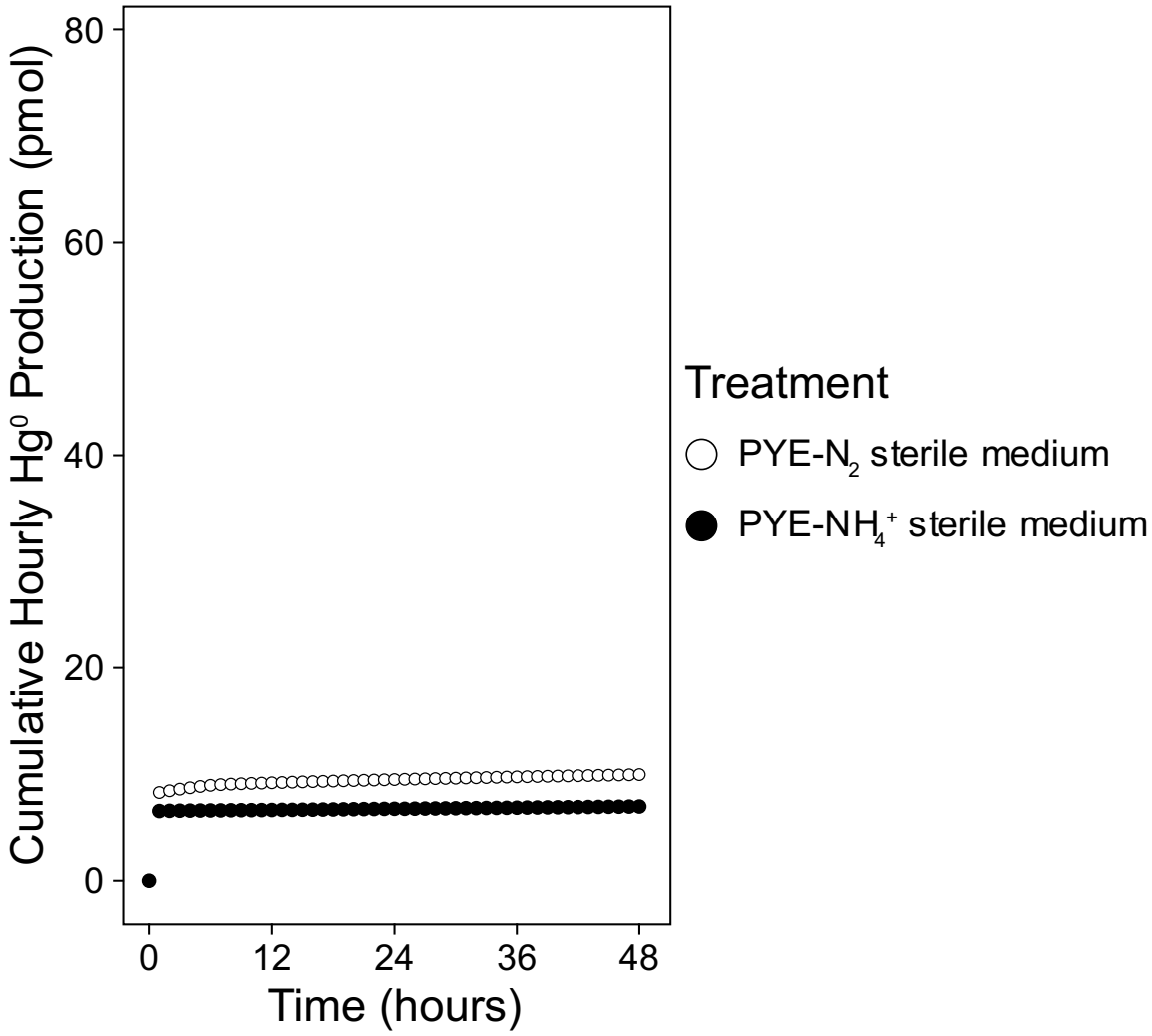

SI Figure 3.3: Hg^0 production by *H. modesticaldum* Ice1 grown phototrophically in media PYE-N_2 and PYE-NH_4^+ and bubbled with oxygen in the bioreactor. (A) Cumulative hourly Hg^0 production and (B) cell growth (as measured by O.D. 600 nm) during bioreactor experiments. Each cumulative Hg^0 data point was recorded once per time step by the instrument, as such no error bars were included. Hg^{II} was added to a final concentration of 250 pM. The gas source bubbled for all experiments was room air filtered through a Tekran Model 1100 Zero Air Generator.

SUPPLEMENTARY REFERENCES

Arregui, G., Hipólito, P., Pallol, B., Lara-Dampier, V., García-Rodríguez, D., Varela, H. P., Tavakoli Zaniani, P., Balomenos, D., Paape, T., Coba de la Peña, T., Lucas, M. M., & Pueyo, J. J. (2021). Mercury-Tolerant Ensifer medicae Strains Display High Mercuric Reductase Activity and a Protective Effect on Nitrogen Fixation in Medicago truncatula Nodules Under Mercury Stress. Frontiers in Plant Science, 11. https://www.frontiersin.org/articles/10.3389/fpls.2020.560768

Chen, J., Hu, G., Liu, J., Poulain, A. J., Pu, Q., Huang, R., Meng, B., & Feng, X. (2023). The divergent effects of nitrate and ammonium application on mercury methylation, demethylation, and reduction in flooded paddy slurries. Journal of Hazardous Materials, 460, 132457. https://doi.org/10.1016/j.jhazmat.2023.132457

Ghosh, S., Sadhukhan, P. c., Ghosh, D. k., Mandal, A. k., Chaudhuri, J., & Mandal, A. (1996). Studies on the effect of mercury and organomercurial on the growth and nitrogen fixation by mercury-resistant Azotobacter strains. Journal of Applied Bacteriology, 80(3), 319–326. https://doi.org/10.1111/j.1365-2672.1996.tb03226.x

Harada, M., Ito, K., Nakajima, N., Yamamura, S., Tomita, M., Suzuki, H., & Amachi, S. (2019). Genomic Analysis of Pseudomonas sp. Strain SCT, an Iodate-Reducing Bacterium Isolated from Marine Sediment, Reveals a Possible Use for Bioremediation. G3 Genes|Genomes|Genetics, 9(5), 1321–1329. https://doi.org/10.1534/g3.118.200978

Kerin, E. J., Gilmour, C. C., Roden, E., Suzuki, M. T., Coates, J. D., & Mason, R. P. (2006). Mercury methylation by dissimilatory iron-reducing bacteria. Appl Environ Microbiol, 72(12), 7919–7921. https://doi.org/10.1128/AEM.01602-06

McDaniel, E. A., Peterson, B. D., Stevens, S. L. R., Patricia Q. Tran, Tran, P. Q., Anantharaman, K., & McMahon, K. D. (2020). Expanded Phylogenetic Diversity and Metabolic Flexibility of Mercury-Methylating Microorganisms. mSystems, 5(4). https://doi.org/10.1128/msystems.00299-20

Park, S., & Ely, R. L. (2008). Candidate Stress Genes of Nitrosomonas europaea for Monitoring Inhibition of Nitrification by Heavy Metals. Applied and Environmental Microbiology, 74(17), 5475–5482. https://doi.org/10.1128/AEM.00500-08

Ray, S., Pahan, K., Gachhui, R., Chaudhuri, J., & Mandal, A. (1993). Studies on the mercury volatilizing enzymes in nitrogen-fixing Beijerinckia mobilis. World Journal of Microbiology and Biotechnology, 9(2), 184–186. https://doi.org/10.1007/BF00327833

Sonke, J. E., Angot, H., Zhang, Y., Poulain, A., Björn, E., & Schartup, A. (2023). Global change effects on biogeochemical mercury cycling. Ambio, 52(5), 853–876. https://doi.org/10.1007/s13280-023-01855-y

Tada, Y., Marumoto, K., & Takeuchi, A. (2020). Nitrospina-Like Bacteria Are Potential Mercury Methylators in the Mesopelagic Zone in the East China Sea. Frontiers in Microbiology, 11. https://doi.org/10.3389/fmicb.2020.01369

Zheng, J., Liang, J.-L., Jia, P., Feng, S., Lu, J., Luo, Z., Ai, H., Liao, B., Li, J., & Shu, W. (2022). Diverse Methylmercury (MeHg) Producers and Degraders Inhabit Acid Mine Drainage Sediments, but Few Taxa Correlate with MeHg Accumulation. mSystems, 8(1), e00736-22. https://doi.org/10.1128/msystems.00736-22

Appendix C

Supporting information for Chapter 4

Noémie C. Lavoie [a], Alexandre J. Poulain [a]

a - Biology Department, University of Ottawa, 30 Marie Curie, Ottawa, ON, K1N 6N5, Canada.

SUPPLEMENTARY TABLE

SI Table 4.1: Summary of bioreactor assay results with *Heliomicrobium modesticaldum* Ice1 wild-type and gene deletion mutants. Optical density at 600nm ($O.D._{600nm}$) was measured at hours 0, 24, and 48 of the assays to estimate microbial growth.

Gene deletion(s)	Bioreactor condition	Metabolism	Modified growth media element	T0 OD600nm	T24 OD600nm	T48 OD600nm	Cumulative Hg^0 produced (pmol)	Relative Hg^0 produced (%)
wild-type	dark	fermentation	NA	0.052	0.339	0.369	108.4	86.7
wild-type	dark	fermentation	NA	0.045	0.317	0.361	124.6	99.7
wild-type	dark	fermentation	NA	0.033	0.291	0.326	114.8	91.8
pshB1	dark	fermentation	NA	0.056	0.341	0.158	90.6	72.5
pshB2	dark	fermentation	NA	0.020	0.388	0.124	99.0	79.2
pshB1pshB2	dark	fermentation	NA	0.052	0.040	0.041	28.1	22.5
pshB1pshB2	dark	fermentation	NA	0.047	0.300	0.220	100.8	80.7
pshB1pshB2	dark	fermentation	NA	0.045	0.040	0.042	71.2	56.9
fdx3	dark	fermentation	NA	0.037	0.045	0.051	75.3	60.2
fdx3	dark	fermentation	NA	0.045	0.045	0.044	80.0	64.0
fdx3	dark	fermentation	no carbon source	0.033	0.015	0.015	14.9	11.9
HM1_2993	dark	fermentation	NA	0.053	0.322	0.439	94.5	75.6
petCBDA	light	fermentation	no carbon source	0.029	0.034	0.033	14.7	11.8
petCBDA	light	fermentation	NA	0.053	0.315	0.301	104.5	83.6

pshA	light	fermentation	NA	0.045	0.097	0.067	84.3	67.5
wild-type	light	photoheterotrophy	NA	0.208	0.380	0.266	80.5	64.4
wild-type	light	photoheterotrophy	NA	0.209	0.400	0.295	80.4	64.3
wild-type	light	photoheterotrophy	NA	0.236	0.432	0.406	91.0	72.8
pshB1	light	photoheterotrophy	NA	0.162	0.408	0.405	100.5	80.4
pshB2	light	photoheterotrophy	NA	0.116	0.110	0.133	47.5	38.0
pshB2	light	photoheterotrophy	NA	0.080	0.070	0.076	28.2	22.6
pshB2	light	photoheterotrophy	1 mM HCO_3^-	0.160	0.445	0.488	103.1	82.5
pshB2	light	photoheterotrophy	1 mM HCO_3^-	0.089	0.378	0.311	104.6	83.7
pshB2	light	photoheterotrophy	20 mM HCO_3^-	0.076	0.065	0.077	22.6	18.1
pshB1pshB2	light	photoheterotrophy	NA	0.189	0.399	0.291	100.6	80.5
fdx3	light	photoheterotrophy	NA	0.117	0.400	0.305	97.1	77.7
fdx3	light	photoheterotrophy	NA	0.164	0.334	0.321	105.6	84.5

Appendix D

Supporting Information for Chapter 5

Noémie C. Lavoie [a], Alexandre J. Poulain [a]

a - Biology Department, University of Ottawa, 30 Marie Curie, Ottawa, ON, K1N 6N5, Canada.

SUPPLEMENTARY FIGURES

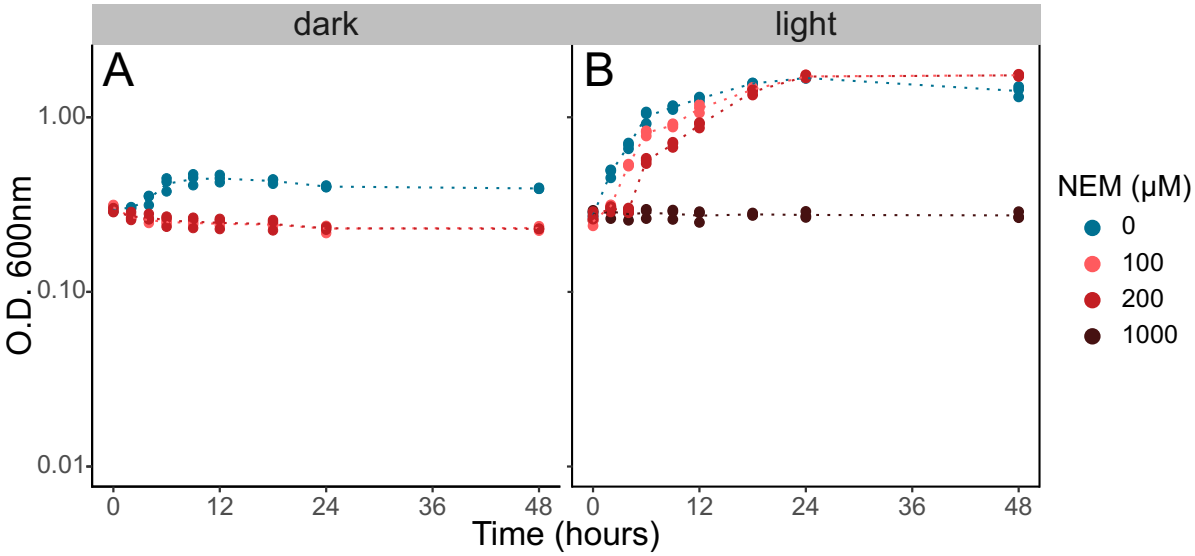

SI Figure 5.1: Minimum inhibitory concentration assays of *H. modesticaldum* Ice1 exposed to a gradient of NEM concentrations for A) fermentative (dark) cultures and B) photoheterotrophic (light) cultures. For each concentration, biological triplicate cultures were prepared to an initial O.D. of ~0.2 in Balch tubes containing 10 mL of medium PYE and O.D. 600 nm was measured over time to assess growth.

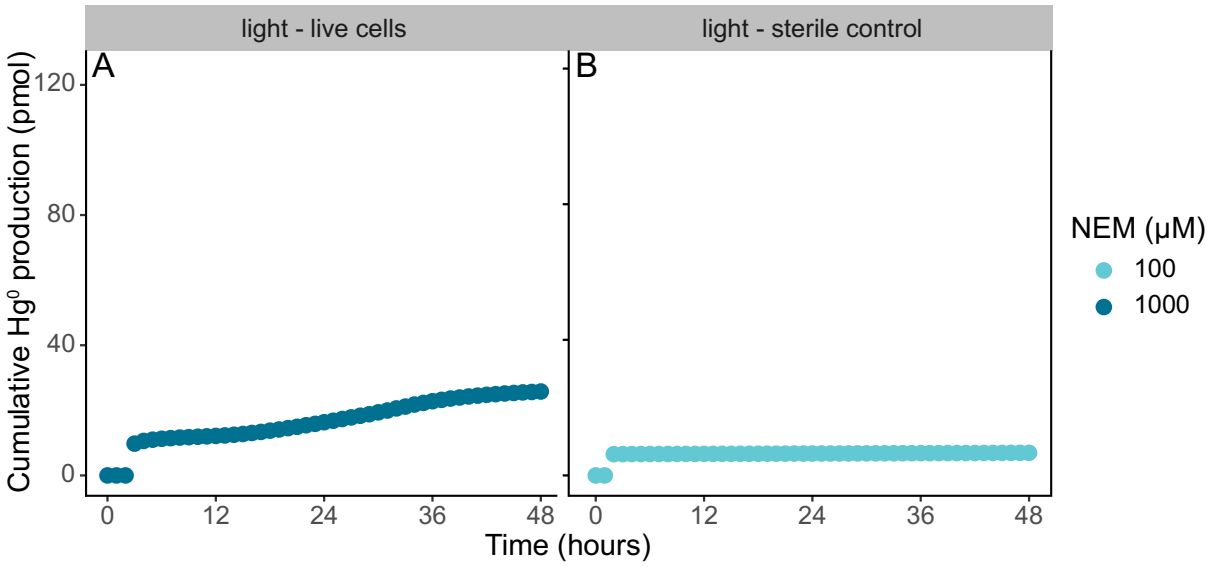

SI Figure 5.2: Hourly cumulative Hg^0 produced for bioreactor experiments with A) live photoheterotrophic (light) cultures of *H. modesticaldum* exposed to 1000 µM of NEM and B) sterile growth medium in the light devoid of cells and exposed to 100 mM.

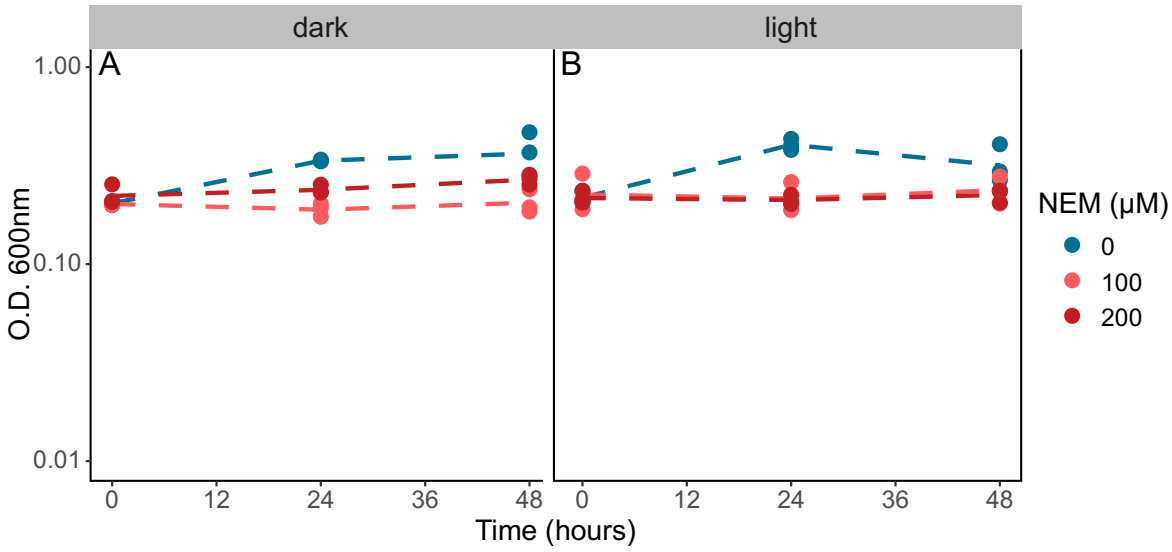

SI Figure 5.3: Measured growth via optical density (O.D. 600nm) of *H. modesticaldum* cultures during bioreactor experiments. A) growth of fermentative (dark) cultures and B) growth of photoheterotrophic (light) cultures. One measurement per bioreactor and per timepoint was taken.

Appendix E

Supporting Information for Chapter 6

Noémie C. Lavoie [a], Alexandre J. Poulain [a]

a - Biology Department, University of Ottawa, 30 Marie Curie, Ottawa, ON, K1N 6N5, Canada.

SUPPLEMENTARY FIGURES

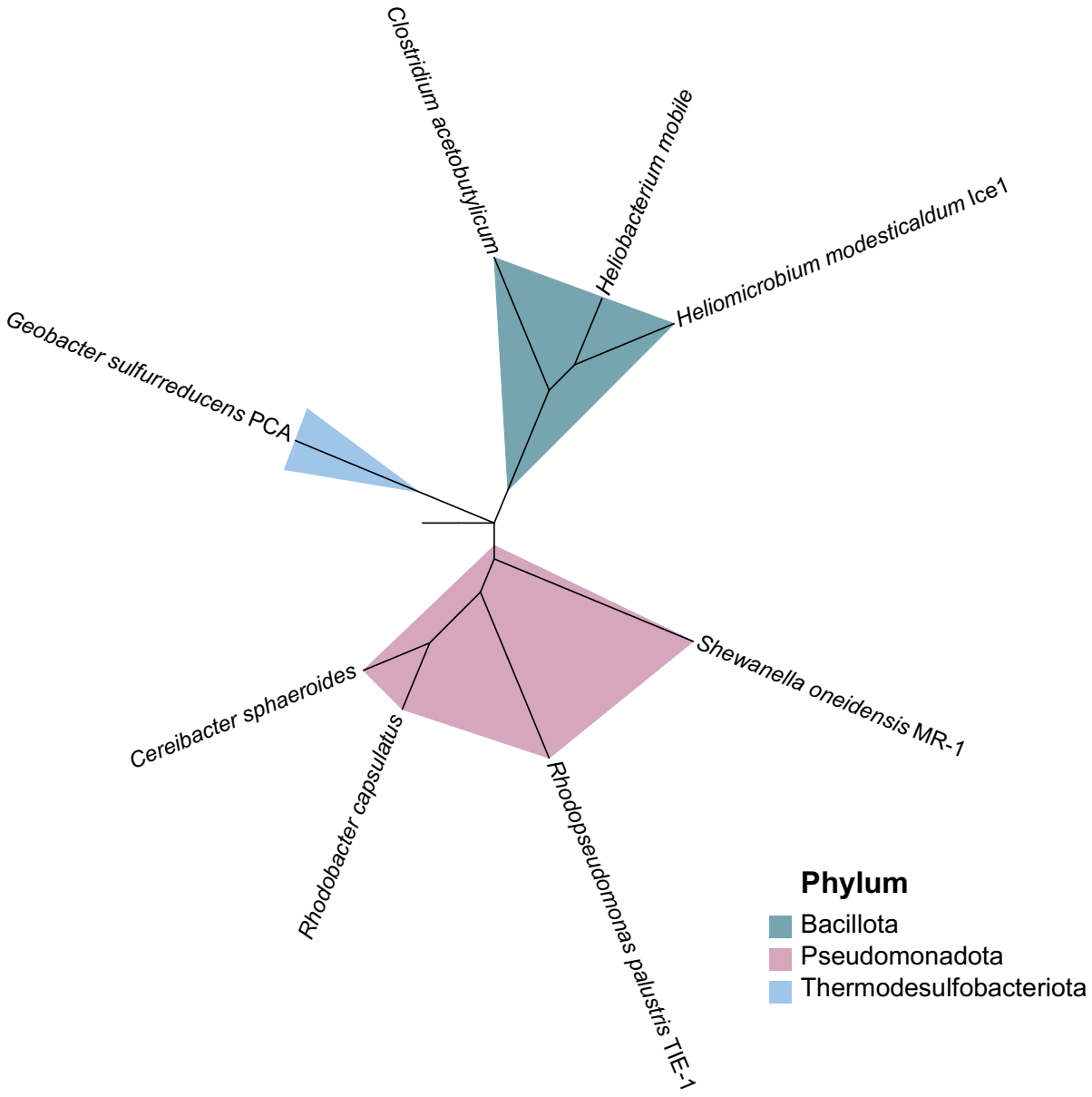

SI Figure 6.1: Unrooted tree of experimentally validated bacteria capable of anaerobic Hg^{II} reduction. Tree generated using phyloT v2 (phylot.biobyte.de) using NCBI taxonomy.

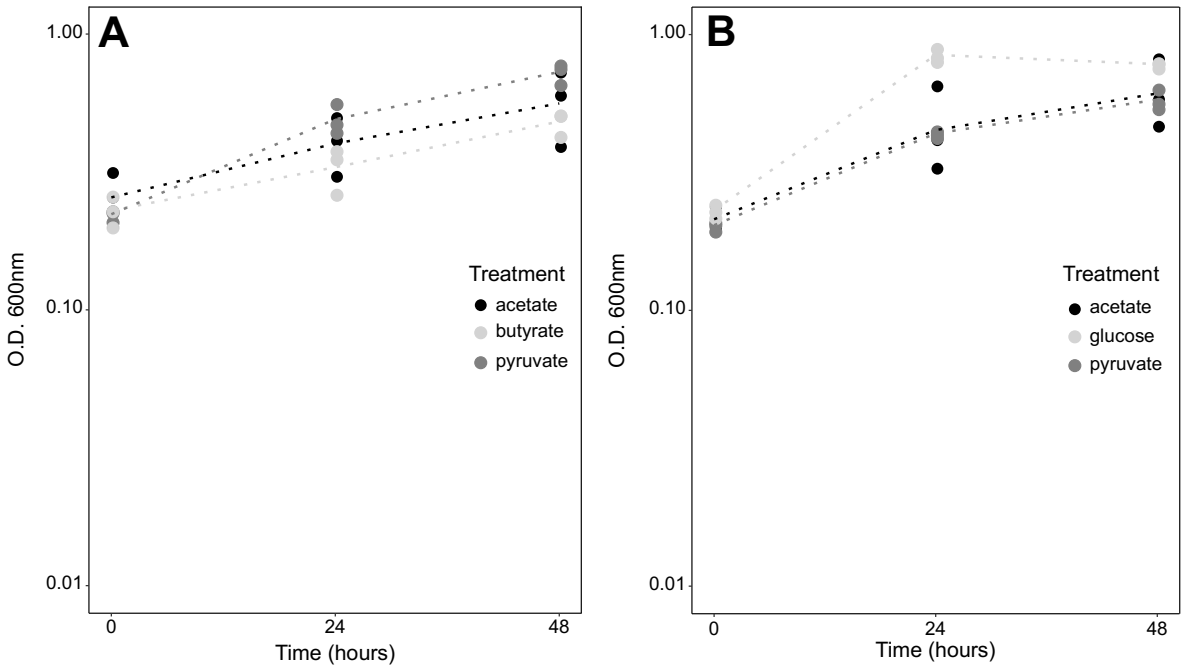

SI Figure 6.2: Growth data for bioreactor experiments with *C. aurantiacus* J10-fl measured at O.D. 600 nm for cultures grown as A) anoxygenic photoheterotrophs and B) aerobic chemoheterotrophs. Single measurements were taken per experiment and per timepoint. Each treatment was assayed in triplicate bioreactor experiments.

SUPPLEMENTARY TABLES

SI Table 6.1: Bioreactor results for sterile growth medium controls (devoid of any cells) exposed to the light or darkness.

Treatment	Carbon source	# of replicates	Conditions	Cumulative Hg^0 production (pmol)	Relative Hg^0 production (%)
sterile growth medium	acetate	1	light	3.5	2.8
		1	dark	2.9	2.3
	pyruvate	1	light	3.7	3.0
		1	dark	3.1	2.5
	butyrate	1	light	4.4	3.5
	CO2	1	light	4.5	3.6
	glucose	1	dark	2.2	1.8

* carbon source 6.1mM for all except 30mM HCO3-

SI Table 6.2: *Zc* of reference proteomes for microbes tested for their ability to reduce Hg^{II}. Zc data from Dick & Tang (2023) *Microbial Ecology*

Microbial strain	**phylum *Zc***	**class *Zc***	**order *Zc***	**non-*mer* Hg^{II} reducer**
Geobacter sulfurreducens PCA	-0.150156	-0.149898	-0.159055	yes
Shewanella oneidensis MR-1	-0.150156	-0.153244	-0.157121	yes
Rhodopseudomonas palustris TIE-1	-0.150156	-0.143236	-0.140223	yes
Rhodobacter capsulatus	-0.150156	-0.143236	-0.137273	yes
Cereibacter sphaeroides	-0.150156	-0.143236	-0.137273	yes
Heliomicrobium modesticaldum Ice1	-0.18071	-0.177419	-	yes
Heliobacterium mobile	-0.18071	-0.177419	-	yes
Clostridium acetobutylicum	-0.18071	-0.177419	-	yes
Chloroflexus aurantiacus J-10-fl	-0.15707	-0.152769	-	no
Escherichia coli K12	-0.150156	-0.153244	-0.158339	no
Cyanobacteria	-0.161369	-0.148958[#]	-	none to date

 # calculated Zc for Gloebacteria class (cyanobacteria)

Appendix F

List of abbreviated terms

Abbreviation	Meaning
3-OHP	3-hydroxypropionate bi-cycle
ATP	Adenosine triphosphate
BMAA	Minimal exposure medium for *E. coli*
BSH	bacillithiol
CVAFS	cold vapour atomic fluorecence spectroscopy
DMRB	Dissimilatory metal reducing bacteria
DMSA	dimercapto succinic acid
DMSO	Dimethylsulphoxide
DOM	Dissolved organic matter
DSMZ	German Collection of Microorganisms and Cell Cultures
EPA	Environmental Protection Agency
EPS	extracellular polymeric substance
ETC	electron transport chain
FAD	Flavin adenine dinucleotide
FADH	Flavin adenine dinucleotide (reduced)
Fd ox	Ferredoxin (oxidized)
Fd red	Ferredoxin (reduced)
FNR	Ferredoxin:NADP+ oxidoreductase
GMM	growth medium for E. coli
HbRC	Heliobacterial photosynthetic reaction center
Hg	Mercury
hgcA/HgcA	corrinoid protein involved in Hg methylation
hgcAB/HgcAB	genes or proteins responsible for Hg methylation
hgcB/HgcB	dicluster ferredoxin involed in Hg methylation
HgS	Cinnabar/mercury sulphide
IRB	Iron reducing bacteria
LMM	low molecular mass
mBBr	Monobromo(trimethylammonio)bimane
MeHg/MMHg	Monomethylmercury
merA/MerA	Mercuric reductase
MerP	periplasmic Hg scavenging protein
MerR	transcriptional activator of mer operon
MerT	inner-membrane bound Hg transporter
MIC	minimum inhibitory concentration
MOPS	3-(N-morpholino)-propanesulphonic acid

NAD(P)H	placeholder when unknown whether NADH or NADPH involved
NAD+	Nicotinamide adenine dinucleotide (oxidized)
NADH	Nicotinamide adenine dinucleotide (reduced)
NADP+	Nicotinamide adenine dinucleotide phosphate (oxidized)
NADPH	Nicotinamide adenine dinucleotide phosphate (reduced)
NEM	N-ethylmaleimide
NfnAB	NADH-dependent ferredoxin:NADP+ oxidoreductase
NOM	natural organic matter
NTZ	Nitazoxanide
O.D. 600	Optical density at 600 nm
OD	Oxidative demethylation
PAR	Photosynthetically active radiation
PBS	phosphate-buffered saline
PCR	Polymerase chain reaction
PEPCK	PEP carboxykinase
pETC	photosynthetic electron transport chain
PFOR	Pyruvate:ferredoxin oxidoreductase
PNSB	Purple non-sulphur bacteria
PYE	Pyruvate yeast extract growth medium
SH/SH-	Thiol group/bond
SRB	Sulphate reducing bacteria
TCA	Tricarboxylic acid cycle
THg	Total mercury
Trx	Thioredoxin
UNEP	United Nations Environmental Programme
YE	Yeast extract